The background of the cover is a watercolor illustration of various cells. The cells are depicted in shades of blue, green, and orange, with some having distinct nuclei or internal structures. The style is soft and artistic, with visible brushstrokes and color blending. The cells are scattered across the page, with some appearing more prominent than others.

Fuelling the fire

Immunometabolism of monocytes and macrophages in obesity & diabetes

Xanthe A.M.H. van Dierendonck

PROPOSITIONS

1. A high glyceic burden drives metabolic and functional alterations in monocytes during diabetes mellitus.
(this thesis)
2. The intracellular accumulation of lipid droplets is not the sole driver of macrophage dysfunction and adipose tissue inflammation during obesity.
(this thesis)
3. While the increasing integration of big data analysis into molecular science opens many new possibilities, one must not lose sight of biological relevance.
4. 'Novel' scientific fields are often not that new, but rather refueled or smartly rebranded.
5. Metabolic health should be the primary focus in preparation for future pandemics.
6. The recipe for flourishing in a scientific career is normalizing failure and a little bit of luck.
7. Learning to communicate science to a broader audience should become an integral part of being a scientist and will counteract the growing public mistrust in science.

Propositions belonging to the thesis entitled:

"Fuelling the fire:

Immunometabolism of monocytes and macrophages in obesity & diabetes"

Xanthe A.M.H. van Dierendonck
Wageningen, 27 August 2021

Fuelling the fire:
Immunometabolism of
monocytes and macrophages
in obesity & diabetes

Xanthe A.M.H. van Dierendonck

Thesis committee

Promotor

Prof. Dr A.H. Kersten

Professor of Nutrition, Metabolism, and Genomics

Division of Human Nutrition and Health

Wageningen University & Research

Co-promotor

Dr R. Stienstra

Assistant professor, Division of Human Nutrition and Health

Wageningen University & Research

Department of Internal Medicine, Radboud University Medical Centre, Nijmegen

Other members

Prof. Dr H.F.J. Savelkoul, Wageningen University & Research

Prof. Dr E. Lutgens, Amsterdam University Medical Centre

Dr M.L. Boes, Utrecht University Medical Centre

Dr K. Wouters, Maastricht University Medical Centre

This research was conducted under the auspices of the Graduate School VLAG (Advanced studies in Food Technology, Agrobiotechnology, Nutrition and Health Sciences).

Fuelling the fire: Immunometabolism of monocytes and macrophages in obesity & diabetes

Xanthe A.M.H. van Dierendonck

Thesis

submitted in fulfilment of the requirements for the degree of doctor
at Wageningen University

by the authority of the Rector Magnificus

Prof. Dr A.P.J. Mol,

in the presence of the

Thesis Committee appointed by the Academic Board

to be defended in public

on Friday 27 August 2021

at 4 p.m. in the Aula.

Xanthe A.M.H. van Dierendonck

Fuelling the fire:

Immunometabolism of monocytes and macrophages in obesity & diabetes

PhD thesis, Wageningen University, The Netherlands (2021)

With references, with summary in English.

ISBN: 978-94-6395-795-3

DOI: <https://doi.org/10.18174/545884>

Contents

Chapter 1	General introduction	8
Chapter 2	Glycolytic activity in human immune cells: inter-individual variation and functional implications in healthy subjects and patients with diabetes	36
Chapter 3	A high glycemic burden relates to functional and metabolic alterations of human monocytes in patients with type 2 diabetes	66
Chapter 4	The role of uncoupling protein 2 in macrophages and its impact on obesity-induced adipose tissue inflammation and insulin resistance	94
Chapter 5	HILPDA uncouples lipid droplet accumulation in adipose tissue macrophages from inflammation and metabolic dysregulation	126
Chapter 6	Triglyceride breakdown from lipid droplets regulates the inflammatory response in macrophages	164
Chapter 7	General summary	200
Chapter 8	General discussion	206
Appendices	Dutch summary Nederlandse samenvatting	236
	Acknowledgements Dankwoord	243
	About the author	251



General introduction

Xanthe A.M.H. van Dierendonck

The global epidemic of metabolic disorders

Over the past years, the prevalence of metabolic disorders, including obesity and diabetes mellitus, has risen to pandemic-like proportions and is expected to increase even further in the coming years [1–4]. In 2016, 39% of all adults worldwide were overweight, with 13% of them being obese [5], whereas the prevalence of diabetes mellitus was 8.5% in this population [6]. The occurrence of obesity and diabetes mellitus often goes hand in hand with the development of cardiometabolic complications, including enhanced susceptibility to infections and increased cardiovascular risk. The latter has become one of the major causes of mortality worldwide [7]. Aberrant responses of the immune system form a common denominator in both the initiation of diabetes mellitus and the development of diabetes-associated complications. Understanding the molecular mechanisms underlying these aberrations in immune cells is of utmost importance in identifying therapeutic strategies to decrease morbidity and mortality. Since metabolism is an important regulator of immune cell function, alterations in metabolic rewiring of immune cell populations may facilitate aberrant functional changes, which may, in turn, become key drivers of the progression of metabolic disorders.

The aim of this thesis is to investigate the role of innate immune cell metabolism in altering innate immune cell function leading to (1) the development of diabetes mellitus and (2) diabetes-related complications.

Obesity as a risk factor for metabolic disorders

Obesity is a chronic disorder primarily characterized by a disequilibrium between energy intake and energy expenditure, leading to weight gain by excessive deposition of fat. In reality, obesity can hardly be viewed as a simple result of overnutrition but instead has a complex aetiology that involves socioeconomic, environmental and psychological factors besides a broad array of physiological interactions [8,9]. Consequently, obesity is a heterogeneous disease that can be difficult to prevent or treat. An obese or overweight state of the body promotes the development of metabolic complications and comorbidities. In the mechanisms underlying these complications, the immune system plays an important role. During the development of obesity, different types of immune cells become dysregulated, which leads to low-grade inflammation in the body [10]. This inflammatory state likely plays a role in the development of many comorbidities to obesity, including cancer [11], cardiovascular diseases [12,13] and diabetes mellitus.

An important role in the development of obesity-associated diabetes mellitus is reserved for the white adipose tissue (WAT) [14]. The WAT forms an important endocrine organ, mediating metabolic processes throughout the body by releasing hormones and

adipokines [15]. Besides adipocytes, the WAT harbours many different types of immune cells that support its homeostasis. During obesity, excess storage of lipids in the WAT can lead to dysfunction of both adipocytes and immune cells, resulting in local development of low-grade inflammation. When this state of low-grade inflammation remains unresolved, it may become chronic, potentially interfering with peripheral glucose signalling by insulin and ultimately progressing toward the development of diabetes mellitus [16,17].

Diabetes mellitus

In healthy conditions, plasma glucose levels are under tight control by various hormones. One of the most important hormones is insulin, responsible for effectively regulating glucose uptake from the circulation into tissues. Insulin directly stimulates facilitated diffusion of glucose into cells, where it is either converted and stored or shuttled toward energy production [18]. Diabetes mellitus is a collection of metabolic diseases caused by defects in the insulin-directed processing of glucose, generally characterized by disordered uptake of glucose from the circulation, resulting in chronic hyperglycemia.

Aberrations in the immune response may play a key role in the pathogenesis of diabetes mellitus and diabetes-associated complications. Type 1 diabetes mellitus (T1DM) is often characterized as an autoimmune disease where a dysfunctional immune response causes the destruction of insulin-producing β -cells in the pancreas, potentially in response to β -cell stress [19]. The absence of insulin signalling due to a lack of functional β -cells subsequently leads to chronic hyperglycemia. Whereas T1DM often reveals itself at a young age, type 2 diabetes mellitus (T2DM) can develop at any stage in life and is associated with lifestyle. As the most prevalent type of diabetes mellitus, the development of T2DM is primarily driven by an insensitivity to insulin, which can be caused by obesity-driven chronic inflammation [20]. As tissues become increasingly resistant to insulin and its signals, the production of insulin is often upregulated. T2DM develops in obese patients when insulin sensitivity cannot be counteracted with increased insulin production, leading to downregulation of insulin receptors, chronic hyperglycemia and further derangement of insulin production [21]. Thus, whereas the origins of both T1DM and T2DM differ, the absence of insulin signalling and the emergence of chronic hyperglycemia are often the common result. Since hyperglycemia is an important factor in driving diabetes-related complications, they are often similar in T1DM and T2DM [22]. These complications involve further dysregulation of the immune system, chronic inflammation and vascular complications, leading to increased cardiovascular risk and impaired acute immune responses [23–25].

The innate immune system

Both obesity and diabetes mellitus are associated with immune cell dysfunction and a state of low-grade inflammation. In a healthy state, the induction of inflammation is under tight control by the immune system, which helps the body to ward off invading pathogens. This system consists of numerous immune cell types that belong to either the innate or the adaptive arm. The first line of defence against pathogens is accounted for by innate immune cells, albeit a less specific type of defence. After recognition of the invading pathogen, innate immune cells produce substantial amounts of cytokines and chemokines. Hereby, they orchestrate a pro-inflammatory response and recruit immune cells of the adaptive immune system, which elicit a more specific response to eliminate the pathogen and protect the host. Since especially innate immune responses are highly associated with the pathophysiology of diabetes mellitus and its complications [21], the innate immune system will be the point of focus in this thesis.

Two important cell types belonging to the innate part of immune defence are monocytes and macrophages, both mononuclear phagocytes that emanate from myeloid progenitors [26,27]. Monocytes are generally short-lived cells that patrol the blood circulation or are nested in the bone marrow or spleen and can be recruited to sites of infection, inflammation or tissue damage. After recruitment, monocytes can differentiate into specific macrophages, rapidly adjusting to their new environment [28]. Besides attracting monocyte-derived macrophages, most tissues also contain stable pools of tissue-specific resident macrophages, which are believed to originate from a different lineage and are not replenished by circulating monocytes [29–34]. Macrophages generally play important roles in initiating and resolving inflammation but also support tissue repair and cell turnover [35]. Their phagocytic capacity enables them to aid cell turnover through efferocytosis of apoptotic cells, but also allows them to quickly eliminate invading microbes during acute infections. Comparable to monocytes, this broad range of seemingly contrasting effector functions is mediated by the high phenotypic plasticity these cells possess. This plasticity facilitates a rapid response to changing microenvironments through polarization, thereby effectively adjusting and re-adjusting their functional programs to different needs [36–38].

Innate immune cell polarization

Both monocytes and macrophages exist in various different flavours. For monocytes, the broad distinction is often made between classical monocytes, intermediate monocytes and non-classical 'patrolling' monocytes [39,40]. Nevertheless, the exact characterization in terms of pro- or anti-inflammatory phenotypes is still a subject of discussion due to

conflicting results and subset heterogeneity [41]. The focus on macrophage polarization has steadily increased over the past years, as various macrophage phenotypes with concurrent functional programs were discovered [37]. Originally, researchers believed in a sharp discrimination between two phenotypes: the pro-inflammatory, so-called classically activated macrophages (M1) versus the anti-inflammatory or alternatively activated macrophages (M2) [35,42]. *In vitro*, classical activation of macrophages is frequently modelled by treatment of naïve macrophages with bacterial lipopolysaccharide (LPS), potentially in combination with interferon (IFN)- γ [43], whereas alternatively activated macrophages are generated by stimulation with interleukin (IL)-4 and IL-13 [44]. However, in contrast to the traditional dogma of the M1- and M2-phenotypic distinction, a plethora of different pathogen-associated molecular patterns (PAMPs), damage-associated molecular patterns (DAMPs) or other cytokines actually give rise to a broad spectrum of different macrophage phenotypes [45–47].

These molecular patterns are often recognized by specialized pattern-recognition receptors (PRRs) that can reside intracellularly or on the plasma membrane of monocytes and macrophages. Particularly the family of Toll-like receptors (TLRs) and its ligands are widely believed to play an important role in regulating innate immune activation [48]. The recognition of PAMPs or DAMPs by different TLRs activates specific intracellular signalling pathways, involving different transcription factors such as nuclear factor-kappa-B (NF κ B) and several signal transducer and activator of transcription (STAT) proteins, which control the transcription of genes that regulate cytokine production and cell survival [49].

Immunometabolism: the interplay between metabolism and immunity

The fact that different functional phenotypes in immune cells associate with specific changes in their metabolism has been reported in studies as early as the 1960s [50–52]. Due to the past years of scientific advancement and technological progress in the fields of immunology and metabolism, the interest in exploring the crossroads of both fields has seen an enormous surge. As a result, the field of ‘immunometabolism’ re-emerged, which comprises two main aspects in the interplay between metabolism and immunity. The first aspect involves the regulation of immune cell function by intracellular metabolic rewiring [53], whereas the second aspect explores how immune responses affect the homeostasis of whole-body (systemic) metabolism and vice versa [54]. Firstly, the regulation of innate immune cell function by metabolism will be considered, and subsequently the focus will be on the interplay between immune function and systemic metabolism.

In monocytes and macrophages, different phenotypes also associate with, or even depend

on, specific metabolic programmes [55,56]. Besides general inflammatory phenotypes, effector functions, such as efferocytosis, are also effectuated by certain metabolic pathways [57]. Important metabolic pathways involved in functional reprogramming include glycolysis, the TCA-cycle, oxidative phosphorylation and the oxidation and synthesis of lipids [53]. Interestingly, the immunometabolic regulation of immune cells can be modulated, which may allow the adjustment of functional programmes by inducing specific metabolic rewiring [58]. Hence, studying the association of metabolic pathways with specific immune cell functions could provide an important foundation to identify new therapeutic possibilities.

Glycolysis

In the first steps of glycolysis, glucose that is taken up by the cell is converted into pyruvate. Subsequently, pyruvate can be reduced into lactate, completing full glycolysis (**Figure 1**). Glycolysis is a relatively inefficient way to produce energy from glucose, although its ability to be rapidly upregulated can be beneficial for activated or proliferating cells. Additionally, it provides important biosynthetic intermediates that support proliferation and cellular growth. Although glucose was originally thought to be converted to lactate only in the absence of oxygen, the so-called 'Warburg effect' describes the use of aerobic glycolysis by rapidly proliferating cells [59]. In macrophages, the Warburg effect is an important hallmark of robust metabolic rewiring following inflammatory activation [60,61], for instance after TLR-mediated activation [55,62]. By upregulating aerobic glycolysis, immune cells can meet the acute need for energy and biosynthetic intermediates that is required during pro-inflammatory activation [63]. Hence, glycolytic enzymes are often observed to be crucial for pro-inflammatory macrophage polarization [61,64–67].

TCA-cycle and oxidative phosphorylation

Instead of its conversion into lactate, pyruvate can additionally be converted into acetyl-CoA and shuttled toward the TCA cycle in the mitochondria. Since the TCA cycle can be fed with derivatives of different carbon sources, including fatty acids and amino acids, it is often seen as a central metabolic hub that links various metabolic and signalling pathways in the cell [68]. In the TCA cycle, several enzymes oxidize acetyl-CoA into metabolic intermediates through a series of chemical reactions. Together, these reactions yield NADH and FADH₂, which are subsequently used to fuel the process of oxidative phosphorylation (OXPHOS). OXPHOS takes place in the electron transport chain, a set of proteins located in the mitochondrial membrane that use proton-motive force to synthesize energy in the form of ATP [53,69] (**Figure 1**). Macrophages with anti-inflammatory phenotypes are thought to synthesize ATP mainly by using the TCA cycle and OXPHOS [70,71], although

the use of OXPHOS may be dispensable [72].

In the early phase of the dynamic, metabolic remodelling following inflammatory activation, certain TCA cycle intermediates are increasingly needed as substrates for biosynthesis through anaplerosis. As a result, the TCA cycle becomes interrupted, leading to the accumulation of different intermediates [70,73]. Consequently, the flux through the electron transport chain diminishes, which decreases OXPHOS and ATP production through this route [74]. Instead, the mitochondrial membrane potential may be repurposed to produce reactive oxygen species (ROS) via reverse electron transport (RET) [75,76] (**Figure 1**). The interruption of the TCA cycle and accumulation of certain intermediates is regularly coupled to aerobic glycolysis, thereby associated with TLR-driven pro-inflammatory polarization of macrophages [74,77]. However, metabolic rewiring following inflammatory activation is often observed to be more complex and dynamic than solely a shift of energetics from OXPHOS toward aerobic glycolysis [73]. In human monocytes, different PAMPs were seen to induce unique metabolic signatures. Depending on the type of activation and the resulting needs of the cell, some PAMPs even led to upregulation of both aerobic glycolysis and OXPHOS [56]. Furthermore, besides an upregulation of aerobic glycolysis, macrophages may still require the oxidation of fatty acids for pro-inflammatory functions [78].

In addition to forming important biosynthetic precursors in anabolic processes, TCA cycle intermediates and their derivatives are also becoming appreciated as direct signalling molecules that can be actively involved in immune regulation [79–83]. One of the best-studied intermediates is itaconate, which directly affects the production of cytokines [84,85] (**Figure 1**) and modifies host-pathogen interactions in macrophages [86,87].

Lipid metabolism: oxidation and synthesis

Besides the conversion of glucose-derived pyruvate, another important source of acetyl-CoA to feed into the TCA cycle is supplied through the oxidation of fatty acids. Fatty acids are shuttled over the mitochondrial membrane via conjugation to carnitine and converted to large amounts of acetyl-CoA through β -oxidation, additionally yielding NADH and FADH_2 . The oxidation of fatty acids is a consistently observed characteristic of anti-inflammatory macrophages [88], although likely not indispensable for their phenotypic polarization [89]. Important sources of fatty acids for β -oxidation are intracellular lipid droplets, where fatty acids are stored in the form of triacylglycerols (TGs), which are synthesized through the esterification of fatty acids to a glycerol backbone [90] (**Figure 1**). Fatty acids can be liberated from stored TGs through lipolysis by intracellular lipases, often located on the outside of the lipid droplets. The rate-limiting intracellular lipase for TGs is adipose

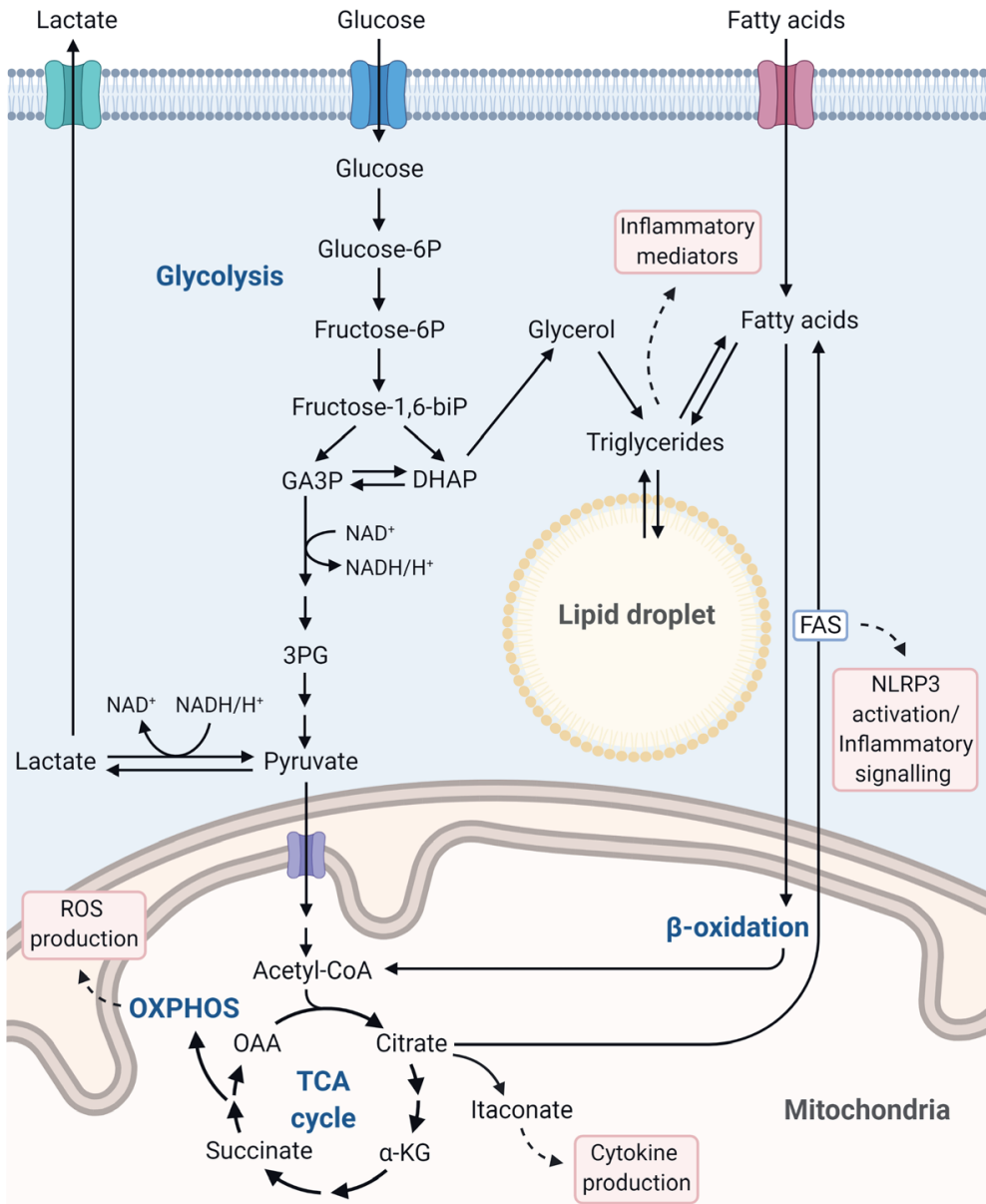


Figure 1. Overview of immunometabolism in innate immune cells.

Glucose is taken up through facilitated diffusion and converted into pyruvate. Pyruvate can be directly reduced to lactate or shuttled toward the TCA cycle in the mitochondria. The TCA cycle is a series of enzymatic reactions that can fuel the electron transport chain, which subsequently synthesizes ATP via OXPHOS, or yields intermediates such as citrate and succinate when interrupted. Diminished flux through OXPHOS can lead to ROS production, whereas accumulation of TCA cycle intermediates, including derivative itaconate, is involved in regulating cytokine production. Another source for acetyl-CoA entering the TCA cycle can be derived from β-oxidation of fatty acids. During inflammatory activation, β-oxidation is often halted, and citrate is used for de novo lipogenesis of fatty acids through FAS. FAS is an important player in activating the NLRP3 inflammasome

and regulating inflammatory signalling. Fatty acids can be esterified to a glycerol backbone, which can be derived from glucose, and resulting triglycerides can be stored in the lipid droplet. The lipid droplet provides precursors for inflammatory mediators.

triglyceride lipase (ATGL), which ensures the tight regulation of fatty acid release from intracellular lipid droplets [91–93].

During inflammatory activation of immune cells, the demand for TGs and phospholipids increases. Lipids are crucial for cellular processes such as membrane remodelling, proliferation or the synthesis of lipid-derived inflammatory mediators. Following activation, lipolysis of TGs seems more tightly regulated, and β -oxidation of fatty acids is largely halted [94]. In exchange, the process of de novo lipogenesis is upregulated [95,96], which likely starts by the conversion of TCA cycle intermediate citrate toward acetyl-CoA [97], possibly fuelled by the increased uptake of glucose. The synthesis of fatty acids by fatty acid synthase (FAS) is a crucial regulator for inflammatory signalling in innate immune cells. In monocytes, fatty acid synthesis is a key component for their differentiation into macrophages [98], whereas FAS in pro-inflammatory macrophages is required for activation of the NLRP3 inflammasome [99] and TLR/MYD88-dependent inflammatory signalling [100,101] (**Figure 1**). However, although the role of FAS seems consistent, recent studies have cast doubts whether de novo fatty acid synthesis is derived from the increased glucose flux after classical inflammation in macrophages. Evidence of direct incorporation of carbon from glucose toward fatty acids was absent, whereas increased incorporation of glucose-derived carbon was found in the glycerol backbones of newly synthesized TGs instead [102] (**Figure 1**).

Regardless of their origin, fatty acids are esterified toward TGs and accumulated in lipid droplets [103]. Lipid droplets support the inflammatory process by providing a steady pool of lipid precursors for the synthesis of inflammatory mediators (**Figure 1**). Interestingly, activation of TLRs by different PAMPs induce specific reprogramming of the lipidome in macrophages, minutely adjusting the composition of lipids to the specific cellular demands that arise after activation [104,105]. Besides specific reprogramming of the lipid content, the lipid droplet itself was also recently observed to play a unique role in regulating immune responses, specifically in recruiting antimicrobial peptides [106].

Immunometabolism: the interplay between metabolism and immunity

The second main aspect of immunometabolism comprises the effect of immune responses on the homeostasis of systemic metabolism [54]. The continuous cross-talk between immune cells and metabolic cells, such as adipocytes, affects the function of

both cell types, which could eventually affect systemic metabolism [107]. As cells with high plasticity, monocytes and macrophages are especially sensitive to metabolic changes in their microenvironment [108–110]. For instance, changed metabolic cues and stressors in the obese adipose tissue microenvironment may lead to altered immune responses, which eventually initiate or amplify chronic, low-grade inflammation, driving insulin resistance and diabetes development [111] (**Figure 2**). Furthermore, during the progression of diabetes mellitus, the altered function of monocytes and macrophages could underlie diabetes-associated complications in several ways (**Figure 2**). The influence of monocytes and macrophages in the development of diabetes and its complications are discussed below.

Chronic low-grade inflammation and development of diabetes

In patients with obesity or diabetes mellitus, a state of chronic low-grade inflammation can develop, ultimately contributing to various complications. Chronic inflammation is characterized by increased pro-inflammatory activation of immune cells, exemplified by circulating mononuclear cells that display an increased transcription of inflammatory genes during obesity [112], or circulating monocytes that show increased inflammasome activation, increased expression of toll-like receptors and increased secretion of pro-inflammatory cytokines in diabetes mellitus [113–115]. In addition to the inflammatory activation of innate immune cells, their number also increases, as both obesity and diabetes mellitus are associated with enhanced myelopoiesis and monocytosis [116–118]. Particularly hyperglycemia was found to promote monocytosis through increased myelopoiesis, which accelerates atherosclerosis development [119–121]. Correspondingly, in the circulation, elevated levels of inflammatory factors can be found, including hs-CRP, which is highly predictive for cardiovascular disease development [112,115,122–124]. On the tissue level, low-grade inflammation also develops in several peripheral tissues, including the liver, adipose tissue, muscle and the central nervous system [108]. Furthermore, although macrophage populations in the pancreas normally maintain tissue homeostasis, inflammatory activated monocytes and macrophages play a significant part in the autoimmune destruction of beta-cells, leading to insulin insufficiency and hyperglycemia [19,125–127] (**Figure 2**).

A crucial role in the development of insensitivity to insulin in obesity and T2DM could be appointed to the chronic inflammatory state of the adipose tissue [128]. The increased presence of the pro-inflammatory cytokine TNF α was found as one of the first factors linking obese adipose tissue inflammation to decreased signalling of insulin receptors and subsequent development of insulin resistance [129,130]. Accordingly, obese

individuals that experience a high degree of inflammation in the adipose tissue are often more resistant to insulin compared with obese individuals that display less adipose tissue inflammation [131]. The origin of pro-inflammatory signals in the adipose tissue has long since the observation of TNF α in the adipose tissue been attributed to an accumulation of inflammatory immune cells, of which the macrophage is the most abundant [132].

In healthy adipose tissue, macrophages are dispersed throughout the tissue and generally display anti-inflammatory phenotypes. These adipose tissue macrophages (ATMs) play important roles in supporting the high rate of adipocyte turnover that takes place in the adipose tissue [133] by effectively clearing apoptotic adipocytes through efferocytosis and promoting remodelling of the extracellular matrix [134]. Furthermore, ATMs act as lipid buffers during activation of lipolysis in adipocytes, for instance during fasting [135]. During the obesity-driven increase in fat disposition, expansion of the adipose tissue leads to adipocyte hypertrophy and increased adipocyte death [136]. In response, ATMs start to accumulate in the adipose tissue [132], forming 'crown-like structures' (CLSs) around dead adipocytes [137,138]. The ATMs in CLSs buffer excess lipids and store them in lipid droplets, which gives these ATMs a foam cell-like appearance reminiscent of foam cells present in atherosclerotic plaques [139] (**Figure 2**). Additionally, ATMs in obese adipose tissue display complex inflammatory signatures [140–143]. These signatures do not conform to the M1- or M2-like phenotypes [144]. Instead, the changing microenvironment in obese adipose tissue gives rise to 'metabolic activation' of ATMs, a phenotype characterized by increased lipid metabolism, lysosomal biogenesis and low-intensity inflammatory traits [145,146]. Although initially crucial for adequate ATM functioning [147], prolonged metabolic activation of ATMs is thought to play a role in the initiation of low-grade inflammation in the adipose tissue, contributing to the development of systemic insulin resistance [148–151]. Indeed, specifically silencing pro-inflammatory genes in ATMs may even improve systemic glucose intolerance in obese mice [152]. Although it is unclear how metabolic activation of ATMs is mediated by the microenvironment of obese adipose tissue, the evident resemblance to foam cells in atherosclerotic plaques suggests a corresponding form of lipotoxicity that instigates pro-inflammatory signalling [139,153]. Metabolic flexibility may be an important factor in ATM function, as suggested by the aggravation of the inflammatory phenotype in ATMs after inhibiting the transport of fatty acids [154] or glucose [60]. Therefore, the metabolic inflexibility that follows the buffering of excess lipids [144] may also lead to disordered functional programs in ATMs during obesity.

Complications of diabetes mellitus

Next to the development of diabetes mellitus, immune dysfunction also plays a role in driving diabetes-related complications during the progression of diabetes mellitus. These

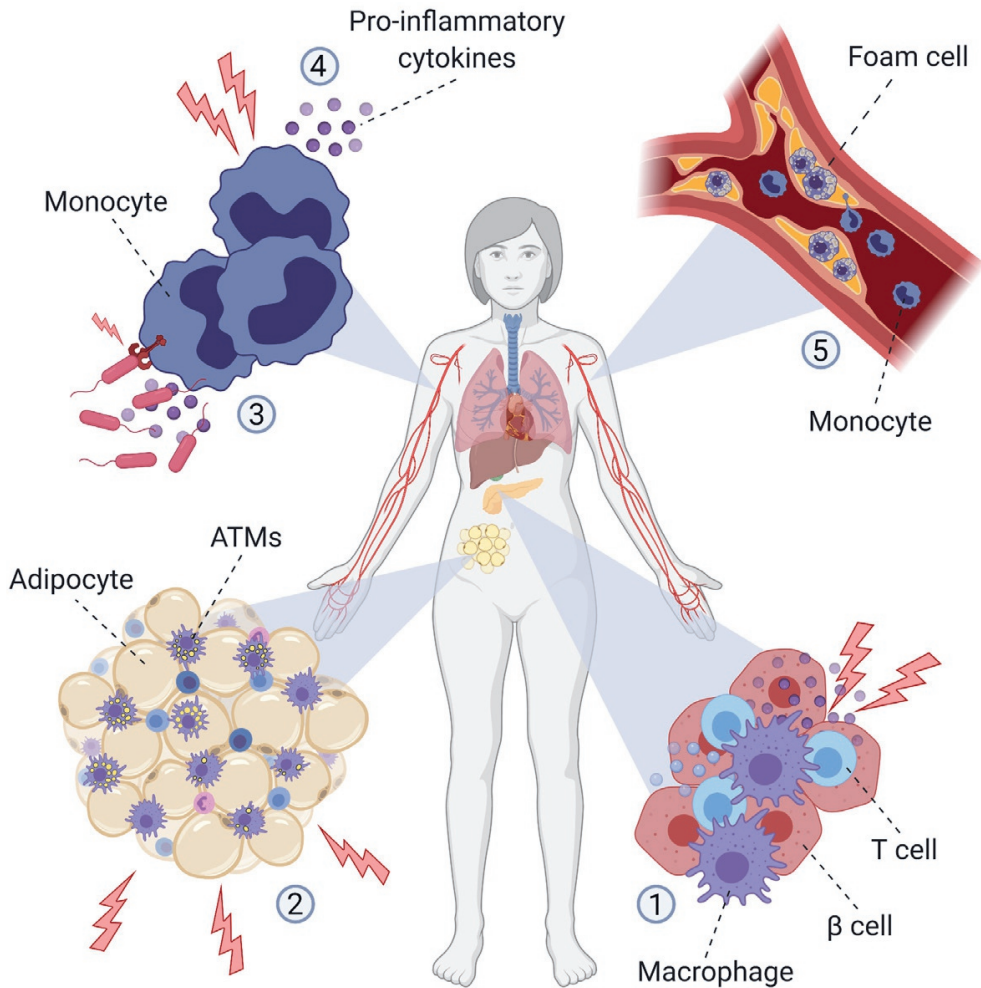


Figure 2. The innate immune system in the development of diabetes mellitus and its complications.

(1) Together with T cells, macrophages contribute to the autoimmune destruction of insulin-producing beta-cells in the pancreas. (2) In obese adipose tissue, adipose tissue macrophages (ATMs) form structures around dead adipocytes and buffer excess lipids. Metabolic activation of ATMs amplifies chronic inflammation in the adipose tissue, leading to insulin resistance. (3) General dysfunction of innate immune cells induces an increased susceptibility to infections and causes aggravation of disease development and outcome. (4) Chronic activation and increased myelopoiesis of circulating monocytes in obesity and diabetes mellitus leads to systemic inflammation and cardiovascular risk. (5) Hyperglycemia-induced monocyto-sis and systemic inflammation facilitate the development of atherosclerotic plaques, wherein activated monocytes and macrophages develop into foam cells.

complications include vascular complications, which lead to increased cardiovascular risk, but also dysfunction of acute immune responses [23–25]. Cardiovascular complications are the major cause of death in patients with diabetes mellitus, and especially circulating inflammatory factors are highly associated with cardiovascular risk in these patients [112,115,122–124]. Whereas multiple factors can induce cardiovascular disease progression, monocytes and macrophages play an undeniable role, particularly in the pathophysiology of atherosclerosis. The formation of atherosclerotic lesions likely starts as a local inflammation in the vascular wall, promoted by the recruitment of monocytes, which invade the subendothelial space and differentiate to macrophages. These macrophages can accumulate oxidized low-density lipoprotein (LDL) cholesterol and develop into foam cells, further accelerating local inflammation and eventually leading to the formation of atherosclerotic plaques (**Figure 2**). Hyperglycemia is one of the most important risk factors that underlies these vascular complications in patients with diabetes mellitus, through processes including protein glycation, glycosylation, increased oxidative stress, and monocytosis and the persistence of chronic inflammation in particular [155]. Indeed, intensive treatment of hyperglycemia can substantially prevent cardiovascular risk [156].

Despite the chronic pro-inflammatory activation of immune cells, epidemiological studies also observed a striking increase in the susceptibility to infections in patients with diabetes mellitus [157] (**Figure 2**). In both type 1 and type 2 diabetes, increased risk for hospitalization after different types of infections was found to be robustly associated with glycemic control, which can be estimated by measurement of glycated haemoglobin (HbA_{1c}) [158,159]. Examples also include the severity of infection with *Mycobacterium tuberculosis*, which is strongly predicted by glycemic control, leading to a tripling of the risk of tuberculosis development in patients with diabetes mellitus [160]. In addition, both obesity and diabetes mellitus were associated with an increased risk of morbidity and mortality for specific Streptococcus infections [161]. More recently, studies emphasized the increased incidence and severity of SARS-CoV-2 (COVID-19) infection in patients with diabetes mellitus or obesity, leading to a dramatically higher risk of hospitalization and ICU admission [162–165]. The increased susceptibility to these infections, which affects incidence, severity and outcome of the disease, suggests strong impairment of adequate acute immune responses toward pathogens during obesity and diabetes mellitus.

Immunometabolism: the interplay between metabolism and immunity

Simply put, cellular metabolism consists of an enormous network of bidirectional biochemical pathways. If one pathway is restricted due to changing fuel availability or cues from the microenvironment, energetics are shunted to another pathway. These forms of

metabolic rewiring can determine the functional plasticity of immune cells. Myeloid cells, especially macrophages and monocytes, possess high metabolic and functional plasticity [166]. Therefore, it is unsurprising that many studies in the field of immunometabolism have focused on myeloid cells. Together with their ubiquitous presence and their intricate cross-talk with metabolic cells, macrophages and monocytes form the ideal cell types for the study of immunometabolic targets in the context of obesity and diabetes mellitus.

During obesity and diabetes development, many systemic metabolic processes lose their delicate homeostatic equilibrium, which profoundly changes the environmental cues perceived by immune cells. Inevitable metabolic and functional rewiring follows, exemplified by the distinct metabolic signatures of ATMs in obese adipose tissue [144,145]. Subsequent immune dysfunction facilitates chronic inflammation, promoting the progression of diabetes and its complications [167], thereby fuelling the 'fire'. Hypothetically, this vicious cycle of disease progression could be broken by specifically modulating metabolic signatures of monocytes and macrophages, preventing dysfunction and attenuating chronic inflammation.

In this thesis, the boundaries of immunometabolic rewiring during health, obesity and diabetes are explored. The focus will be on the role of innate immune cell metabolism in altering immune functioning, contributing to the development of diabetes mellitus and diabetes-related complications. Furthermore, the potential use of targeting metabolism to improve these functional consequences is investigated.

Outline of this thesis

The innate immune system is often referred to as the immune system's first line of defence against unwanted pathogens, facilitating early recognition and removal. For that purpose, innate immune cells produce and release large amounts of cytokines. Interestingly, large inter-individual variations exist in the magnitude of cytokine production in response to pathogens. Since glycolytic metabolism is a robust and consistent hallmark of metabolic rewiring after immune cell activation, we set out to study its role in determining cytokine responses in human immune cells during health and disease. In **chapter 2**, we explore to what extent a normal range of increased aerobic glycolysis could be responsible for the inter-individual variation in immune responses and whether this relationship is altered in patients with type 1 diabetes mellitus.

Type 1 diabetes mellitus is often linked to increased susceptibility to infections, yet is also described to increase the risk for cardiovascular disease by causing a chronic inflammatory state in the body. Both associations suggest an ineffective functioning of (innate) immune

cells. Whereas earlier studies provide examples for alterations in innate immune cell functioning, potentially driven by chronically elevated glucose levels, it remains unknown how these alterations are linked to metabolic rewiring of innate immune cells. In **chapter 3**, we study extracellular metabolic flux and cytokine release from isolated monocytes from healthy subjects and patients with type 1 diabetes to examine changes in monocyte function and metabolism and try to identify the disease-related factors that drive these changes.

Specific metabolic and functional alterations in innate immune cells may not only drive diabetes-related complications, but can also support the development of diabetes mellitus itself. In obese adipose tissue, metabolic activation of macrophages leads to a low-grade inflammatory phenotype, coupled to distinct metabolic reprogramming. This metabolic activation could thereby contribute to increased adipose tissue inflammation, promoting insulin resistance and the development of type 2 diabetes mellitus. In this context, we investigated whether specific metabolic genes could be identified as important players that support the function of adipose tissue macrophages, to eventually attenuate obesity-driven adipose tissue inflammation. Therefore, we first consider uncoupling protein 2 (UCP2) as a potential metabolic target for adipose tissue macrophage function in **chapter 4**. UCP2 is a mitochondrial carrier suggested to be involved in regulating metabolic pathways, but is also known for its potential role in immune regulation. Using a murine model with myeloid-specific deletion of *Ucp2*, we address its role in regulating metabolism and cytokine production in macrophages during classical inflammation and high-fat diet-induced obesity. During obesity, lipid influx in the obese adipose tissue requires adipose tissue macrophages to handle a lipid-rich environment. Hypoxia-inducible lipid droplet-associated (HILPDA), a lipid-droplet associated protein, was identified as a lipid inducible protein in adipose tissue macrophages. In **chapter 5**, we determine the role of HILPDA in regulating the accumulation of lipid droplets in macrophages and its relation to adipose triglyceride lipase (ATGL) using a murine myeloid-specific knockout model. Hereby, we also investigate the exact role of lipid droplet accumulation in adipose tissue macrophages in the development of adipose tissue inflammation and insulin resistance in obesity.

The accumulation of lipid droplets is a phenomenon that is not only observed in macrophages in response to lipid-rich environments, including obese adipose tissue. Instead, macrophages consistently accumulate triglycerides in lipid droplets in response to inflammatory stimuli as well. In **chapter 6**, we build further on the role of HILPDA in macrophages by studying its function in the context of classical inflammation. We elaborate on the relationship between HILPDA and ATGL and determine how triglycerides accumulate in macrophages in response to LPS. Thereby, we demonstrate the importance

of lipid droplet accumulation in regulating the inflammatory response in macrophages.

Lastly, all the results obtained in this thesis are summarized in **chapter 7**. Subsequently, in **chapter 8**, the insights that were gained are evaluated and integrated into the context of the current literature. On this basis, I discuss future research perspectives of immunometabolism in the context of inflammatory responses in monocytes and macrophages with the goal to ultimately attenuate the progression of diabetes and the development of diabetes-associated complications.

References

Figures are created with BioRender.com

1. The GBD 2015 Obesity Collaborators. Health Effects of Overweight and Obesity in 195 Countries over 25 Years. *New England Journal of Medicine*. 2017; 377(1): 13–27.
2. Dai H, Alsalhe TA, Chalghaf N, Riccò M, Bragazzi NL, Wu J. The global burden of disease attributable to high body mass index in 195 countries and territories, 1990–2017: An analysis of the Global Burden of Disease Study. *PLoS Medicine*. 2020; 17(7).
3. Ampofo AG, Boateng EB. Beyond 2020: Modelling obesity and diabetes prevalence. *Diabetes Research and Clinical Practice*. 2020; 167.
4. (NCD-RisC) NRFC. Trends in adult body-mass index in 200 countries from 1975 to 2014: a pooled analysis of 1698 population-based measurement studies with 19.2 million participants. *The Lancet*. 2016; 387(10026): 1377–96.
5. World Health Organization. Obesity and overweight - WHO factsheet [Internet]. <https://www.who.int/news-room/fact-sheets/detail/obesity-and-overweight>.
6. World Health Organization. Diabetes - WHO factsheet [Internet]. <https://www.who.int/news-room/fact-sheets/detail/diabetes>.
7. WHO. The top 10 causes of death [Internet]. <https://www.who.int/news-room/fact-sheets/detail/the-top-10-causes-of-death>.
8. Malik VS, Willett WC, Hu FB. Global obesity: Trends, risk factors and policy implications. *Nature Reviews Endocrinology*. 2013; 9(1): 13–27.
9. Bhupathiraju SN, Hu FB. Epidemiology of obesity and diabetes and their cardiovascular complications. *Circulation Research*. 2016; 118(11): 1723–35.
10. Lackey DE, Olefsky JM. Regulation of metabolism by the innate immune system. *Nature reviews Endocrinology*. 2016; 12(1): 15–28.
11. Deng T, Lyon CJ, Bergin S, Caligiuri MA, Hsueh WA. Obesity, Inflammation, and Cancer. *Annual Review of Pathology: Mechanisms of Disease*. 2016; 11(1): 421–49.
12. Mathieu P, Lemieux I, Després JP. Obesity, inflammation, and cardiovascular risk. *Clinical Pharmacology and Therapeutics*. 2010; 87(4): 407–16.
13. Després JP. Body fat distribution and risk of cardiovascular disease: An update. *Circulation*. 2012; 126(10): 1301–13.
14. Longo M, Zatterale F, Naderi J, Parrillo L, Formisano P, Raciti GA, et al. Adipose tissue dysfunction as determinant of obesity-associated metabolic complications. *International Journal of Molecular Sciences*. 2019; 20(9).
15. Trayhurn P, Wood IS. Adipokines: inflammation and the pleiotropic role of white adipose tissue. *British Journal of Nutrition*. 2004; 92(03): 347.
16. Samuel VT, Shulman GI. The pathogenesis of insulin resistance: integrating signaling pathways and substrate flux. *The Journal of clinical investigation*. 2016; 126(1): 12–22.
17. Shoelson SE, Lee J, Goldfine AB. Inflammation and insulin resistance. *Journal of Clinical Investigation*. 2006; 116(7): 1793–801.
18. Petersen MC, Shulman GI. Mechanisms of insulin action and insulin resistance. *Physiological Reviews*. 2018; 98(4): 2133–223.
19. Roep BO, Thomaidou S, van Tienhoven R, Zaldumbide A. Type 1 diabetes mellitus as a disease

- of the β -cell (do not blame the immune system?). *Nature reviews Endocrinology*. 2020; 17: 1–12.
20. Arkan MC, Hevener AL, Greten FR, Maeda S, Li ZW, Long JM, et al. IKK- β links inflammation to obesity-induced insulin resistance. *Nature Medicine*. 2005; 11(2): 191–8.
 21. Donath MY, Shoelson SE. Type 2 diabetes as an inflammatory disease. *Nature reviews Immunology*. 2011; 11(2): 98–107.
 22. Brownlee M. Biochemistry and molecular cell biology of diabetic complications. *Nature*. 2001; 414(6865): 813–20.
 23. Laakso M. Cardiovascular disease in type 2 diabetes from population to man to mechanisms: The Kelly West award lecture 2008. *Diabetes Care*. 2010; 33(2): 442–9.
 24. Harcourt BE, Penfold SA, Forbes JM. Coming full circle in diabetes mellitus: From complications to initiation. *Nature Reviews Endocrinology*. 2013; 9(2): 113–23.
 25. Donath MY, Dinarello CA, Mandrup-Poulsen T. Targeting innate immune mediators in type 1 and type 2 diabetes. *Nature Reviews Immunology*. 2019; : 1–13.
 26. van Furth R, Cohn ZA, Hirsch JG, Humphrey JH, Spector WG, Langevoort HL. The mononuclear phagocyte system: a new classification of macrophages, monocytes, and their precursor cells. *Bulletin of the World Health Organization*. 1972; 46(6): 845–52.
 27. van Furth R, Cohn ZA. The origin and kinetics of mononuclear phagocytes. *The Journal of experimental medicine*. 1968; 128(3): 415–35.
 28. Jung S. Macrophages and monocytes: Of tortoises and hares. *Nature Reviews Immunology*. 2018; 18(2): 85–6.
 29. Soucie EL, Weng Z, Geirsdóttir L, Molawi K, Maurizio J, Fenouil R, et al. Lineage-specific enhancers activate self-renewal genes in macrophages and embryonic stem cells. *Science*. 2016; 351(6274).
 30. Hashimoto D, Chow A, Noizat C, Teo P, Beasley MB, Leboeuf M, et al. Tissue-resident macrophages self-maintain locally throughout adult life with minimal contribution from circulating monocytes. *Immunity*. 2013; 38(4): 792–804.
 31. Yona S, Kim KW, Wolf Y, Mildner A, Varol D, Breker M, et al. Fate Mapping Reveals Origins and Dynamics of Monocytes and Tissue Macrophages under Homeostasis. *Immunity*. 2013; 38(1): 79–91.
 32. Gibbings SL, Goyal R, Desch AN, Leach SM, Prabagar M, Atif SM, et al. Transcriptome analysis highlights the conserved difference between embryonic and postnatal-derived alveolar macrophages. *Blood*. 2015; 126(11): 1357–66.
 33. Gomez Perdiguero E, Klapproth K, Schulz C, Busch K, Azzoni E, Crozet L, et al. Tissue-resident macrophages originate from yolk-sac-derived erythro-myeloid progenitors. *Nature*. 2015; 518(7540): 547–51.
 34. Mass E, Ballesteros I, Farlik M, Halbritter F, Günther P, Crozet L, et al. Specification of tissue-resident macrophages during organogenesis. *Science*. 2016; 353(6304).
 35. Mantovani A, Biswas SK, Galdiero MR, Sica A, Locati M. Macrophage plasticity and polarization in tissue repair and remodelling. *Journal of Pathology*. 2013; 229(2): 176–85.
 36. Stout RD, Jiang C, Matta B, Tietzel I, Watkins SK, Suttles J. Macrophages Sequentially Change Their Functional Phenotype in Response to Changes in Microenvironmental Influences. *The Journal of Immunology*. 2005; 175(1): 342–9.
 37. Sica A, Mantovani A. Macrophage plasticity and polarization: In vivo veritas. *Journal of Clinical Investigation*. 2012; 122(3): 787–95.
 38. Liu SX, Gustafson HH, Jackson DL, Pun SH, Trapnell C. Trajectory analysis quantifies

- transcriptional plasticity during macrophage polarization. *Scientific Reports*. 2020; 10(1).
39. Wong KL, Tai JJY, Wong WC, Han H, Sem X, Yeap WH, et al. Gene expression profiling reveals the defining features of the classical, intermediate, and nonclassical human monocyte subsets. *Blood*. 2011; 118(5).
 40. Zawada AM, Rogacev KS, Rotter B, Winter P, Marell RR, Fliser D, et al. SuperSAGE evidence for CD14⁺⁺CD16⁺ monocytes as a third monocyte subset. *Blood*. 2011; 118(12).
 41. Merah-Mourah F, Cohen SO, Charron D, Mooney N, Haziot A. Identification of Novel Human Monocyte Subsets and Evidence for Phenotypic Groups Defined by Interindividual Variations of Expression of Adhesion Molecules. *Scientific Reports*. 2020; 10(1): 4397.
 42. Mills CD, Kincaid K, Alt JM, Heilman MJ, Hill AM. M-1/M-2 Macrophages and the Th1/Th2 Paradigm. *The Journal of Immunology*. 2000; 164(12): 6166–73.
 43. Bosisio D, Polentarutti N, Sironi M, Bernasconi S, Miyake K, Webb GR, et al. Stimulation of toll-like receptor 4 expression in human mononuclear phagocytes by interferon- γ : A molecular basis for priming and synergism with bacterial lipopolysaccharide. *Blood*. 2002; 99(9): 3427–31.
 44. Van Dyken SJ, Locksley RM. Interleukin-4- and interleukin-13-mediated alternatively activated macrophages: Roles in homeostasis and disease. *Annual Review of Immunology*. 2013; 31: 317–43.
 45. Mosser DM, Edwards JP. Exploring the full spectrum of macrophage activation. *Nature Reviews Immunology*. 2008; 8(12): 958–69.
 46. Xue J, Schmidt S V., Sander J, Draffehn A, Krebs W, Quester I, et al. Transcriptome-Based Network Analysis Reveals a Spectrum Model of Human Macrophage Activation. *Immunity*. 2014; 40(2): 274–88.
 47. Guilliams M, van de Laar L. A hitchhiker's guide to myeloid cell subsets: Practical implementation of a novel mononuclear phagocyte classification system. *Frontiers in Immunology*. 2015; 6: 406.
 48. O'Neill LAJ, Golenbock D, Bowie AG. The history of Toll-like receptors-redefining innate immunity. *Nature Reviews Immunology*. 2013; 13(6): 453–60.
 49. Akira S, Uematsu S, Takeuchi O. Pathogen recognition and innate immunity. *Cell*. 2006; 124(4): 783–801.
 50. Oren R, Farnham AE, Saito K, Milofsky E, Karnovsky ML. Metabolic patterns in three types of phagocytizing cells. *The Journal of Cell Biology*. 1963; 17(3).
 51. Newsholme P, Curi R, Gordont S, Newsholme EA. Metabolism of glucose, glutamine, long-chain fatty acids and ketone bodies by murine macrophages. *Biochem J*. 1986; 239: 121–5.
 52. Michl J, Ohlbaum DJ, Silverstein SC. 2-Deoxyglucose selectively inhibits Fc and complement receptor-mediated phagocytosis in mouse peritoneal macrophages. *Journal of Experimental Medicine*. 1976; 144(6): 1484–93.
 53. O'Neill LAJ, Kishton RJ, Rathmell J. A guide to immunometabolism for immunologists. *Nature Reviews Immunology*. 2016; 16(9): 553–65.
 54. Biswas SK, Mantovani A. Orchestration of metabolism by macrophages. *Cell Metabolism*. 2012; 15(4): 432–7.
 55. Rodríguez-Prados J-C, Través PG, Cuenca J, Rico D, Aragonés J, Martín-Sanz P, et al. Substrate Fate in Activated Macrophages: A Comparison between Innate, Classic, and Alternative Activation. *The Journal of Immunology*. 2010; 185(1): 605–14.
 56. Lachmandas E, Boutens L, Ratter JM, Hijmans A, Hooiveld GJ, Joosten LAB, et al. Microbial stimulation of different Toll-like receptor signalling pathways induces diverse metabolic

- programmes in human monocytes. *Nature Microbiology*. 2016; 2: 16246.
57. Yurdagul A, Subramanian M, Wang X, Crown SB, Ilkayeva OR, Darville L, et al. Macrophage Metabolism of Apoptotic Cell-Derived Arginine Promotes Continual Efferocytosis and Resolution of Injury. *Cell Metabolism*. 2020; 31(3): 518-533.e10.
 58. Loftus RM, Finlay DK. Immunometabolism: Cellular Metabolism Turns Immune Regulator. *Journal of Biological Chemistry*. 2016; 291(1): 1-10.
 59. Warburg O, Wind F, Negelein E. The metabolism of tumors in the body. *Journal of General Physiology*. 1927; 8(6): 519-30.
 60. Freemerman AJ, Johnson AR, Sacks GN, Milner JJ, Kirk EL, Troester MA, et al. Metabolic reprogramming of macrophages: Glucose transporter 1 (GLUT1)-mediated glucose metabolism drives a proinflammatory phenotype. *Journal of Biological Chemistry*. 2014; 289(11): 7884-96.
 61. Palsson-Mcdermott EM, Curtis AM, Goel G, Lauterbach MAR, Sheedy FJ, Gleeson LE, et al. Pyruvate kinase M2 regulates hif-1 α activity and il-1 β induction and is a critical determinant of the warburg effect in LPS-activated macrophages. *Cell Metabolism*. 2015; 21(1).
 62. Krawczyk CM, Holowka T, Sun J, Blagih J, Amiel E, DeBerardinis RJ, et al. Toll-like receptor-induced changes in glycolytic metabolism regulate dendritic cell activation. *Blood*. 2010; 115(23): 4742-9.
 63. Puchalska P, Huang X, Martin SE, Han X, Patti GJ, Crawford PA. Isotope Tracing Untargeted Metabolomics Reveals Macrophage Polarization-State-Specific Metabolic Coordination across Intracellular Compartments. *iScience*. 2018; 9: 298-313.
 64. Tan Z, Xie N, Cui H, Moellering DR, Abraham E, Thannickal VJ, et al. Pyruvate Dehydrogenase Kinase 1 Participates in Macrophage Polarization via Regulating Glucose Metabolism. *The Journal of Immunology*. 2015; 194(12): 6082-9.
 65. Galván-Peña S, Carroll RG, Newman C, Hinchey EC, Palsson-McDermott E, Robinson EK, et al. Malonylation of GAPDH is an inflammatory signal in macrophages. *Nature Communications*. 2019; 10(1).
 66. Haschemi A, Kosma P, Gille L, Evans CR, Burant CF, Starkl P, et al. The sedoheptulose kinase CARKL directs macrophage polarization through control of glucose metabolism. *Cell metabolism*. 2012; 15(6): 813-26.
 67. Xie M, Yu Y, Kang R, Zhu S, Yang L, Zeng L, et al. PKM2-Dependent glycolysis promotes NLRP3 and AIM2 inflammasome activation. *Nature Communications*. 2016; 7.
 68. Martínez-Reyes I, Chandel NS. Mitochondrial TCA cycle metabolites control physiology and disease. *Nature Communications*. 2020; 11(1): 1-11.
 69. Ryan DG, O'Neill LAJ. Krebs Cycle Reborn in Macrophage Immunometabolism. *Annual Review of Immunology*. 2020; .
 70. Jha AK, Huang SCC, Sergushichev A, Lampropoulou V, Ivanova Y, Loginicheva E, et al. Network integration of parallel metabolic and transcriptional data reveals metabolic modules that regulate macrophage polarization. *Immunity*. 2015; 42(3).
 71. Vats D, Mukundan L, Odegaard JI, Zhang L, Smith KL, Morel CR, et al. Oxidative metabolism and PGC-1 β attenuate macrophage-mediated inflammation. *Cell Metabolism*. 2006; 4(1): 13-24.
 72. Divakaruni AS, Hsieh WY, Minarrieta L, Duong TN, Kim KKO, Desousa BR, et al. Etomoxir Inhibits Macrophage Polarization by Disrupting CoA Homeostasis. *Cell Metabolism*. 2018; 28(3): 490-503.e7.
 73. Seim GL, Britt EC, John S V., Yeo FJ, Johnson AR, Eisenstein RS, et al. Two-stage metabolic remodelling in macrophages in response to lipopolysaccharide and interferon- γ stimulation.

- Nature Metabolism. 2019; 1(7): 731–42.
74. Van den Bossche J, Baardman J, Otto NA, van der Velden S, Neele AE, van den Berg SM, et al. Mitochondrial Dysfunction Prevents Repolarization of Inflammatory Macrophages. *Cell Reports*. 2016; 17(3): 684–96.
 75. Mills EL, Kelly B, Logan A, Costa ASH, Varma M, Bryant CE, et al. Succinate Dehydrogenase Supports Metabolic Repurposing of Mitochondria to Drive Inflammatory Macrophages. *Cell*. 2016; 167(2): 457–470.e13.
 76. Chouchani ET, Pell VR, Gaude E, Aksentijević D, Sundier SY, Robb EL, et al. Ischaemic accumulation of succinate controls reperfusion injury through mitochondrial ROS. *Nature*. 2014; 515(7527): 431–5.
 77. Lauterbach MA, Hanke JE, Serefidou M, Mangan MSJ, Kolbe CC, Hess T, et al. Toll-like Receptor Signaling Rewires Macrophage Metabolism and Promotes Histone Acetylation via ATP-Citrate Lyase. *Immunity*. 2019; 51(6): 997–1011.e7.
 78. Moon JS, Nakahira K, Chung KP, DeNicola GM, Koo MJ, Pabón MA, et al. NOX4-dependent fatty acid oxidation promotes NLRP3 inflammasome activation in macrophages. *Nature Medicine*. 2016; 22(9): 1002–12.
 79. Lampropoulou V, Sergushichev A, Bambouskova M, Nair S, Vincent EE, Loginicheva E, et al. Itaconate Links Inhibition of Succinate Dehydrogenase with Macrophage Metabolic Remodeling and Regulation of Inflammation. *Cell Metabolism*. 2016; .
 80. Tannahill GM, Curtis AM, Adamik J, Palsson-McDermott EM, McGettrick AF, Goel G, et al. Succinate is an inflammatory signal that induces IL-1 β through HIF-1 α . *Nature*. 2013; 496(7444): 238–42.
 81. Liu PS, Wang H, Li X, Chao T, Teav T, Christen S, et al. α -ketoglutarate orchestrates macrophage activation through metabolic and epigenetic reprogramming. *Nature Immunology*. 2017; 18(9): 985–94.
 82. Arts RJW, Novakovic B, ter Horst R, Carvalho A, Bekkering S, Lachmandas E, et al. Glutaminolysis and Fumarate Accumulation Integrate Immunometabolic and Epigenetic Programs in Trained Immunity. *Cell Metabolism*. 2016; 24(6): 807–19.
 83. Williams NC, O'Neill LAJ. A role for the krebs cycle intermediate citrate in metabolic reprogramming in innate immunity and inflammation. *Frontiers in Immunology*. 2018; 9(FEB).
 84. Swain A, Bambouskova M, Kim H, Andhey PS, Duncan D, Auclair K, et al. Comparative evaluation of itaconate and its derivatives reveals divergent inflammasome and type I interferon regulation in macrophages. *Nature Metabolism*. 2020; 2(7): 594–602.
 85. Mills EL, Ryan DG, Prag HA, Dikovskaya D, Menon D, Zaslona Z, et al. Itaconate is an anti-inflammatory metabolite that activates Nrf2 via alkylation of KEAP1. *Nature*. 2018; 556(7699): 113–7.
 86. Chen M, Sun H, Boot M, Shao L, Chang SJ, Wang W, et al. Itaconate is an effector of a Rab GTPase cell-autonomous host defense pathway against Salmonella. *Science*. 2020; 369(6502): 450–5.
 87. Michelucci A, Cordes T, Ghelfi J, Pailot A, Reiling N, Goldmann O, et al. Immune-responsive gene 1 protein links metabolism to immunity by catalyzing itaconic acid production. *Proceedings of the National Academy of Sciences of the United States of America*. 2013; 110(19): 7820–5.
 88. Namgaladze D, Brüne B. Macrophage fatty acid oxidation and its roles in macrophage polarization and fatty acid-induced inflammation. *Biochimica et Biophysica Acta (BBA) - Molecular and Cell Biology of Lipids*. 2016; 1861(11): 1796–807.
 89. Namgaladze D, Brüne B. Fatty acid oxidation is dispensable for human macrophage IL-4-induced polarization. *Biochimica et Biophysica Acta - Molecular and Cell Biology of Lipids*.

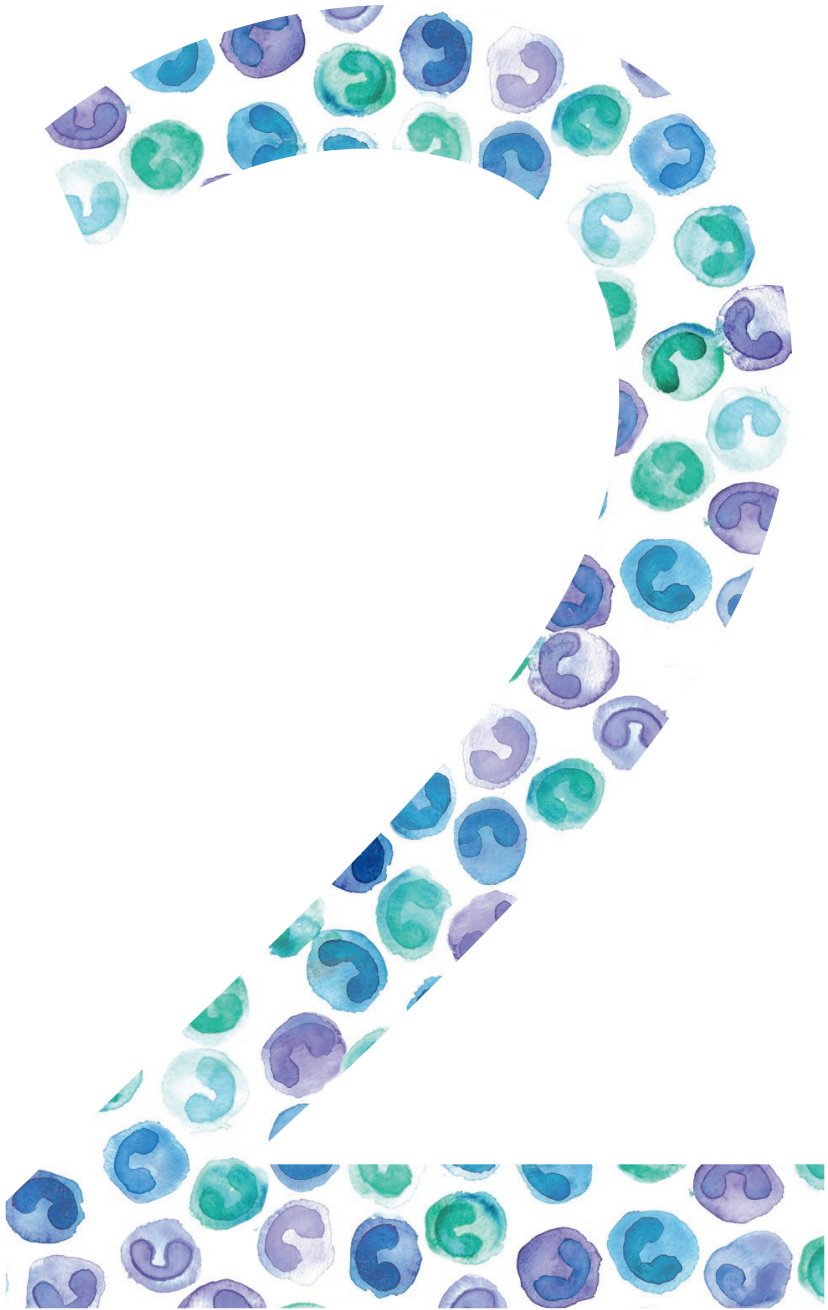
- 2014; 1841(9): 1329–35.
90. Walther TC, Farese R V. Lipid droplets and cellular lipid metabolism. *Annual Review of Biochemistry*. 2012; 81: 687–714.
 91. Zimmermann R, Strauss JG, Haemmerle G, Schoiswohl G, Birner-Gruenberger R, Riederer M, et al. Fat mobilization in adipose tissue is promoted by adipose triglyceride lipase. *Science*. 2004; 306(5700): 1383–6.
 92. Villena JA, Roy S, Sarkadi-Nagy E, Kim KH, Hei SS. Desnutrin, an adipocyte gene encoding a novel patatin domain-containing protein, is induced by fasting and glucocorticoids: Ectopic expression of desnutrin increases triglyceride hydrolysis. *Journal of Biological Chemistry*. 2004; 279(45): 47066–75.
 93. Jenkins CM, Mancuso DJ, Yan W, Sims HF, Gibson B, Gross RW. Identification, cloning, expression, and purification of three novel human calcium-independent phospholipase A2 family members possessing triacylglycerol lipase and acylglycerol transacylase activities. *Journal of Biological Chemistry*. 2004; 279(47): 48968–75.
 94. Huang Y, Morales-Rosado J, Ray J, Myers TG, Kho T, Lu M, et al. Toll-like Receptor Agonists Promote Prolonged Triglyceride Storage in Macrophages. *Journal of Biological Chemistry*. 2014; 289(5): 3001–12.
 95. Feingold KR, Shigenaga JK, Kazemi MR, McDonald CM, Patzek SM, Cross AS, et al. Mechanisms of triglyceride accumulation in activated macrophages. *Journal of Leukocyte Biology*. 2012; 92(4): 829–39.
 96. Im SS, Yousef L, Blaschitz C, Liu JZ, Edwards RA, Young SG, et al. Linking lipid metabolism to the innate immune response in macrophages through sterol regulatory element binding protein-1a. *Cell Metabolism*. 2011; 13(5): 540–9.
 97. Infantino V, Iacobazzi V, Palmieri F, Menga A. ATP-citrate lyase is essential for macrophage inflammatory response. *Biochemical and Biophysical Research Communications*. 2013; 440(1): 105–11.
 98. Ecker J, Liebisch G, Englmaier M, Grandl M, Robenek H, Schmitz G. Induction of fatty acid synthesis is a key requirement for phagocytic differentiation of human monocytes. *Proceedings of the National Academy of Sciences of the United States of America*. 2010; 107(17): 7817–22.
 99. Moon J-S, Lee S, Park M-A, Siempos II, Haslip M, Lee PJ, et al. UCP2-induced fatty acid synthase promotes NLRP3 inflammasome activation during sepsis. *Journal of Clinical Investigation*. 2015; 125(2): 665–80.
 100. Kim YC, Lee SE, Kim SK, Jang HD, Hwang I, Jin S, et al. Toll-like receptor mediated inflammation requires FASN-dependent MYD88 palmitoylation. *Nature Chemical Biology*. 2019; 15(9): 907–16.
 101. Carroll RG, Zasłona Z, Galván-Peña S, Koppe EL, Sévin DC, Angiari S, et al. An unexpected link between fatty acid synthase and cholesterol synthesis in proinflammatory macrophage activation. *Journal of Biological Chemistry*. 2018; 293(15): 5509–21.
 102. Rosas-Ballina M, Guan XL, Schmidt A, Bumann D. Classical Activation of Macrophages Leads to Lipid Droplet Formation Without de novo Fatty Acid Synthesis. *Frontiers in Immunology*. 2020; 11: 131.
 103. Castoldi A, Monteiro LB, van Teijlingen Bakker N, Sanin DE, Rana N, Corrado M, et al. Triacylglycerol synthesis enhances macrophage inflammatory function. *Nature Communications*. 2020; 11(1).
 104. Hsieh WY, Zhou QD, York AG, Williams KJ, Scumpia PO, Kronenberger EB, et al. Toll-Like Receptors Induce Signal-Specific Reprogramming of the Macrophage Lipidome. *Cell Metabolism*. 2020; 32(1): 128-143.e5.

105. Dennis EA, Deems RA, Harkewicz R, Quehenberger O, Brown HA, Milne SB, et al. A mouse macrophage lipidome. *Journal of Biological Chemistry*. 2010; 285(51): 39976–85.
106. Bosch M, Sánchez-Álvarez M, Fajardo A, Kapetanovic R, Steiner B, Dutra F, et al. Mammalian lipid droplets are innate immune hubs integrating cell metabolism and host defense. *Science*. 2020; 370(6514).
107. Schipper HS, Prakken B, Kalkhoven E, Boes M. Adipose tissue-resident immune cells: Key players in immunometabolism. *Trends in Endocrinology and Metabolism*. 2012; 23(8): 407–15.
108. Okabe Y, Medzhitov R. Tissue-specific signals control reversible program of localization and functional polarization of macrophages. *Cell*. 2014; 157(4): 832–44.
109. Amit I, Winter DR, Jung S. The role of the local environment and epigenetics in shaping macrophage identity and their effect on tissue homeostasis. *Nature Immunology*. 2016; 17(1): 18–25.
110. Van den Bossche J, Saraber DL. Metabolic regulation of macrophages in tissues. *Cellular Immunology*. 2018; .
111. Odegaard JI, Chawla A. The Immune System as a Sensor of the Metabolic State. *Immunity*. 2013; 38(4): 644–54.
112. Ghanim H, Aljada A, Hofmeyer D, Syed T, Mohanty P, Dandona P. Circulating mononuclear cells in the obese are in a proinflammatory state. *Circulation*. 2004; 110(12): 1564–71.
113. Lee HM, Kim JJ, Kim HJ, Shong M, Ku BJ, Jo EK. Upregulated NLRP3 inflammasome activation in patients with type 2 diabetes. *Diabetes*. 2013; 62(1): 194–204.
114. Devaraj S, Dasu MR, Rockwood J, Winter W, Griffen SC, Jialal I. Increased toll-like receptor (TLR) 2 and TLR4 expression in monocytes from patients with type 1 diabetes: Further evidence of a proinflammatory state. *Journal of Clinical Endocrinology and Metabolism*. 2008; 93(2): 578–83.
115. Devaraj S, Glaser N, Griffen S, Wang-Polagruto J, Miguelino E, Jialal I. Increased monocytic activity and biomarkers of inflammation in patients with type 1 diabetes. *Diabetes*. 2006; 55(3): 774–9.
116. Poitou C, Dalmas E, Renovato M, Benhamo V, Hajduch F, Abdennour M, et al. CD14^{dim}CD16⁺ and CD14⁺CD16⁺ monocytes in obesity and during weight loss: Relationships with fat mass and subclinical atherosclerosis. *Arteriosclerosis, Thrombosis, and Vascular Biology*. 2011; 31(10): 2322–30.
117. Devèvre EF, Renovato-Martins M, Clément K, Sautès-Fridman C, Cremer I, Poitou C. Profiling of the Three Circulating Monocyte Subpopulations in Human Obesity. *The Journal of Immunology*. 2015; 194(8): 3917–23.
118. Nagareddy PR, Kraakman M, Masters SL, Stizaker RA, Gorman DJ, Grant RW, et al. Adipose tissue macrophages promote myelopoiesis and monocytosis in obesity. *Cell Metabolism*. 2014; 19(5): 821–35.
119. Nagareddy PR, Murphy AJ, Stizaker RA, Hu Y, Yu S, Miller RG, et al. Hyperglycemia promotes myelopoiesis and impairs the resolution of atherosclerosis. *Cell Metabolism*. 2013; 17(5): 695–708.
120. Flynn MC, Kraakman MJ, Tikellis C, Lee MKS, Hanssen NMJ, Kammoun HL, et al. Transient Intermittent Hyperglycemia Accelerates Atherosclerosis by Promoting Myelopoiesis. *Circulation Research*. 2020; 127(7): 877–92.
121. Heyde A, Rohde D, McAlpine CS, Zhang S, Hoyer FF, Gerold JM, et al. Increased stem cell proliferation in atherosclerosis accelerates clonal hematopoiesis. *Cell*. 2021; 184(5): 1348-1361.e22.

122. Basu S, Larsson A, Vessby J, Vessby B, Berne C. Type 1 Diabetes Is Associated With Increased Cyclooxygenase- and Cytokine-Mediated Inflammation. *Diabetes Care*. 2005; 28(6): 1371 LP – 1375.
123. Dogan Y, Akarsu S, Ustundag B, Yilmaz E, Gurgoze MK. Serum IL-1 β , IL-2, and IL-6 in insulin-dependent diabetic children. *Mediators of Inflammation*. 2006; 2006(1).
124. 124. Pai JK, Pischon T, Ma J, Manson JE, Hankinson SE, Joshipura K, et al. Inflammatory Markers and the Risk of Coronary Heart Disease in Men and Women. *New England Journal of Medicine*. 2004; 351(25): 2599–610.
125. Yang LJ. Big mac attack: Does it play a direct role for monocytes/macrophages in type 1 diabetes? *Diabetes*. 2008; 57(11): 2922–3.
126. Martin AP, Rankin S, Pitchford S, Charo IF, Furtado GC, Lira SA. Increased expression of CCL2 in insulin-producing cells of transgenic mice promotes mobilization of myeloid cells from the bone marrow, marked insulinitis, and diabetes. *Diabetes*. 2008; 57(11): 3025–33.
127. Jensen DM, Hendricks K V., Mason AT, Tessem JS. Good Cop, Bad Cop: The Opposing Effects of Macrophage Activation State on Maintaining or Damaging Functional β -Cell Mass. *Metabolites*. 2020; 10(12): 485.
128. Xu H, Barnes GT, Yang Q, Tan G, Yang D, Chou CJ, et al. Chronic inflammation in fat plays a crucial role in the development of obesity-related insulin resistance. *Journal of Clinical Investigation*. 2003; 112(12): 1821–30.
129. Hotamisligil GS, Shargill NS, Spiegelman BM. Adipose expression of tumor necrosis factor- α : Direct role in obesity-linked insulin resistance. *Science*. 1993; 259(5091): 87–91.
130. Uysal KT, Wiesbrock SM, Marino MW, Hotamisligil GS. Protection from obesity-induced insulin resistance in mice lacking TNF- α function. *Nature*. 1997; 389(6651): 610–4.
131. Barbarroja N, López-Pedrería R, Mayas MD, García-Fuentes E, Garrido-Sánchez L, Macías-González M, et al. The obese healthy paradox: Is inflammation the answer? *Biochemical Journal*. 2010; 430(1): 141–9.
132. Weisberg SP, McCann D, Desai M, Rosenbaum M, Leibel RL, Ferrante AW. Obesity is associated with macrophage accumulation in adipose tissue. *Journal of Clinical Investigation*. 2003; 112(12): 1796–808.
133. Spalding KL, Arner E, Westermark PO, Bernard S, Buchholz BA, Bergmann O, et al. Dynamics of fat cell turnover in humans. *Nature*. 2008; 453(7196): 783–7.
134. Fischer-Posovszky P, Wang QA, Asterholm IW, Rutkowski JM, Scherer PE. Targeted deletion of adipocytes by apoptosis leads to adipose tissue recruitment of alternatively activated M2 macrophages. *Endocrinology*. 2011; 152(8): 3074–81.
135. Kosteli A, Sgaru E, Haemmerle G, Martin JF, Lei J, Zechner R, et al. Weight loss and lipolysis promote a dynamic immune response in murine adipose tissue. *The Journal of Clinical Investigation*. 2010; 120(10): 3466–79.
136. Strissel KJ, Stancheva Z, Miyoshi H, Perfield JW, DeFuria J, Jick Z, et al. Adipocyte death, adipose tissue remodeling, and obesity complications. *Diabetes*. 2007; 56(12): 2910–8.
137. Cinti S, Mitchell G, Barbatelli G, Murano I, Ceresi E, Faloia E, et al. Adipocyte death defines macrophage localization and function in adipose tissue of obese mice and humans. *Journal of Lipid Research*. 2005; 46(11): 2347–55.
138. Murano I, Barbatelli G, Parisani V, Latini C, Muzzonigro G, Castellucci M, et al. Dead adipocytes, detected as crown-like structures, are prevalent in visceral fat depots of genetically obese mice. *Journal of Lipid Research*. 2008; 49(7): 1562–8.
139. Shapiro H, Pecht T, Shaco-Levy R, Harman-Boehm I, Kirshtein B, Kuperman Y, et al. Adipose

- Tissue Foam Cells Are Present in Human Obesity. *The Journal of Clinical Endocrinology & Metabolism*. 2013; 98(3): 1173–81.
140. Lumeng CN, Bodzin JL, Saltiel AR. Obesity induces a phenotypic switch in adipose tissue macrophage polarization. *Journal of Clinical Investigation*. 2007; 117(1): 175–84.
141. Lumeng CN, DelProposto JB, Westcott DJ, Saltiel AR. Phenotypic Switching of Adipose Tissue Macrophages With Obesity Is Generated by Spatiotemporal Differences in Macrophage Subtypes. *Diabetes*. 2008; 57(12): 3239–46.
142. Shaul ME, Bennett G, Strissel KJ, Greenberg AS, Obin MS. Dynamic, M2-like remodeling phenotypes of CD11c+ adipose tissue macrophages during high-fat diet - Induced obesity in mice. *Diabetes*. 2010; 59(5): 1171–81.
143. Zeyda M, Farmer D, Todoric J, Aszmann O, Speiser M, Györi G, et al. Human adipose tissue macrophages are of an anti-inflammatory phenotype but capable of excessive pro-inflammatory mediator production. *International Journal of Obesity*. 2007; 31(9): 1420–8.
144. Kratz M, Coats BR, Hisert KB, Hagman D, Mutskov V, Peris E, et al. Metabolic Dysfunction Drives a Mechanistically Distinct Proinflammatory Phenotype in Adipose Tissue Macrophages. *Cell Metabolism*. 2014; 20(4): 614–25.
145. Xu X, Grijalva A, Skowronski A, van Eijk M, Serlie MJ, Ferrante AW. Obesity Activates a Program of Lysosomal-Dependent Lipid Metabolism in Adipose Tissue Macrophages Independently of Classic Activation. *Cell Metabolism*. 2013; 18(6): 816–30.
146. Boutens L, Hooiveld GJ, Dhingra S, Cramer RA, Netea MG, Stienstra R. Unique metabolic activation of adipose tissue macrophages in obesity promotes inflammatory responses. *Diabetologia*. 2018; 61(4): 942–53.
147. Coats BR, Schoenfelt KQ, Barbosa-Lorenzi VC, Peris E, Cui C, Hoffman A, et al. Metabolically Activated Adipose Tissue Macrophages Perform Detrimental and Beneficial Functions during Diet-Induced Obesity. *Cell Reports*. 2017; 20(13): 3149–61.
148. Jung S-B, Choi MJ, Ryu D, Yi H-S, Lee SE, Chang JY, et al. Reduced oxidative capacity in macrophages results in systemic insulin resistance. *Nature Communications*. 2018; 9(1): 1551.
149. Odegaard JI, Ricardo-Gonzalez RR, Goforth MH, Morel CR, Subramanian V, Mukundan L, et al. Macrophage-specific PPAR γ controls alternative activation and improves insulin resistance. *Nature*. 2007; 447(7148): 1116–20.
150. Lee YS, Li P, Huh JY, Hwang IJ, Lu M, Kim JI, et al. Inflammation is necessary for long-term but not short-term high-fat diet-induced insulin resistance. *Diabetes*. 2011; 60(10): 2474–83.
151. Patsouris D, Li P-P, Thapar D, Chapman J, Olefsky JM, Neels JG. Ablation of CD11c-Positive Cells Normalizes Insulin Sensitivity in Obese Insulin Resistant Animals. *Cell Metabolism*. 2008; 8(4): 301–9.
152. Aouadi M, Tencerova M, Vangala P, Yawe JC, Nicoloso SM, Amano SU, et al. Gene silencing in adipose tissue macrophages regulates whole-body metabolism in obese mice. *Proceedings of the National Academy of Sciences of the United States of America*. 2013; 110(20): 8278–83.
153. Aouadi M, Vangala P, Yawe JC, Tencerova M, Nicoloso SM, Cohen JL, et al. Lipid storage by adipose tissue macrophages regulates systemic glucose tolerance. *American Journal of Physiology-Endocrinology and Metabolism*. 2014; 307(4): E374–83.
154. Johnson AR, Qin Y, Cozzo AJ, Freerman AJ, Huang MJ, Zhao L, et al. Metabolic reprogramming through fatty acid transport protein 1 (FATP1) regulates macrophage inflammatory potential and adipose inflammation. *Molecular Metabolism*. 2016; 5(7): 506–26.
155. Flynn MC, Pernes G, Lee MKS, Nagareddy PR, Murphy AJ. Monocytes, macrophages, and metabolic disease in atherosclerosis. *Frontiers in Pharmacology*. 2019; 10:666.

156. "The Diabetes Control and Complications Trial/Epidemiology of Diabetes Interventions and Complications (DCCT/EDIC) Study Research Group." *Intensive Diabetes Treatment and Cardiovascular Disease in Patients with Type 1 Diabetes*. *New England Journal of Medicine*. 2005; 353(25): 2643–53.
157. Carey IM, Critchley JA, Dewilde S, Harris T, Hosking FJ, Cook DG. Risk of infection in type 1 and type 2 diabetes compared with the general population: A matched cohort study. *Diabetes Care*. 2018; 41(3): 513–21.
158. Critchley JA, Carey IM, Harris T, DeWilde S, Hosking FJ, Cook DG. Glycemic control and risk of infections among people with type 1 or type 2 diabetes in a large primary care cohort study. *Diabetes Care*. 2018; 41(10): 2127–35.
159. McGovern AP, Hine J, de Lusignan S. Infection risk in elderly people with reduced glycaemic control. *The Lancet Diabetes and Endocrinology*. 2016; 4(4): 303–4.
160. Dooley KE, Chaisson RE. Tuberculosis and diabetes mellitus: convergence of two epidemics. *The Lancet Infectious Diseases*. 2009; 9(12): 737–46.
161. Langley G, Hao Y, Pondo T, Miller L, Petit S, Thomas A, et al. The Impact of Obesity and Diabetes on the Risk of Disease and Death due to Invasive Group A Streptococcus Infections in Adults. *Clinical Infectious Diseases*. 2016; 62(7): 845–52.
162. Singh AK, Gupta R, Ghosh A, Misra A. Diabetes in COVID-19: Prevalence, pathophysiology, prognosis and practical considerations. *Diabetes and Metabolic Syndrome: Clinical Research and Reviews*. 2020; 14(4): 303–10.
163. Popkin BM, Du S, Green WD, Beck MA, Algaith T, Herbst CH, et al. Individuals with obesity and COVID-19: A global perspective on the epidemiology and biological relationships. *Obesity Reviews*. 2020; 21(11):e13128.
164. Zhou Y, Chi J, Lv W, Wang Y. Obesity and diabetes as high-risk factors for severe coronavirus disease 2019 (Covid-19). *Diabetes/Metabolism Research and Reviews*. 2020; 37(2):e3377.
165. Kruglikov IL, Shah M, Scherer PE. Obesity and diabetes as comorbidities for COVID-19: Underlying mechanisms and the role of viral–bacterial interactions. *eLife*. 2020; 9: 1–21.
166. Stienstra R, Netea-Maier RT, Riksen NP, Joosten LAB, Netea MG. Specific and Complex Reprogramming of Cellular Metabolism in Myeloid Cells during Innate Immune Responses. *Cell Metabolism*. 2017; 26(1): 142–56.
167. Chawla A, Nguyen KD, Goh YPS. Macrophage-mediated inflammation in metabolic disease. *Nature reviews Immunology*. 2011; 11(11): 738–49.



Glycolytic activity in human immune cells: inter-individual variation and functional implications in healthy subjects and patients with type 1 diabetes

Xanthe A.M.H. van Dierendonck^{1,2}, Frank Vrieling², Martin Jaeger¹, Anna W.M. Janssen¹, Anneke Hijmans¹, Mihai G. Netea^{1,3}, Cees J. Tack¹ and Rinke Stienstra^{1,2}

¹Department of Internal Medicine (463) and Radboud Institute for Molecular Life Sciences, Radboud University Medical Center, Nijmegen, the Netherlands

²Division of Human Nutrition and Health, Wageningen University, Wageningen, the Netherlands

³Department for Genomics and Immunoregulation, Life and Medical Sciences Institute (LIMES), University of Bonn, Bonn, Germany

Manuscript in preparation

Abstract

Immune cell metabolism has widely been recognized as a crucial driver of immune cell function. Particularly an increase in aerobic glycolysis is a robust and consistent hallmark of metabolic rewiring, enabling a rapid immune response toward pathogens. Innate immune cells play a key role in the early recognition of pathogens. The release of cytokines is one of the most important mechanisms in the innate immune response. Interestingly, large inter-individual differences can be found in the magnitude of this cytokine response. In patients with diabetes mellitus, impaired immune responses lead to a chronic inflammatory state, which could contribute to the development of diabetes-associated complications. The hyperglycemic microenvironment associated with diabetes mellitus may play a role in driving aberrations in the innate immune cell response. Here, we explore how increased aerobic glycolysis relates to the inter-individual variation in immune responses, and whether this association is altered in patients with type 1 diabetes mellitus. Our results suggest a robust association between lactate production and the concentrations of cytokines, with the strongest association for the production of IL-1RA. Based on the relative production of lactate, distinct clusters of responders could be identified, reflecting glycolytic flexibility. In patients with diabetes mellitus, a diminished correlation was found between lactate and IL-6 production, and the associations following stimulation with *S. aureus* were attenuated.

Introduction

Intracellular metabolism has been increasingly recognized as a key regulator of immune cell function [1–3]. This has been illustrated by the observation that a well-orchestrated immune response toward different pathogens is accompanied by specific metabolic rewiring in immune cells [4]. In particular, a metabolic shift from oxidative phosphorylation to aerobic glycolysis, also known as the Warburg effect [5], is seen as a hallmark for immune cell activation, both in the innate [6–8] and adaptive arm [9–12] of host defence. In innate immune cells, the upregulation of aerobic glycolysis enables the cell to fuel key processes, including differentiation and inflammatory activation [8,13]. Aerobic glycolysis comprises the conversion of glucose into pyruvate, followed by conversion of pyruvate into lactate, which is considered the end product of glycolysis and is subsequently secreted by the cell. Direct metabolism of pyruvate into lactate enables the cell to rapidly increase the rate of adenosine triphosphate (ATP) production at the cost of a lower total ATP yield, with pyruvate being diverted from the tricarboxylic acid (TCA) cycle [14]. Simultaneously, this process accommodates the accumulation of TCA cycle intermediates that contribute to inflammatory signalling [15,16].

Inhibition of glycolytic metabolic reprogramming in innate immune cells, such as monocytes and macrophages, can directly interfere with the activation of inflammation and the response toward different pathogen-associated molecular patterns (PAMPs). This process is best illustrated by altering the production and release of cytokines through specific modulation of the glycolytic route. For instance, pre-treating inflammatory macrophages with the glycolytic inhibitor 2-deoxyglucose (2-DG) reduced the expression and production of IL-1 β [17–19]. Interestingly, treatment with 2-DG also reveals a certain specificity in the association between glycolytic metabolism and cytokine production, since the production of TNF α generally seems unaffected by glycolytic inhibition [18,19].

Within human populations, large variations exist in the production of cytokines: one of the most important drivers of the host immune response. These variations are established by a variety of different host-related factors, including genetic predisposition, gut microbiome composition and environmental factors [20–25]. Whether variations exist in the capacity of immune cells to mount glycolytic metabolism and what factors may influence glycolysis in immune cells remains to be investigated. Since metabolism is a crucial determinant of immune cell function, potential differences in aerobic glycolysis of innate immune cells would serve to explain the observed variations in immune responses between individuals.

Metabolic disorders, such as diabetes mellitus, are often linked to dysregulated immune responses and a chronic, low-grade inflammatory state of the body [26]. The chronic inflammatory state may increase cardiovascular risk on the one hand, while defective responsiveness to pathogens will result in a higher susceptibility to infection on the other hand [27–30]. Since cellular metabolism is an important driver of the innate inflammatory response, signals that can influence cellular metabolism will ultimately also drive immune function. In patients with diabetes mellitus who suffer from chronic hyperglycemia [31], immune cells reside in a different extracellular environment that may play a pivotal role in determining inflammatory responses [31,32]. These hyperglycemic conditions could impact on the metabolic status of circulating innate immune cells, thereby driving changes in their inflammatory responses. For instance, a high glycemic burden may increase the availability of glucose, inducing a pro-inflammatory transcriptional signature in circulating monocytes [33].

The majority of studies performed in the field of immunometabolism to date have focused on the effects of specific metabolites in murine systems. Although these studies clarify important molecular mechanisms underlying immunometabolic rewiring, findings are difficult to extrapolate to human populations. Furthermore, large-scale cohorts exploring the role of cellular metabolism in driving differential immune responses in humans have been lacking.

In the current study, we explored the importance of aerobic glycolysis for the innate immune response to different PAMPs in cohorts of healthy subjects and patients with type 1 diabetes mellitus (T1DM). These cohorts are part of the Human Functional Genomics Project, which aims to study inter-individual variations of immune responses in humans [34]. Using lactate as a marker for glycolytic rate [35], we determined the relationship between lactate production and secretion of important cytokines after *ex vivo* stimulation of circulating immune cells with different PAMPs. We mapped inter-individual variations in glycolytic activation of monocytes and defined subsequent contribution to functional responses in healthy subjects. We also studied whether the association between glycolysis and immune cell function in healthy individuals was altered in patients with T1DM. Our results suggest specificity regarding both cytokines and PAMPs in the association between the production of lactate and different cytokines, which is slightly altered in patients with T1DM.

Results

A schematic overview of the study setup is presented in **Figure 1**. Peripheral blood mononuclear cells (PBMCs) were isolated from healthy volunteers and patients with T1DM and subsequently stimulated with the Toll-like receptor (TLR)-4 ligand lipopolysaccharide (LPS), TLR-2 ligand Pam3CysK4 (Pam3Cys), heat-killed *Staphylococcus aureus* (*S. aureus*) or heat-killed *Candida albicans conidia* (*C. albicans*) for 24 hours. These stimuli were chosen to include a broad array of synthetic and heat-killed PAMPs, reflecting bacterial or fungal-induced immune responses.

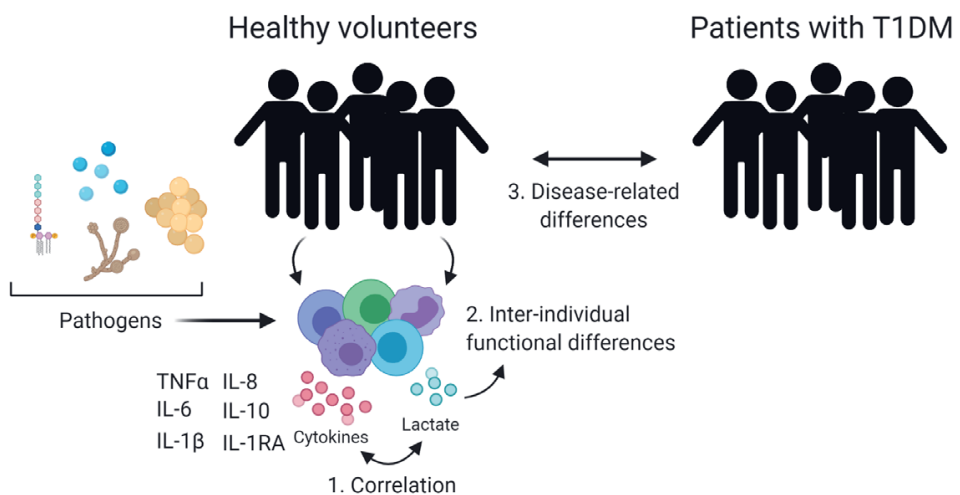


Figure 1. Overview of the study.

Peripheral blood mononuclear cells (PBMCs) were isolated from healthy volunteers and patients with type 1 diabetes mellitus. After isolation, PBMCs were treated with RPMI (non-treated control), LPS, Pam3Cys, *S. aureus* or *C. albicans* for 24 hours. The production of lactate was measured as a marker for aerobic glycolysis, and cytokines (TNF α , IL-6, IL-1 β , IL-8, IL-10 and IL-1RA) were determined as an indication of the immune response.

Pathogenic stimulation leads to a robust increase in the production of lactate and cytokines

We first assessed the host characteristics of healthy individuals (**Supplemental Figure 1A**) and the production of lactate after pathogenic stimulation. Although the production of lactate at baseline and after stimulation varied considerably among individuals, it robustly increased after all pathogenic stimulations compared to untreated PBMCs (RPMI) (**Figure 2A**). This is in line with the well-established increase in glycolytic rate of immune cells upon activation [5], which supports functional changes in the cells, including cytokine release [18,36]. The production of IL-1 β , IL-6, TNF α , IL-10, IL-8 and IL-1RA was increased upon stimulation (**Figure 2B**), with each stimulus leading to a different pattern in cytokine

secretion. The large range in the production of lactate and cytokines could be indicative of significant inter-individual variation both in immune effector function and metabolism. Because glycolysis and immune cell function are closely intertwined, we next investigated the association between lactate and cytokine production for all pathogenic stimuli. The results (shown in **Figure 2C**) indicate that the positive association between lactate and cytokine production is cytokine-specific across different stimuli and generally seems stronger for IL-8 and IL-1RA. Indeed, different stimuli lead to specific relationships between lactate and cytokine production, where Pam3Cys and *S. aureus* often elicit the strongest associations, whereas the least strong associations are induced by *C. albicans* (**Figure 2C**).

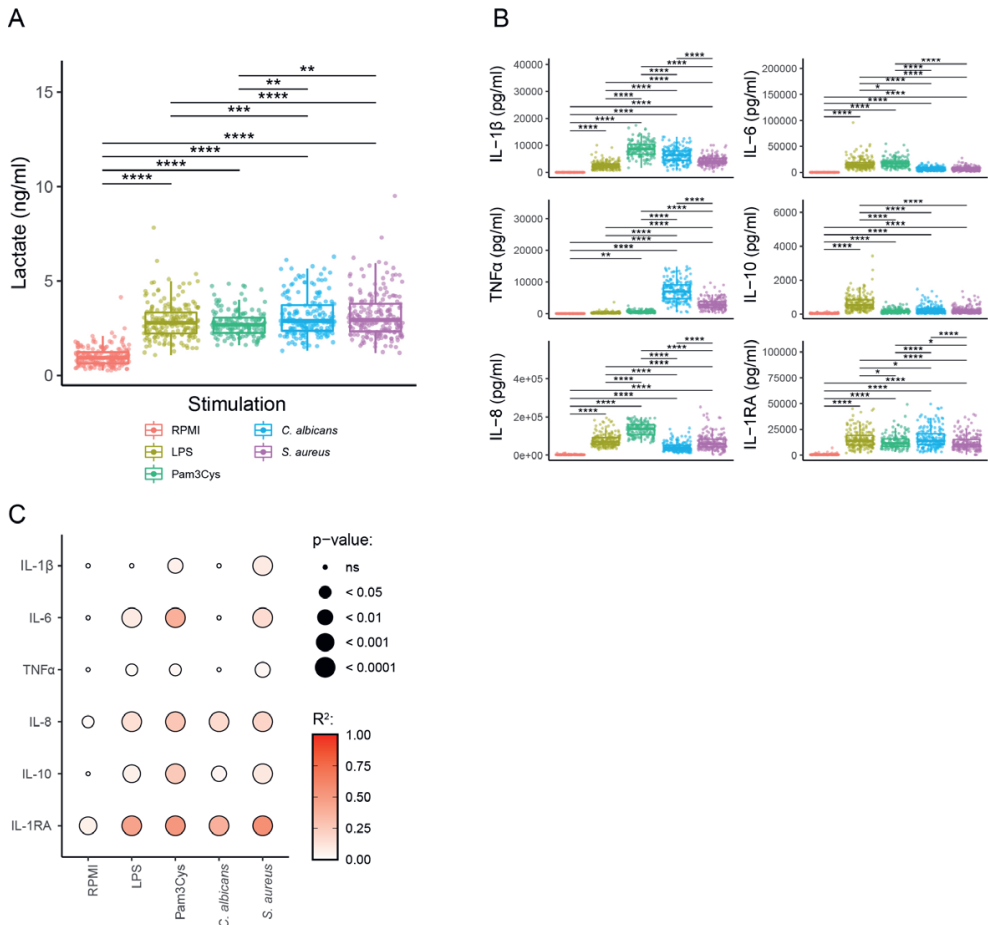


Figure 2. Pathogenic stimulation robustly increases the production of both lactate and cytokines in parallel.

PBMCs were isolated from healthy volunteers and treated with either RPMI (non-treated control), LPS (100 ng/mL), Pam3Cys (10 μ g/mL), *S. aureus* (1×10^6 /mL) or *C. albicans* (1×10^6 /mL) for 24 hours. The production of lactate (**A**) and IL-1 β , IL-6, TNF α , IL-10, IL-8 and IL-1RA (**B**) were determined. (**C**) R^2 and p -value of the correlation

between the production of lactate and each cytokine after each stimulus. LPS: lipopolysaccharide. * $p < 0.05$, ** $p < 0.01$, *** $p < 0.001$, **** $p < 0.0001$

The production of lactate by PBMCs after pathogenic stimulation is affected by host characteristics

Within the PBMC fraction, monocytes are potent producers of TNF α , IL-1 β , IL-6 and IL-8 [37]. Since innate immune responses are often most acutely regulated, we assumed that monocytes were the cell population that was largely responsible for the concentrations of lactate and cytokines measured in supernatants after 24 h. Variations in monocyte numbers between individuals may therefore explain part of the variation in lactate production. Additionally, other host factors such as age, BMI, and gender, known to determine host immune response [25], could also impact on the correlation between lactate and cytokine production. To explore whether these host characteristics could explain the inter-individual differences in the glycolytic rate of immune cells, we performed linear regression of lactate levels versus the percentage of monocytes (**Figure 3A**), age (**Figure 3B**), BMI (**Figure 3C**), and gender (**Figure 3D**) we found that age, BMI and gender only showed a minor impact, whereas the percentage of monocytes was an important determinant of lactate production by PBMCs across all stimulations, confirming their importance in lactate production. Therefore, the correlations between lactate and cytokine production could be driven by inter-individual variations in the percentage of monocytes in PBMCs used for *ex vivo* stimulations.

The correlation between lactate production and cytokine production is cytokine- and stimulus-specific

To determine intrinsic differences in lactate and cytokine responses between individuals, separate mixed models were fitted for each cytokine-stimulation combination, for which host factors (including the percentage of monocytes) were added as covariates in a stepwise fashion to evaluate their individual impact on model parameters (**Supplemental Figure 2**). Since the included host factors all displayed a minor impact on the model parameters, all were included as covariates in the final model to account for their influence. Subsequently, regression coefficients (slopes) and associated p -values were extracted for all covariates from each individual model to compare their relative contribution to the production of IL-1 β , IL-6, TNF α , IL-10, IL-8 and IL-1RA. For all pathogenic stimuli, lactate production was the most relevant indicator for the production of several cytokines (**Figure 4A**). Other host factors sporadically displayed significant associations for specific cases, such as an observed inverse relationship between age and production of IL-1 β , IL-6 and TNF α after LPS stimulation, or the specific association between monocyte percentages and IL-1RA levels (**Figure 4A**). When focusing in detail on the correlation between lactate

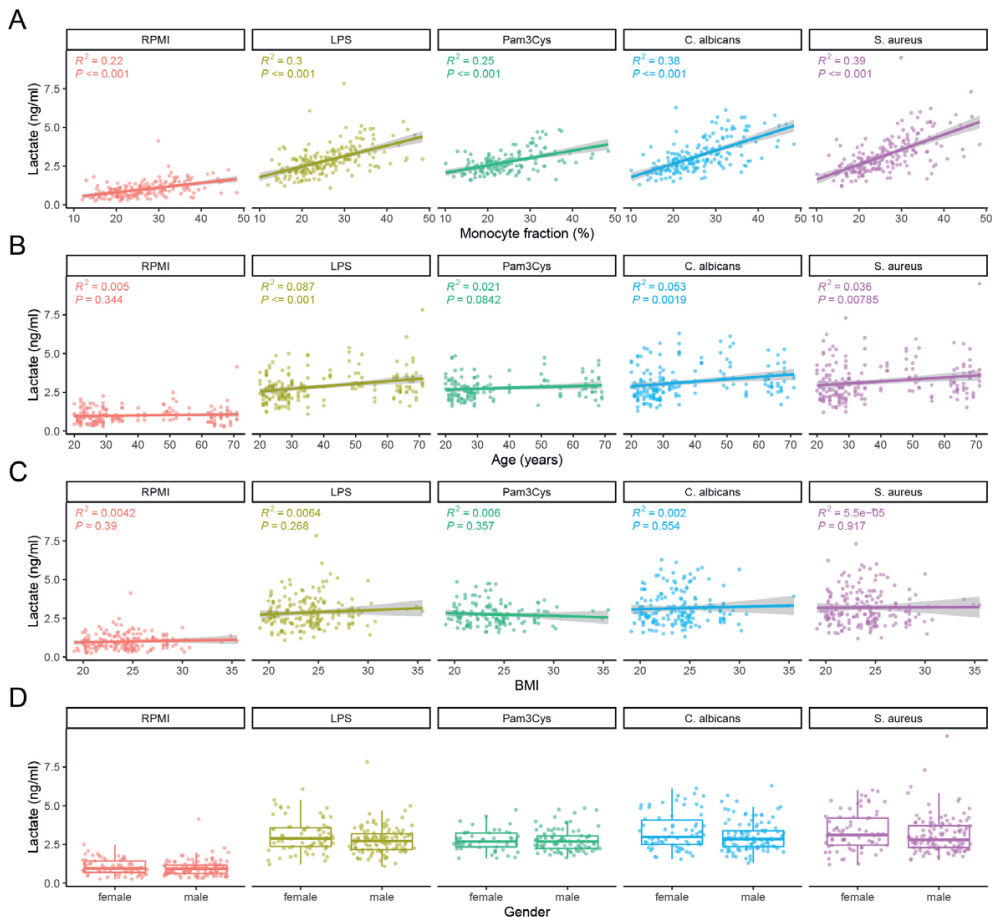


Figure 3. The associations between lactate production and host characteristics.

PBMCs were isolated from healthy volunteers and treated with either RPMI (non-treated control), LPS (100 ng/mL), Pam3Cys (10 μ g/mL), *S. aureus* (1×10^6 /mL) or *C. albicans* (1×10^6 /mL) for 24 hours. The production of lactate was plotted against the percentage of monocytes (A), age (B) and BMI (C) and gender (D). LPS: lipopolysaccharide; BMI: Body Mass Index.

and cytokine production in the adjusted model, we observed that lactate showed a significant positive correlation with the production of several cytokines for the majority of the pathogenic stimuli (Figure 4B). However, the strength and significance of the correlation varied, depending on specific cytokines and stimuli. Interestingly, these data were largely congruent with the uncorrected results in Figure 2C, although the strength of the associations between lactate and cytokine production diminished for IL-1 β and TNF α and increased for IL-6. For IL-1 β , the correlation between lactate is only significant after stimulation with *S. aureus*. IL-6 responses are significantly correlated to lactate for all stimuli, with the strongest association for Pam3Cys and LPS. Of all cytokines, the production of

TNF α was least significantly correlated to lactate production, only after stimulation with *S. aureus*. IL-10 production was significantly correlated to lactate production after all stimuli, except *C. albicans*, and the strongest correlation can be seen for LPS. The production of IL-8 was correlated to lactate production for all stimuli, with the strongest correlations for Pam3Cys, LPS and *S. aureus*. Similarly, IL-1RA production was also significantly correlated to lactate production after all stimuli, with strong correlations found after each stimulus. *C. albicans* seems to be the stimulus that leads to the weakest correlations between cytokine and lactate production (**Figure 4B**). In general, the relationship between lactate and cytokine production seems partly cytokine-specific, with the strongest correlations for IL-6, IL-10, IL-8 and IL-1RA. On the other hand, the relationship between cytokine and lactate production also shows clear specificity for different stimuli, where stimulation with *S. aureus* most often elicits a significant relationship between the two parameters.

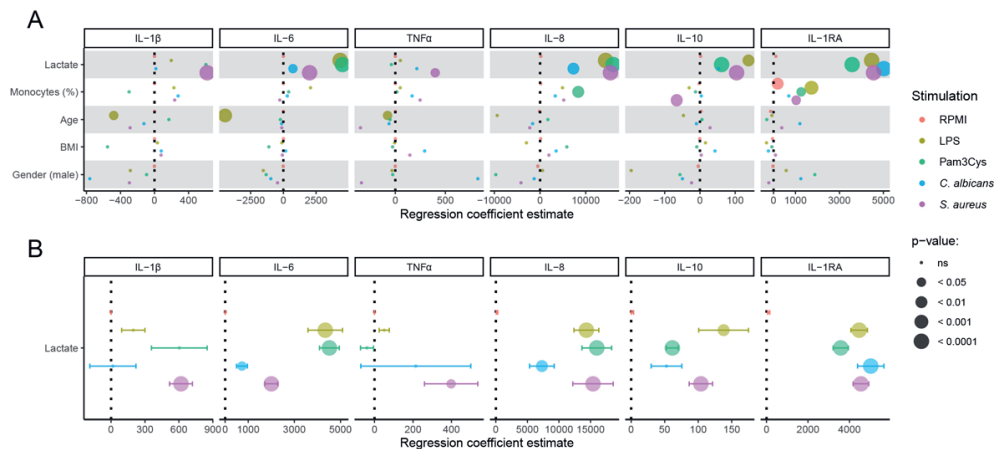


Figure 4. The increase of lactate and cytokine secretion after pathogenic stimulation is predominantly cytokine-specific.

PBMCs were isolated from healthy volunteers and treated with either RPMI (non-treated control), LPS (100 ng/mL), Pam3Cys (10 μ g/mL), *S. aureus* (1×10^6 /mL) or *C. albicans* (1×10^6 /mL) for 24 hours. The relationship between lactate, host factors and cytokine secretion was explored by fitting separate mixed models for each combination of cytokine/stimulation, including the percentage of monocytes, age, BMI and gender as covariates (scaled) (**A**). The correlation between the production of lactate with the production of each cytokine was determined for all stimuli as the regression coefficient estimate (**B**). LPS: lipopolysaccharide; BMI: Body Mass Index. *P*-values were adjusted for multiple testing by FDR correction.

Clustering of subjects based on inter-individual differences in lactate production reveals the existence of high- and low-responders

The measured lactate concentrations shown in **Figure 2A** show that lactate production of immune cells varies between individuals. To explore potential underlying causes and functional consequences, we aimed to identify group patterns of different glycolytic

responders based on relative lactate response. Using k-means clustering, data was partitioned into three groups representing between-subject differences in lactate production after the different stimuli (**Figure 5A**). The identified clusters suggest the existence of high- (red), intermediate- (green), and low- (blue) responders in the relative production of lactate after pathogenic stimuli (**Figure 5B**). Indeed, when plotting the production of cytokines for each of the three clusters after treatment with different stimuli, the production of cytokines followed this high, intermediate and low pattern after pathogenic stimulation (**Figure 5C**). Especially the differences in cytokine production between the high- and low-responding group were distinct, with significant differences for IL-1RA after stimulation with LPS; for IL-1 β and IL-8 after stimulation with Pam3Cys; for IL-1RA after stimulation with *C. albicans*; and for IL-6, IL-8, IL-10 and IL-1RA after stimulation with *S. aureus*. Between the intermediate- and low-responding group, differences were also well-defined, reaching significance for the production of IL-8 and IL-1RA after stimulation with LPS; for IL-6, IL-8, IL-10 and IL-1RA after stimulation with Pam3Cys; for IL-1RA after stimulation with *C. albicans*; and for IL-6, IL-8 and IL-1RA after stimulation with *S. aureus*. Differences between the high- and intermediate-responding group were less evident, where only the production of IL-1RA was significantly different after stimulation with *S. aureus*, although this could partly be due to lack of power.

Although host factors such as age, gender and BMI were seen to play minimal roles in the association between lactate and cytokine production, we next assessed their relevance for the formation of the clusters reflecting relative lactate responses. The formation of these clusters could not be convincingly explained by the host factors that were accounted for in the model, although univariate plotting of host factors did still reveal the importance of monocyte frequency in these clusters, and revealed a non-significant skewing toward a lower age for the low-responding group (**Supplemental Figure 3A**). Although the observed clusters seem to predict the magnitude of the functional response through the production of several cytokines, they likely represent healthy variations in the upregulation of aerobic glycolysis after immune cell activation, reflecting glycolytic flexibility.

The relationships between cytokine and lactate production are altered in patients with T1DM compared with healthy subjects

Diabetes mellitus is a metabolic disease that is known to associate with aberrated innate immune responses. Monocytes in patients with T1DM with high glycemic burden show basal hyperinflammatory gene signatures, but inadequate inflammatory responses upon pathogenic stimulation. Increased glycolysis may provide an explanation for these aberrations [33]. Therefore, we next sought to explore whether the observed associations

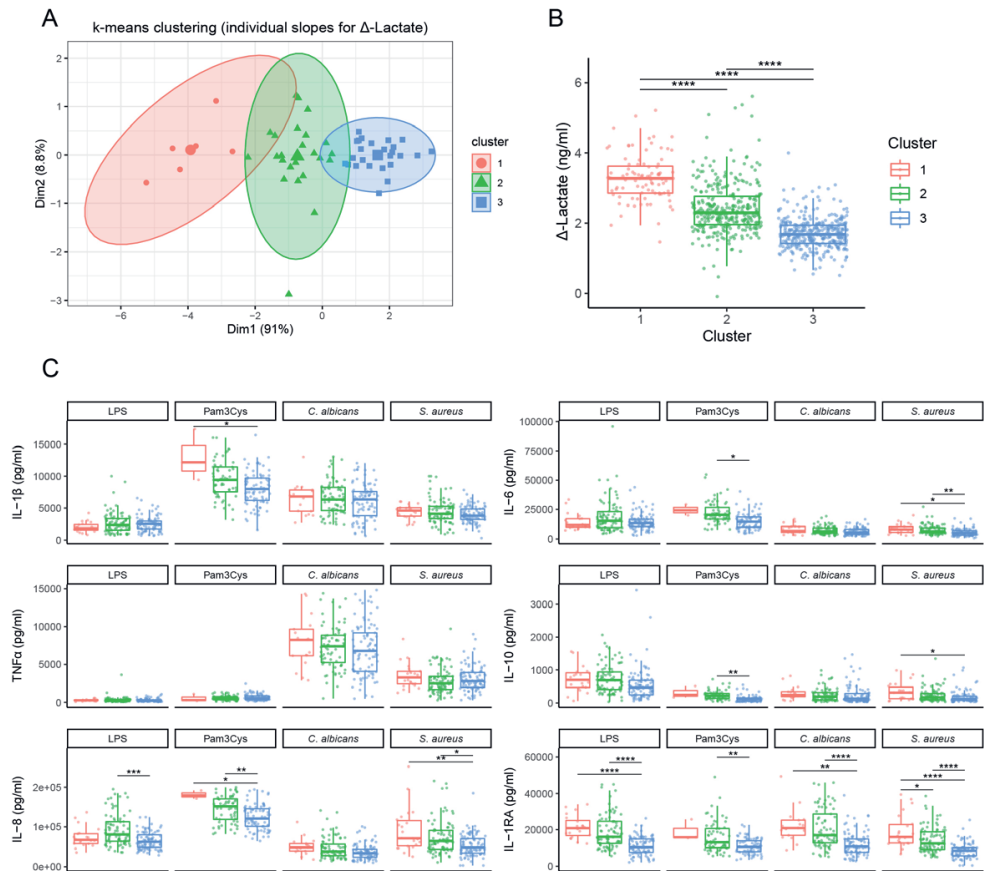


Figure 5. Clustering inter-individual lactate production reveals the existence of high- and low-responders.

A random slope model was fitted on all samples, and individual slopes of the effect of stimulation on delta lactate production were extracted for each subject. Extracted slopes were subsequently used for k-means clustering of subjects into three clusters (**A**). The delta of the lactate response (**B**) and the production of IL-1 β , IL-6, TNF α , IL-10, IL-8, and IL-1RA (**C**) was plotted for each cluster. LPS: lipopolysaccharide. * $p < 0.05$, ** $p < 0.01$, *** $p < 0.001$, **** $p < 0.0001$

between lactate and cytokine production in healthy subjects were altered in patients with T1DM. The production of lactate was plotted against the percentage of monocytes (**Supplemental Figure 4A**), age (**Supplemental Figure 4B**), BMI (**Supplemental Figure 4C**) and gender (**Supplemental Figure 4D**) as a first exploration of the existent associations. Next, these parameters were included as covariates in a multiple linear regression model for each combination of cytokine and stimulation. Regression coefficient estimates (slopes) and associated p -values were subsequently extracted for each covariate (**Figure 6A**).

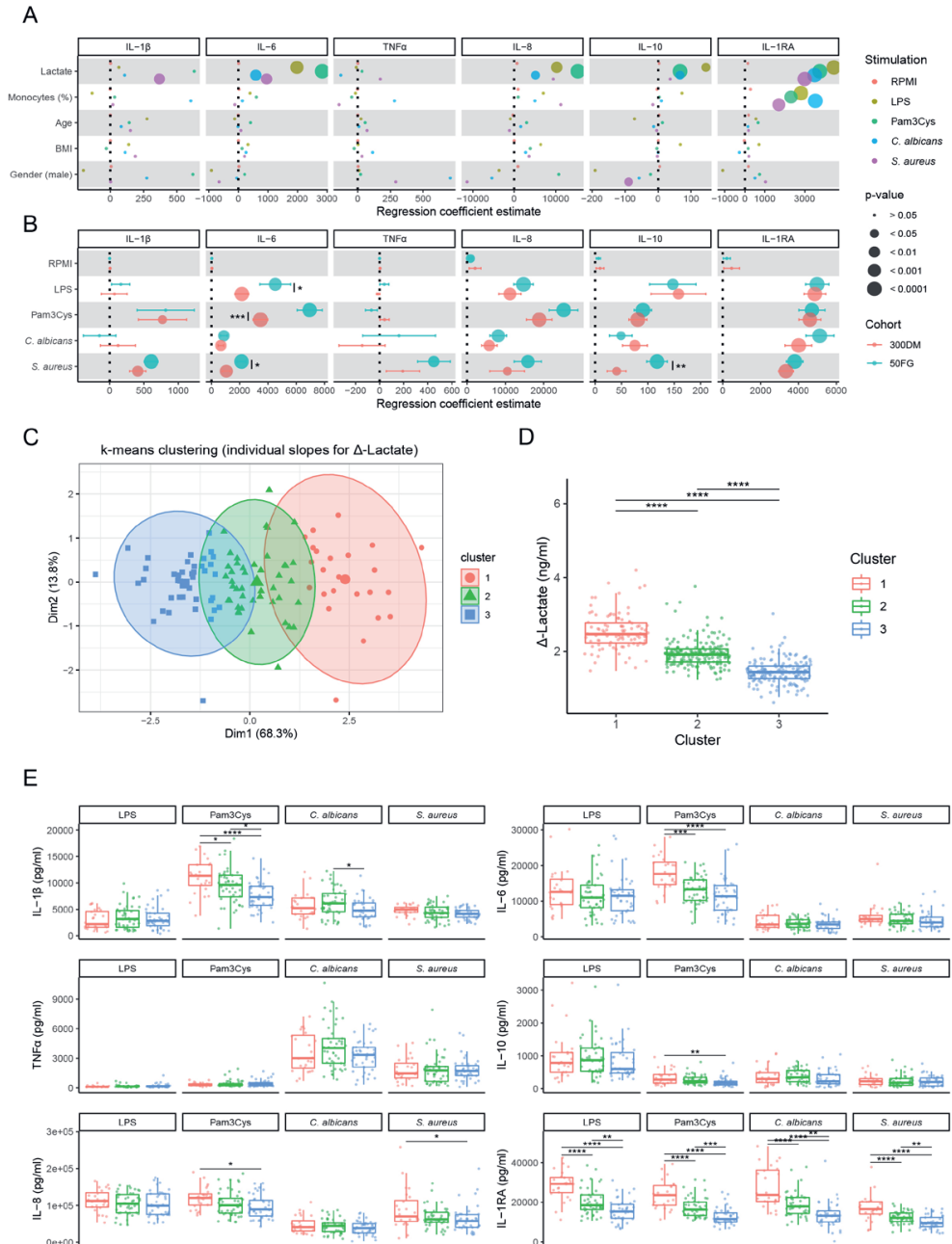


Figure 6. The relationships between subject characteristics or cytokine production and lactate production are altered in patients with T1DM compared with healthy subjects.

PBMCs were isolated from patients with T1DM and treated with either RPMI (non-treated control), LPS (100 ng/mL), Pam3Cys (10 μ g/mL), *S. aureus* (1×10^6 /mL) or *C. albicans* (1×10^6 /mL) for 24 hours. The relationship between lactate, host factors and cytokine secretion was explored by fitting separate multiple linear regression

models for each combination of cytokine/stimulation, including the percentage of monocytes, age, BMI and gender as covariates (scaled) (A). From each individual model, the regression coefficient (slope) for lactate was extracted and directly compared with those extracted from the mixed model fitted for healthy subjects in **Figure 4B** (not scaled) (B). K-means clustering was performed for the individual slopes based on the delta of the lactate response for all subjects, corrected for the percentage of monocytes, gender, BMI and age (C) and the concentrations of lactate (D) and IL-1 β , IL-6, TNF α , IL-10, IL-8, and IL-1RA (E) were plotted for each cluster. LPS: lipopolysaccharide; BMI: Body Mass Index. * $p < 0.05$, ** $p < 0.01$, *** $p < 0.001$, **** $p < 0.0001$

In patients with T1DM, we observed a new inverse relationship between gender and IL-10 production after *S. aureus* stimulation, whereas the relationship between age and IL-1 β , IL-6 or TNF α production was not reproduced in this population (**Figure 6A**), arguing that the presence of diabetes supersedes the impact of age. When directly comparing the relationship between lactate and cytokine production in healthy subjects versus patients with T1DM (**Figure 6B**), it can be seen that the correlations observed for IL-10 or IL-6 and lactate production after stimulation with *S. aureus* were significantly attenuated, and the relationship with lactate production and TNF α disappeared (**Figure 6B**). Additionally, the relationship between IL-6 and lactate production was significantly weaker for patients with T1DM after Pam3Cys and LPS stimulation (**Figure 6B**). Based on these observed changes in the relationship between lactate and cytokine production compared with the healthy cohort, the relationship between glycolytic metabolism and function of innate immune cells seems to be partly attenuated in patients with T1DM.

Following the clustering approach that led to the identification of high-, intermediate- and low-responders in lactate production of healthy individuals, we used k-means clustering on the delta of the lactate response to identify similar groups in the patients with T1DM. Clustering led to the identification of distinct groups, differing in their lactate response to stimuli (**Figure 6C** and **D**). The relative lactate responses seemed to display a lower degree of variation compared with healthy subjects in **Figure 5B**, and similar patterns were found with univariate plotting of host factors, except for the distribution of age (**Supplemental Figure 3B**). When comparing the production of IL-1 β , IL-6, TNF α , IL-10, IL-8, and IL-1RA among the three clusters, patterns were found to be generally comparable to the clustering based on healthy subjects, although differences are present for specific cytokines or stimuli. Several significant differences found between clusters in healthy subjects after treatment with *S. aureus* were not found in patients with T1DM, for instance for the production of IL-6, IL-10 and IL-8 (**Figure 6E**). Similarly, several differences found in IL-8 production after LPS or Pam3Cys stimulation in the clusters based on healthy subjects were not significant in the clusters based on patients with T1DM (**Figure 6E**). In contrast, some of the T1DM-based clusters actually displayed stronger distinctions,

exemplified by the response to Pam3Cys, which results in significant differences between each of the groups for the production of IL-1 β , IL-6 and IL-1RA (**Figure 6E**). Furthermore, the differences between the high- and intermediate-responding groups seem more evident for IL-1RA after treatment with LPS or *C. albicans*, although there is a significant difference between the intermediate- and low-responding groups in the production of IL-1 β after *C. albicans*. In general, the clusters of high, intermediate, and low-responders in T1DM show less distinct differences in the production of cytokines after treatment with *S. aureus*, but more pronounced differences in the production of cytokines after treatment with Pam3Cys or *C. albicans*.

Discussion

In this study, we explored the link between the glycolytic response of stimulated immune cells and the cytokine production capacity in human volunteers, using lactate as a marker for glycolytic rate. Our data collectively confirm the robust link between upregulated aerobic glycolysis and increased cytokine production in immune cells from healthy subjects and patients with T1DM. Stimulation of immune cells by Pam3Cys or *S. aureus* elicited the strongest relationships between lactate and cytokine production in healthy subjects, and the production of IL-1RA was robustly linked to lactate production for all pathogenic stimuli. Although the inter-individual variation in lactate levels was relatively high, clustering analysis of individual stimuli-specific lactate responses resulted in the identification of distinct clusters which represented high, intermediate and low responders. The identification of these groups most likely represents the normal range of metabolic variation in immune responses between individuals but is still predictive of cytokine production. However, in patients with T1DM, the correlation between lactate and IL-6 production was found to be weaker compared with healthy individuals. Furthermore, the strength of the relationship between lactate and cytokine production elicited by *S. aureus* stimulation seemed to be attenuated. Although clustering of patients with T1DM resulted in similar identification of high, intermediate and low responders based on lactate production, metabolic variation in these groups could not be explained by age, gender or BMI.

The observed correlations between lactate and cytokine production are confirmative of previously found correlations between immune cell metabolism and function. Interestingly, the magnitude of this association seems to differ for various cytokines, but is also affected by the type of stimulus that induces immune cell activation. The specificity regarding cytokines is in line with earlier reports from *in vitro* studies demonstrating attenuated cytokine release after treatment with 2-DG. Hence, it seems that the production of some cytokines depends more on glycolysis compared with others. Interestingly, the production of IL-1 β , IL-6 and IL-10, but not TNF α , could be inhibited by the addition of 2-DG [18,38], which is in line with the results of this study. TNF α showed only a weak correlation with lactate production for all stimuli, demonstrating apparent independence of TNF α from glycolytic regulation.

The cytokine that was most unambiguously associated with lactate production in this study was IL-1RA. IL-1RA functions as an anti-inflammatory cytokine by binding the IL-1 receptor (IL-1R1/IL-R2), thereby acting as a natural antagonist for IL-1 α and IL-1 β in response to their production [39]. IL-1 β can exert large effects in low concentrations, and therefore

its secretion may be kept relatively limited, possibly impeding a strong association with lactate production. In comparison, the secretion of IL-1RA is several magnitudes higher, as a high molar ratio is needed to inhibit IL-1 bioactivity and is thus used as a surrogate marker for the biological effect of IL-1 β [39]. The consistent association of IL-1RA with lactate production may therefore underline that its production, or the production of the entire IL-1 cytokine family, is highly dependent on the upregulation of aerobic glycolysis.

In the specific association between cytokines and aerobic glycolysis, relative kinetics should be taken into account. Cytokines such as IL-1 β and TNF α are often upregulated relatively early in response to pathogens, whereas the production of IL-1RA starts in response to IL-1 β [39]. Because both lactate and cytokines were measured after 24 h, the correlation could be stronger for cytokines that still accumulate and did not yet pass the peak of their production. These kinetics may partly explain the stronger associations found for anti-inflammatory cytokines with lactate production, since their production starts in a later phase of the inflammatory response. Additionally, lactate itself can affect the production of certain cytokines and form a negative feedback loop toward the induction of glycolysis [40–43]. Furthermore, lactate may even specifically reduce the production of TNF α [42], possible also partly explaining the relative lack of association between lactate and TNF α production.

The associations between lactate and cytokine production seemed uniquely driven by different types of stimuli. The observed differences could potentially be explained by the various activation pathways that follow recognition of PAMPs by different Toll-like receptors (TLRs). TLRs play pivotal roles in the recognition of PAMPs by innate immune cells, leading to the activation of transcription factors that regulate specific immune responses, including the production of cytokines [44]. In this study, particularly the activation of immune cells with Pam3Cys or *S. aureus* led to strong associations between lactate and cytokine production. Both Pam3Cys and *S. aureus* are mainly recognized by TLR-1/2 [45–47]. Therefore, TLR-1/2-mediated recognition of both PAMPs could underly the observed strong associations between cytokine and lactate production, indicating that TLR-1/2-mediated recognition leads to similar upregulation of aerobic glycolysis and cytokine production. It is also possible that TLR1/2-mediated signalling is more dependent on aerobic glycolysis compared with TLR-4. Unpublished data from our group indeed suggests that LPS-mediated immune cell activation takes longer to activate glycolysis than P3C-mediated activation, further supporting a strong association between TLR-1/2-signalling and robust induction of aerobic glycolysis. Moreover, for the association of IL-1 β and lactate, TLR-1/2 ligands Pam3Cys and *S. aureus* are the only inducers, and the TLR-4 ligand LPS [48] is not able to induce a significant association. However, TLR-1/2-mediated

signalling by Pam3Cys and *S. aureus* does not always lead to identical associations, as can be seen by the stronger associations with lactate production that are induced by Pam3Cys stimulation for IL-6, IL-10 and IL-8. Similarly, *S. aureus* is the only stimulus that leads to a significant correlation between TNF α and lactate production, further underlining that the differences between stimuli cannot solely be explained by their TLR-mediated recognition.

The observed spread in lactate production indicates that large variations can also be found in the glycolytic metabolism of immune cells in human populations, alongside those in the production of cytokines. Furthermore, the observed associations between lactate and cytokine production suggest that the differences in aerobic glycolysis may partly explain the observed variations in immune responses between individuals. However, which host-related factors could be responsible for the differences in glycolytic metabolism in immune cells remains unknown. In order to elucidate these factors, we used clustering analysis to identify high, intermediate and low-responding individuals based on the delta of the lactate production after immune cell activation, reflective of their glycolytic flexibility. We investigated whether different patterns could be found within these clusters regarding monocyte count, gender, BMI, or age. Whereas the effect of gender, BMI or age did not seem to play an important role in the formation of the clusters, differences in monocyte numbers could be seen between the groups, which were also found in the uncorrected associations between lactate and cytokine prediction. This validates the assumption that a major fraction of the measured cytokines and lactate are indeed produced by monocytes. To investigate the intrinsic differences between individuals, we accounted for monocyte frequencies by including them as a covariate in the mixed models. However, although lactate production was found to be a better predictor for cytokine responses than the monocyte count using mixed models, it proved difficult to fully correct for the differences in monocyte populations in PBMCs in the formation of the producer clusters. Even after correcting for absolute monocyte count, a residual effect remains, which is potentially a biological intercellular amplifying effect driven by increased monocyte frequencies. Although using PBMC fractions better resemble the *in vivo* situation and circumvents laborious isolation steps, it would be advisable to isolate single cell populations to fully rule out the amplifying or dampening effects of variations in monocyte count in order to draw more specific conclusions.

Differences in the glycolytic metabolism of immune cells depend on a myriad of factors besides the ones investigated in the current study, such as genetic predispositions or differences in microbiome [20–25], environmental factors such as diet [49], or previous encounters with certain pathogens [50,51]. Likely, the involvement of epigenetic factors plays an important role, as these are increasingly found to be regulated by metabolic

pathways in immune cells [52–55]. Although the distinct groups in healthy individuals display differences in glycolytic flexibility and functional responses of their immune cells, all variations likely fall within the adequate and healthy range of immune responses to pathogens. Nevertheless, it is plausible to assume that consequences in disease susceptibility could be connected to the differences in responses of these groups. Therefore, future studies could focus on unravelling the possible immune-related consequences that correspond to each group.

Diabetes mellitus is generally associated with a chronic inflammatory state on the one hand, but an increased susceptibility to infections on the other hand [26–30]. Therefore, we investigated if the aforementioned relationships between lactate and cytokine production could be altered in patients with T1DM. Although many of the relationships between lactate and specific cytokines could be reproduced, the association between IL-6 and lactate was significantly diminished. Furthermore, a slightly decreased production of certain cytokines was found relative to the production of lactate, compared with healthy individuals. These results are in accordance with earlier work, where a decreased association between glycolysis and cytokine production was found in monocytes of patients with T1DM that have a high glycemic burden. These attenuated associations were linked to a more inflammatory phenotype of circulating monocytes, which led to a certain desensitization to *ex vivo* stimulation. This resulted in a higher glycolytic rate, but relatively lower production of cytokines [33]. A similar mechanism could underlie the general attenuation that was seen for the relationship between lactate and cytokine production in patients with T1DM in the current study. Especially the differential response to *S. aureus* may be disadvantageous for the host and could be related to the higher frequency of infections that is often associated with T1DM [27,28]. In the high-, intermediate- and low-responding clusters that were identified based on the relative glycolytic flexibility, the distinct differences in response to *S. aureus* also seemed to be attenuated among the different clusters. Interestingly, however, cytokine responses to other PAMPs, including Pam3Cys and *C. albicans*, showed a more profound distinction between the different groups of responders. This finding is intriguing, especially because patients with T1DM are often seen to be more susceptible to infection with *Candida* [56], and stimulation of monocytes from T1DM patients with Pam3Cys has revealed uncoupling of glycolysis and cytokine production before [33].

In the current study, we report that lactate production correlates robustly to the production of several cytokines across an array of different PAMPs. Therefore, in future cohort studies, lactate may be included as an easy and feasible additional measurement of innate immune cell activation and glycolytic flexibility. Furthermore, future studies could

focus on unravelling the possible causes and consequences of the high, intermediate and low-responding groups and whether these clusters can be found consistently among other (metabolic) diseases. If beneficial effects could be attributed to any of these groups, elucidating the responsible host factors could lead to the identification of (epi)genetic targets of immune cell metabolism, which could be modulated to obtain improved immune cell functioning.

Acknowledgements

We thank all the volunteers for their participation. The authors also thank Sanne Smeekens, Marije Doppenberg-Oosting, Clementine Verhulst, Lisa van de Wijer, Wouter van der Heijden and Lian van Meijel for their assistance during the setup of the cohorts; recruitment of study subjects or assistance during clinical visits. We thank Sanne Smeekens, Lisa van de Wijer, Wouter van der Heijden, Heidi Lemmers and Helga Dijkstra for assistance during experimental bench work; and Rob ter Horst for assistance during data processing.

Methods

Study population

The study was performed using two well-characterized, independent cohorts, which are both parts of the HFGP (www.humanfunctionalgenomics.org) and were recruited simultaneously. The 50FG cohort is a population-based cohort that consists of 56 healthy individuals with a Western European background and is a subset of the 500FG cohort [34]. The absence of diabetes in the 50FG cohort was based on self-report. The 300DM cohort consists of 239 patients with type 1 diabetes mellitus, selected from the outpatient clinic at the Radboud University Medical Centre, the Netherlands. The HFGP was approved by the Ethical Committee of Radboud University Nijmegen, the Netherlands (NL54214.091.15, 2015-1930 and NL42561.091.12, 2012-550). All participants gave written informed consent before participation, and experiments were conducted according to the principles expressed in the Declaration of Helsinki.

Isolation of peripheral blood mononuclear cells and *in vitro* stimulation

In each cohort, blood from the cubital vein of volunteers was collected in 10 mL EDTA tubes (Monoject), and the PBMC fraction was isolated by density centrifugation using Ficoll-Paque (Pharmacia Biotech), followed by three washes in phosphate-buffered saline. 5×10^5 PBMCs were plated in 96-well plates in 100 μ L Roswell Park Memorial Institute (RPMI) 1640 medium (Dutch modified) supplemented with gentamycin, L-glutamine and pyruvate. 100 μ L of either RPMI or RPMI containing LPS, Pam3Cys, heat-killed *Candida albicans* conidia or heat-killed *Staphylococcus aureus* was added to obtain a final concentration of 100 ng/mL LPS, 10 μ g/mL Pam3Cys, or 1×10^6 parts/mL of either *C. albicans* or *S. aureus*. Supernatants were collected after 24 hours and stored at -20°C until assayed.

Enzyme-linked immunosorbent assays (ELISA)

In cell supernatants, IL-1 β , IL-6, TNF α , IL-10, IL-8 and IL-1RA levels were measured using DuoSet sandwich ELISA kits (R&D Systems) according to manufacturer's instructions.

Lactate measurements

The produced concentrations of lactate were determined in cell supernatants using the conversion of lactate by lactate oxidase (Merck). The subsequent oxidation of the Amplex Red reagent (ThermoFisher Scientific) to resorufin via HRP (ThermoFisher Scientific) was measured as a fluorescent signal.

Statistical analysis

Data analysis was performed using R version 1.3.6 and RStudio version 1.2.1335. Samples with incomplete measurements for cytokines and lactate, or one of the two, were excluded before analysis. Delta lactate values were calculated by subtracting the baseline lactate production under control (RPMI) condition from the lactate induced by immune cell activation (if baseline measurement was available). Mixed-effects models of 50FG cohort samples were fitted and analyzed using the lme4 (version 1.1.23) [57] and lmerTest (version 3.1.2) [58] packages. Models included individual cytokines as dependent variables, a random intercept for each subject and the following covariates: Time + Lactate + Monocyte fraction + Age + BMI + Gender. For 300DM cohort samples, individual multiple linear regression models were fitted for each cytokine using the lm function from the stats package (version 3.6.1.) and included the following covariates: Lactate + Monocyte fraction + Age + BMI + Gender. Regression coefficient estimates (slopes) and associated p -values were subsequently extracted from individual models and plotted. Regression coefficients of 50DG and 300DM models were directly compared by Z-test [59]. To investigate interindividual variation in lactate responses, individual slopes were extracted per subject from a model which specified the stimulation as a predictor variable and delta lactate as a dependent variable. Subsequent k-means clustering on extracted slopes was performed using the factoextra package (version 1.0.7) [60]. Comparisons depicted in boxplots were tested for significance by Tukey's test with Holm correction. Where indicated, p -values were adjusted for multiple testing by False Discovery Rate (FDR). Plots were generated using ggplot2 (version 3.3.2) [61] and cowplot (version 1.1.0) [62].

References

Figure 1 was created with BioRender.com

1. Buck MD, Sowell RT, Kaech SM, Pearce EL. Metabolic Instruction of Immunity. *Cell*. 2017; 169(4): 570–86.
2. O'Neill LAJ, Kishton RJ, Rathmell J. A guide to immunometabolism for immunologists. *Nature Reviews Immunology*. 2016; 16(9): 553–65.
3. Makowski L, Chaib M, Rathmell JC. Immunometabolism: From basic mechanisms to translation. *Immunological Reviews*. 2020; 295(1): 5–14.
4. Lachmandas E, Boutens L, Ratter JM, Hijmans A, Hooiveld GJ, Joosten LAB, et al. Microbial stimulation of different Toll-like receptor signalling pathways induces diverse metabolic programmes in human monocytes. *Nature Microbiology*. 2016; 2: 16246.
5. Krawczyk CM, Holowka T, Sun J, Blagih J, Amiel E, DeBerardinis RJ, et al. Toll-like receptor-induced changes in glycolytic metabolism regulate dendritic cell activation. *Blood*. 2010; 115(23): 4742–9.
6. Galván-Peña S, Carroll RG, Newman C, Hinchey EC, Pålsson-McDermott E, Robinson EK, et al. Malonylation of GAPDH is an inflammatory signal in macrophages. *Nature Communications*. 2019; 10(338).
7. Rodríguez-Prados J-C, Través PG, Cuenca J, Rico D, Aragonés J, Martín-Sanz P, et al. Substrate Fate in Activated Macrophages: A Comparison between Innate, Classic, and Alternative Activation. *The Journal of Immunology*. 2010; 185(1): 605–14.
8. Jha AK, Huang SCC, Sergushichev A, Lampropoulou V, Ivanova Y, Loginicheva E, et al. Network integration of parallel metabolic and transcriptional data reveals metabolic modules that regulate macrophage polarization. *Immunity*. 2015; 42(3):419-30.
9. De Rosa V, Galgani M, Porcellini A, Colamatteo A, Santopaolo M, Zuchegna C, et al. Glycolysis controls the induction of human regulatory T cells by modulating the expression of FOXP3 exon 2 splicing variants. *Nature Immunology*. 2015; 16(11): 1174–84.
10. Chang CH, Curtis JD, Maggi LB, Faubert B, Villarino A V., O'Sullivan D, et al. XPosttranscriptional control of T cell effector function by aerobic glycolysis. *Cell*. 2013; 153(6): 1239.
11. Michalek RD, Gerriets VA, Jacobs SR, Macintyre AN, MacIver NJ, Mason EF, et al. Cutting Edge: Distinct Glycolytic and Lipid Oxidative Metabolic Programs Are Essential for Effector and Regulatory CD4 + T Cell Subsets . *The Journal of Immunology*. 2011; 186(6): 3299–303.
12. Wang R, Dillon CP, Shi LZ, Milasta S, Carter R, Finkelstein D, et al. The transcription factor Myc controls metabolic reprogramming upon T lymphocyte activation. *Immunity*. 2011; 35(6): 871–82.
13. Mills EL, Kelly B, Logan A, Costa ASH, Varma M, Bryant CE, et al. Succinate Dehydrogenase Supports Metabolic Repurposing of Mitochondria to Drive Inflammatory Macrophages. *Cell*. 2016; 167(2): 457-470.e13.
14. Pfeiffer T, Schuster S, Bonhoeffer S. Cooperation and competition in the evolution of ATP-producing pathways. *Science*. 2001; 292(5516): 504–7.
15. Harber KJ, de Goede KE, Verberk SGS, Meinster E, de Vries HE, van Weeghel M, et al. Succinate is an inflammation-induced immunoregulatory metabolite in macrophages. *Metabolites*. 2020; 10(9): 1–14.
16. Swain A, Bambouskova M, Kim H, Andhey PS, Duncan D, Auclair K, et al. Comparative evaluation of itaconate and its derivatives reveals divergent inflammasome and type I interferon

- regulation in macrophages. *Nature Metabolism*. 2020; 2(7): 594–602.
17. Izquierdo E, Cuevas VD, Fernández-Arroyo S, Riera-Borrull M, Orta-Zavalza E, Joven J, et al. Reshaping of Human Macrophage Polarization through Modulation of Glucose Catabolic Pathways. *The Journal of Immunology*. 2015; 195(5): 2442–51.
 18. Tannahill G, Curtis A, Adamik J, Palsson-McDermott E, McGettrick A, Goel G, et al. Succinate is a danger signal that induces IL-1 β via HIF-1 α . *Nature*. 2013; 496(7444): 238–42.
 19. Moon JS, Hisata S, Park MA, DeNicola GM, Rytter SW, Nakahira K, et al. MTORC1-Induced HK1-Dependent Glycolysis Regulates NLRP3 Inflammasome Activation. *Cell Reports*. 2015; 12(1): 102–15.
 20. Aguirre-Gamboa R, Joosten I, Urbano PCM, van der Molen RG, van Rijssen E, van Cranenbroek B, et al. Differential Effects of Environmental and Genetic Factors on T and B Cell Immune Traits. *Cell Reports*. 2016; 17(9): 2474–87.
 21. Schirmer M, Smeekens SP, Vlamakis H, Jaeger M, Oosting M, Franzosa EA, et al. Linking the Human Gut Microbiome to Inflammatory Cytokine Production Capacity. *Cell*. 2016; 167(4): 1125-1136.e8.
 22. Li Y, Oosting M, Deelen P, Ricaño-Ponce I, Smeekens S, Jaeger M, et al. Inter-individual variability and genetic influences on cytokine responses to bacteria and fungi. *Nature Medicine*. 2016; 22(8): 952–60.
 23. Li Y, Oosting M, Smeekens SP, Jaeger M, Aguirre-Gamboa R, Le KTT, et al. A Functional Genomics Approach to Understand Variation in Cytokine Production in Humans. *Cell*. 2016; 167(4): 1099-1110.e14.
 24. Bakker OB, Aguirre-Gamboa R, Sanna S, Oosting M, Smeekens SP, Jaeger M, et al. Integration of multi-omics data and deep phenotyping enables prediction of cytokine responses. *Nature Immunology*. 2018; 19(7): 776–86.
 25. ter Horst R, Jaeger M, Smeekens SP, Oosting M, Swertz MA, Li Y, et al. Host and Environmental Factors Influencing Individual Human Cytokine Responses. *Cell*. 2016; 167(4): 1111-1124.e13.
 26. Hotamisligil GS. Inflammation, metaflammation and immunometabolic disorders. *Nature*. 2017; 542(7640): 177–85.
 27. Carey IM, Critchley JA, Dewilde S, Harris T, Hosking FJ, Cook DG. Risk of infection in type 1 and type 2 diabetes compared with the general population: A matched cohort study. *Diabetes Care*. 2018; 41(3): 513–21.
 28. Critchley JA, Carey IM, Harris T, DeWilde S, Hosking FJ, Cook DG. Glycemic control and risk of infections among people with type 1 or type 2 diabetes in a large primary care cohort study. *Diabetes Care*. 2018; 41(10): 2127–35.
 29. Nathan DM, Bebu I, Braffett BH, Lachin JM, Orchard TJ, Cowie CC, et al. Risk factors for cardiovascular disease in type 1 diabetes. *Diabetes*. 2016; 65(5): 1370–9.
 30. Laakso M. Cardiovascular disease in type 2 diabetes from population to man to mechanisms: The Kelly West award lecture 2008. *Diabetes Care*. 2010; 33(2): 442–9.
 31. Caputa G, Castoldi A, Pearce EJ. Metabolic adaptations of tissue-resident immune cells. *Nature Immunology*. 2019; 20(7): 793–801.
 32. Norata GD, Caligiuri G, Chavakis T, Matarese G, Netea MG, Nicoletti A, et al. The Cellular and Molecular Basis of Translational Immunometabolism. *Immunity*. 2015; 43(3): 421-434.
 33. Thiem K, van Dierendonck XAMH, Janssen AWM, Boogaard JP, Riksen NP, Tack CJ, et al. A High Glycemic Burden Relates to Functional and Metabolic Alterations of Human Monocytes in Patients with Type 1 Diabetes. *Diabetes*. 2020; 69(12): 2735-2746.
 34. Netea MG, Joosten LAB, Li Y, Kumar V, Oosting M, Smeekens S, et al. Understanding human

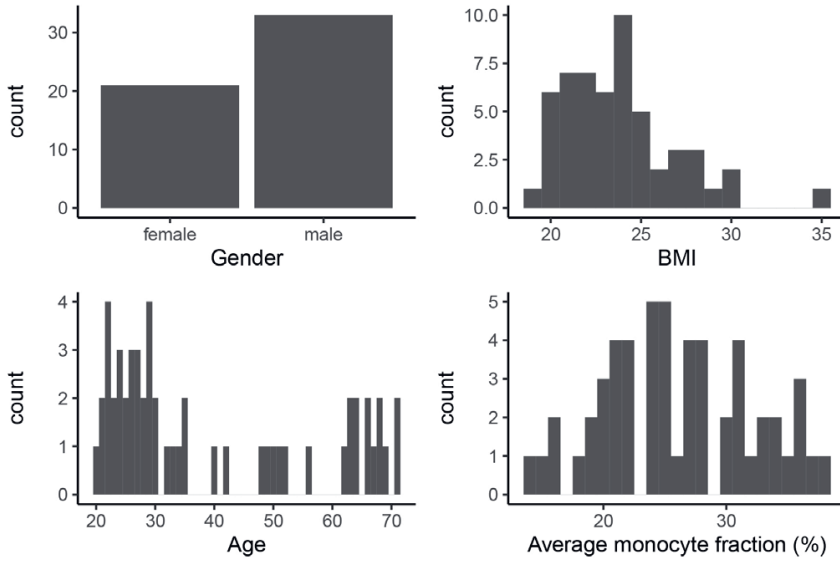
- immune function using the resources from the Human Functional Genomics Project. *Nature Medicine*. 2016; 22(8): 831–3.
35. Teslaa T, Teitell MA. Techniques to monitor glycolysis. *Methods in Enzymology*. 2014; 542: 91–114.
 36. Palsson-Mcdermott EM, Curtis AM, Goel G, Lauterbach MAR, Sheedy FJ, Gleeson LE, et al. Pyruvate kinase M2 regulates hif-1 α activity and il-1 β induction and is a critical determinant of the warburg effect in LPS-activated macrophages. *Cell Metabolism*. 2015; 21(1): 65–80.
 37. Kany S, Vollrath JT, Relja B. Cytokines in Inflammatory Disease. *International Journal of Molecular Sciences*. 2019; 20(23): 6008.
 38. Chiba S, Hisamatsu T, Suzuki H, Mori K, Kitazume MT, Shimamura K, et al. Glycolysis regulates LPS-induced cytokine production in M2 polarized human macrophages. *Immunology Letters*. 2017; 183: 17–23.
 39. Dinarello CA. Biologic basis for interleukin-1 in disease. *Blood*. 1996; 87(6): 2095–147.
 40. Zhang D, Tang Z, Huang H, Zhou G, Cui C, Weng Y, et al. Metabolic regulation of gene expression by histone lactylation. *Nature*. 2019; 574: 575–580.
 41. Haas R, Smith J, Rocher-Ros V, Nadkarni S, Montero-Melendez T, D’Acquisto F, et al. Lactate Regulates Metabolic and Pro-inflammatory Circuits in Control of T Cell Migration and Effector Functions. Marrack P, editor. *PLOS Biology*. 2015; 13(7): e1002202.
 42. Dietl K, Renner K, Dettmer K, Timischl B, Eberhart K, Dorn C, et al. Lactic Acid and Acidification Inhibit TNF Secretion and Glycolysis of Human Monocytes. *The Journal of Immunology*. 2010; 184(3): 1200–9.
 43. Ratter JM, Rooijackers HMM, Hooiveld GJ, Hijmans AGM, de Galan BE, Tack CJ, et al. In vitro and in vivo Effects of Lactate on Metabolism and Cytokine Production of Human Primary PBMCs and Monocytes. *Frontiers in immunology*. 2018; 9: 2564.
 44. Kawasaki T, Kawai T. Toll-like receptor signaling pathways. *Frontiers in Immunology*. 2014; 5: 461.
 45. Jin MS, Kim SE, Heo JY, Lee ME, Kim HM, Paik SG, et al. Crystal Structure of the TLR1-TLR2 Heterodimer Induced by Binding of a Tri-Acylated Lipopeptide. *Cell*. 2007; 130(6): 1071–82.
 46. Jin MS, Lee JO. Structures of the Toll-like Receptor Family and Its Ligand Complexes. *Immunity*. 2008; 29(2): 182–91.
 47. Fournier B, Philpott DJ. Recognition of *Staphylococcus aureus* by the innate immune system. *Clinical Microbiology Reviews*. 2005; 18(3): 521–40.
 48. Beutler B. Tlr4: Central component of the sole mammalian LPS sensor. *Current Opinion in Immunology*. 2000; 12(1): 20–6.
 49. Christ A, Günther P, Lauterbach MAR, Duewell P, Biswas D, Pelka K, et al. Western Diet Triggers NLRP3-Dependent Innate Immune Reprogramming. *Cell*. 2018; 172(1–2): 162–175.e14.
 50. Netea MG, Domínguez-Andrés J, Barreiro LB, Chavakis T, Divangahi M, Fuchs E, et al. Defining trained immunity and its role in health and disease. *Nature Reviews Immunology*. 2020; 20(6): 375–88.
 51. Domínguez-Andrés J, Joosten LA, Netea MG. Induction of innate immune memory: the role of cellular metabolism. *Current Opinion in Immunology*. 2019; 56: 10–6.
 52. Cheng SC, Quintin J, Cramer RA, Shepardson KM, Saeed S, Kumar V, et al. MTOR- and HIF-1 α -mediated aerobic glycolysis as metabolic basis for trained immunity. *Science*. 2014; 345(6204).
 53. Phan AT, Goldrath AW, Glass CK. Metabolic and Epigenetic Coordination of T Cell and Macrophage Immunity. *Immunity*. 2017; 46(5): 714–729.
 54. Fanucchi S, Domínguez-Andrés J, Joosten LAB, Netea MG, Mhlanga MM. The Intersection of

- Epigenetics and Metabolism in Trained Immunity. *Immunity*. 2020; 54(1): 32-43.
55. Wellen KE, Hatzivassiliou G, Sachdeva UM, Bui T V., Cross JR, Thompson CB. ATP-citrate lyase links cellular metabolism to histone acetylation. *Science*. 2009; 324(5930): 1076–80.
 56. Rodrigues CF, Rodrigues ME, Henriques M. *Candida* sp. Infections in Patients with Diabetes Mellitus. *Journal of Clinical Medicine*. 2019; 8(1): 76.
 57. Bates D, Mächler M, Bolker BM, Walker SC. Fitting linear mixed-effects models using lme4. *Journal of Statistical Software*. 2015; 67(1): 1–48.
 58. Kuznetsova A, Brockhoff PB, Christensen RHB. lmerTest Package: Tests in Linear Mixed Effects Models . *Journal of Statistical Software*. 2017; 82(13): 1–26.
 59. Clogg CC, Petkova E, Haritou A. Statistical Methods for Comparing Regression Coefficients Between Models. *American Journal of Sociology*. 1995; 100(5): 1261–93.
 60. Kassambara A, Mundt F. factoextra: Extract and Visualize the Results of Multivariate Data Analyses [R package factoextra version 1.0.7] [Internet]. Comprehensive R Archive Network (CRAN); 2020.
 61. Wickham H. ggplot2: Elegant Graphics for Data Analysis. ggplot2: Elegant Graphics for Data Analysis. Springer-Verlag New York; 2009.
 62. Wilke CO. cowplot: Streamlined Plot Theme and Plot Annotations for “ggplot2” [R package cowplot version 1.1.1] [Internet]. Comprehensive R Archive Network (CRAN); 2020.

Supplemental material

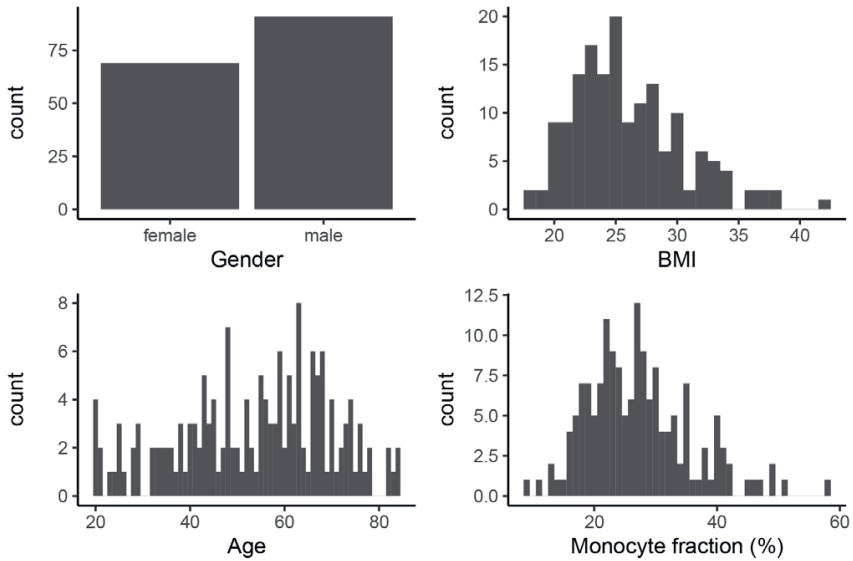
A

50FG

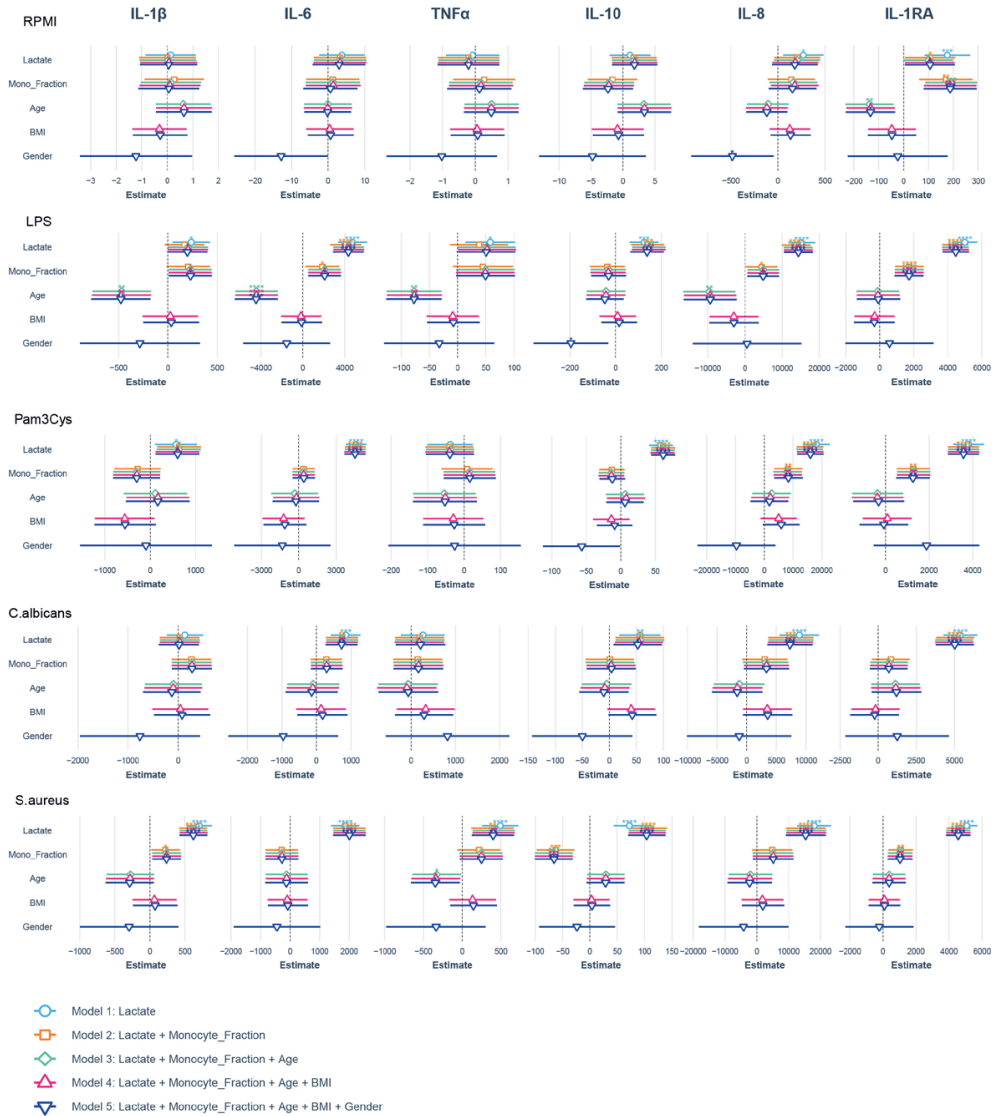


B

300DM

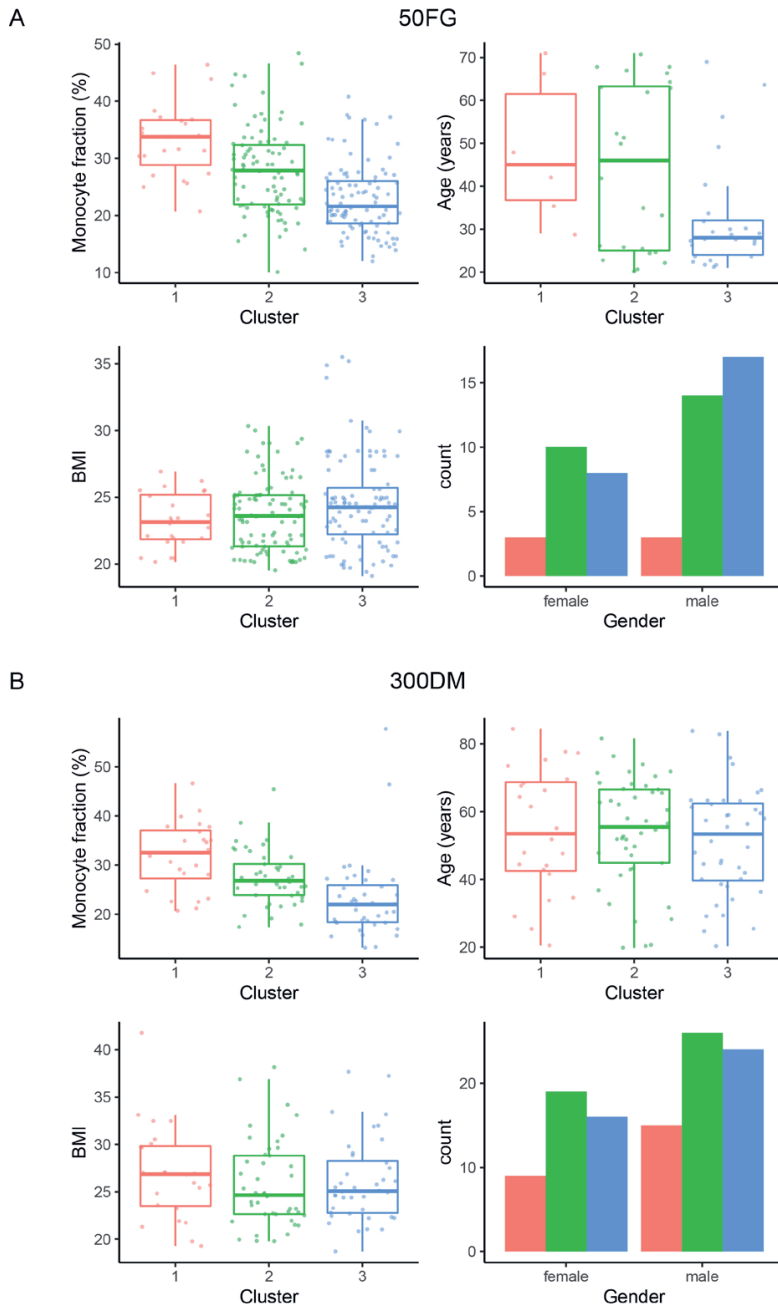
**Supplemental Figure 1. Subject characteristics of the cohorts.**

Subject characteristics of the 50FG (A) and 300DM (B) cohorts.



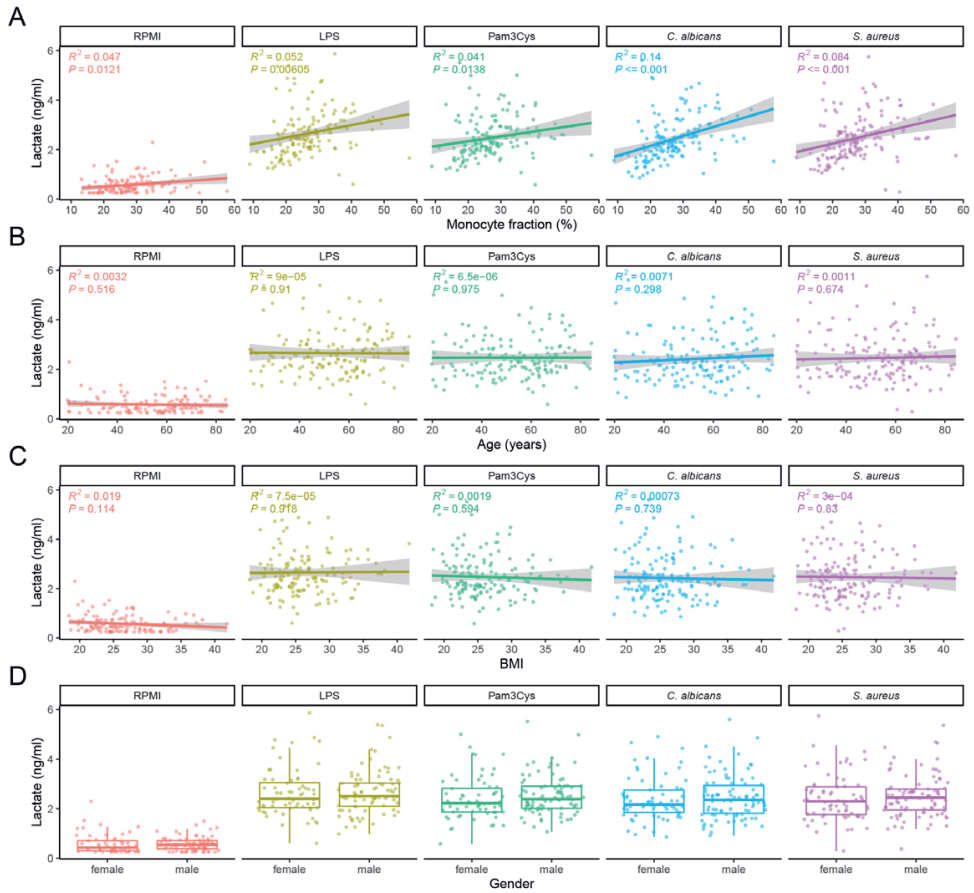
Supplemental Figure 2. Evaluation of covariates in the mixed models.

Separate mixed models were fitted for each of the cytokine-stimulation combinations. The host factors were added as covariates in a stepwise fashion to evaluate their individual impact on model parameters. All host factors were included as covariates in the final mixed model.



Supplemental Figure 3. Univariate evaluation of host factors for all clusters.

Univariate plotting of the host factors for each of the three clusters distinguished by k-means clustering for healthy subjects (A) and patients with T1DM (B). BMI: Body Mass Index.



Supplemental Figure 4. Linear relationships between lactate production in PBMCs and host factors.

Linear relation between lactate production in PBMCs and monocyte fraction (A), age (B), BMI (C) and gender (D) for patients with T1DM. LPS: lipopolysaccharide; BMI: Body Mass Index.

2



A high glyceic burden relates to functional and metabolic alterations of human monocytes in patients with type 1 diabetes

Kathrin Thiem^{1*}, Xanthe A.M.H. van Dierendonck^{1,2*}, Anna W.M. Janssen^{1*}, Joline P. Boogaard², Niels P. Riksen¹, Cees J. Tack^{1#}, Rinke Stienstra^{1,2#}

¹Department of Internal Medicine (463) & Radboud Institute for Molecular Life Sciences, Radboud University Medical Center, Nijmegen, the Netherlands.

²Division of Human Nutrition and Health, Wageningen University, the Netherlands.

*joint first authors

#joint senior authorship

Diabetes. 2020; 69(12):2735-2746.

Abstract

Diabetes mellitus is associated with increased cardiovascular risk and higher occurrence of infections. These complications suggest altered responses of the innate immune system. Recent studies have shown that energy metabolism of monocytes is crucial in determining their functionality. Here we investigate whether monocyte metabolism and function are changed in patients with diabetes and aim to identify diabetes-associated factors driving these alterations. Patients with type 1 diabetes (T1D) (n=41) and healthy age-, sex- and BMI-matched controls (n=20) were recruited. Monocytes were isolated from peripheral blood to determine immune functionality, metabolic responses and transcriptome profiles. Upon *ex vivo* stimulation with TLR-4 or TLR-2 agonists, monocytes of patients with T1D secreted lower levels of various cytokines and showed lower glycolytic rates in comparison to monocytes isolated from matched controls. Stratification based on HbA_{1c} levels revealed that lower cytokine secretion was coupled to higher glycolytic rate of monocytes in patients with higher glycemic burden. Circulating monocytes displayed an enhanced inflammatory gene expression profile associated with high glycemic burden. These results suggest that a high glycemic burden in patients with T1D is related to expression of inflammatory genes of monocytes and is associated with an impaired relationship between metabolism and inflammatory function upon activation.

Introduction

The presence of diabetes is associated with an altered innate immune cell function [1, 2]. Diabetes is known to increase the risk for infection [3], suggestive of ineffective (innate) immune cell function, yet is also characterized by a chronic inflammatory state which contributes to the development of cardiovascular disease (CVD) driven by inflammatory monocytes and macrophages [4, 5]. In patients with diabetes, a number of systemic alterations occur, most significant being varying levels of hyperglycemia and incidental hypoglycemia in patients treated with insulin. Also dyslipidemia, changes in fibrinolytic factors and other metabolic changes related to obesity occur [6], mainly in diabetes type 2 (T2D). These systemic alterations have been associated with various complications. For example, an association between glyceic burden (HbA_{1c} levels) and the risk for CVD has been well established [7]. In addition to CVD, large cohort studies have demonstrated that the increased risk for infections in patients with diabetes is associated with HbA_{1c} levels, age, presence of obesity and the duration of diabetes [8, 9].

On a functional level, various diabetes-associated alterations have been described in innate immune cells. *Ex vivo* studies using monocytes from patients with T2D link altered cytokine secretion to atherosclerotic complications [10, 11]. Furthermore, gene expression levels of pro-inflammatory cytokines interleukin (IL)-1 and IL-6 were elevated in unstimulated monocytes from patients with type 1 diabetes (T1D) or T2D [12]. Other functional alterations of innate immune cells have also been observed, including impairments in *ex vivo* bacterial killing and phagocytic function of polymorphonuclear leukocytes [13].

Recent evidence from the field of immunology has established the relevance of innate immune cell metabolism in determining functional output. This is illustrated both by robust intracellular metabolic rewiring after encountering a pathogen and by specific metabolic signatures accompanying innate immune cell polarization [14]. In monocytes, pathogenic stimulation promotes unique metabolic adaptations to build an effective response [15]. One of the most prominent features of activated immune cells is activation of glycolysis; the metabolic rewiring relies on intracellular changes to increase glycolytic rate, yet also depends on extracellular factors including substrate availability. For example, increasing glucose availability by enhancing glucose transporter 1 (GLUT1) activity promotes a pro-inflammatory phenotype in macrophages [16]. In diabetes, circulating monocytes are exposed to chronically elevated glucose concentrations [1], which can lead to functional changes [17], possibly by promoting alterations in their metabolic signature. A detailed assessment of changes in function and metabolism of monocytes during diabetes and

identification of potential factors that drive these alterations is currently lacking.

The purpose of this study was to investigate whether monocyte metabolism and function are changed in patients with diabetes and to identify diabetes-associated factors driving these alterations. We report that circulating monocytes from patients with T1D are characterized by a pro-inflammatory transcriptome. Upon stimulation *ex vivo*, however, the capacity to boost proinflammatory cytokine production is reduced, and an increased glycolytic rate after stimulation was seen in patients displaying a high glycemic burden.

Research design and methods

Experimental design

This study was a single-center cross-sectional case control study in patients with T1D and healthy control (HC) subjects. The study population consisted of three groups: patients with well-controlled type 1 diabetes, patients with poorly-controlled type 1 diabetes and healthy control subjects. The study was powered on the primary study outcome: vascular wall inflammation in the carotid and femoral arteries, quantified by 2-deoxy-2-[18F] fluoro-D-glucose–positron emission tomography (PET) scanning. One of the secondary outcomes was the *ex vivo* determination of the inflammatory/atherogenic phenotype and the cellular metabolism of circulating monocytes, the focus of this manuscript. The formal sample size calculation was based on the primary outcome and resulted in 20 subjects per group. Ethical approval for this study was obtained from the Institutional Review Board of the Radboud University Medical Center (NL62200.091.17 2017-3555), and registered at ClinicalTrials.gov (NCT03441919). The study was conducted according to the principles expressed in the Declaration of Helsinki. All participants gave written consent before participation.

Patients and control subjects

A total of 41 patients with T1D and 20 healthy nondiabetic control subjects were included, carefully matched for age, sex and BMI. Inclusion criteria for patients with diabetes were: diagnosis based on clinical criteria; duration of diabetes ≥ 10 years; age ≥ 20 years ≤ 60 years; group 1: $\text{HbA}_{1c} > 64$ mmol/mol, group 2: $\text{HbA}_{1c} \leq 64$ mmol/mol. Inclusion criteria for HC subjects were: absence of disease, no use of medication; matched for age, gender and BMI; $\text{HbA}_{1c} < 42$ mmol/mol. Exclusion criteria for all groups were: inability to provide informed consent; smoking; specific medication use (immunosuppressive drugs, use of statins < 2 weeks before the PET-CT, use of acetylsalicylic acid); previous cardiovascular events (ischemic stroke/TIA, myocardial infarction, peripheral arterial disease); auto-inflammatory or auto-immune diseases; current or recent infection (< 3 months); previous

vaccination (<3 months); renal failure (MDRD <45 mL/min per 1.73 m²); BMI>30kg/m²; pregnancy or breastfeeding; claustrophobia; severe hypoglycemia <1 week before PET-CT. Patients included in the study were recruited from the outpatient clinic of the Radboud University Medical Center (Radboudumc) Nijmegen. Clinical characteristics are given in **Table 1**, HbA_{1c} levels were averaged from the last ten visits.

Cells and culture

Peripheral blood mononuclear cells (PBMCs) were isolated by dilution of blood with pyrogen-free PBS and differential density centrifugation over Ficoll-Plaque gradient media (GE Healthcare, Eindhoven, The Netherlands). Obtained PBMCs were further purified to CD14⁺ monocytes using negative selection by depleting non-monocyte cells using the classical monocyte isolation kit (Miltenyi Biotec B.V., Leiden, The Netherlands). Cells were resuspended in RPMI culture medium containing 11mM of glucose (1640, Invitrogen, ThermoFisher Scientific, Eindhoven, The Netherlands) supplemented with 50 µg/mL gentamicin (Centraform), 2mM glutaMAX (Gibco, ThermoFisher Scientific), and 1mM pyruvate (Gibco, ThermoFisher Scientific). For *in vitro* stimulation experiments, 1x10⁵ CD14⁺ monocytes were cultured in 96-well flat bottom plates using RPMI medium containing 10% human pooled serum at 37°C and 5% CO₂. CD14⁺ monocytes were stimulated for 24 hours with Pam3CysK (10 µg/mL), *Escherichia coli* LPS (10 ng/mL, serotype 055:B5, Sigma-Aldrich, Zwijndrecht, The Netherlands) or only RPMI as control. Supernatants were stored at -20°C for future batchwise ELISA analyses.

Transcriptome analysis

Total RNA was isolated from monocytes that were directly frozen at -80°C in TRIzol reagent (Invitrogen, ThermoFisher Scientific) after isolation and was purified with the RNeasy Micro kit (Qiagen, Venlo, The Netherlands). For microarray analysis, the integrity of the RNA was verified with RNA 6000 Nano chips using an Agilent 2100 Bioanalyzer (Agilent Technologies, Amstelveen, The Netherlands). RNA was considered suitable for array hybridization with an RNA integrity number of minimally 7. Per sample, 100 ng of purified RNA was labeled with the Whole-Transcript Sense Target Assay kit (Affymetrix, Santa Clara, CA, USA; P/N 900652) which was hybridized to Affymetrix GeneChip Human Gene 2.1 ST arrays (Affymetrix). Hybridization, washing, and scanning of the peg arrays were carried out on the Affymetrix GeneTitan platform according to the manufacturer's instructions. The quality control and data analysis pipeline have been described in detail previously [18]. Briefly, normalized expression estimates of probe sets were computed by the robust multiarray analysis (RMA) algorithm [19] as implemented in the Bioconductor library oligo [20]. Probe sets were redefined using current genome information according to Dai et al.

[21] based on annotations provided by the Entrez Gene database, which resulted in the profiling of 29,635 unique genes (custom CDF v23). Differentially expressed probe sets (genes) were identified by using linear models (limma) and an intensity-based moderated t-statistic [22, 23]. The heterogeneity in gene expression profiles that was observed in both study groups was taken into account by fitting a heteroskedastic model that included relative quality weights that were computed for each sample per group [24, 25]. *P*-values were corrected for multiple testing according to Benjamini & Hochberg [26]. Probe sets that satisfied the criterion of $FDR < 0.01$ were considered to be significantly regulated. Functional analysis of the transcriptome data was performed using Ingenuity Pathway Analysis (IPA, Qiagen).

Real-time PCR

For gene expression analysis by real-time PCR, cDNA was generated by reverse transcription of 400 ng purified RNA with the iScript cDNA synthesis kit (Bio-Rad Laboratories, Hercules, CA, USA) following manufacturer's instructions. Nucleic acid quantification and purity was assessed by using the NanoDrop spectrophotometer (ThermoFisher Scientific). Gene expression analysis was performed in duplicate with SYBR green reactions using the SensiMix™ (BioLine, London, UK) protocol with the CFX384 Touch™ Real-Time detection system (Bio-Rad Laboratories). Negative template controls (NTC) did not show any amplification. CFX Maestro software (Bio-Rad Laboratories) was used to analyze qPCR data and Cq values were calculated with the use of a calibration curve. Primers that were used for real-time PCR analysis are listed in **Supplementary Table 1**, together with measured efficiency and R^2 of calibration curves. Expression of B2M and 36B4 were assessed as housekeeping gene, expression of B2M was stable (average Cq: 18.97, standard deviation: 0.36) and was used for normalization.

Mitochondrial respiration and glycolytic rate

Directly after isolation, CD14⁺ monocytes were seeded in XF96 microplates (Agilent Technologies, Amstelveen, The Netherlands; 2×10^5 cells per well in quintuple) in RPMI 1640 medium containing 11 mM glucose and rested for 1 hour at 37°C, 5% CO₂. Thereafter, cells were incubated in non-buffered DMEM medium without glucose (D5030, Sigma-Aldrich), supplemented with 1 or 2 mM L-glutamine (Sigma-Aldrich) in a CO₂-free incubator (37°C) for 45 minutes. Measurements of oxygen consumption and extracellular acidification were performed at 37°C using a Seahorse XF96 Extracellular Flux Analyzer (Agilent Technologies). The Seahorse XF Cell Glyco Stress Test kit was used to characterize the dynamics of glycolytic rate according to the extracellular acidification rate (ECAR). The cells were treated according to the manufacturer's protocol with glucose (11 mM),

oligomycin (1 μ M), 2-DG (22 mM) at time points indicated in **Figure 2A**. For measurement of different dynamics in mitochondrial oxygen consumption rate (OCR), the Seahorse XF Cell Mito Stress Test kit was used, with slight adjustments to the protocol. Cells were first treated with glucose (11 mM), then oligomycin (1 μ M), FCCP (1 μ M) in combination with pyruvate (1 mM) and lastly Rotenone and Antimycin A (1.25 μ M and 2.5 μ M) at time points indicated in **Figure 2B**. To assess parameters of OCR and ECAR during pathogenic stimulation, cells were injected with glucose (11 mM), then P3C (10 μ g/mL) or LPS (10 ng/mL) at time points indicated in **Figure 2J** and **M**.

Cytokine measurements

Cytokine concentrations in supernatants were determined by enzyme-linked immunosorbent assays (ELISA) using commercially available kits for TNF α and IL-6, IL-1 β , IL-1Ra and IL-8 (R&D Systems, Bio-Techne, Minneapolis, MN).

Statistical analysis

Participant characteristics were analyzed by one-way ANOVA using SPSS Statistics 25 software (IBM Corp., Armonk, NY, USA) after normality was assessed using Q-Q plots. Stratification was based on calculated quartiles of the data. For parts of the analysis, clinical HbA_{1c} cut-off points were used. While these cut-offs are biologically relevant and valid for this study, they may hamper statistical power. Data in **Table 1** are presented as mean \pm SD. Data are shown as box plots with median and spread (whiskers), or as graphs and bar plots with means \pm SDs. In box plots and bar plots, all single data points are visualized. For all data, normality was assessed by generating Q-Q plots, using the *qnorm* function with R software. Significance was assessed using Mann Whitney-U test when comparing two groups, and Kruskal-Wallis test when comparing more than two groups followed by the Dunn test for multiple comparisons. Correlations were assessed by calculating Spearman's ρ . A two-sided *p*-value below 0.05 was considered statistically significant. All data were visualized and analyzed using Prism version 5.0 or 8.0 (GraphPad Software, San Diego, CA) or R Studio (PBC, Boston, MA; <http://www.rstudio.com/>).

Data and Resource Availability

The datasets generated during the current study are available from the corresponding author upon reasonable request. The microarray dataset that was generated and analyzed during the current study has been submitted to the Gene Expression Omnibus repository (GEO number: GSE154609). No applicable resources were generated or analyzed during the current study.

Results

Demographics of the subjects included in the study are shown in **Table 1**. HC subjects and patients with T1D were matched for age and BMI. The average duration of diabetes was 27.3 years. HbA_{1c} levels in patients with T1D ranged from 39 mmol/mol (5.8%) to 91 mmol/mol (10.5%) with an average value of 63.4 mmol/mol (7.9%). In HC subjects, the average HbA_{1c} value was 34 mmol/mol (5.2%) (**Table 1**).

Table 1. Demographic and anthropometric characteristics of the subjects.

Values are given in mean \pm SD (range).

	T1D	HC	<i>p-value</i>
Age, yr (range)	43 \pm 13.2 (22-60)	43 \pm 12.2 (23-59)	<i>p</i> = 0.954
Height, cm (range)	175 \pm 9 (159-198)	175 \pm 9 (158-191)	<i>p</i> = 0.764
Weight, kg (range)	76.3 \pm 11.3 (53-100)	75.8 \pm 14.4 (51-99)	<i>p</i> = 0.874
BMI, kg/m ² (range)	24.8 \pm 2.7 (19.9-30.1)	24.7 \pm 3.3 (18.7-29.9)	<i>p</i> = 0.935
Female, n (%)	21 (51)	10 (50)	<i>p</i> = 0.930
HbA _{1c} , mmol/mol (range)	64 \pm 10 (39-91)	34 \pm 4.3 (26-40)	<i>p</i> < 0.00001
Duration of T1D, yr (range)	27 \pm 11.2 (10-47)	-	

Inflammatory response of monocytes is reduced in patients with T1D compared with HC subjects.

To test the inflammatory function of monocytes, cells were exposed to a TLR-2 agonist (Pam3CysK, P3C) and a TLR-4 agonist (LPS) to induce activation, and cytokine secretion was used as final readout. Although a robust induction of cytokines was observed in response to P3C and LPS both in patients with T1D and HC subjects (**Figure 1**), the production of TNF α , IL-1 β and IL-1Ra was significantly lower in patients with T1D (**Figure 1A, D-F, I and J**). Also the secretion of IL-6 tended to be reduced upon P3C stimulation and was lower upon LPS stimulation (**Figure 1B, G**) in patients with T1D compared with HC subjects. Not all cytokines were affected: IL-8 secretion by monocytes was not different between patients with T1D and HC subjects after P3C or LPS stimulation.

Metabolism of monocytes from patients with T1D differs compared with HC subjects.

Directly after isolation, the metabolism of the monocytes was measured with the Agilent Seahorse Extracellular Flux Analyzer using Seahorse XF Cell Glyco- and Cell Mito-Stress tests (**Figure 2A, B**). No differences in maximal glycolytic capacity (**Figure 2C**) or glycolytic reserve (**Figure 2D**) existed between monocytes from patients with T1D and HC subjects. Also measurements of oxygen consumption revealed no differences in maximal respiration (**Figure 2E**), and spare respiratory capacity (**Figure 2F**) of monocytes from patients with T1D and HC subjects. Combining all glycolytic extracellular flux measurements at baseline and after glucose injection (**Figure 2G**) revealed that basal glycolytic rates did not differ

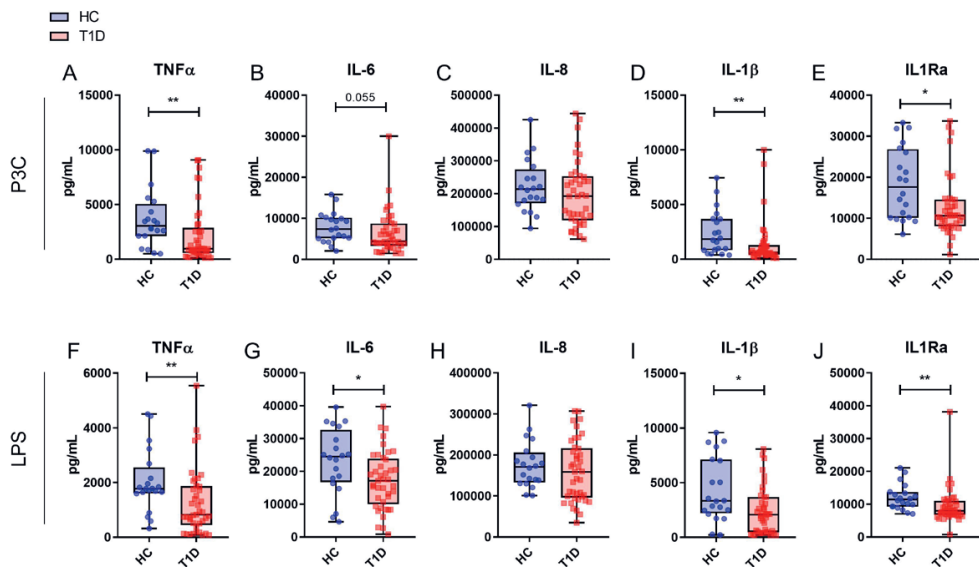


Figure 1. Inflammatory cytokine secretion in monocytes from patients with T1D and HC subjects.

CD14⁺ monocytes were stimulated for 24 hours with P3C or LPS. TNF α (**A**, $p = 0.0054$ and **F**, $p = 0.0098$), IL-6 (**B**, $p = 0.055$ and **G**, $p = 0.0269$), IL-8, (**C** and **H**) IL-1 β (**D**, $p = 0.0048$ and **I**, $p = 0.0137$) and IL-1Ra (**E**, $p = 0.0159$ and **J**, $p = 0.0015$) were determined in cell supernatants. HC subjects, $n = 20$; T1D patients, $n = 41$. * $p < 0.05$, ** $p < 0.01$.

(**Figure 2H**), but were significantly lower after glucose injection in monocytes derived from patients with T1D compared with cells from HC subjects (**Figure 2I**).

We also determined the metabolic response towards P3C and LPS stimulations, which are both known to result in acute and unique metabolic adaptations of monocytes (15). Glycolytic activity and mitochondrial respiration of CD14⁺ monocytes were measured after P3C or LPS injection and followed over the first hour after stimulation (**Figure 2J**, **M** and **Supplementary Figure 1**). Stimulation with P3C increased glycolytic activity approximately twofold (**Figure 2K** compared with **Figure 2H** and **I**) and induced a subtle increase in OCR with similar responses in patients with T1D and HC subjects (**Figure 2P**, compared with **Figure 2N** and **O**). LPS injection had a smaller acute impact on glycolytic activity (**Figure 2L**, compared with **Figure 2H** and **I**) and mitochondrial respiration (**Figure 2Q**, compared with **Figure 2N** and **O**) in both groups compared with P3C. However, no differences in OCR or ECAR after pathogenic stimulation were observed between monocytes derived from patients with T1D versus HC subjects.

A high glycaemic burden is associated with lower cytokine secretion.

To identify factors contributing to altered responses in monocytes from patients with T1D, we determined the impact of diabetes duration and glucose control (HbA_{1c}) on monocyte

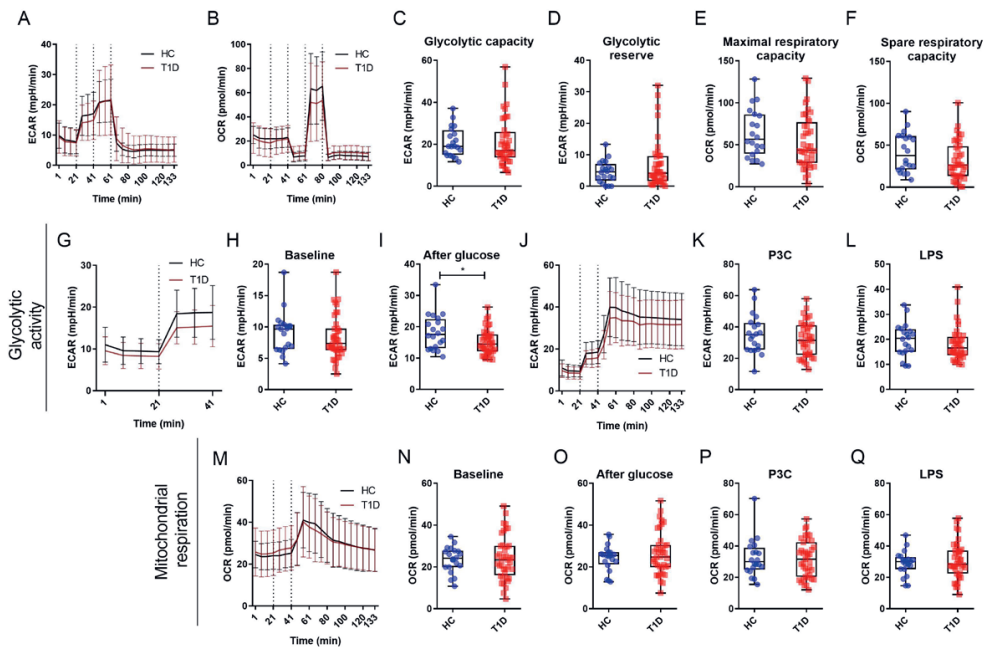


Figure 2. Glycolytic and oxidative metabolism in monocytes from patients with T1D and HC subjects.

Extracellular Flux analysis was performed on monocytes isolated from patients with patients with T1D and HC subjects, measuring extracellular acidification rates (ECAR) and oxygen consumption rates (OCR). Glycolytic stress tests, mitochondrial stress tests and acute stimulations were performed and injections time points are indicated with dotted lines. Extracellular flux curves are shown for glycolytic activity (**A**) (glycolytic stress test, ECAR) and respiratory activity (**B**) (mitochondrial stress test, OCR). Glycolytic capacity (**C**) and glycolytic reserve (**D**) were calculated based on the glycolytic stress test. Maximal respiratory capacity (**E**) and spare respiratory capacity (**F**) were calculated based on the mitochondrial stress test. Effects of pathogenic stimulations on cellular metabolism were tested first injecting glucose (**G, H and I** for ECAR, $p = 0.0355$; **N and O** for OCR) and afterwards either P3C (**J and K** for ECAR, **M and P** for OCR) or LPS (**L** for ECAR, **Q** for OCR). Values presented as means from 3 consecutive measurements within 20 min for baseline and glucose, and as means from 13 consecutive measurements within 90 min for pathogenic stimulations. HC subjects: $n = 20$, patients with T1D: $n = 41$. $*p < 0.05$.

functionality. Stratification based on duration of T1D revealed no major impact on cytokine secretion of TLR-activated monocytes from patients with longer duration of T1D (**Supplementary Figure 2**). To determine the effect of glucose control, cytokine levels upon TLR stimulation were stratified by HbA_{1c} (**Figure 3A – E, Supplementary Figure 3A – E**), using HbA_{1c} quartiles. High glycaemic burden, reflected by high HbA_{1c} levels, was associated with reduced monocyte function after P3C stimulation in patients with the highest HbA_{1c} levels (71-91 mmol/mol; 8.6-10.5%) compared with HC subjects, illustrated by significantly reduced secretion levels of TNF α and IL-1 β (**Figure 3A, D**), but not IL-6, IL-8 and IL-1Ra levels (**Figure 3B, C, E**). Similar patterns for TNF α and a significant effect for IL-1Ra were found after LPS stimulation (**Supplementary Figure 3A, E**).

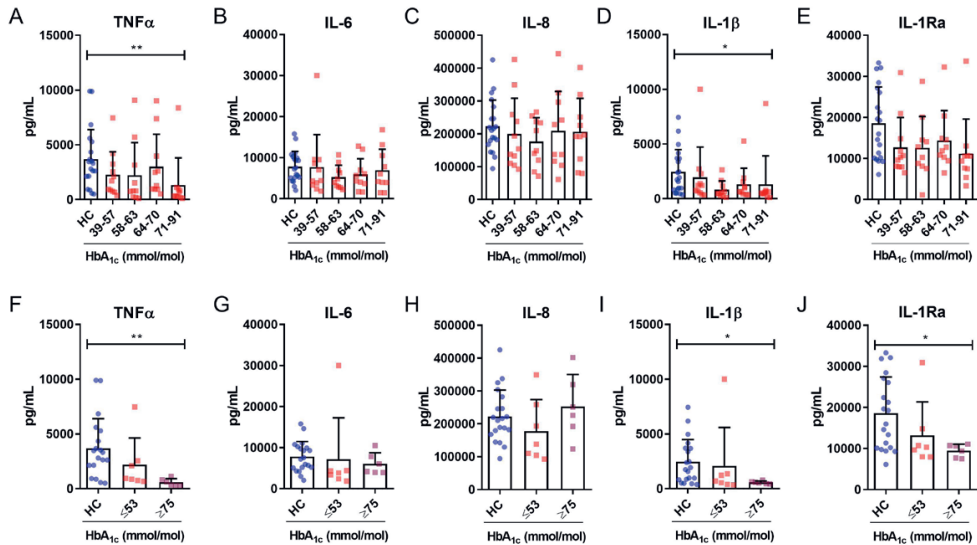


Figure 3. Monocytes of patients with higher HbA_{1c} levels have lower cytokine secretion.

CD14⁺ monocytes were stimulated with P3C and TNF α , IL-6, IL-8, IL-1 β and IL-1Ra were measured. Quartiles of equal size were created for patients with T1D based on HbA_{1c} levels (**A**, $p = 0.0084$; **B**; **C**; **D**, $p = 0.0478$; **E**), and two groups with clinically relevant HbA_{1c} levels (≤ 53 and ≥ 75 mmol/mol) were compared against HC subjects (**F**, $p = 0.002$; **G**; **H**; **I**, $p = 0.0389$; **J**, $p = 0.0428$). HC subjects: $n = 20$; T1D HbA_{1c} quartiles: $n = 10-11$; HbA_{1c} ≤ 53 mmol/mol: $n = 7$, HbA_{1c} ≥ 75 : $n = 6$. * $p < 0.05$, ** $p < 0.01$.

Altered metabolic activity during a high glyceic burden.

Changes in functionality of monocytes were primarily associated to HbA_{1c} levels but not to duration of diabetes. Similarly, duration of diabetes was not associated with differences in metabolic parameters of monocytes (**Supplementary Figure 4**). Next, we set out to determine the relevance of glyceic burden as a driver for metabolic alterations of the cells. Stratifying for HbA_{1c} levels, we observed comparable patterns for the various metabolic readouts related to glycolysis and oxidative phosphorylation. A nonsignificant, J-shaped association between different parameters of monocyte metabolism and glyceic burden was observed as shown in **Figure 4A – J**. This association is mostly illustrated by the metabolic readouts related to ECAR, including maximal glycolytic capacity (**Figure 4A**) and response to P3C (**Figure 4E**) or LPS (**Supplementary Figure 5**). Here, a decreased glycolytic rate in patients in the lower quartiles of HbA_{1c} (between 39-70 mmol/mol) can be seen compared with HC subjects, in addition to an increase in glycolytic rate in patients with high HbA_{1c} levels. Using the HbA_{1c} classifications of ≤ 53 mmol/mol and ≥ 75 mmol/mol led to similar results. As shown in **Figure 4F and H**, glycolytic rate was significantly

higher in monocytes comparing HbA_{1c} levels ≥ 75 mmol/mol versus levels ≤ 53 mmol/mol, although both groups were not significantly different from the HC subjects.

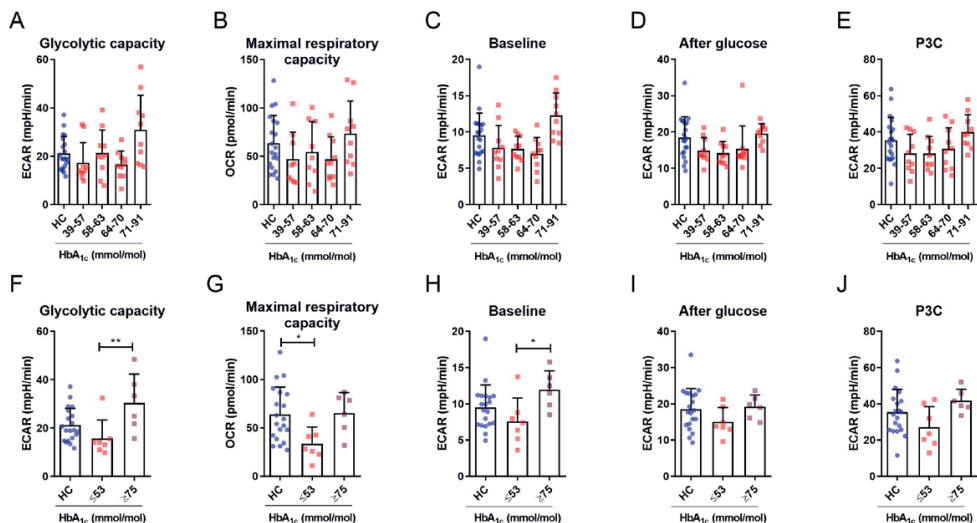


Figure 4. The association of HbA_{1c} levels with monocyte metabolism.

Extracellular flux was measured in monocytes isolated from patients with T1D and HC subjects. Values from patients with T1D are shown grouped into equally sized quartiles based on HbA_{1c} levels and compared with values from HC subjects on glycolytic capacity (A), maximal respiratory capacity (B), ECAR at baseline (C), ECAR after glucose injection (D) or ECAR after P3C stimulation (E). Values from patients with T1D that fall within two groups of extremes are compared with values for HC subjects on glycolytic capacity (F, $p = 0.0062$), maximal respiratory capacity (G, $p = 0.0328$), ECAR at baseline (H, $p = 0.0328$), ECAR after glucose injection (I) or ECAR after P3C stimulation (J). HbA_{1c} quartiles; HC subjects: $n = 20$, T1D quartiles: $n = 10-11$, HbA_{1c} ≤ 53 mmol/mol: $n = 7$, HbA_{1c} ≥ 75 mmol/mol: $n = 6$. * $p < 0.05$, ** $p < 0.01$.

Because glycolytic metabolism and function of monocytes are closely intertwined and we observed significant differences in glycolytic responses of the monocytes between patients with T1D and HC subjects (Figure 2I), we determined the association between glycolysis and cytokine production. To do so, we calculated ratios between ECAR and cytokine secretion (Figure 5A-E). Patients with a low glycemic burden (HbA_{1c} ≤ 53 mmol/mol) and HC subjects had similar ratios. However, in patients with a high glycemic burden (HbA_{1c} ≥ 75 mmol/mol) glycolysis-to-cytokine ratios were significantly increased for TNF α , IL-1 β and IL-1Ra, not for IL-6 and IL-8 secretion upon P3C stimulation compared with HC subjects and patients with a low glycemic burden (Figure 5A - E). For OCR-to-cytokine secretion ratios, similar patterns were found (Supplementary Figure 6A - E). Visualization of the correlation analysis between glycolytic parameters (ECAR and lactate production) and cytokine production versus HbA_{1c} levels further illustrates the altered association between metabolism and function dependent on the glycemic burden (Figure 5E) where

in the higher end of glycemia, an increased metabolic rate is coupled to lower production of TNF α .

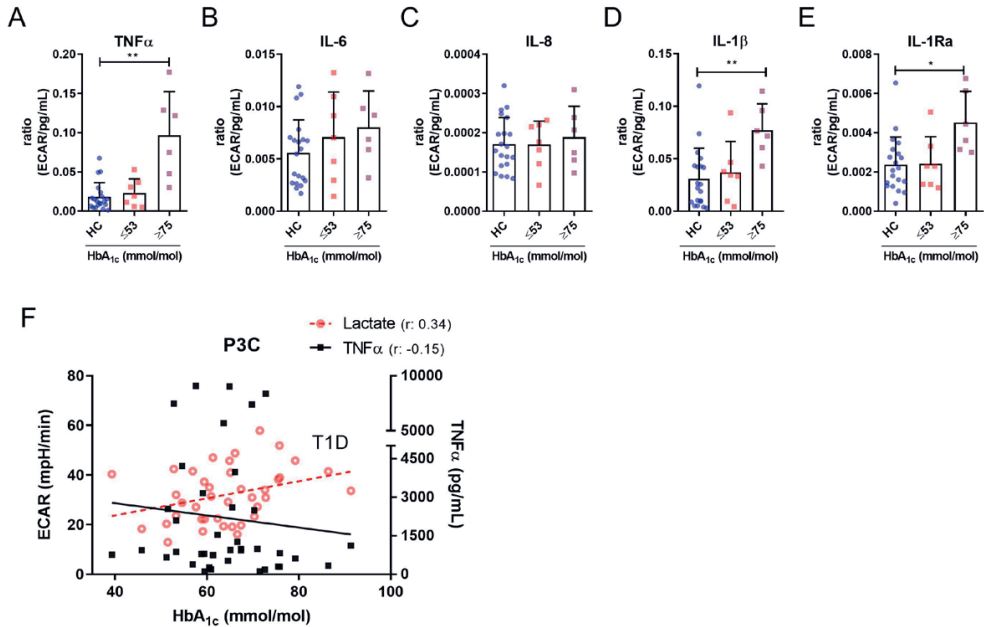


Figure 5. Monocytes of patients with poor glyceic control have higher ECAR-to-cytokine secretion ratio's.

Extracellular Flux analysis was measured in monocytes isolated from patients with T1D and HC subjects, measuring ECARs for 90 consecutive minutes after direct stimulation with P3C. Cytokine secretion was measured after 24 hour stimulation with P3C. A ratio between ECAR and cytokine secretion was calculated and is shown for TNF α (A, $p = 0.0021$), IL-6 (B), IL-8 (C), IL-1 β (D, $p = 0.008$), IL-1Ra (E, $p = 0.0195$). (F) The correlation between ECAR (acute), TNF α secretion (24h), HbA $_{1c}$ and lactate secretion (24h) is shown for monocytes isolated from patients with T1D treated with P3C. HbA $_{1c}$ \leq 53 mmol/mol: $n = 7$, HbA $_{1c}$ \geq 75 mmol/mol: $n = 6$; Correlation: $n = 41$. * $p < 0.05$, ** $p < 0.01$.

Transcriptome analysis of circulating monocytes from HC subjects versus patients with T1D.

To investigate the potential underlying mechanisms, we analyzed the transcriptome of monocytes directly after isolation to obtain insights into reprogramming of circulating monocytes during diabetes that may translate into altered responses upon activation. Because function and metabolism of monocytes was both impacted by HbA $_{1c}$, we compared patients with the highest HbA $_{1c}$ levels ($n = 12$) with HC subjects ($n = 12$). The two groups did not differ regarding BMI, sex and age. A heat map of the most differentially regulated genes (top 50 up- or downregulated with an adjusted p -value < 0.01) revealed upregulation of several inflammatory genes in the monocytes from patients with T1D

versus HC subjects, including *JUN*, *CXCL8* (IL-8), *FOSB*, and *CXCL5* (**Figure 6A, B**). This was corroborated by Ingenuity pathway analysis identifying enrichment of the IL-17A-induced signalling/activation pathway in monocytes from patients with T1D compared with HC subjects (**Figure 6C**). The most significantly upregulated gene was *JUN* (c-JUN/AP1), a transcription factor known for mediating inflammatory responses [27, 28]. To further confirm these results, we measured the gene expression of pro-inflammatory genes *JUN* and *CXCL5* by real-time PCR in monocytes obtained from patients with a low glycemic burden ($HbA_{1c} \leq 53$ mmol/mol) and a high glycemic burden (HbA_{1c} levels ≥ 75 mmol/mol). As shown, expression of *JUN* (**Figure 6D**) and *CXCL5* (**Figure 6E**) mRNA are significantly enhanced in monocytes from patients with a high glycemic burden compared with HC subjects.

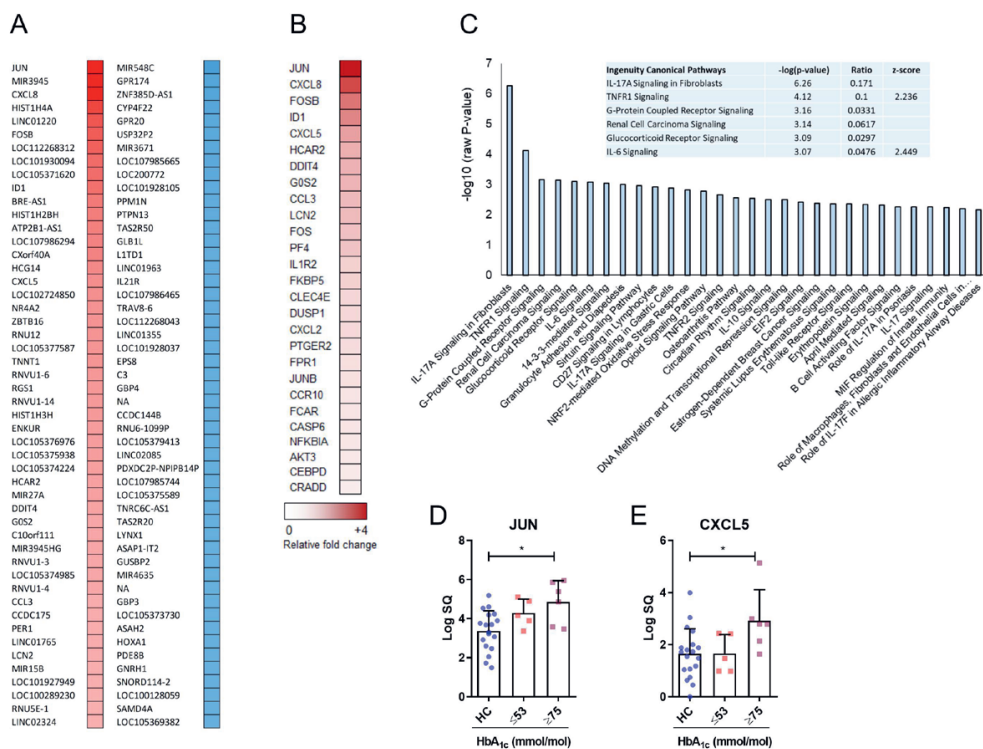


Figure 6. Monocytes of patients with higher HbA_{1c} levels show a pro-inflammatory gene expression signature.

Gene expression levels were measured in mRNA isolated from CD14⁺ monocytes of patients with T1D and HC subjects by means of microarray. (**A**) Relative fold changes of the top 50 up- (red) or downregulated (blue) genes are shown for patients with T1D versus HC subjects (only genes with a *p*-value <0.01 are shown). Ingenuity pathway analyses revealed the pathways that are most changed in patients with T1D versus HC subjects (**B**). (**C**) Inflammatory response heat map containing fold changes of the highest up- or downregulated genes in patients

with T1D versus HC subjects based on the Ingenuity disease analysis. qPCR analysis of *JUN* (**D**, $p = 0.0413$) and *CXCL5* (**E**, $p = 0.0345$) in monocytes of HC subjects, and patients with $\text{HbA}_{1c} \leq 53$ mmol/mol ($n = 7$) or $\text{HbA}_{1c} \geq 75$ mmol/mol ($n = 6$). HC subjects: $n = 12$; T1D: $n = 12$. 7, $\text{HbA}_{1c} \geq 75$ mmol/mol: $n = 6$. * $p < 0.05$.

Discussion

Our results demonstrate that circulating monocytes from patients with T1D display a pro-inflammatory gene expression signature compared with HC subjects, which translates into a reduced reserve capacity (lower cytokine production) upon acute TLR stimulation. These changes appear to be mainly associated to the glycemic burden. In parallel, the higher glycolytic activity in monocytes from patients with T1D also associates with high glycemic burden. Altogether these results suggest that a high glycemic burden links to a pro-inflammatory signature in circulating monocytes that upon acute stimulation translates into a lower functional response and may explain both susceptibility to infections as well as enhanced vascular inflammation in the diabetic state.

In the current study, the release of several cytokines by monocytes of patients with T1D differed from HC subjects, with some specificity regarding the affected cytokines. The production and secretion of various cytokines is differentially regulated and therefore, the diabetic state may only impact on specific pathways. Previous studies have also demonstrated alterations in cytokine secretion of innate immune cells from diabetic patients. *Ex vivo* studies performed with total mononuclear cells from patients with T1D showed similar reductions in IL-1 β secretion upon LPS stimulation [29], although no reduction in TNF α or IL-1Ra secretion was found [29, 30]. The latter observation is in contrast to our results, yet might be explained by the fact that these studies used a mixture of mononuclear cells from male patients with T1D, whereas we specifically measured monocyte responses from both male and female patients with T1D. Although total mononuclear cells might more closely resemble the situation *in vivo*, variations in cellular composition between study participants may hamper interpretation of the results. Furthermore, this setup enables us to specifically address the functional changes in monocytes. Our results revealed an altered response of monocytes to *ex vivo* stimulation with inflammatory stimuli characterized by a reduced capacity to produce cytokines, which appears to be linked to a high glycemic burden in patients with T1D. Other studies previously looking at monocyte function in T1D found inconsistent results on cytokine release, reporting either lower IL-1 and IL-6 [31] or higher IL-6 release in monocytes from patients with T1D [32]. However, none of these studies stratified the data for HbA_{1c} level, nor coupled the functional data to extensive metabolic phenotyping of the cells.

Optimal glycemic control is the main treatment goal to reduce long-term complications in the management of T1D [33-35]. Our results link poor glycemic control to aberrant monocyte functioning, which may both contribute to accelerated vascular damage and to an increased infection rate. From a mechanistic point of view, multiple explanations

for our observation exist. For once, several biochemical pathways are known to increase oxidative stress mediated by hyperglycemia [36-39], which has already been coupled to the metabolic activation of monocytes in patients with T2D [40]. Although these pathways have mainly been studied in the context of microvascular complications such as retinopathy and neuropathy, similar pathways might be altered in monocytes residing in hyperglycemic conditions, promoting functional changes. However, the transcriptomics analyses did not reveal major differences in oxidative pathways in monocytes of patients with T1D versus HC subjects. Since the glycolytic rate of innate immune cells is known to determine functional output, including cytokine production [41], changes in glucose availability as direct substrate for monocytes might also explain our observations. Without stratifying for HbA_{1c}, we observed a general decrease in glycolytic rate *ex vivo* after addition of glucose in monocytes derived from patients with T1D versus HC subjects. Because the glycolytic rate has been proposed as one of the main drivers of monocyte/macrophage activation [42], these metabolic changes may explain the reduced cytokine secretion.

Interestingly, our transcriptome analysis of circulating monocytes revealed an enhanced inflammatory signature associated to a high glyceic load. One of the most differentially regulated genes is *JUN*, which is known to be activated in LPS-stimulated human monocytes [43]. Although these results may seem in contrast to the reduced cytokine levels upon *ex vivo* stimulation, they are in accordance with the presence of immune tolerance. It has been well established that LPS can induce tolerance with a robust initial response followed by a non-responsive cell upon a second exposure to LPS [44]. A similar phenomenon may occur in monocytes exposed to the chronic diabetic milieu. Possibly, the hyperglycemic environment *in vivo* leads to chronic activation of monocytes, explaining the upregulated *JUN* mRNA expression in circulating monocytes from patients with T1D in the current study. This chronic activation translates into a lower reserve for the immune response upon a second activation *ex vivo*, due to immune tolerance.

The enrichment of the IL-17A signaling pathway, that included *JUN* upregulation, has been previously identified in the context of type 1 diabetes. In a comparison of the transcriptome of mononuclear cells of patients with T1D to those of healthy individuals, Li and colleagues found new molecular dynamic clusters that were highly enriched in the IL-17A pathway [45]. It could be argued that the inflammatory changes found are related to autoimmunity involved in the pathogenesis of T1D [46], yet the specific increase in patients with a high glyceic load compared with those individuals with lower HbA_{1c} levels points to an important role of glucose in regulating these pathways.

Although glycolytic rate after glucose injection was significantly lower in monocytes

from patients with T1D compared with HC subjects, stratification based on glycemic load revealed a specific pattern with lower baseline and maximal glycolytic activity in well-controlled patients and higher baseline and maximal glycolytic activity in patients with a high glycemic burden ($\text{HbA}_{1c} \geq 75$ mmol/mol). In the group of patients with high glycemic burden, the higher basal and maximal glycolytic activity was coupled to lower cytokine secretion. Possibly, the monocytes attempt to compensate for low cytokine secretion by upregulation of their metabolic rate. Importantly, this effect seems only to be apparent in patients with a high glycemic burden, suggesting that monocytes can tolerate hyperglycemia up to a certain extent. Another potential explanation could be glucose desensitization of monocytes from patients with T1D, although this process cannot be demonstrated or excluded based on the current study.

One could speculate that the metabolic signature of monocytes is not the main determinant of cytokine release, but instead controls different functional properties of the cell, which are known to be altered during T1D, including phagocytosis [47] and adhesion [32, 48, 49]. Furthermore, the subtle changes in glycolytic rate and oxidative phosphorylation imply other pathways beyond metabolism controlling alterations in function including cytokine secretion. Alternatively, metabolic changes other than H^+ production (ECAR) or oxygen consumption (OCR), the parameters which are measured by extracellular flux, might be altered. Recently, metabolomic analyses performed with mononuclear cells derived from children susceptible to T1D development revealed decreased intracellular levels of lipid species and other polar metabolites [50]. Possibly, changes in intracellular fluxes of specific metabolites that are induced by T1D development might also impact on the function of monocytes, leading to changed cytokine secretion levels. We were not able to observe robust metabolic differences in the transcriptomics analyses (measured before stimulation), suggesting that the metabolic changes only become apparent after a pathogenic trigger, and might not yet be obvious in unstimulated circulating monocytes.

The results of this study elicit several important questions that would require follow-up studies. Firstly, it would be important to establish whether the changes we have observed in monocytes from patients with T1D are reversible, in other words, could better glycemic control revert the changes in function and metabolism observed in patients with high HbA_{1c} levels? Secondly, since monocytes function as precursor cells for macrophages, it would be interesting to investigate whether alterations in monocytes, linked to a high glycemic load, also translate into alterations in resulting macrophages after differentiation.

In summary, our results show that circulating monocytes in the diabetic state display an inflammatory gene expression signature, which is coupled to higher glycolytic activity

and lower cytokine production upon activation. In patients with T1D, it seems that a high glyceic burden is linked to an altered ratio between metabolism and function of monocytes that may ultimately contribute to the development of various diabetes-associated complications.

Acknowledgements

We thank Anneke Hijmans (Radboud university medical center, Nijmegen, The Netherlands) and Jenny Jansen (Wageningen University, Wageningen, The Netherlands) for their technical assistance.

Funding

This work was funded by the Dutch Diabetes Foundation (2015.82.1824) and the European Foundation for the Study of Diabetes (EFSD EFSD/AZ Macrovascular Programme 2015). N.P.R received an IN-CONTROL CVON grant from the Dutch Heart Foundation (CVON2018-27) and a grant of the ERA-CVD Joint Transnational Call 2018, which is supported by the Dutch Heart Foundation (JTC2018, project MEMORY; 2018T093).

Duality of interest

No potential conflicts of interest relevant to this article were reported.

Author contributions

K.T., A.W.M.J., N.P.R, C.T. and R.S. conceived and planned the study. K.T. and A.W.M.J. carried out the study. K.T., A.W.M.J., J.P.B. and X.A.M.H.v.D. performed the experiments and analyzed the data. K.T. and X.A.M.H.v.D. wrote the first drafts of the manuscript. All authors provided critical feedback and helped to shape the research and manuscript. R.S. is the guarantor of this work and, as such, had full access to all the data in the study and takes responsibility for the integrity of the data and the accuracy of the data analysis.

References

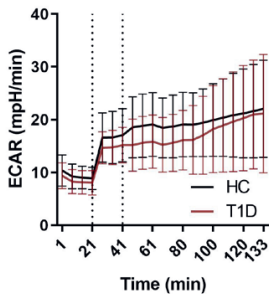
1. Ratter JM, Tack CJ, Netea MG, Stienstra R. Environmental Signals Influencing Myeloid Cell Metabolism and Function in Diabetes. *Trends in Endocrinology and Metabolism*. 2018; 29:468-480
2. Lachmandas E, Thiem K, van den Heuvel C, Hijmans A, de Galan BE, Tack CJ, Netea MG, van Crevel R, van Diepen JA. Patients with type 1 diabetes mellitus have impaired IL-1beta production in response to *Mycobacterium tuberculosis*. *European Journal of Clinical Microbiology and Infectious Diseases* 2018; 37:371-380
3. Pearson-Stuttard J, Blundell S, Harris T, Cook DG, Critchley J. Diabetes and infection: assessing the association with glycaemic control in population-based studies. *Lancet Diabetes and Endocrinology*. 2016; 4:148-158
4. Flynn MC, Kraakman MJ, Tikellis C, Lee MK, Hanssen NM, Kammoun HL, Pickering R, Dragoljevic D, Al-Sharea A, Barrett TJ, Hortle F, Byrne FL, Olzomer E, McCarthy DA, Schalkwijk CG, Forbes JM, Hoehn K, Makowski L, Lancaster GI, El-Osta A, Fisher EA, Goldberg IJ, Cooper ME, Nagareddy PR, Thomas MC, Murphy AJ. Transient Intermittent Hyperglycemia Accelerates Atherosclerosis by Promoting Myelopoiesis. *Circulation Research*. 2020; 127:877-892
5. Flynn MC, Pernes G, Lee MKS, Nagareddy PR, Murphy AJ. Monocytes, Macrophages, and Metabolic Disease in Atherosclerosis. *Frontiers in Pharmacology*. 2019; 10:666
6. Harcourt BE, Penfold SA, Forbes JM. Coming full circle in diabetes mellitus: from complications to initiation. *Nature Reviews Endocrinology*. 2013; 9:113-123
7. Hainsworth DP, Bebu I, Aiello LP, Sivitz W, Gubitosi-Klug R, Malone J, White NH, Danis R, Wallia A, Gao X, Barkmeier AJ, Das A, Patel S, Gardner TW, Lachin JM, Diabetes C, Complications Trial /Epidemiology of Diabetes I, Complications Research G. Risk Factors for Retinopathy in Type 1 Diabetes: The DCCT/EDIC Study. *Diabetes Care*. 2019; 42:875-882
8. Carey IM, Critchley JA, DeWilde S, Harris T, Hosking FJ, Cook DG. Risk of Infection in Type 1 and Type 2 Diabetes Compared With the General Population: A Matched Cohort Study. *Diabetes Care*. 2018; 41:513-521
9. Critchley JA, Carey IM, Harris T, DeWilde S, Hosking FJ, Cook DG. Glycemic Control and Risk of Infections Among People With Type 1 or Type 2 Diabetes in a Large Primary Care Cohort Study. *Diabetes Care*. 2018; 41:2127-2135
10. Corrales JJ, Almeida M, Burgo RM, Hernandez P, Miralles JM, Orfao A. Decreased production of inflammatory cytokines by circulating monocytes and dendritic cells in type 2 diabetic men with atherosclerotic complications. *Journal of Diabetes and its Complications*. 2007; 21:41-49
11. Gacka M, Dobosz T, Szymaniec S, Bednarska-Chabowska D, Adamiec R, Sadakierska-Chudy A. Proinflammatory and atherogenic activity of monocytes in type 2 diabetes. *Journal of Diabetes and its Complications*. 2010; 24:1-8
12. Giulietti A, van Etten E, Overbergh L, Stoffels K, Bouillon R, Mathieu C. Monocytes from type 2 diabetic patients have a pro-inflammatory profile. 1,25-Dihydroxyvitamin D(3) works as anti-inflammatory. *Diabetes Research and Clinical Practice*. 2007; 77:47-57
13. Marhoffer W, Stein M, Maeser E, Federlin K. Impairment of polymorphonuclear leukocyte function and metabolic control of diabetes. *Diabetes Care*. 1992; 15:256-260
14. Jha AK, Huang SC, Sergushichev A, Lampropoulou V, Ivanova Y, Loginicheva E, Chmielewski K, Stewart KM, Ashall J, Everts B, Pearce EJ, Driggers EM, Artyomov MN. Network integration of parallel metabolic and transcriptional data reveals metabolic modules that regulate

- macrophage polarization. *Immunity*. 2015; 42:419-430
15. Lachmandas E, Boutens L, Ratter JM, Hijmans A, Hooiveld GJ, Joosten LA, Rodenburg RJ, Fransen JA, Houtkooper RH, van Crevel R, Netea MG, Stienstra R. Microbial stimulation of different Toll-like receptor signalling pathways induces diverse metabolic programmes in human monocytes. *Nature Microbiology*. 2016; 2:16246
 16. Freemerman AJ, Johnson AR, Sacks GN, Milner JJ, Kirk EL, Troester MA, Macintyre AN, Goraksha-Hicks P, Rathmell JC, Makowski L. Metabolic reprogramming of macrophages: glucose transporter 1 (GLUT1)-mediated glucose metabolism drives a proinflammatory phenotype. *Journal of Biological Chemistry*. 2014; 289:7884-7896
 17. Barry JC, Shakibakho S, Durrer C, Simtchouk S, Jawanda KK, Cheung ST, Mui AL, Little JP. Hyporesponsiveness to the anti-inflammatory action of interleukin-10 in type 2 diabetes. *Scientific Reports*. 2016; 6:21244
 18. Lin K, Kools H, de Groot PJ, Gavai AK, Basnet RK, Cheng F, Wu J, Wang X, Lommen A, Hooiveld GJ, Bonnema G, Visser RG, Muller MR, Leunissen JA. MADMAX - Management and analysis database for multiple ~omics experiments. *Journal of Integrative Bioinformatics*. 2011; 8:160
 19. Irizarry RA, Hobbs B, Collin F, Beazer-Barclay YD, Antonellis KJ, Scherf U, Speed TP. Exploration, normalization, and summaries of high density oligonucleotide array probe level data. *Biostatistics*. 2003; 4:249-264
 20. Carvalho BS, Irizarry RA. A framework for oligonucleotide microarray preprocessing. *Bioinformatics*. 2010; 26:2363-2367
 21. Dai M, Wang P, Boyd AD, Kostov G, Athey B, Jones EG, Bunney WE, Myers RM, Speed TP, Akil H, Watson SJ, Meng F. Evolving gene/transcript definitions significantly alter the interpretation of GeneChip data. *Nucleic Acids Research*. 2005; 33:e175
 22. Ritchie ME, Phipson B, Wu D, Hu Y, Law CW, Shi W, Smyth GK. Limma powers differential expression analyses for RNA-sequencing and microarray studies. *Nucleic Acids Research*. 2015; 43:e47
 23. Sartor MA, Tomlinson CR, Wesselkamper SC, Sivaganesan S, Leikauf GD, Medvedovic M. Intensity-based hierarchical Bayes method improves testing for differentially expressed genes in microarray experiments. *BMC Bioinformatics*. 2006; 7:538
 24. Ritchie ME, Diyagama D, Neilson J, van Laar R, Dobrovic A, Holloway A, Smyth GK. Empirical array quality weights in the analysis of microarray data. *BMC Bioinformatics*. 2006; 7:261
 25. Liu R, Holik AZ, Su S, Jansz N, Chen K, Leong HS, Blewitt ME, Asselin-Labat ML, Smyth GK, Ritchie ME. Why weight? Modelling sample and observational level variability improves power in RNA-seq analyses. *Nucleic Acids Research*. 2015; 43:e97
 26. Benjamini Y, Hochberg Y. Controlling the False Discovery Rate - a Practical and Powerful Approach to Multiple Testing. *Journal of the Royal Statistical Society: Series B*. 1995; 57:289-300
 27. Johnson GL, Nakamura K. The c-jun kinase/stress-activated pathway: regulation, function and role in human disease. *Biochimica Biophysica Acta*. 2007; 1773:1341-1348
 28. Schonhaler HB, Guinea-Viniegra J, Wagner EF. Targeting inflammation by modulating the Jun/AP-1 pathway. *Annals of the Rheumatic Diseases*. 2011; 70 Suppl 1:i109-112
 29. Mooradian AD, Reed RL, Meredith KE, Scuderi P. Serum levels of tumor necrosis factor and IL-1 alpha and IL-1 beta in diabetic patients. *Diabetes Care*. 1991; 14:63-65
 30. Foss-Freitas MC, Foss NT, Rassi DM, Donadi EA, Foss MC. Evaluation of cytokine production from peripheral blood mononuclear cells of type 1 diabetic patients. *Annals of the New York Academy of Sciences*. 2008; 1150:290-296
 31. Ohno Y, Aoki N, Nishimura A. In vitro production of interleukin-1, interleukin-6, and tumor

- necrosis factor-alpha in insulin-dependent diabetes mellitus. *The Journal of Clinical Endocrinology and Metabolism*. 1993; 77:1072-1077
32. Devaraj S, Glaser N, Griffen S, Wang-Polagruto J, Miguelino E, Jialal I. Increased monocytic activity and biomarkers of inflammation in patients with type 1 diabetes. *Diabetes*. 2006; 55:774-779
 33. Zerr KJ, Furnary AP, Grunkemeier GL, Bookin S, Kanhere V, Starr A. Glucose control lowers the risk of wound infection in diabetics after open heart operations. *Annals of Thoracic Surgery*. 1997; 63:356-361
 34. Diabetes Complications Trial Research Group: Nathan DM, Genuth S, Lachin J, Cleary P, Crofford O, Davis M, Rand L, Siebert C. The effect of intensive treatment of diabetes on the development and progression of long-term complications in insulin-dependent diabetes mellitus. *New England Journal of Medicine*. 1993; 329:977-986
 35. Nathan DM, Cleary PA, Backlund JY, Genuth SM, Lachin JM, Orchard TJ, Raskin P, Zinman B, Diabetes C, Complications Trial/Epidemiology of Diabetes I, Complications Study Research G. Intensive diabetes treatment and cardiovascular disease in patients with type 1 diabetes. *New England Journal of Medicine*. 2005; 353:2643-2653
 36. Meza CA, La Favor JD, Kim DH, Hickner RC. Endothelial Dysfunction: Is There a Hyperglycemia-Induced Imbalance of NOX and NOS? *International Journal of Molecular Sciences*. 2019; 20:3775
 37. Oyama T, Miyasita Y, Watanabe H, Shirai K. The role of polyol pathway in high glucose-induced endothelial cell damages. *Diabetes Research and Clinical Practice*. 2006; 73:227-234
 38. Chung SS, Ho EC, Lam KS, Chung SK. Contribution of polyol pathway to diabetes-induced oxidative stress. *Journal of the American Society of Nephrology*. 2003; 14:S233-236
 39. Yamagishi S, Maeda S, Matsui T, Ueda S, Fukami K, Okuda S. Role of advanced glycation end products (AGEs) and oxidative stress in vascular complications in diabetes. *Biochimica et Biophysica Acta*. 2012; 1820:663-671
 40. Kitahara M, Eyre HJ, Lynch RE, Rallison ML, Hill HR. Metabolic activity of diabetic monocytes. *Diabetes*. 1980; 29:251-256
 41. Kelly B, O'Neill LA. Metabolic reprogramming in macrophages and dendritic cells in innate immunity. *Cell Research*. 2015; 25:771-784
 42. O'Neill LA, Pearce EJ. Immunometabolism governs dendritic cell and macrophage function. *Journal of Experimental Medicine*. 2016; 213:15-23
 43. Guha M, Mackman N. LPS induction of gene expression in human monocytes. *Cellular Signalling*. 2001; 13:85-94
 44. Biswas SK, Lopez-Collazo E. Endotoxin tolerance: new mechanisms, molecules and clinical significance. *Trends in Immunology*. 2009; 30:475-487
 45. Li L, Pan Z, Yang X. Identification of dynamic molecular networks in peripheral blood mononuclear cells in type 1 diabetes mellitus. *Diabetes, Metabolic Syndrome and Obesity*. 2019; 12:969-982
 46. Honkanen J, Nieminen JK, Gao R, Luopajarvi K, Salo HM, Ilonen J, Knip M, Otonkoski T, Vaarala O. IL-17 immunity in human type 1 diabetes. *Journal of Immunology*. 2010; 185:1959-1967
 47. Katz S, Klein B, Elian I, Fishman P, Djaldetti M. Phagocytotic activity of monocytes from diabetic patients. *Diabetes Care*. 1983; 6:479-482
 48. Setiadi H, Wautier JL, Courillon-Mallet A, Passa P, Caen J. Increased adhesion to fibronectin and Mo-1 expression by diabetic monocytes. *Journal of Immunology*. 1987; 138:3230-3234
 49. Kunt T, Forst T, Fruh B, Flohr T, Schneider S, Harzer O, Pfutzner A, Engelbach M, Lobig M, Beyer J. Binding of monocytes from normolipidemic hyperglycemic patients with type 1 diabetes to

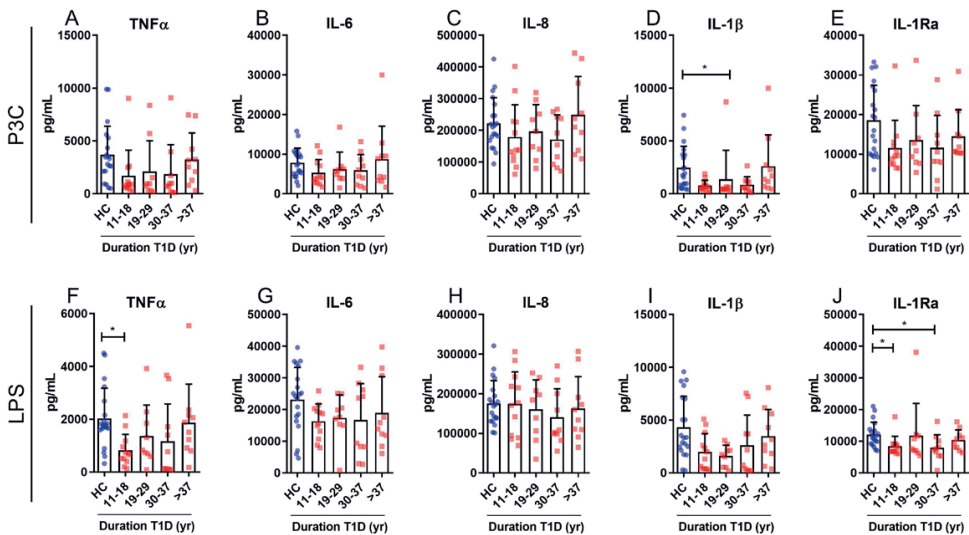
- endothelial cells is increased in vitro. *Experimental and Clinical Endocrinology and Diabetes*. 1999; 107:252-256
50. Sen P, Dickens AM, Lopez-Bascon MA, Lindeman T, Kemppainen E, Lamichhane S, Ronkko T, Ilonen J, Toppari J, Veijola R, Hyoty H, Hyotylainen T, Knip M, Oresic M. Metabolic alterations in immune cells associate with progression to type 1 diabetes. *Diabetologia*. 2020; 63:1017-1031

Supplemental material



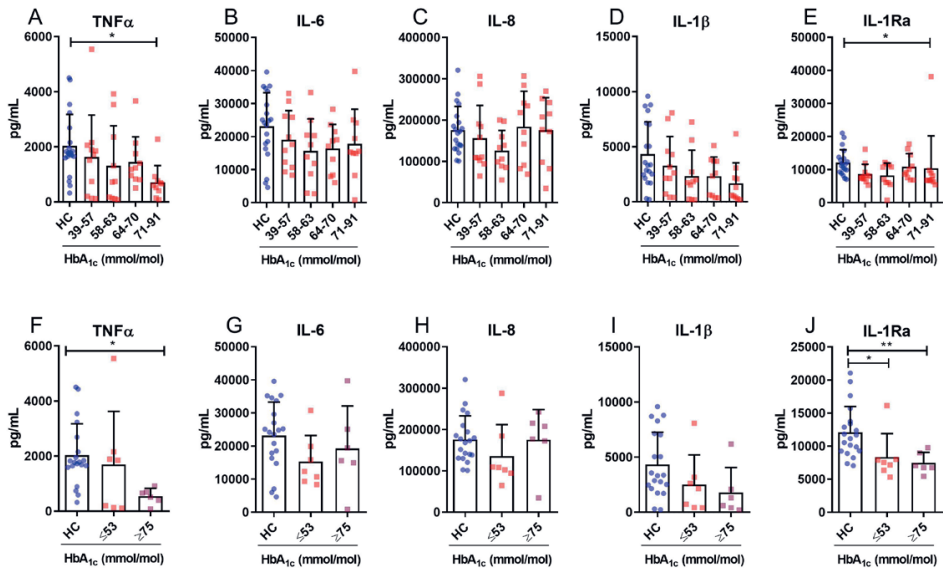
Supplemental Figure 1. Extracellular acidification rate from patients with T1D and HC subjects.

The extracellular acidification rate of CD14⁺ monocytes isolated from patients with T1D and HC subjects was measured basally, after injection of glucose (first dotted line) and after injection of LPS (second dotted line).



Supplemental Figure 2. Cytokine secretion in monocytes from patients with T1D and HC subjects treated with LPS or P3C and stratified for duration of T1D.

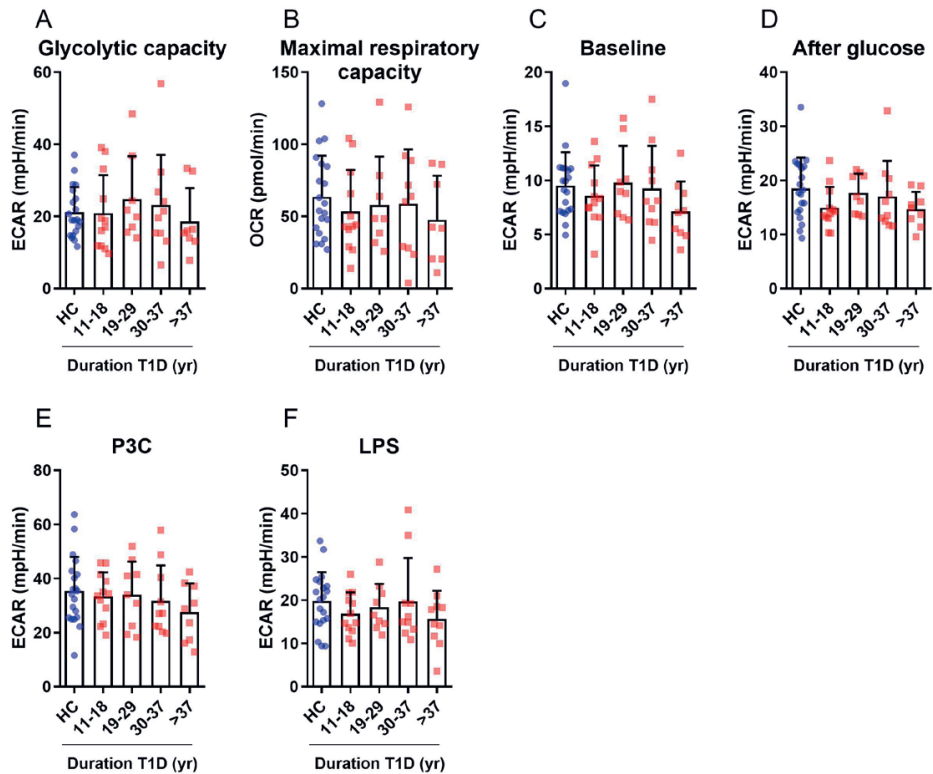
CD14⁺ monocytes were stimulated with P3C or LPS and TNF α (**A** and **F**, $p = 0.0373$), IL-6 (**B** and **G**), IL-8 (**C** and **H**), IL-1 β (**D**, $p = 0.0324$ and **I**) and IL-1Ra (**E** and **J**, $p = 0.0185$ and $p = 0.0354$) were measured. Quartiles of equal size were created for patients with T1D based on duration of diabetes. Duration quartiles: HC: $n = 20$; T1D quartiles: $n = 10-12$; * $p < 0.05$.



Supplemental Figure 3. Cytokine secretion in monocytes from patients with T1D and HC subjects treated with LPS and stratified for HbA_{1c} levels.

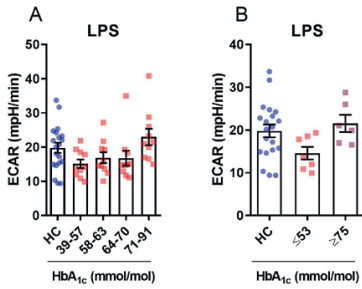
CD14⁺ monocytes were stimulated with LPS, after which TNF α , IL-6, IL-8, IL-1 β and IL-1Ra were measured. Quartiles of equal size were created for patients with T1D based on HbA_{1c} levels (A, $p = 0.0179$; B; C; D; E, $p = 0.0220$), and two groups with clinically relevant HbA_{1c} levels (≤ 53 and ≥ 75 mmol/mol) were compared against HC subjects (F, $p = 0.0184$; G; H; I; J, $p = 0.0276$ and $p = 0.0090$). HbA_{1c} quartiles HC: $n = 20$; T1D quartiles: $n = 10-11$; HbA_{1c} ≤ 53 mmol/mol: $n = 7$, HbA_{1c} ≥ 75 : $n = 6$. * $p < 0.05$, ** $p < 0.01$.

3



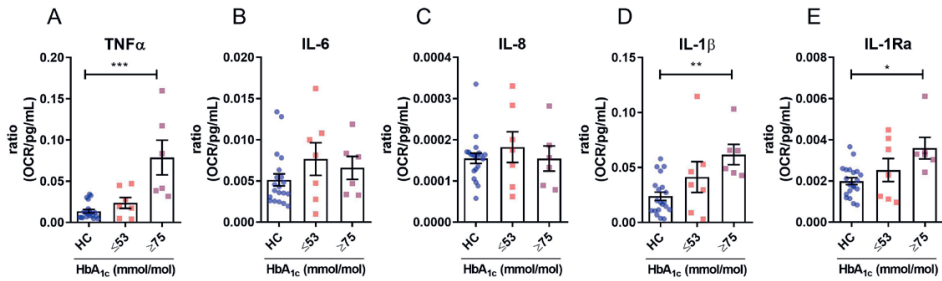
Supplemental Figure 4. Extracellular flux of monocytes from patients with T1D and HC subjects stratified for duration of T1D.

The extracellular flux of monocytes isolated from patients with T1D and HC subjects was measured. Values of patients with T1D are shown grouped into equally sized quartiles based on duration of diabetes and compared with values of HC subjects on glycolytic capacity (A), maximal respiratory capacity (B), ECAR at baseline (C), ECAR after glucose injection (D), ECAR after P3C stimulation (E) or ECAR after LPS stimulation (F). Quartiles; HC: n = 20, T1D quartiles: n = 10-11.



Supplemental Figure 5. Extracellular flux of monocytes from patients with T1D and HC subjects stratified for HbA_{1c}.

Extracellular flux of monocytes isolated from patients with T1D and HC subjects was measured after injection of LPS. Values of patients with T1D are shown grouped into equally sized quartiles based on HbA_{1c} levels and compared with values of HC subjects. Values of patients with T1D that fall within two groups of extremes are compared with values of HC subjects. HbA_{1c} quartiles; HC subjects: n = 20, T1D quartiles: n = 10-11, HbA_{1c} ≤53 mmol/mol: n = 7, HbA_{1c} ≥75 mmol/mol: n = 6.



Supplemental Figure 6. Monocytes of patients with poor glycaemic control have higher OCR-to-cytokine secretion ratios.

Oxygen consumption rates (OCR) were measured by extracellular flux in CD14⁺ cells for 90 consecutive minutes after direct stimulation with P3C. Cytokine secretion was measured after 24 hour stimulation with P3C. The ratio between OCR and cytokine secretion was calculated and is shown for TNFα (A, $p = 0.0011$), IL-6 (B), IL-8 (C), IL-1β (D, $p = 0.0106$), IL-1Ra (E, $p = 0.0292$). HbA_{1c} ≤53 mmol/mol: n = 7, HbA_{1c} ≥75 mmol/mol: n = 6; * $p < 0.05$, ** $p < 0.01$, *** $p < 0.001$.

Supplementary Table 1. Primer sequences for real-time PCR

Gene	Forward primer	Reverse primer	Measured efficiency	Measured R ²
B2M	GATGAGTATGCCTGCCGTGT	CTGCTTACATGTCTCGATCCCA	98.8%	0.995
JUN	AACAGGTGGCACAGCTTAAAC	CAACTGCTCGTTAGCATGAG	91.5%	0.998
CXCL5	AGCTGCGTTGCGTTTGTTTAC	TGGCGAACACTTGCAGATTAC	100.4%	0.991



The role of uncoupling protein 2 in macrophages and its impact on obesity-induced adipose tissue inflammation and insulin resistance

Xanthe A.M.H. van Dierendonck^{1,2}, Tiphaine Sancerni³, Marie-Clotilde Alves-Guerra³, Rinke Stienstra^{1,2}

¹Nutrition, Metabolism, and Genomics Group, Division of Human Nutrition and Health, Wageningen University, Wageningen, the Netherlands

²Department of Internal Medicine, Radboud University Nijmegen Medical Centre, Nijmegen

³Université de Paris, Institut Cochin, INSERM, CNRS F-75014 PARIS, France

Abstract

The development of a chronic, low-grade inflammation originating from adipose tissue in obese subjects is widely recognized to induce insulin resistance, leading to the development of type 2 diabetes. The adipose tissue microenvironment drives specific metabolic reprogramming of adipose tissue macrophages, contributing to the induction of tissue inflammation. Uncoupling protein 2 (UCP2), a mitochondrial anion carrier, is thought to separately modulate inflammatory and metabolic processes in macrophages and is up-regulated in macrophages in the context of obesity and diabetes. Here, we investigate the role of UCP2 in macrophage activation in the context of obesity-induced adipose tissue inflammation and insulin resistance. Using a myeloid-specific knockout of UCP2 (*Ucp2^{ΔLysM}*), we found that UCP2 deficiency significantly increases glycolysis and oxidative respiration, both unstimulated and after inflammatory conditions. Strikingly, fatty acid loading abolished the metabolic differences between *Ucp2^{ΔLysM}* macrophages and their floxed controls. Furthermore, *Ucp2^{ΔLysM}* macrophages show attenuated pro-inflammatory responses toward Toll-like receptor-2 and -4 stimulation. To test the relevance of macrophage-specific *Ucp2* deletion *in vivo*, *Ucp2^{ΔLysM}* and *Ucp2^{fl/fl}* mice were rendered obese and insulin resistant through high-fat feeding. Although no differences in adipose tissue inflammation or insulin resistance was found between the two genotypes, adipose tissue macrophages isolated from diet-induced obese *Ucp2^{ΔLysM}* mice showed decreased TNF α secretion after *ex vivo* lipopolysaccharide stimulation compared with their *Ucp2^{fl/fl}* littermates. Together, these results demonstrate that although UCP2 regulates both metabolism and the inflammatory response of macrophages, its activity is not crucial in shaping macrophage activation in the adipose tissue during obesity-induced insulin resistance.

Introduction

The occurrence of obesity and related metabolic disturbances, including insulin resistance and development of type 2 diabetes, have risen to epidemic proportions [1,2]. The chronic inflammatory processes that closely associate with a state of obesity are now widely recognized as important drivers of insulin resistance that may eventually evolve into type 2 diabetes [3]. In particular the activation of macrophages in expanding adipose tissue has been linked to this chronic, low-grade inflammation [3–7].

Dynamic changes in tissue microenvironments can drive specific metabolic alterations in tissue-resident immune cells in an attempt to accommodate appropriate changes in immune cell functioning [8]. It is well known that modifications in metabolic signatures are closely related to immune cell functioning, demonstrated for instance by pro-inflammatory immune cells that rely on glycolytic pathways [9]. Activation of macrophages in the context of obese adipose tissue was found to lead to unique changes in the metabolic signature of these adipose tissue macrophages (ATMs) [5,7]. This “metabolic activation” of macrophages was also linked to functional changes, such as the release of inflammatory cytokines [10]. It is clear that modifications in metabolic signatures are crucial for appropriate immune cell functioning, yet might also drive immune cell dysfunction [11]. Hence, specific metabolic reprogramming of adipose tissue macrophages driven by the lipid-enriched adipose tissue microenvironment during obesity might contribute to increased adipose tissue inflammation.

Uncoupling protein 2 (UCP2) is a mitochondrial carrier protein belonging to the SLC25 family of transporters [12]. Although *Ucp2* mRNA is widely expressed throughout different tissues in mice, UCP2 protein can only be detected in spleen, lung, stomach, adipose tissue and isolated immune cells including macrophages [13–15]. These findings underline the clear discrepancy between mRNA expression and protein expression [16]. Potentially, the presence of UCP2 protein in immune-cell rich tissues such as spleen, lung and adipose tissue could largely be attributable to the infiltration of immune cells. UCP2 shows a 59% homology to its family member uncoupling protein 1 (UCP1), known for robust uncoupling activity, although any uncoupling activity attributed to UCP2 is likely not physiological [12,17–19]. Nonetheless, in line with its presence in immune cells, UCP2 appears to play an important role in immune regulation, with UCP2 knockout mice showing increased survival after infections accompanied by an up-regulation in pro-inflammatory cytokines [20,21].

UCP2 has been suggested to regulate metabolic pathways, determining the oxidation of glucose versus fatty acids in different cell types *in vitro* [22,23] and in colorectal cancer

cells *in vivo* [24]. Possibly, UCP2 regulates cellular metabolism by being involved in the export of four-carbon substrates out of the mitochondria [25]. In addition to its proposed metabolic role, several SNPs in UCP2 were found to be related to obesity and type 2 diabetes [26–32].

Due to its involvement in both immune cell functioning and defining cellular metabolism of glucose versus fatty acids, UCP2 potentially provides an interesting target in elucidating the molecular mechanisms underlying immunometabolic reprogramming and activation of macrophages in the context of obesity-induced adipose tissue inflammation and insulin resistance. To investigate whether UCP2 plays a role in activation of adipose tissue macrophages, we first set out to determine the role of UCP2 in macrophages during inflammatory activation. Secondly, we evaluated the consequences of the absence of UCP2 in macrophages on the development of HFD-induced obesity and its complications including adipose tissue inflammation, glucose tolerance and insulin resistance.

Our results reveal that UCP2 deficiency drives a distinct increase in glycolytic and oxidative metabolism in activated macrophages. Furthermore, specific *Ucp2* deletion attenuates pro-inflammatory activation in macrophages but does not alter the development of obesity-induced adipose tissue inflammation and insulin resistance.

Results

Regulation of uncoupling protein 2 in macrophages during obesity and diabetes

We compared the regulation of UCP2 in three adipose tissue macrophage models: ATMs isolated from mice fed a high-fat diet (HFD) versus a low-fat diet (LFD) [10]; bone marrow-derived macrophages (BMDMs) co-cultured with obese versus lean adipose tissue; and human ATMs isolated from obese diabetic patients versus obese nondiabetic patients [33]; (**Figure 1A** and **Figure S1**). In all three macrophage-related models, *Ucp2* mRNA expression was up-regulated. Furthermore, after 10 to 16 weeks of HFD feeding in mice, *Ucp2* expression was increased in the adipose tissue (**Figure 1B**). These levels likely correspond with the influx of immune cells into the adipose tissue, because increased *Ucp2* expression in the adipose tissue of HFD-fed versus LFD-fed (Ctrl) mice is mainly attributable to the stromal vascular fraction, including ATMs, and not to adipocytes (**Figure 1C**). To be able to determine the role of UCP2 in regulating macrophage metabolism and activation in more detail, we generated mice with a myeloid-specific deletion of UCP2, using the Cre/loxP system coupled to the *Lys2* (*LysM*) promoter, resulting in *Ucp2*^{Δ*LysM*} mice and their floxed control littermates (*Ucp2*^{*fl/fl*}). The myeloid-specific deletion of UCP2 significantly silenced protein expression of UCP2 in BMDMs derived from *Ucp2*^{Δ*LysM*} mice compared to

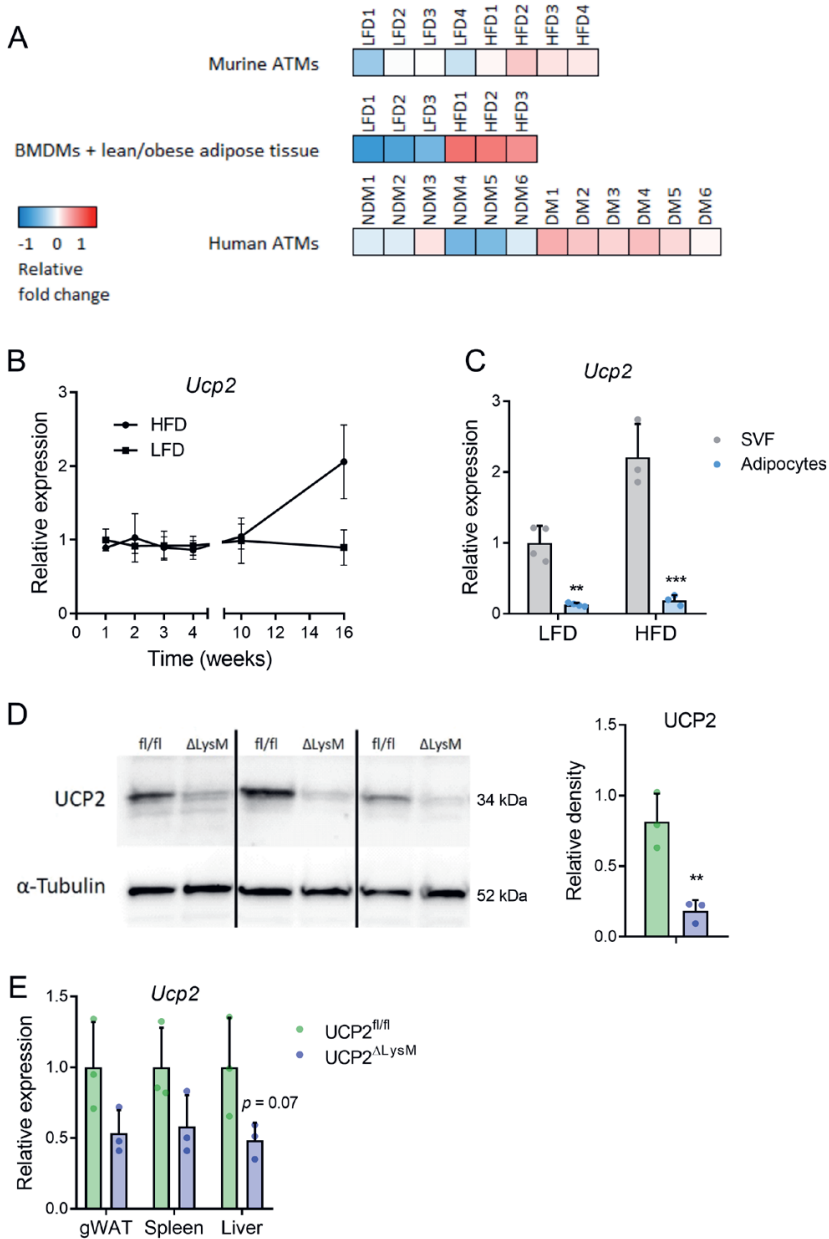


Figure 1. Regulation of uncoupling protein 2 in macrophages during obesity and diabetes.

(A) Relative fold changes of *Ucp2* in adipose tissue macrophages isolated from lean and obese mice ($n = 4$ mice per group); bone marrow-derived macrophages co-cultured with lean or obese adipose tissue explants ($n = 3$ replicates per group) and CD14⁺ adipose tissue macrophages isolated from obese subjects with (DM) or without (NDM) type 2 diabetes ($n = 6$ subjects per group). Per dataset, group means were significantly different ($p < 0.05$, $p < 0.01$ and $p < 0.05$ respectively). (B) Relative expression of *Ucp2* in gonadal adipose tissue of C57Bl/6J mice fed a LFD or HFD for 1, 2, 3, 4, 10 and 16 weeks ($n = 6$ per diet). (C) Relative expression of *Ucp2* in stromal vascular

and adipocyte fractions of C57Bl/6J mice fed a LFD or HFD for 7 days (n= 3-4). **(D)** Protein expression of UCP2 in *Ucp2*^{ΔLysM} and *Ucp2*^{fl/fl} bone-marrow derived macrophages. **(E)** Relative mRNA expression of *Ucp2* measured in gWAT, spleen and liver of *Ucp2*^{ΔLysM} and *Ucp2*^{fl/fl} mice (n = 3). Data are presented as mean ± SD. BMDM: bone marrow-derived macrophage, ATM: adipose tissue macrophage, NDM: no diabetes mellitus, DM: diabetes mellitus, HFD: high-fat diet, LFD: low-fat diet, SVF: stromal vascular fraction, gWAT: gonadal white adipose tissue. **, $p < 0.01$; ***, $p < 0.001$.

Ucp2^{fl/fl} control mice (**Figure 1D**) and resulted in a nonsignificant trend toward decreased *Ucp2* mRNA expression in macrophage-rich tissues such as gonadal adipose tissue, spleen and liver (**Figure 1E**).

Deficiency of UCP2 increases glycolytic and oxidative metabolism in macrophages, which is attenuated by fatty acids

To understand the impact of UCP2 on cellular metabolism, we used extracellular flux assays. Basal glycolysis (**Figure 2A**) and maximal glycolytic capacity (**Figure 2B**) were significantly increased in *Ucp2*^{ΔLysM} versus *Ucp2*^{fl/fl} macrophages, both during control conditions and during TLR-4 agonist LPS-induced inflammation. Furthermore, relative mRNA expression of the glycolytic enzyme *Pfkfb3* was increased in *Ucp2*^{ΔLysM} macrophages after LPS treatment, as was the production of lactate (**Figure S2, A and B**). Basal (**Figure 2C**) and maximal (**Figure 2D**) respiration were significantly increased in *Ucp2*^{ΔLysM} macrophages compared to *Ucp2*^{fl/fl} cells during control conditions, and only basal respiration followed this pattern after LPS-induced inflammation. Strikingly, fatty acid loading abolished all differences observed in basal and maximal glycolysis (**Figure 2, E and F**) and respiration (**Figure 2, G and H**) between *Ucp2*^{ΔLysM} and *Ucp2*^{fl/fl} macrophages, in addition to abolishing differences in *Cpt1a* expression (**Figure S2C**). Hence, UCP2 deficiency abolishes OA:PA-stimulated increases in glycolysis and maximal respiration.

Lack of UCP2 specifically attenuates macrophage response to inflammatory activation

Obesity-induced low-grade adipose tissue inflammation is linked to inflammatory activation of macrophages in adipose tissue with an important contribution of TLR-2 and TLR-4 receptor activation in driving metabolic inflammation [34]. To study the role of UCP2 in macrophage activation, we tested the inflammatory response of *Ucp2*^{ΔLysM} and *Ucp2*^{fl/fl} macrophages toward TLR-2 receptor agonist Pam3CysK (P3C) and TLR-4 receptor agonist lipopolysaccharide (LPS) on both a transcriptional and functional level (**Figure 3, A-E** and **Figure 4, A-D**). Treatment for 6 or 24 h with either LPS or P3C significantly increased the mRNA expression and protein secretion of all measured cytokines. Although most differences were relatively subtle, the pro-inflammatory response was generally attenuated in *Ucp2*^{ΔLysM} versus *Ucp2*^{fl/fl} macrophages treated with LPS, illustrated by lower

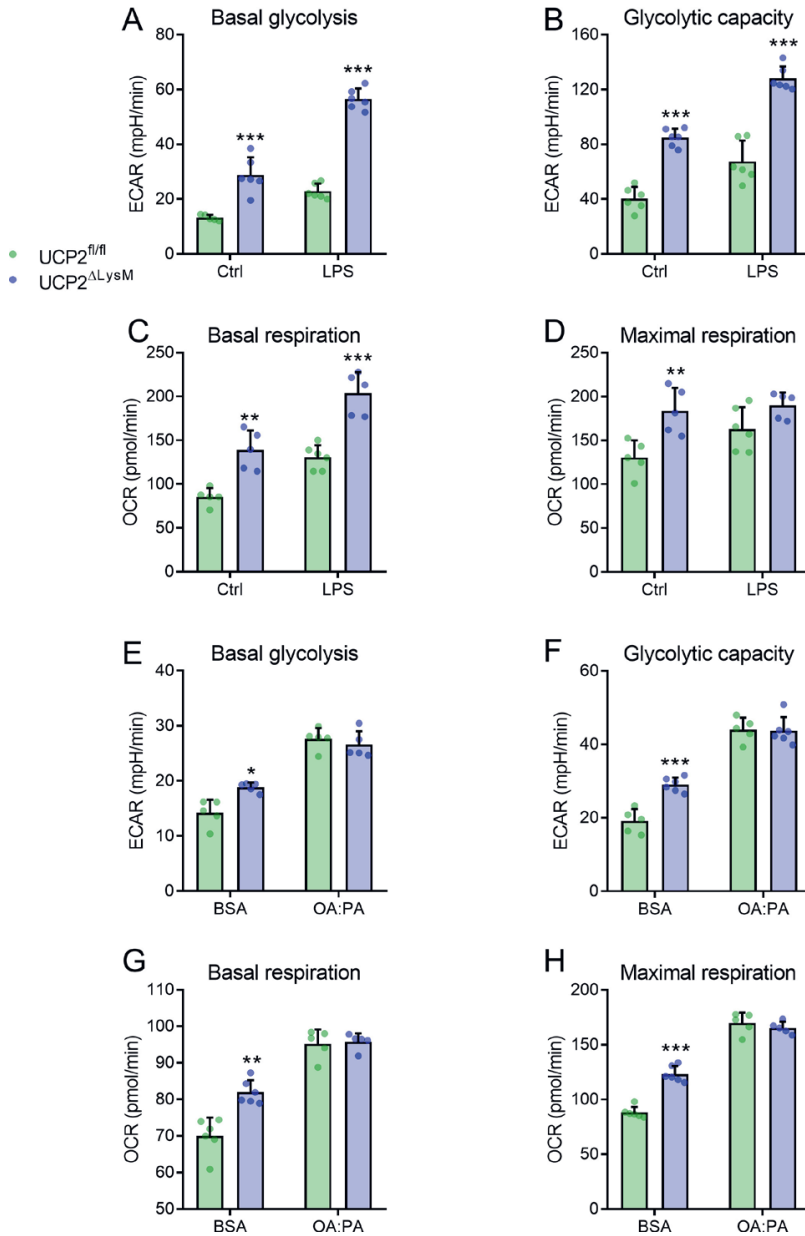


Figure 2. Deficiency of UCP2 increases glycolytic and oxidative metabolism in macrophages; metabolic differences are attenuated by fatty acid influx.

Basal glycolysis (A) and glycolytic capacity (B) based on extracellular acidification rates of *Ucp2^{fl/fl}* and *Ucp2^{ΔLysM}* BMDMs, treated with or without LPS for 24h and subjected to glycolytic stress tests. Basal (C) and maximal respiration (D) based on oxygen consumption rates of *Ucp2^{fl/fl}* and *Ucp2^{ΔLysM}* BMDMs, treated with or without LPS for 24h and subjected to mitochondrial stress tests. Basal glycolysis (E) and glycolytic capacity (F) based on extracellular acidification rates of *Ucp2^{fl/fl}* and *Ucp2^{ΔLysM}* BMDMs treated with oleate:palmitate conjugated to

BSA or BSA alone for 24h and subjected to glycolytic stress tests. Basal (E) and maximal respiration (F) based on oxygen consumption rates of *Ucp2^{fl/fl}* and *Ucp2^{ΔLysM}* BMDMs treated with oleate:palmitate conjugated to BSA or BSA alone for 24h and subjected to mitochondrial stress tests. Data presented as mean ± standard deviation for representative runs. ECAR: extracellular acidification rate, OCR: oxygen consumption rate, Ctrl: vehicle control, LPS: lipopolysaccharide, BSA: bovine serum albumin, OA:PA: mixture of oleic acid and palmitic acid (2:1). *, $p < 0.05$; **, $p < 0.01$; ***, $p < 0.001$.

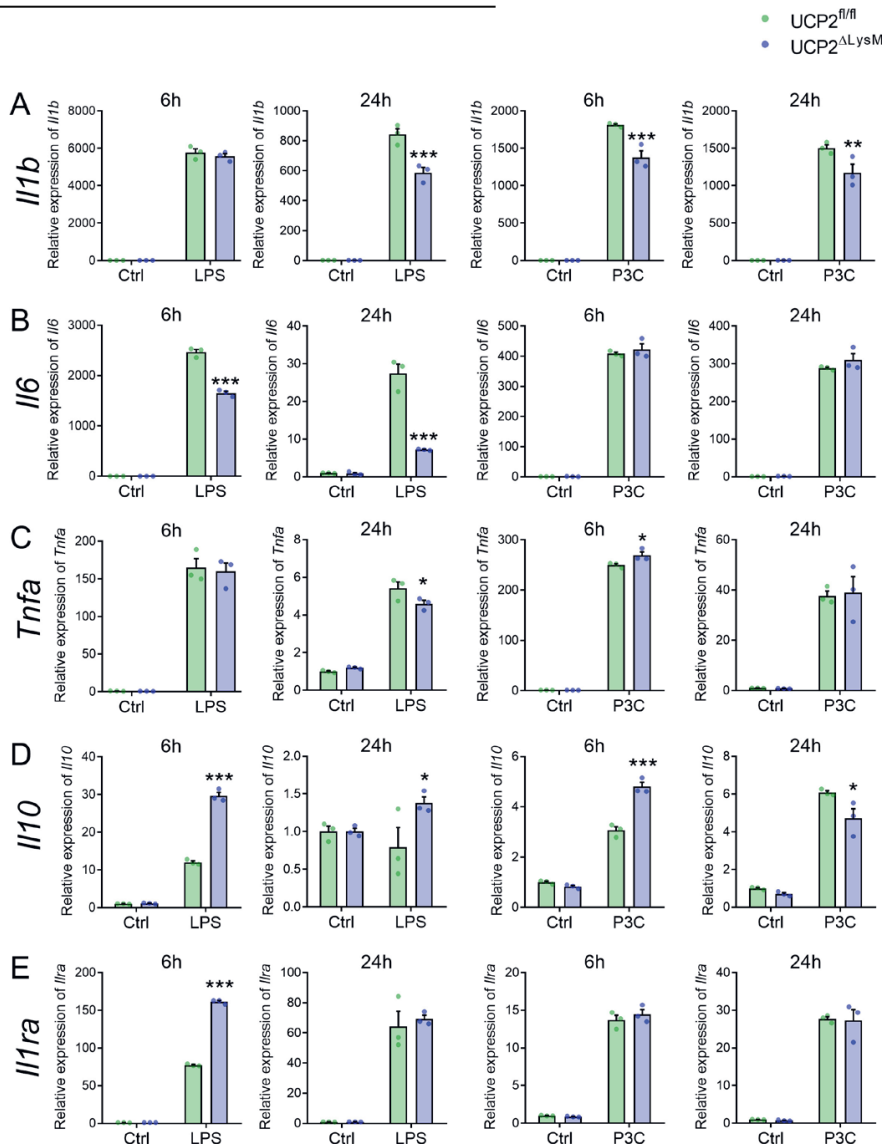


Figure 3. Lack of UCP2 specifically attenuates transcriptional pro-inflammatory activation of macrophages.

Relative expression of *Il1b* (A), *Il6* (B), *Tnfa* (C), *Il10* (D) and *Il1ra* (E) in *Ucp2^{fl/fl}* and *Ucp2^{ΔLysM}* BMDMs treated with 10 ng/mL LPS or 5 μg/mL P3C for 6 or 24h. Data are presented as mean ± SD. Ctrl: vehicle control, LPS:

lipopolysaccharide, P3C: Pam3CysK. *, $p < 0.05$; ***, $p < 0.001$.

Il1b expression after 24 h and lower *Il6* expression for both time points; *Tnfa* expression was not different (**Figure 4, A-C**). For P3C, the differential effect was seen in *Il1b* expression for both time points. Accordingly, anti-inflammatory *Il10* expression was mostly up-regulated in *Ucp2^{ΔLysM}* compared to *Ucp2^{fl/fl}* macrophages, whereas *Il1ra* was clearly up-regulated after 6 h following LPS stimulation (**Figure 3D**). On protein level, macrophage-specific deficiency of UCP2 generally subtly decreased the secretion of inflammatory cytokines IL6 and TNF α following LPS treatment while increasing IL10 secretion (**Figure 4, A-D**).

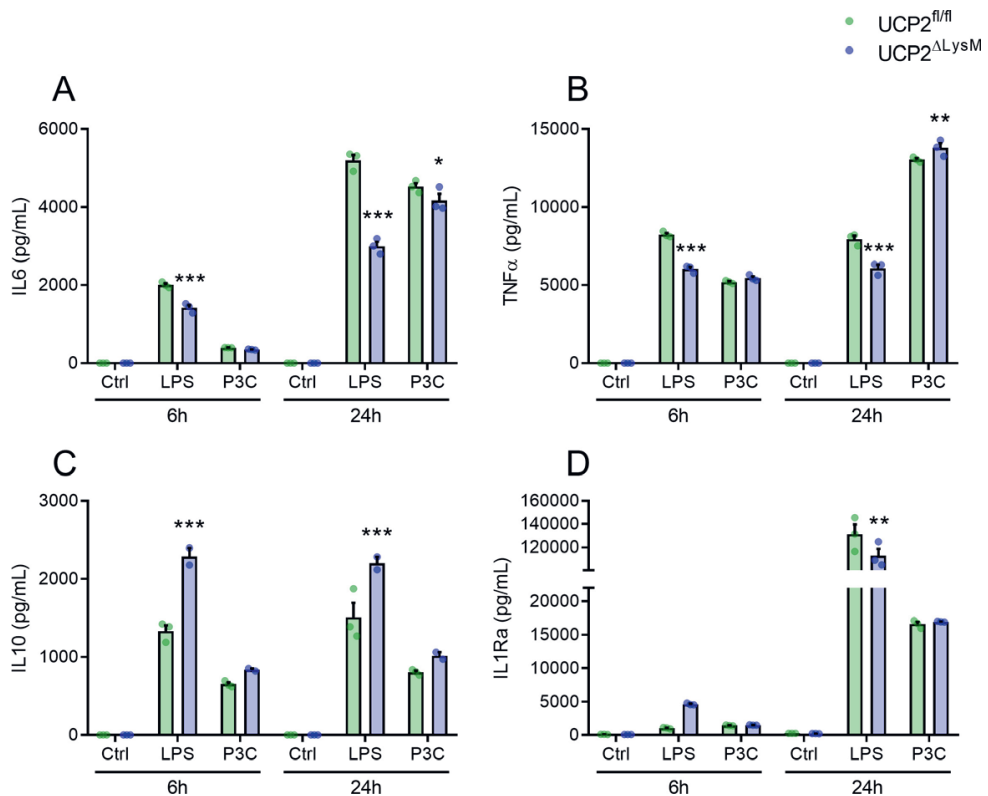


Figure 4. Lack of UCP2 modulates cytokine secretion toward a less pro-inflammatory phenotype in macrophages.

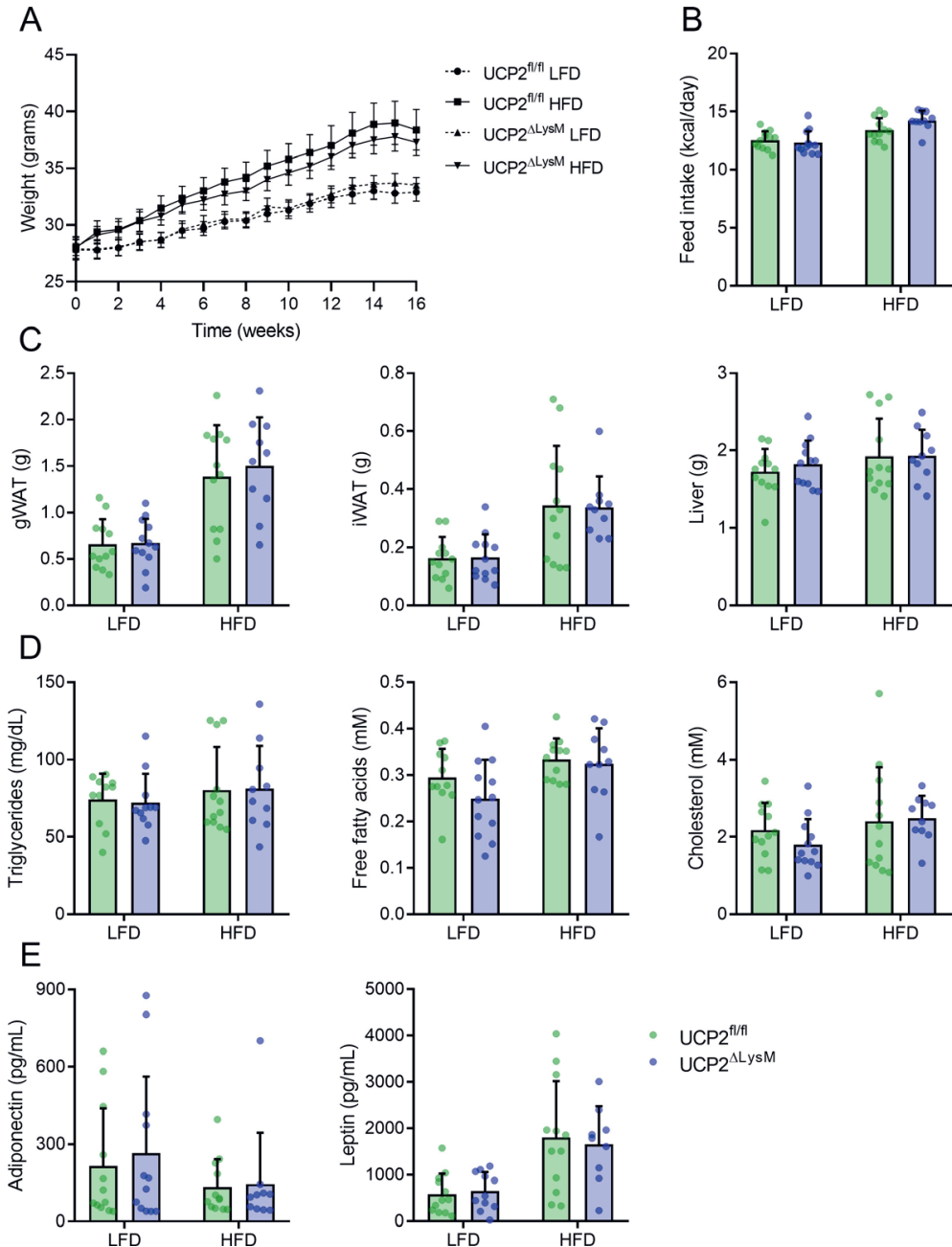
Production of IL6 (A), TNF α (B), IL10 (C) and IL1Ra (D) in *Ucp2^{fl/fl}* and *Ucp2^{ΔLysM}* BMDMs treated with 10 ng/mL LPS or 5 μg/mL P3C for 6 or 24 h. Data are presented as mean \pm SD. Ctrl: vehicle control, LPS: lipopolysaccharide, P3C: Pam3CysK. *, $p < 0.05$; **, $p < 0.01$; ***, $p < 0.001$.

Myeloid-specific UCP2 deficiency affects adipose tissue macrophage activation without affecting overall adipose tissue inflammation

Our next step was to test whether UCP2 in macrophages impacts adipose tissue inflammation and insulin resistance in an *in vivo* model of high-fat diet-induced obesity (DIO). *Ucp2*^{ΔLysM} and their *Ucp2*^{fl/fl} littermates were rendered obese and insulin resistant by being fed a high-fat diet for 16 weeks, using a low-fat diet as control. No differences between the two genotypes were found in body weight gain (**Figure 5A**), feed intake (**Figure 5B**) or adipose tissue and liver weights (**Figure 5C** and **Figure S3**). Additionally, plasma levels of triglycerides, nonesterified fatty acids, cholesterol, adiponectin and leptin did not show any differences between *Ucp2*^{ΔLysM} and *Ucp2*^{fl/fl} mice (**Figure 5, D and E**).

Subsequently, we isolated ATMs from the *Ucp2*^{ΔLysM} and *Ucp2*^{fl/fl} mice fed a high-fat diet. To compare these to macrophages that did not reside in a lipid-rich microenvironment, we additionally isolated macrophages from the peritoneum of these mice and measured the release of inflammatory cytokines of both types of macrophages unstimulated, or upon an inflammatory stressor (LPS). In the *Ucp2*^{ΔLysM} ATMs, no decrease was found in IL6 (**Figure 6A**), but a significant decrease was found in the levels of TNFα (**Figure 6B**) and IL1Ra (**Figure 6D**), and a similar trend for IL10 (**Figure 6C**) after LPS stimulation. In contrast, both IL6 and TNFα levels remained unchanged in peritoneal macrophages isolated from *Ucp2*^{ΔLysM} versus *Ucp2*^{fl/fl} mice after *ex vivo* LPS stimulation (**Figure 6, E and F**).

Next, we assessed inflammation of total adipose tissue. Flow cytometry of the stromal vascular fraction derived from gonadal adipose tissue (gWAT) of obese *Ucp2*^{ΔLysM} and *Ucp2*^{fl/fl} mice revealed that there was no relative difference in general (F4/80⁺) or pro-inflammatory (F4/80⁺CD11c⁺) macrophage populations between the two genotypes (**Figure 7A**). Additionally, relative mRNA expression of macrophage markers *Cd68* and *Adgre1* (F4/80) did not differ significantly (**Figure 7B**). Moreover, mRNA expression of cytokines involved in the inflammatory response of adipose tissue (*Il1b*, *Tnfa*, *Il6* and *Il10*) was not found to be significantly altered between the genotypes (**Figure 7C**), as was the release of IL6 and IL10 (**Figure 7D**). The density of crown-like structures (CLS) stained for macrophage marker F4/80 did not differ between obese adipose tissue from *Ucp2*^{ΔLysM} versus their *Ucp2*^{fl/fl} littermates (**Figure 7E**). Also, no differences were found in the mRNA expression of inflammatory markers in the liver, nor any differences in liver histology (**Figure S4, A-C**). On a systemic level, we found no significant differences in either insulin tolerance (**Figure 8, A and B**) or glucose tolerance (**Figure 8, C and D**) in *Ucp2*^{ΔLysM} and *Ucp2*^{fl/fl} mice. Furthermore, nonfasted levels of both insulin and glucose did not differ significantly between the two genotypes, either after low-fat or high-fat diet feeding (**Figure 8, E and F**).



4

Figure 5. Macrophage specific UCP2 deletion does not lead to general differences in LFD or HFD-fed mice. Body weight (A), feed intake (B), gWAT, iWAT and liver weight (C), plasma concentrations of triglycerides, free fatty acids, cholesterol (D), adiponectin and leptin (E) of *Ucp2*^{fl/fl} and *Ucp2*^{ΔLysM} mice (n = 24 *Ucp2*^{fl/fl} and 22 *Ucp2*^{ΔLysM}) fed either LFD or HFD for 16 weeks. Data are presented as mean ± SD or mean ± SEM (A). LFD: low-fat diet, HFD: high-fat diet, gWAT: gonadal white adipose tissue, iWAT: inguinal white adipose tissue.

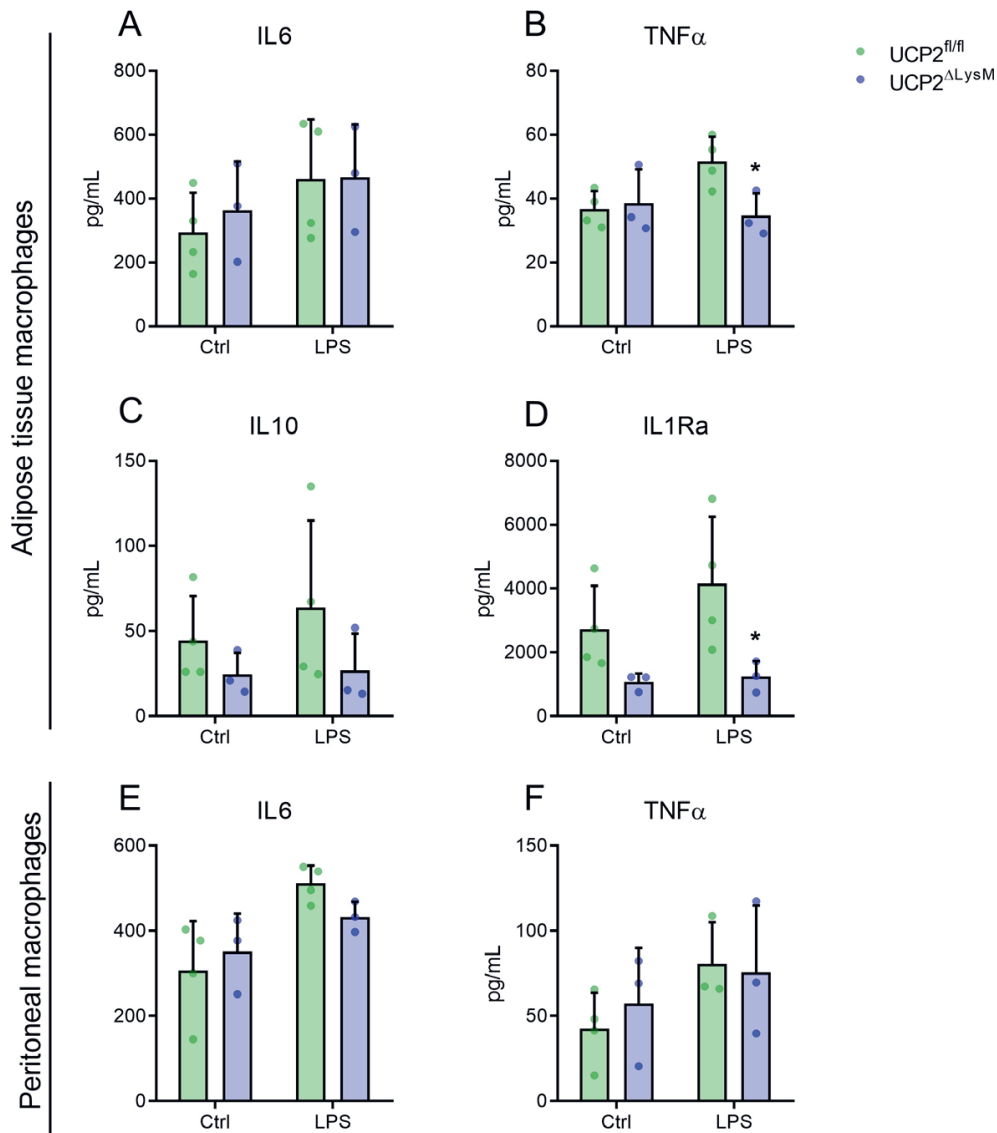


Figure 6. UCP2 deficiency impacts cytokine secretion in adipose tissue macrophages, but not peritoneal macrophages in HFD-fed mice.

Production of IL6 (A), TNFα (B), IL1ra (C) and IL10 (D) in adipose tissue macrophages and IL6 (E) and TNFα (F) in peritoneal macrophages isolated from *Ucp2*^{fl/fl} and *Ucp2*^{ΔLysM} mice fed a HFD for 16 weeks and treated with LPS or vehicle (Ctrl) for 24h. Data are normalized to DNA concentrations per well and are presented as mean ± SD. Ctrl: control, LPS: lipopolysaccharide. *, $p < 0.05$.

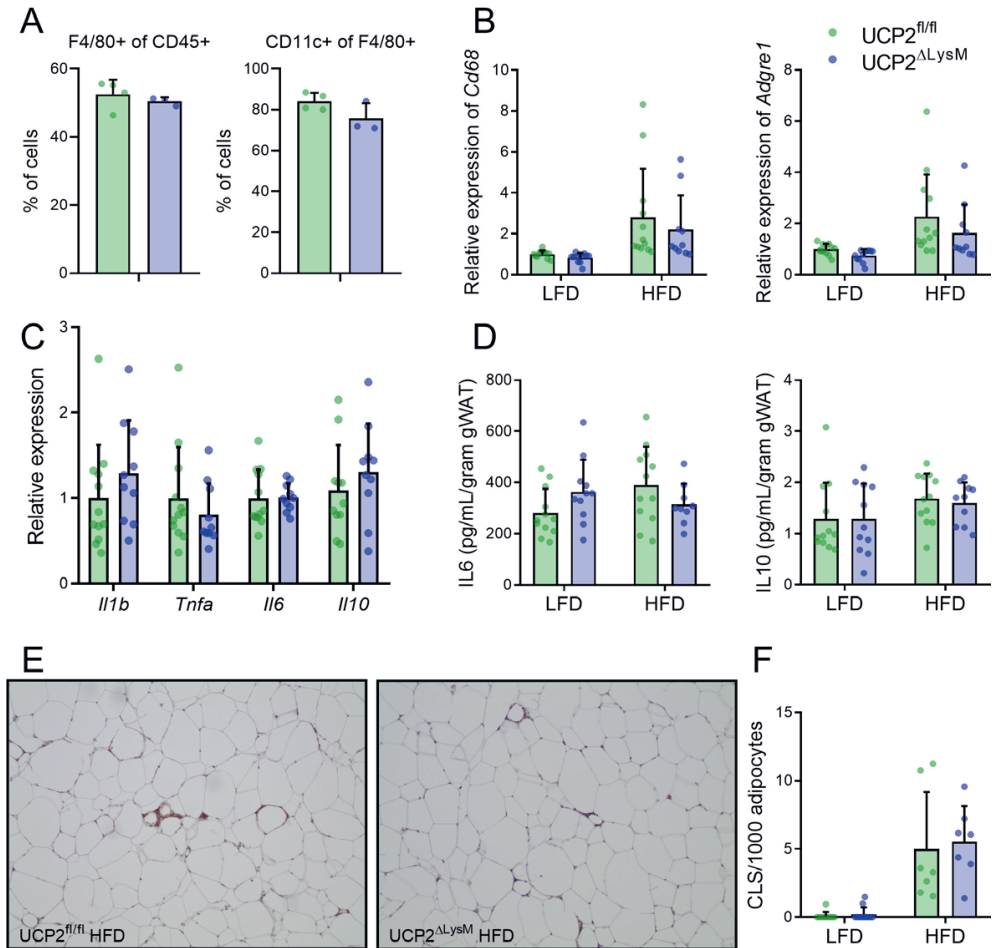


Figure 7. Macrophage-specific UCP2 deletion does not impact adipose tissue inflammation after HFD feeding.

(A) Flow cytometry analysis of CD45+F4/80+ cells and CD45+F4/80+CD11c+ cells in the stromal vascular fractions isolated from $Ucp2^{fl/fl}$ and $Ucp2^{\Delta LysM}$ mice fed a HFD for 16 weeks. Relative mRNA expression of immune cell markers *Cd68* and *Adgre1* (B), relative expression of inflammatory cytokines *Il1b*, *Tnfa*, *Il6* and *Il10* (C, only for HFD) and production of IL6 and IL10 in gWAT from $Ucp2^{fl/fl}$ and $Ucp2^{\Delta LysM}$ mice fed either a LFD or a HFD for 16 weeks (D). (E and F) Density of crown-like structures (CLS) in gWAT F4/80-stained coupes from $Ucp2^{fl/fl}$ and $Ucp2^{\Delta LysM}$ mice fed a HFD for 16 weeks. Data are presented as mean \pm SD. LFD: low-fat diet, HFD: high-fat diet, gWAT: gonadal white adipose tissue, CLS: crown-like structure.

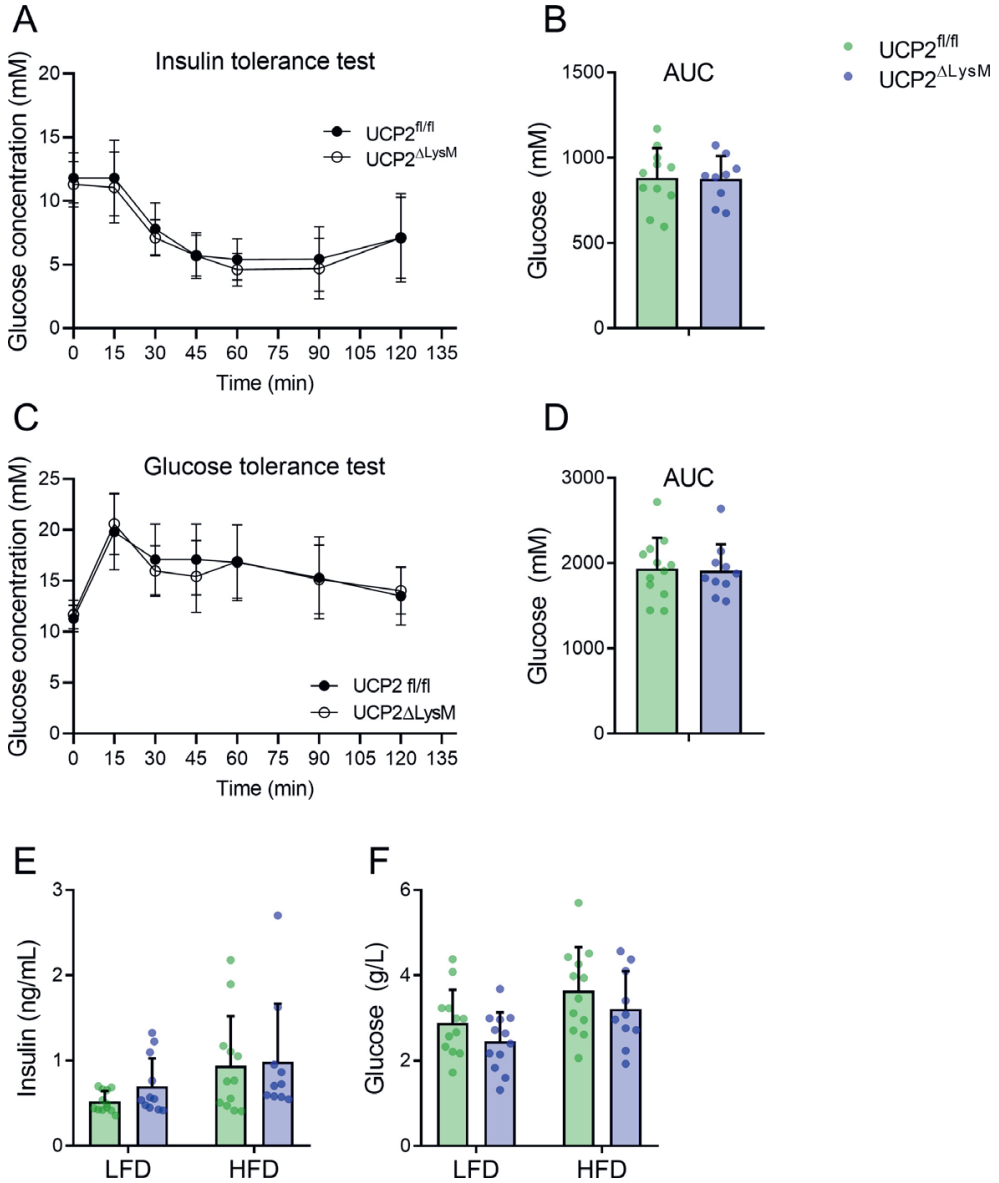


Figure 8. UCP2 deletion in macrophages does not impact systemic insulin or glucose tolerance. Intraperitoneal insulin tolerance test (**A** and **B**) and oral glucose tolerance test (**C** and **D**) of $Ucp2^{fl/fl}$ and $Ucp2^{\Delta LysM}$ mice fed a HFD for 16 weeks. Nonfasted insulin (**E**) and glucose (**F**) levels in plasma of $Ucp2^{fl/fl}$ and $Ucp2^{\Delta LysM}$ mice fed either LFD or HFD for 16 weeks. Data presented as mean \pm SD. LFD: low-fat diet, HFD: high-fat diet, AUC: area under the curve.

Discussion

This is the first study determining the function of UCP2 in macrophages during low-grade adipose tissue inflammation in the context of obesity and type 2 diabetes. Here, we demonstrate that lack of UCP2 leads to an up-regulation of both glycolytic and oxidative metabolism in macrophages, which is overruled after an influx of lipids. Furthermore, UCP2-deficiency specifically attenuates the macrophage response to inflammation, without impacting overall adipose tissue inflammation or systemic glucose homeostasis.

The expression of UCP2 protein is not linked to mRNA expression levels because of translational regulation of UCP2 [16]. In this study, we use a macrophage-specific deletion of UCP2 that was confirmed by using a highly specific, nonambiguous UCP2 antibody [13], which enables us to study UCP2 while minimizing the induction of nonphysiological changes.

The results of our research confirm the immunomodulatory role that was previously attributed to UCP2. We were able to show that lack of UCP2 leads to general attenuation of the pro-inflammatory response of macrophages toward LPS and P3C *in vitro*. Additionally, *Ucp2*^{ΔLysM} ATMs isolated from obese adipose tissue displayed an overall blunted response to LPS treatment *ex vivo*, with decreased TNF α and IL1Ra levels. Interestingly, in earlier studies, loss of *Ucp2* was shown to promote inflammation, translating into prolonged survival of mice in infection models [20,21]. However, these models used whole-body *Ucp2*^{-/-} mice, which still leaves macrophage-specific roles unclear. Furthermore, the enhancement of inflammation by *Ucp2* knockout is often attributed to increased ROS production, although the induction of ROS in *Ucp2*^{-/-} cells is not always present or consistent [23]. Particularly macrophage-specific *Ucp2*^{-/-} models have led to inconsistent results regarding ROS induction [35,36], leading to contradictory results related to the contribution of UCP2 in modulating inflammatory responses specifically in macrophages. A more recent study showed that enhanced survival of *Ucp2*^{-/-} mice in a model of sepsis was coupled to a decreased inflammatory phenotype [37]. In their study, Moon and colleagues [37] suggest that macrophage-specific loss of UCP2 leads to reduced inflammasome activation through inhibition of fatty acid synthase signaling, resulting in lower inflammatory activation. Together with these findings, our results underline the importance of UCP2 in linking metabolic signatures and inflammatory output in macrophages. Hereby, UCP2-deficient macrophages are less equipped to successfully adapt to inflammatory environments and subsequently demonstrate an attenuated inflammatory response.

UCP2 was previously identified as a protein that can regulate cellular metabolism by exporting four-carbon substrates, favoring oxidative respiration [22,23,25,35]. Loss of

UCP2 had earlier been found to lead to metabolic shifts in glucose utilization [24] and to limit metabolic flexibility in resting macrophages due to incomplete oxidation [38]. Accordingly, in UCP2-deficient macrophages we observed an increased glycolytic rate, both in resting, nontreated cells as well as after LPS treatment. Although increased glycolytic flux is seen as a key characteristic for inflammatory macrophages [39], *Ucp2*^{ΔLysM} macrophages actually display an attenuated pro-inflammatory response after treatment. In these macrophages, enforced metabolic inflexibility likely disconnects metabolic rewiring from inflammatory activation, exemplified by the impaired adaptation to inflammatory environments.

Interestingly, after exposure to fatty acids, relevant for macrophages residing in adipose tissue, differences in glycolytic and oxidative metabolism between *Ucp2*^{ΔLysM} and *Ucp2*^{fl/fl} macrophages disappear. This finding is in accordance with data from Xu et al. [35], who found no difference in fatty-acid induced β -oxidation between UCP2-deficient and control macrophages after lipid loading. The abolishment of metabolic differences after fatty acid loading suggests that changes in immune cell metabolism are uncoupled from the presence or activation of UCP2 during the influx of lipids. Therefore, although UCP2 seems an important component in determining effective metabolic adaptation during basal or inflammatory states, it is not a crucial component in controlling macrophage metabolism in the presence of high amounts of lipids. Instead, after knockdown of UCP2, the cell is able to bypass the UCP2-driven mechanism and relies on other mechanisms to deal with the increased influx of fatty acids. Likely, these lipids activate the nuclear receptor PPAR γ , which controls the expression of numerous lipid-related genes in macrophages [40] next to regulating *Ucp2* [41].

Based on our *in vitro* studies, we hypothesized that UCP2 deficiency in ATMs might attenuate inflammatory activation, leading to a decrease in adipose tissue inflammation in obese *Ucp2*^{ΔLysM} mice. The blunted inflammatory response of *Ucp2*^{ΔLysM} versus *Ucp2*^{fl/fl} ATMs after *ex vivo* stimulation with LPS is in line with our hypothesis. However, no evidence of decreased adipose tissue inflammation nor reduced glucose tolerance was found *in vivo*. Several explanations may exist as to why loss of UCP2 in macrophages does not impact on inflammation of the adipose tissue or glucose tolerance upon HFD-induced obesity. Although the blunted response of ATMs hints toward a difference in inflammatory phenotype between *Ucp2*^{ΔLysM} and *Ucp2*^{fl/fl} macrophages, this phenotype only became apparent after *ex vivo* stimulation with LPS. Because UCP2 seems to be a more subtle regulator of cellular metabolism [24], which is dispensable for most metabolic processes in the absence of constraints [12], substantial stressors are needed to uncover the consequences of UCP2 deletion. Hence, the inflammatory factors present in obese

adipose tissue that lead to metabolic activation of adipose tissue macrophages [42] might not be potent enough to lead to a phenotype similar to activation by LPS. Next to that, as seen *in vitro*, the presence of high amounts of lipids leads to an unaltered metabolic status in both *Ucp2*^{ΔLysM} and *Ucp2*^{fl/fl} macrophages, likely similar to the *in vivo* situation in the adipose tissue. These observations together could serve to explain the lack of differences in adipose tissue inflammation between *Ucp2*^{ΔLysM} and *Ucp2*^{fl/fl} mice.

Several potential limitations existed in this study. Because functional UCP2 antibody is scarce, and UCP2 protein expression is not directly linked to mRNA expression, detailed mechanistic studies are complicated. Furthermore, because the *Ucp2*^{ΔLysM} model is myeloid-specific in the whole organism, any potential differences in the *in vivo* phenotype could have been attributable to deletion of UCP2 in myeloid cells in other organs, including the brain [43]. Lastly, only male mice were used for the *in vivo* studies, possibly leading to bias.

In conclusion, UCP2 has a role in modulating both metabolism and inflammatory response in macrophages. When UCP2 is specifically deleted in macrophages, both glycolytic and oxidative metabolism are up-regulated, although metabolic differences equalize after fatty acid loading. Furthermore, UCP2 deficiency in macrophages attenuates the pro-inflammatory response toward LPS, also in adipose tissue macrophages, but does not impact adipose tissue inflammation after high-fat feeding. Therefore, although UCP2 modulates macrophage metabolism and subsequent inflammatory responses, its presence is not essential to shape ATM activation during lipid influx or obesity.

Experimental procedures

Animal studies

For the animal studies, purebred wild-type C57BL/6J animals (Jackson Laboratories, Bar Harbor, ME), *Ucp2*^{ΔLysM} mice and their floxed littermates were used. *Ucp2*^{fl^{ox}/fl^{ox}} mice were acquired from Jackson Laboratories (B6;129S-Ucp2tm2.1Lowl/J, Bar Harbor, ME) and crossed at least 5 generations with C57Bl/6J mice. Subsequently, *Ucp2*^{fl^{ox}/fl^{ox}} mice were crossed with lysM-Cre transgenic mice (Jackson Laboratories, Bar Harbor, ME; B6.129P2-Lyz2tm1(cre)lfo/J, #004781) to generate mice with a specific Cre-mediated deletion of UCP2 in the mature myeloid cell fraction. Mice were housed individually under normal light-dark cycles in temperature- and humidity-controlled specific pathogen-free conditions. Mice had *ad libitum* access to food and water. All animal experiments were carried out in accordance with the EU Directive 2010/63/EU for animal experiments.

To induce obesity and insulin resistance, male *Ucp2*^{ΔLysM} mice aged 9-12 weeks and their male floxed littermates were placed on a high-fat diet for 16 weeks. To calculate the power, previous data on fasting glucose values were used. Fasting glucose values of mice fed a high-fat diet may differ on average 3mM (± 8 mM – 11mM) compared to mice fed a low-fat diet. Differences in responses might lead to an SD around 2mM or higher. To perform the power calculation, we used a one-way analysis of variance with a significance level of 0.05 and a power of 90%, leading to an estimation of around $n = 11$ mice needed per group. To allow for the compensation of unforeseen circumstances or potential loss of mice during the study, $n = 12$ mice were included per group. Thus, 12 mice per genotype were randomly allocated to a standardized high-fat diet or a low-fat diet for 16 weeks (D12451 and D12450H, Research Diets, New Brunswick, NJ, USA; γ -irradiated with 10-20 kilograys).

Body weight and food intake were assessed weekly. At the end of the study, mice were anesthetized with isoflurane and blood was collected via orbital puncture in tubes containing EDTA (Sarstedt, Nümbrecht, Germany). Subsequently, mice were immediately euthanized by cervical dislocation, after which tissues were excised, weighed, and frozen in liquid nitrogen or prepared for histology. Samples from liquid nitrogen were stored at -80°C . All animal experiments were approved by the local animal welfare committee of Wageningen University (2016.W-0093.002). The experimenter was blinded to group assignments during all analyses.

Intraperitoneal glucose and insulin tolerance test

Glucose and insulin tolerance tests were performed after 14 or 15 weeks by oral gavage of glucose (0.8g/kg, Baxter) or intraperitoneal injection of insulin (0.75 units/kg, Novo

Nordisk). Mice were fasted for 5 h prior to the tolerance tests and blood was collected at 0, 15, 30, 45, 60, 90, and 120 min after administration of glucose or insulin by tail bleeding. Blood glucose was measured using glucose sensor strips and a GLUCOFIX Tech glucometer (GLUCOFIX Tech, Menarini Diagnostics, Valkenswaard, The Netherlands).

Plasma measurements

Blood collected in EDTA tubes was spun down for 15 min at 5000 rpm and at 4°C. Plasma was aliquoted and stored at -80°C. Measurement of insulin (ultra-sensitive mouse insulin ELISA kit, Crystal Chem Inc., Elk Grove Village, IL, USA), glucose (Liquicolor, Human GmbH, Wiesbaden, Germany), adiponectin (adiponectin ELISA DuoSet kit, R&D Systems), leptin (leptin ELISA DuoSet kit, R&D Systems), cholesterol (Liquicolor), triglycerides (Liquicolor) and nonesterified fatty acids (NEFA-HR set R1, R2 and standard, WAKO Diagnostics, Instruchemie, Delfzijl, The Netherlands).

Explants and isolation of adipose tissue macrophages

After collection of gonadal adipose tissue (gWAT), part of the gWAT was separated and transferred on ice in Dulbecco's modified Eagle's medium (DMEM, Corning, NY, USA), supplemented with 1% penicillin/streptomycin (p/s) (Corning) and 1% FFA-free Bovine Serum Albumin (BSA fraction V, Roche via Merck, Darmstadt, Germany). For each mouse, an explant of 50 mg was kept in culture for 24 h in DMEM supplemented with 10% FCS (BioWest, Nuaillé, France) and 1% p/s, after which supernatant was collected for ELISA measurements or harvested as conditioned medium. Stromal vascular fractions of gWAT were isolated by collagenase digestion for 45 min in RPMI 1630 medium (Lonza, Basel, Switzerland) supplemented with 10% FCS, 1% p/s, 0.5% FFA-free BSA, 1M CaCl₂, 1M HEPES and 0.15% collagenase (from *Clostridium histolyticum*, Merck). gWAT was pooled for three mice of the same group after digestion, mature adipocytes were stored separately, and erythrocytes were lysed with ACK buffer. From the resulting stromal vascular cells, 500 000 cells were sampled for flow cytometry; remaining cells were used for ATM isolation. ATMs were isolated by magnetic separation using the OctoMACS Cell Separator System with MS columns, mouse anti-F4/80-FITC antibody and anti-FITC MicroBeads (all Miltenyi Biotec, Bergisch Gladbach, Germany). ATMs were kept in culture in RPMI 1630 with 10% FCS and 1%p/s for 24 h in the presence or absence of 10ng/mL LPS (Merck) to obtain supernatants.

Flow cytometry

Stromal vascular cells were stained with antibodies against CD45-ECD (Beckman Coulter, Brea, CA, USA), F4/80-FITC, CD206-APC, CD11c-PE-Cy7 and CD11b-PE (Biolegend, San Diego, CA, USA). Samples were measured on a flow cytometer (FC500, Beckman Coulter)

and results were analyzed using Kaluza analysis software 2.1 (Beckman Coulter).

Histological studies

gWAT and liver samples were fixed in 3.7% paraformaldehyde and embedded in paraffin. Sectioned slides were stained with hematoxylin eosin according to standard protocols. Sectioned slides were incubated 20% normal goat serum, before overnight incubation with F4/80 antibody (MCA497G, Bio-Rad Laboratories, Hercules, CA, USA). Secondary antibodies used were anti-rat or anti-rabbit IgG conjugated to HRP (Cell Signaling Technology Danvers, MA, USA). No primary antibody was used for negative controls.

Primary cell isolation

Peritoneal macrophages were harvested from the mice by washing the peritoneal cavity with ice-cold PBS and F4/80 based magnetic separation was used to ensure purity (see isolation ATMs). Peritoneal macrophages were kept in culture for 24 h in RPMI 1630 with 10% FCS and 1%p/s with or without the presence of 10ng/mL LPS (Merck) to obtain supernatants. For BMDM isolation, 8- to 12-week-old *Ucp2^{ΔLysM}* and their *Ucp2^{fl/fl}* littermates were euthanized by cervical dislocation. Femurs were isolated, bone marrow was extracted and differentiated in DMEM, supplemented with 10% FCS, 1% p/s and 15% L929 conditioned medium. After seven days of differentiation, BMDMs were scraped and plated as appropriate.

Cell culture experiments

Palmitate (Merck) and oleate (Merck) were solubilized using EtOH and KOH and conjugated to FFA-free BSA in sterile water (Versol, Aguettant, Lyon, France) at 37°C for 30 min. Oleate was used at a concentration of 200 μM or a mixture of oleate and palmitate (oleate:palmitate) was made in a ratio of 2:1 and used in a final concentration of 600 μM. BSA was used as control for fatty acid treatments. LPS (Merck) was used in a concentration of 10 ng/mL, P3C (Merck) was used in a concentration of 5 μg/mL, both were diluted in PBS. All cells were washed with PBS (Corning) before treatment. For macrophage-adipose tissue co-cultures (**Figure 1A**), BMDMs were plated in 12-well plates and after adhesion, an insert was added with 100 mg of carefully minced live adipose tissue isolated from mice fed a HFD or LFD for 13 – 16 weeks. BMDMs were co-cultured with adipose tissue for 24 h.

Extracellular flux assay

To measure extracellular flux in BMDMs, the Agilent Seahorse XF-96 Analyzer (Agilent Technologies, Santa Clara, CA, USA) was used. Cells were seeded in XF-96 plates (Agilent Technologies) in a density of 200 000 cells/well, and treated with LPS or fatty acids

appropriately. Before flux measurement, cells were washed and cultured for an hour in Seahorse XF base medium (Agilent Technologies) at 37°C in a non-CO₂ incubator until the measurement. The base medium was set to a pH of 7.4 and was supplemented with 2 mM L-glutamine for glycolytic stress tests or 2 mM L-glutamine and 25 mM glucose for mitochondrial stress tests. Glycolytic stress tests included the injection of glucose (25 mM) after which basal glycolysis was measured, oligomycin (1.5 µM) after which glycolytic capacity was measured and 2-deoxyglucose (50 mM). Mitochondrial stress tests included the injection of oligomycin (1.5 µM), FCCP (1.5 µM) plus pyruvate (1 mM) after which maximal respiration was measured, and antimycin A (2.5 µM) plus rotenone (1.25 µM). Basal respiration was measured unstimulated. All experiments were performed at least with quadruplicates. OCR and ECAR were measured at baseline and following the injections, calculations were made using Wave Desktop 2.6 (Agilent Technologies).

Real-time PCR and microarray

For cells and liver tissue, total RNA was isolated using TRIzol® Reagent (Invitrogen, Thermo Fisher Scientific). For gWAT, total RNA was isolated with the RNeasy Micro Kit (Qiagen, Venlo, The Netherlands). The iScript cDNA kit was used to synthesize cDNA (Bio-Rad Laboratories) according to manufacturer's instructions. The CFX384 Touch™ Real-Time detection system (Bio-Rad Laboratories) was used to perform real time polymerase chain reaction (RT-PCR), using a SensiMix™ (BioLine, London, UK) based protocol. Human *B2M* and mouse *36b4* expression were used to normalize values for human and mouse samples, respectively. The microarray datasets used for **Figure 1A** were described earlier [10,33].

Immunoblotting

Cell protein lysates were separated by electrophoresis on a precast 4-20% Tris-glycine gel (SDS-PAGE) (Bio-Rad Laboratories) and transferred onto nitrocellulose membranes using a liquid transfer cell (all purchased from Bio-Rad Laboratories), blocked in nonfat milk and incubated overnight at 4°C with primary antibody and subsequently for 1 h with appropriate peroxidase conjugate antibody at room temperature. Membranes were developed with the chemiluminescence substrate (SuperSignal West Pico PLUS, Thermo Fisher Scientific) and images were captured with the ChemiDoc MP system (Bio-Rad Laboratories). The primary antibodies for UCP2 were described earlier [13].

Enzyme-linked immunosorbent assays (ELISA)

TNFα, IL10, IL1Ra and IL6 levels were measured in cell or explant supernatant with DuoSet sandwich ELISA kits (R&D systems) according to manufacturer's instructions. To normalize the data, the concentration of DNA per well was measured for adipose tissue macrophages and peritoneal macrophages (Quant-iT dsDNA Assay Kit high sensitivity, Thermo Fisher

Scientific). For gWAT explants, the exact weight per explant was used for normalization.

Lactate assay

Proteins were removed from cell supernatants using perchloric acid precipitation to avoid contamination with lactate dehydrogenase. Lactate concentrations were determined using conversion of lactate by lactate oxidase (Merck), and subsequent oxidation of Amplex Red reagent (Thermo Fisher Scientific) into resorufin by HRP (Thermo Fisher Scientific), which was measured as a fluorescent signal.

Data and statistical analysis

Data are represented as means \pm SD as indicated in the legend. Statistical analyses were carried out using the unpaired Student's t test or two-way analysis of variance followed by Bonferroni's post hoc multiple comparisons test, if genotype and diet or genotype and treatment were both found significant (GraphPad Software, San Diego, CA, USA). A value of $p < 0.05$ was considered statistically significant.

Data availability

All data are contained within the manuscript. Microarray datasets that were used were described earlier [10,33].

Acknowledgements

We would like to thank Shohreh Keshtkar, Jenny Jansen, Desiree Vorstenbosch, Julia van Heck and Anneke Hijmans for their technical assistance.

Author contributions

X. A. M. H. v. D. and R. S. conceptualization; X. A. M. H. v. D. data curation; X. A. M. H. v. D. formal analysis; X. A. M. H. v. D. validation; X. A. M. H. v. D. investigation; X. A. M. H. v. D. visualization; X. A. M. H. v. D. and T. S. methodology; X. A. M. H. v. D. writing-original draft; X. A. M. H. v. D. and R. S. project administration; X. A. M. H. v. D., T. S., M.-C. A.-G., and R. S. writing-review and editing; T. S. and M.-C. A.-G. resources; R. S. supervision; R. S. funding acquisition.

Funding source

This work was supported by a Vidi Grant from the NWO and by the Dutch Diabetes Foundation senior fellowship 2015.82.1824 (to R.S.).

Conflict of interest

The authors declare that they have no conflicts of interest with the contents of this article.

Abbreviations

The abbreviations used are: ATM, adipose tissue macrophage; gWAT, gonadal white adipose tissue; HFD, high-fat diet; LFD, low-fat diet; BMDM, bone marrow-derived macrophages; Ctrl, control; LPS, lipopolysaccharide; OA:PA, mixture of oleic acid and palmitic acid; p/s, penicillin/streptomycin.

References

1. NCD-RisC NRFC. Trends in adult body-mass index in 200 countries from 1975 to 2014: a pooled analysis of 1698 population-based measurement studies with 19.2 million participants. *The Lancet*. 2016; 387(10026): 1377–96.
2. Cornier M-A, Després J-P, Davis N, Grossniklaus DA, Klein S, Lamarche B, et al. Assessing Adiposity. *Circulation*. 2011; 124(18): 1996–2019.
3. Odegaard JI, Chawla A. Mechanisms of macrophage activation in obesity-induced insulin resistance. *Nature Clinical Practice Endocrinology & Metabolism*. 2008; 4(11): 619–26.
4. Weisberg SP, McCann D, Desai M, Rosenbaum M, Leibel RL, Ferrante AW. Obesity is associated with macrophage accumulation in adipose tissue. *Journal of Clinical Investigation*. 2003; 112(12): 1796–808.
5. Xu X, Grijalva A, Skowronski A, van Eijk M, Serlie MJ, Ferrante AW. Obesity Activates a Program of Lysosomal-Dependent Lipid Metabolism in Adipose Tissue Macrophages Independently of Classic Activation. *Cell Metabolism*. 2013; 18(6): 816–30.
6. Cinti S, Mitchell G, Barbatelli G, Murano I, Ceresi E, Faloia E, et al. Adipocyte death defines macrophage localization and function in adipose tissue of obese mice and humans. *Journal of Lipid Research*. 2005; 46(11): 2347–55.
7. Kratz M, Coats BR, Hisert KB, Hagman D, Mutskov V, Peris E, et al. Metabolic Dysfunction Drives a Mechanistically Distinct Proinflammatory Phenotype in Adipose Tissue Macrophages. *Cell Metabolism*. 2014; 20(4): 614–25.
8. Loftus RM, Finlay DK. Immunometabolism: Cellular Metabolism Turns Immune Regulator. *Journal of Biological Chemistry*. 2016; 291(1): 1–10.
9. Lachmandas E, Boutens L, Ratter JM, Hijmans A, Hooiveld GJ, Joosten LAB, et al. Microbial stimulation of different Toll-like receptor signalling pathways induces diverse metabolic programmes in human monocytes. *Nature Microbiology*. 2016; 2: 16246.
10. Boutens L, Hooiveld GJ, Dhingra S, Cramer RA, Netea MG, Stienstra R. Unique metabolic activation of adipose tissue macrophages in obesity promotes inflammatory responses. *Diabetologia*. 2018; 61(4): 942–53.
11. O'Neill LAJ, Kishton RJ, Rathmell J. A guide to immunometabolism for immunologists. *Nature Reviews Immunology*. 2016; 16(9): 553–65.
12. Bouillaud F, Alves-Guerra M-C, Ricquier D. UCPs, at the interface between bioenergetics and metabolism. *Biochimica et Biophysica Acta (BBA) - Molecular Cell Research*. 2016; 1863(10): 2443–56.
13. Pecqueur C, Alves-Guerra MC, Gelly C, Levi-Meyrueis C, Couplan E, Collins S, et al. Uncoupling protein 2, in vivo distribution, induction upon oxidative stress, and evidence for translational regulation. *The Journal of Biological Chemistry*. 2001; 276(12): 8705–12.
14. Alves-Guerra M-C, Rousset S, Pecqueur C, Mallat Z, Blanc J, Tedgui A, et al. Bone Marrow Transplantation Reveals the in Vivo Expression of the Mitochondrial Uncoupling Protein 2 in Immune and Nonimmune Cells during Inflammation. *Journal of Biological Chemistry*. 2003; 278(43): 42307–12.
15. Mattiasson G, Sullivan PG. The emerging functions of UCP2 in health, disease, and therapeutics. *Antioxidants and Redox Signaling*. 2006; 8: 1–38.
16. Hurtaud C, Gelly C, Bouillaud F, Lévi-Meyrueis C. Translation control of UCP2 synthesis by the upstream open reading frame. *Cellular and Molecular Life Sciences*. 2006; 63(15): 1780–9.

17. Bouillaud F. UCP2, not a physiologically relevant uncoupler but a glucose sparing switch impacting ROS production and glucose sensing. *Biochimica et Biophysica Acta (BBA) - Bioenergetics*. 2009; 1787(5): 377–83.
18. Couplan E, del Mar Gonzalez-Barroso M, Alves-Guerra MC, Ricquier D, Goubern M, Bouillaud F. No evidence for a basal, retinoic, or superoxide-induced uncoupling activity of the uncoupling protein 2 present in spleen or lung mitochondria. *The Journal of Biological Chemistry*. 2002; 277(29): 26268–75.
19. Li N, Karaca M, Maechler P. Upregulation of UCP2 in beta-cells confers partial protection against both oxidative stress and glucotoxicity. *Redox Biology*. 2017; 13: 541–9.
20. Arsenijevic D, Onuma H, Pecqueur C, Raimbault S, Manning BS, Miroux B, et al. Disruption of the uncoupling protein-2 gene in mice reveals a role in immunity and reactive oxygen species production. *Nature Genetics*. 2000; 26(4): 435–9.
21. Rousset S, Emre Y, Join-Lambert O, Hurtaud C, Ricquier D, Cassard-Doulcier A-M. The uncoupling protein 2 modulates the cytokine balance in innate immunity. *Cytokine*. 2006; 35(3–4): 135–42.
22. Esteves P, Pecqueur C, Ransy C, Esnous C, Lenoir V, Bouillaud F, et al. Mitochondrial retrograde signaling mediated by UCP2 inhibits cancer cell proliferation and tumorigenesis. *Cancer Research*. 2014; 74(14): 3971–82.
23. Pecqueur C, Bui T, Gelly C, Hauchard J, Barbot C, Bouillaud F, et al. Uncoupling protein-2 controls proliferation by promoting fatty acid oxidation and limiting glycolysis-derived pyruvate utilization. *The FASEB Journal*. 2008; 22(1): 9–18.
24. Aguilar E, Esteves P, Sancerni T, Lenoir V, Aparicio T, Bouillaud F, et al. UCP2 Deficiency Increases Colon Tumorigenesis by Promoting Lipid Synthesis and Depleting NADPH for Antioxidant Defenses. *Cell Reports*. 2019; 28(9): 2306-2316.e5.
25. Vozza A, Parisi G, De Leonardi F, Lasorsa FM, Castegna A, Amorese D, et al. UCP2 transports C4 metabolites out of mitochondria, regulating glucose and glutamine oxidation. *Proceedings of the National Academy of Sciences*. 2014; 111(3): 960–5.
26. Oktavianthi S, Trimarsanto H, Febinia CA, Suastika K, Saraswati MR, Dwipayana P, et al. Uncoupling protein 2 gene polymorphisms are associated with obesity. *Cardiovascular Diabetology*. 2012; 11(1): 41.
27. Martinez-Hervas S, Mansego ML, de Marco G, Martinez F, Alonso MP, Morcillo S, et al. Polymorphisms of the UCP2 gene are associated with body fat distribution and risk of abdominal obesity in Spanish population. *European Journal of Clinical Investigation*. 2012; 42(2): 171–8.
28. Meyer TE, Boerwinkle E, Morrison AC, Volcik KA, Sanderson M, Coker AL, et al. Diabetes Genes and Prostate Cancer in the Atherosclerosis Risk in Communities Study. *Cancer Epidemiology Biomarkers & Prevention*. 2010; 19(2): 558–65.
29. Salopuro T, Pulkkinen L, Lindström J, Kolehmainen M, Tolppanen A-M, Eriksson JG, et al. Variation in the UCP2 and UCP3 genes associates with abdominal obesity and serum lipids: The Finnish Diabetes Prevention Study. *BMC Medical Genetics*. 2009; 10(1): 94.
30. Andersen G, Dalgaard LT, Justesen JM, Anthonson S, Nielsen T, Thørner LW, et al. The frequent UCP2 –866G>A polymorphism protects against insulin resistance and is associated with obesity: a study of obesity and related metabolic traits among 17 636 Danes. *International Journal of Obesity*. 2013; 37(2): 175–81.
31. Lyssenko V, Almgren P, Anevski D, Orho-Melander M, Sjögren M, Saloranta C, et al. Genetic Prediction of Future Type 2 Diabetes. Hattersley A, editor. *PLoS Medicine*. 2005; 2(12): e345.

32. Esterbauer H, Schneitler C, Oberkofler H, Ebenbichler C, Paulweber B, Sandhofer F, et al. A common polymorphism in the promoter of UCP2 is associated with decreased risk of obesity in middle-aged humans. *Nature Genetics*. 2001; 28(2): 178–83.
33. Dalmas E, Venticlef N, Caer C, Poitou C, Cremer I, Aron-Wisniewsky J, et al. T cell+derived IL-22 amplifies IL-1 β +driven inflammation in human adipose tissue: Relevance to obesity and type 2 diabetes. *Diabetes*. 2014; 63(6): 1966–77.
34. Könner AC, Brüning JC. Toll-like receptors: linking inflammation to metabolism. *Trends in Endocrinology & Metabolism*. 2011; 22(1): 16–23.
35. Xu H, Hertzler A V., Steen KA, Wang Q, Suttles J, Bernlohr DA. Uncoupling Lipid Metabolism from Inflammation through Fatty Acid Binding Protein-Dependent Expression of UCP2. *Molecular and Cellular Biology*. 2015; 35(6): 1055–65.
36. Emre Y, Nübel T. Uncoupling protein UCP2: When mitochondrial activity meets immunity. *FEBS Letters*. 2010; 584(8): 1437–42.
37. Moon J-S, Lee S, Park M-A, Siempos II, Haslip M, Lee PJ, et al. UCP2-induced fatty acid synthase promotes NLRP3 inflammasome activation during sepsis. *The Journal of Clinical Investigation*. 2015; 125(2): 665–80.
38. Nübel T, Emre Y, Rabier D, Chadeaux B, Ricquier D, Bouillaud F. Modified glutamine catabolism in macrophages of Ucp2 knock-out mice. *Biochimica et Biophysica Acta (BBA) - Bioenergetics*. 2008; 1777(1): 48–54.
39. O’Neill LAJ, Pearce EJ. Immunometabolism governs dendritic cell and macrophage function. *The Journal of Experimental Medicine*. 2016; 213(1): 15–23.
40. Ahmadian M, Suh JM, Hah N, Liddle C, Atkins AR, Downes M, et al. Ppar γ signaling and metabolism: The good, the bad and the future. *Nature Medicine*. 2013; 19(5): 557–66.
41. Medvedev A V., Snedden SK, Raimbault S, Ricquier D, Collins S. Transcriptional regulation of the mouse uncoupling protein-2 gene: Double E-box motif is required for peroxisome proliferator-activated receptor- γ -dependent activation. *Journal of Biological Chemistry*. 2001; 276(14): 10817–23.
42. Hotamisligil GS. Inflammation, metaflammation and immunometabolic disorders. *Nature*. 2017; 542(7640): 177–85.
43. Kim JD, Yoon NA, Jin S, Diano S. Microglial UCP2 Mediates Inflammation and Obesity Induced by High-Fat Feeding. *Cell Metabolism*. 2019; 30(5): 952-962.e5.

Supplemental material

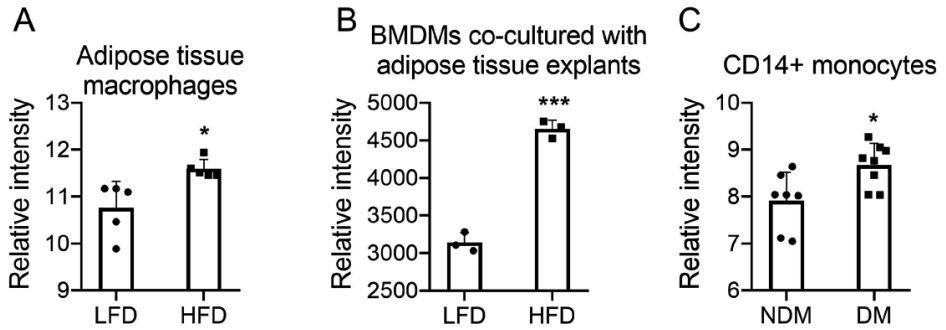


Figure S1 (linked to Figure 1A). *Ucp2* mRNA expression is upregulated in monocytes and macrophages in the context of obesity.

Relative microarray intensity values of *Ucp2* expression in adipose tissue macrophages isolated from (A) lean and obese mice (n = 4 mice per group); (B) bone marrow-derived macrophages co-cultured with lean or obese adipose tissue explants (n = 3 replicates per group) and (C) CD14+ monocytes isolated from subjects with (DM) or without (NDM) diabetes type 2 (n = 6 subjects per group). Data are presented as mean ± SD. BMDM: bone marrow-derived macrophage, ATM: adipose tissue macrophage, NDM: no diabetes mellitus, DM: diabetes mellitus HFD: high-fat diet, LFD: low-fat diet, SVF: stromal vascular fraction, gWAT: gonadal white adipose tissue. $p < 0.01$; ***, $p < 0.001$.

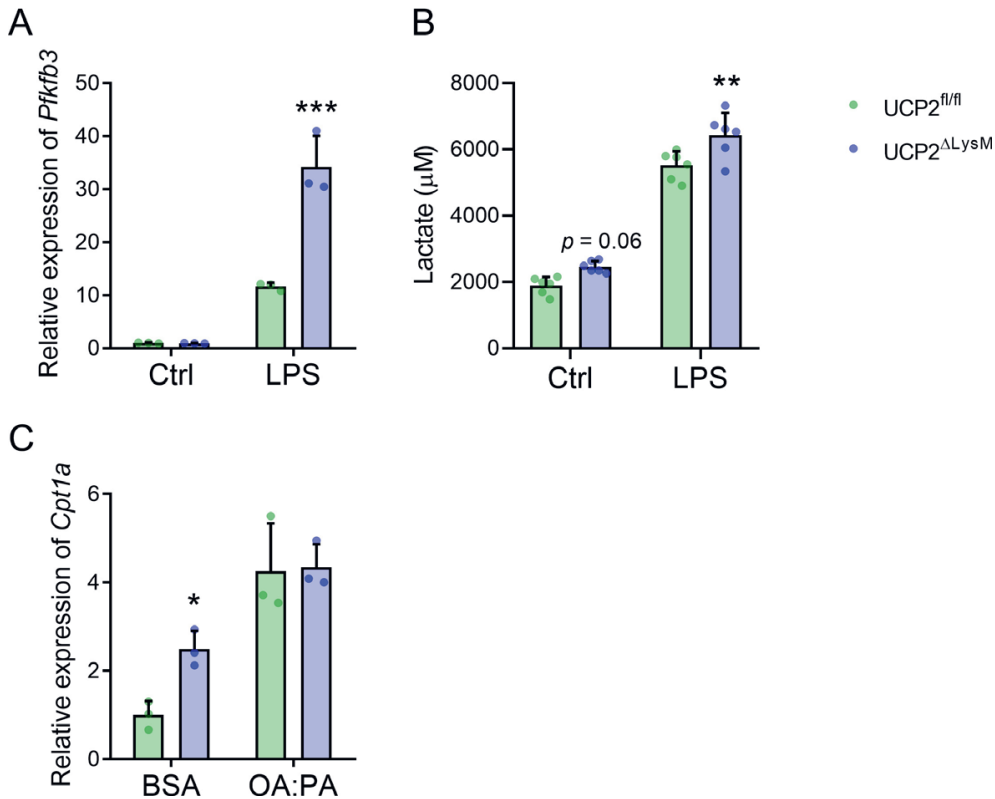


Figure S2 (linked to Figure 2). Expression of metabolic enzymes and lactate after LPS or fatty acid treatment.

Relative expression of *Pfkfb3* mRNA (A) after 6h and production of lactate (B) after 24 h in *Ucp2^{fl/fl}* and *Ucp2^{ΔLysM}* BMDMs treated with 10 ng/mL LPS. (C) Relative expression of *Cpt1a* mRNA in *Ucp2^{fl/fl}* and *Ucp2^{ΔLysM}* BMDMs treated with vehicle (BSA) or a mixture of 0.6 mM OA:PA for 6 h. Data are presented as mean ± SD. Ctrl: vehicle control, LPS: lipopolysaccharide, BSA: bovine serum albumin, OA:PA: oleic acid and palmitic acid. *, $p < 0.05$; **, $p < 0.01$; ***, $p < 0.001$.

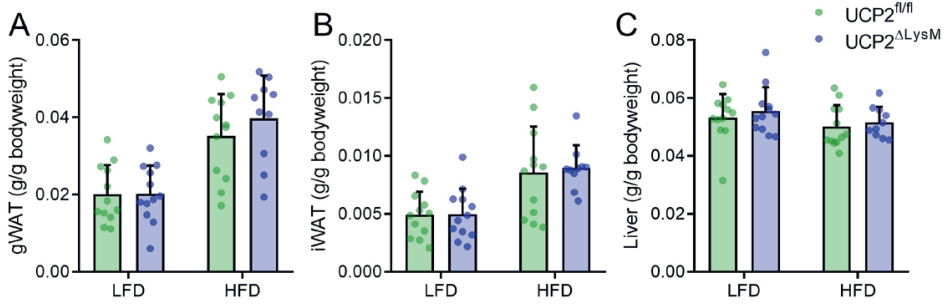


Figure S3 (linked to Figure 5C). Organ weight of *Ucp2*^{fl/fl} and *Ucp2*^{ΔLysM} mice fed a LFD or HFD.

Weight of gWAT (A), iWAT (B) and liver (C) of *Ucp2*^{fl/fl} and *Ucp2*^{ΔLysM} mice (n = 24 *Ucp2*^{fl/fl} and 22 *Ucp2*^{ΔLysM}) fed either LFD or HFD for 16 weeks. Organ weights are normalized to body weight. Data are presented as mean ± SD. LFD: low-fat diet, HFD: high-fat diet, gWAT: gonadal white adipose tissue, iWAT: inguinal white adipose tissue.

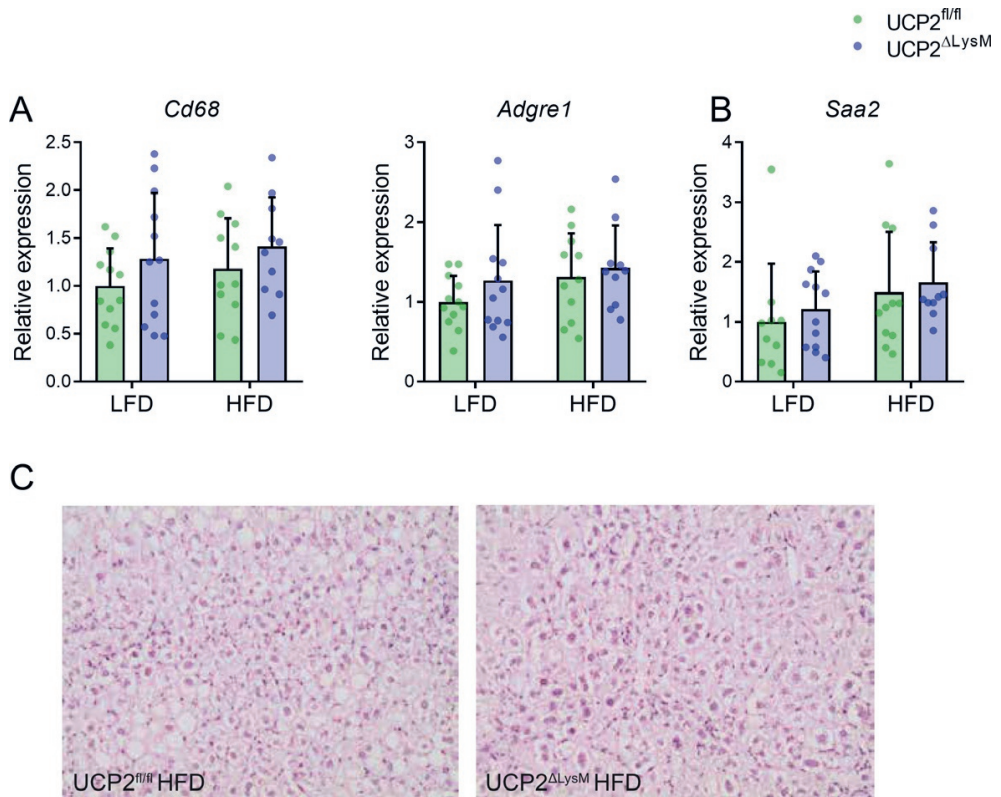


Figure S4. Inflammatory markers in the livers of *Ucp2*^{fl/fl} and *Ucp2*^{ΔLysM} mice fed a LFD or HFD.

Relative mRNA expression of immune cell markers *Cd68* and *Adgre1* (A), liver inflammatory marker *Saa2* (B) and hematoxylin/eosin stained slices (C) from livers of *Ucp2*^{fl/fl} and *Ucp2*^{ΔLysM} mice fed either a LFD or a HFD for 16 weeks. Data are presented as mean ± SD. LFD: low-fat diet, HFD: high-fat diet.

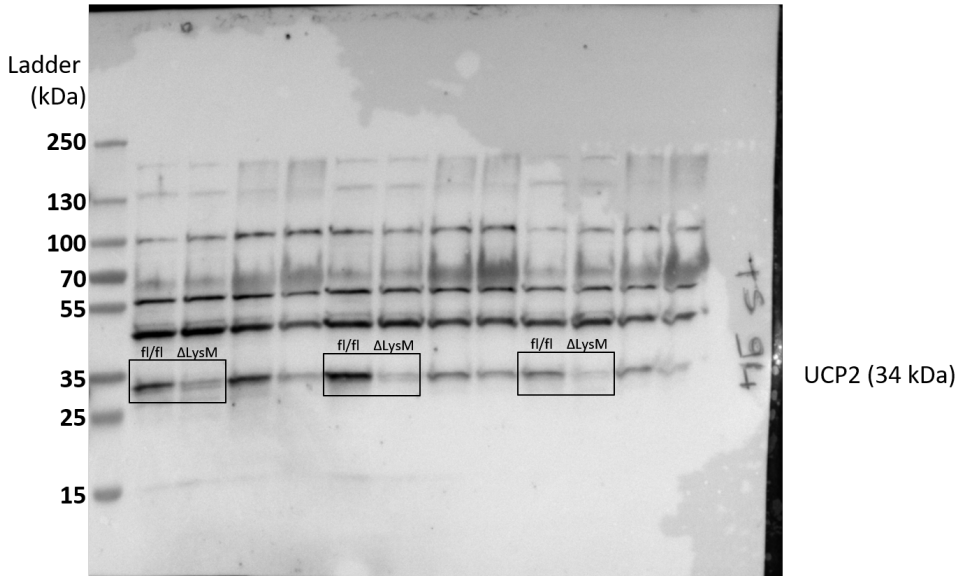


Figure S5 (linked to Figure 1).

Full western blot membrane of UCP2 protein expression in *Ucp2^{fl/fl}* and *Ucp2^{ΔLysM}* bone marrow-derived macrophages, including molecular weight marker (left).



HILPDA uncouples lipid droplet accumulation in adipose tissue macrophages from inflammation and metabolic dysregulation

Xanthe A.M.H. van Dierendonck^{1,2,8}, Montserrat A. de la Rosa Rodriguez^{1,8}, Anastasia Georgiadi^{1,3}, Frits Mattijssen¹, Wieneke Dijk^{1,4}, Michel van Weeghel⁵, Rajat Singh⁶, Jan Willem Borst⁷, Rinke Stienstra^{1,2,9}, Sander Kersten^{1,9}

¹Nutrition, Metabolism and Genomics Group, Division of Human Nutrition and Health, Wageningen University, Wageningen, the Netherlands

²Department of Internal Medicine, Radboud University Medical Center, Nijmegen, the Netherlands

³Present address: Institute for Diabetes and Cancer (IDC), Helmholtz Zentrum München, German Research Center for Environmental Health, Neuherberg, Germany

⁴Present address: L'Institut du Thorax, U1087, INSERM, Nantes, France

⁵Laboratory Genetic Metabolic Diseases, Amsterdam UMC, University of Amsterdam, Amsterdam Gastroenterology and Metabolism, Amsterdam Cardiovascular Sciences, Amsterdam, the Netherlands

⁶Department of Medicine, Albert Einstein College of Medicine, Bronx, NY 10461, USA

⁷Laboratory of Biochemistry, Microspectroscopy Research Facility, Wageningen University, Wageningen, the Netherlands

⁸These authors contributed equally

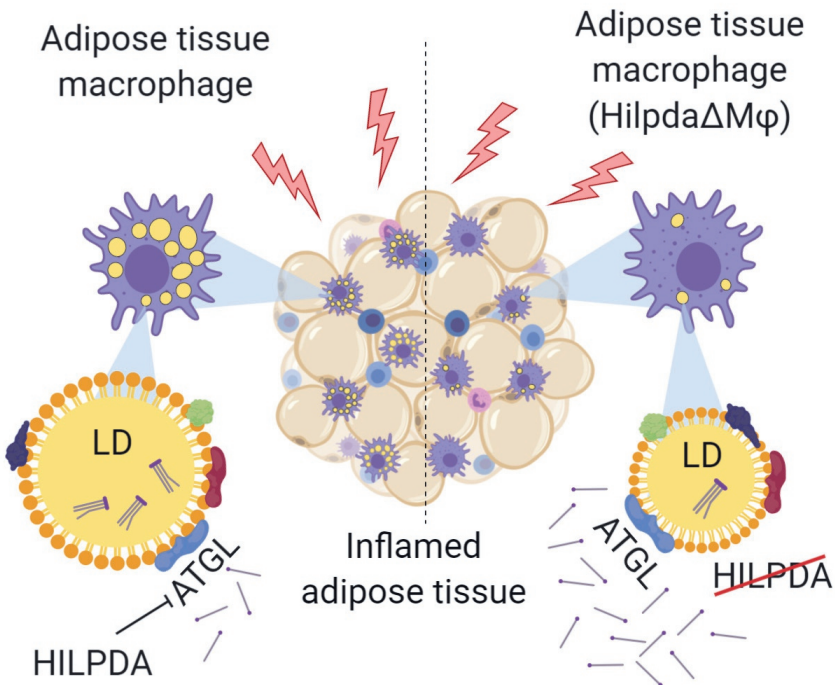
⁹Shared senior authors

Cell Reports. 2020; 30(6):1811:1822.

Abstract

Obesity leads to a state of chronic low-grade inflammation that features the accumulation of lipid-laden macrophages in adipose tissue. Here, we determined the role of macrophage lipid droplet accumulation in the development of obesity-induced adipose tissue inflammation, using mice with myeloid-specific deficiency of the lipid-inducible HILPDA protein. HILPDA deficiency markedly reduced intracellular lipid levels and accumulation of fluorescently labeled fatty acids. Decreased lipid storage in HILPDA-deficient macrophages can be rescued by inhibition of adipose triglyceride lipase (ATGL) and is associated with increased oxidative metabolism. In diet-induced obese mice, HILPDA deficiency does not alter inflammatory and metabolic parameters, despite markedly reducing lipid accumulation in macrophages. Overall, we find that HILPDA is a lipid-inducible, physiological inhibitor of ATGL-mediated lipolysis in macrophages and uncouples lipid storage in adipose tissue macrophages from inflammation and metabolic dysregulation. Our data question the contribution of lipid droplet accumulation in adipose tissue macrophages in obesity-induced inflammation and metabolic dysregulation.

Graphical abstract



Introduction

The prevalence of obesity across the world has risen steeply in the past decades and has become a huge public health concern. It is well established that obesity is associated with a state of chronic, low-grade inflammation. That low-grade inflammation is characterized by increased production of several inflammatory cytokines and adipokines and has been suggested to be an important pathophysiological mechanism underlying many of the adverse health effects of obesity [1]. In particular, the increase in inflammatory cytokines and adipokines is believed to disrupt insulin signalling and contribute to obesity-induced insulin resistance [2].

Adipose tissue mainly consists of adipocytes, but it also harbors numerous immune cells, including macrophages. Those macrophages are important for maintaining homeostasis in healthy adipose tissue but also contribute to the development of inflammation during obesity [3]. In lean states, adipose tissue macrophages mainly show anti-inflammatory phenotypes and are distributed evenly throughout the adipose tissue. In contrast, in obese adipose tissue, macrophages accumulate in so-called crown-like structures around dead adipocytes and display a metabolically activated phenotype [4–6]. Metabolically activated macrophages form multiple intracellular lipid droplets and display distinct transcriptional profiles [6–8]. Those features reflect an attempt by macrophages to buffer excess lipids, which is adaptive in the lean state but becomes maladaptive in obese adipose tissue [3]. The lipid-laden macrophages observed in obese adipose tissue are reminiscent of the foamy macrophages present in atherosclerotic plaques. Although foam cell formation and adipose tissue inflammation are known to co-exist in obesity, the exact role of lipid droplet accumulation in adipose tissue macrophages in the development of obesity-induced adipose tissue inflammation and associated metabolic disturbances remains unclear.

HILPDA (hypoxia inducible lipid droplet associated) is a small lipid droplet-associated protein expressed in several tissues [9]. The expression of *Hilpda* is induced by different stimuli, including hypoxia, beta-adrenergic activation, and PPAR transcription factors [9–11]. Gain- and loss-of-function studies have shown that HILPDA promotes lipid deposition in hepatocytes, adipocytes, and macrophages [9–14]. The mechanism by which HILPDA promotes lipid storage in cells has not been completely elucidated, but evidence has been presented that HILPDA directly binds and inhibits adipose triglyceride lipase (ATGL) [15,16], consistent with the ability of HILPDA to inhibit lipolysis [11,12]. Interestingly, endothelial cell marker *Tie2*-Cre-driven deletion of *Hilpda* was found to decrease fatty acid and oxidized low-density lipoprotein (oxLDL)-driven lipid droplet formation in

macrophages and reduce lesion formation and progression of atherosclerosis in *Apoe*^{-/-} mice [14].

Here, we aimed to determine the exact role of HILPDA in lipid storage in macrophages, and explore the potential causal relationship between lipid droplet accumulation in adipose tissue macrophages, and the development of adipose tissue inflammation and insulin resistance during obesity.

Results

***Hilpda* as gene of interest in obese adipose tissue**

To identify genes that may be able to modify lipid storage in adipose tissue macrophages, we searched for genes that are induced by lipids and upregulated in adipose tissue macrophages by obesity. To that end, we co-analyzed the transcriptomics data from three experiments: (1) adipose tissue macrophages isolated from obese versus lean mice, (2) mouse peritoneal macrophages treated with the fatty acid oleate, (3) mouse peritoneal macrophages treated with intralipid, a triglyceride emulsion. Scatterplot analysis identified *Hilpda* as a gene of particular interest (**Figure 1A**) because it was the only gene that was strongly upregulated in all three experiments. Moreover, *Hilpda* was the most highly induced gene in peritoneal macrophages by oleate. Consistent with a potential role for *Hilpda* in obesity-induced adipose tissue inflammation, transcriptome analysis indicated that *Hilpda* expression in adipose tissue is upregulated by high-fat feeding in mice, in parallel with macrophage and inflammatory markers, such as *Ccl2* (MCP1), *Cd68*, and *Itgax* (*Cd11c*) (**Figure 1B**), as confirmed by qPCR (**Figure 1C**). Immunohistochemistry of adipose tissue of obese mice indicated that HILPDA co-localized with adipose tissue macrophages in crown-like structures, thus supporting the expression of HILPDA in adipose tissue macrophages (**Figure 1D**). Together, these data suggest that HILPDA may be implicated in obesity-induced adipose tissue inflammation and foam cell formation.

***Hilpda* in macrophages is responsive to lipids**

To further investigate the regulation of HILPDA by lipids, we treated RAW264.7 and primary peritoneal macrophages with fatty acids. Confirming the transcriptomics data, oleate markedly upregulated *Hilpda* mRNA in RAW264.7 and peritoneal macrophages (**Figure 1E**). Similarly, intralipid significantly induced *Hilpda* mRNA in both types of macrophages (**Figure 1F**). The induction of HILPDA by intralipid in RAW264.7 and peritoneal macrophages was particularly evident at the protein level (**Figure 1G**). *Hilpda* was originally identified as hypoxia-inducible gene 2 (*Hig2*) [17]. Because hypoxic areas are characteristic of obese adipose tissue [18], we tested the effect of a combination of

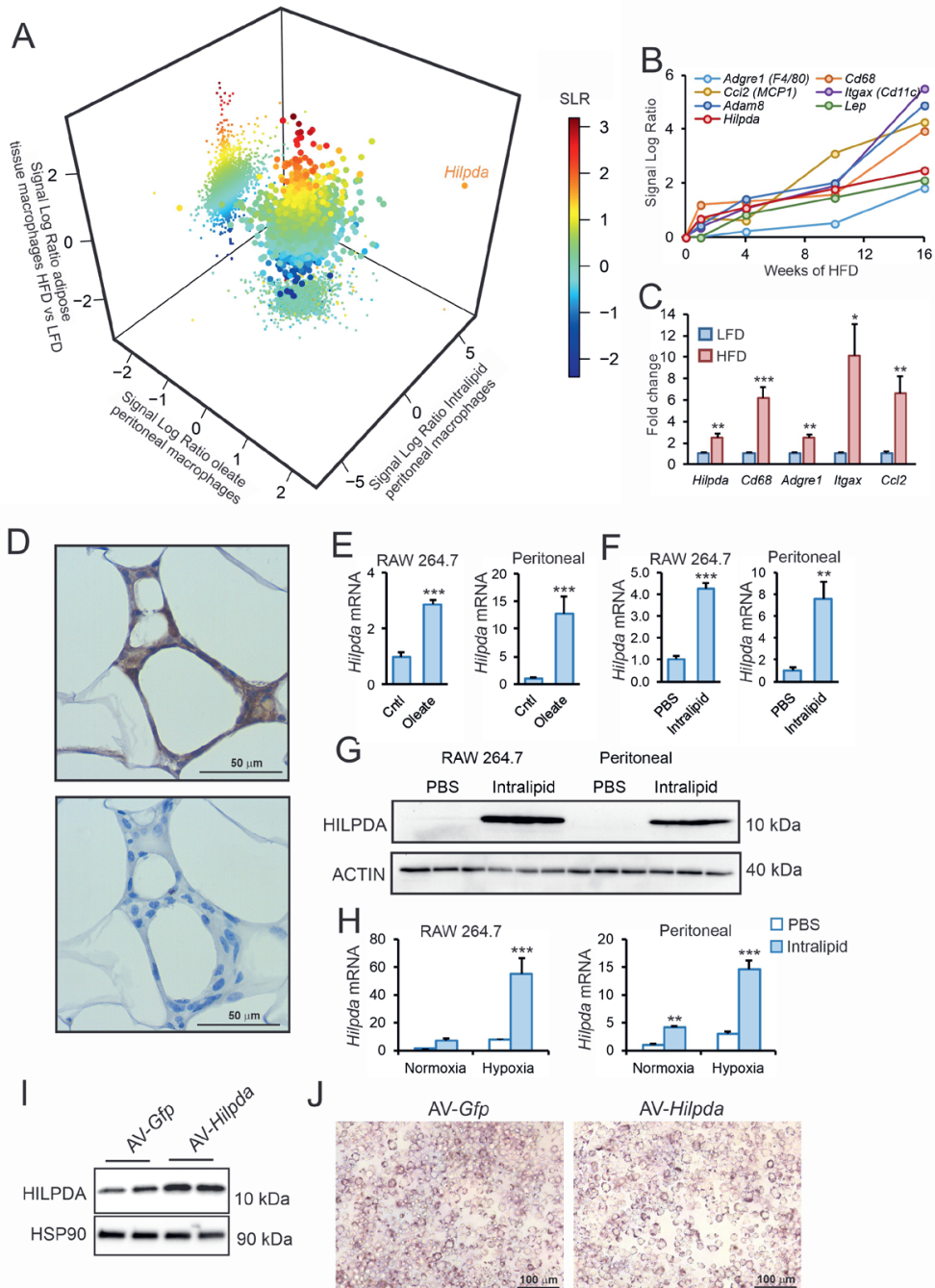


Figure 1. Lipid-responsive *Hilpda* as gene of interest in obese adipose tissue.

(A) Transcriptomics co-analysis of ATMs isolated from C57Bl/6 mice fed a HFD versus a LFD, C57Bl/6 mouse

peritoneal macrophages treated with oleate and C57Bl/6 *Angptl4*^{-/-} mouse peritoneal macrophages treated with intralipid. **(B)** Signal log-ratio of mRNA patterns of *Hilpda*, inflammatory genes and macrophage markers in gonadal adipose tissue of C57Bl/6 mice fed a HFD for 0, 1, 4, 10 or 16 weeks. **(C)** Gene expression of *Hilpda*, *Cd68*, *Adgre1*, *Itgax*, *Ccl2* in gonadal adipose tissue of C57Bl/6 mice fed a HFD for 20 weeks (LFD, n = 8; HFD, n = 10). **(D)** Immunohistochemical staining of HILPDA in gonadal adipose tissue from C57Bl/6 mice fed a HFD for 20 weeks (representative data for n = 10). Bottom panel is without primary antibody. **(E and F)** *Hilpda* mRNA expression in RAW264.7 and C57Bl/6 mouse peritoneal macrophages exposed to 250 μM of oleate **(E)** or 1 mM of intralipid **(F)** for 6 h versus BSA (control [Cntl]) or PBS. **(G)** HILPDA protein levels in RAW 264.7 and peritoneal macrophages exposed to 1 mM of intralipid or PBS for 6 h. ACTIN was used as the loading control. **(H)** *Hilpda* mRNA expression in RAW264.7 and C57Bl/6 mouse peritoneal macrophages exposed to 1 mM of intralipid or PBS in combination with normoxia or chemical hypoxia mimic induced by 100 μM of 2,2'-bipyridyl for 6 h. **(I)** HILPDA protein levels in RAW264.7 macrophages transduced with recombinant adenovirus expressing *Gfp* (AV-*Gfp*) or *Hilpda* (AV-*Hilpda*) at a multiplicity of infection of 500 for 48 h. **(J)** Oil Red O staining of RAW264.7 macrophages transduced with AV-*Gfp* or AV-*Hilpda*, followed by lipid loading with 667 μM of oleate and 333 μM of palmitate or BSA for 24 h. Bar graphs are presented as mean ± SEM (*in vivo* studies) or mean ± SD (*in vitro* studies). Statistical testing was performed by Student's t-test or by two-way ANOVA followed by Bonferroni's post hoc multiple comparisons test. The effect of treatment was significant in **(H)**. **p* < 0.05, ***p* ≤ 0.01, ****p* ≤ 0.001.

intralipid and a chemical hypoxia mimic. Together, they synergistically increased *Hilpda* mRNA **(Figure 1H)**.

Macrophage-specific *Hilpda* deficiency impairs lipid droplet accumulation

To study the effect of HILPDA on lipid storage in macrophages, we overexpressed HILPDA in RAW264.7 macrophages using an adenoviral vector **(Figure 1I)**. Interestingly, the marked increase in HILPDA protein levels was not accompanied by any changes in lipid droplet accumulation, as visualized by Oil Red O staining **(Figure 1J)**. These data indicate that overexpression of HILPDA in macrophages has no discernible effect on lipid storage.

We next switched to bone-marrow-derived macrophages (BMDMs) as a robust primary *in vitro* model. Similar to RAW264.7 and peritoneal macrophages, intralipid and chemical hypoxia synergistically upregulated *Hilpda* mRNA in BMDMs **(Figure 2A)**. To be able to study the effects of HILPDA deficiency in macrophages, we generated mice with a myeloid-specific *Hilpda* inactivation (*Hilpda*^{ΔMΦ}) by crossing *Hilpda*^{flox/flox} with mice expressing Cre-recombinase driven by the LysM promoter. BMDMs obtained from *Hilpda*^{ΔMΦ} mice and their *Hilpda*^{flox/flox} littermates were lipid-loaded with a combination of oleate and palmitate for 12 h to induce maximal lipid droplet formation. The Cre-mediated excision led to an approximate 80% reduction in *Hilpda* mRNA in BMDMs **(Figure 2B)** and a corresponding decrease in HILPDA protein **(Figure 2C)**. Strikingly, staining of neutral lipids by boron-dipyrromethene (BODIPY) in BMDMs showed that lipid droplets were much less visible in fatty acid-loaded *Hilpda*^{ΔMΦ} than *Hilpda*^{flox/flox} macrophages **(Figure 2D)**.

Quantitative analysis indicated that the number of lipid droplets per cell and the size of

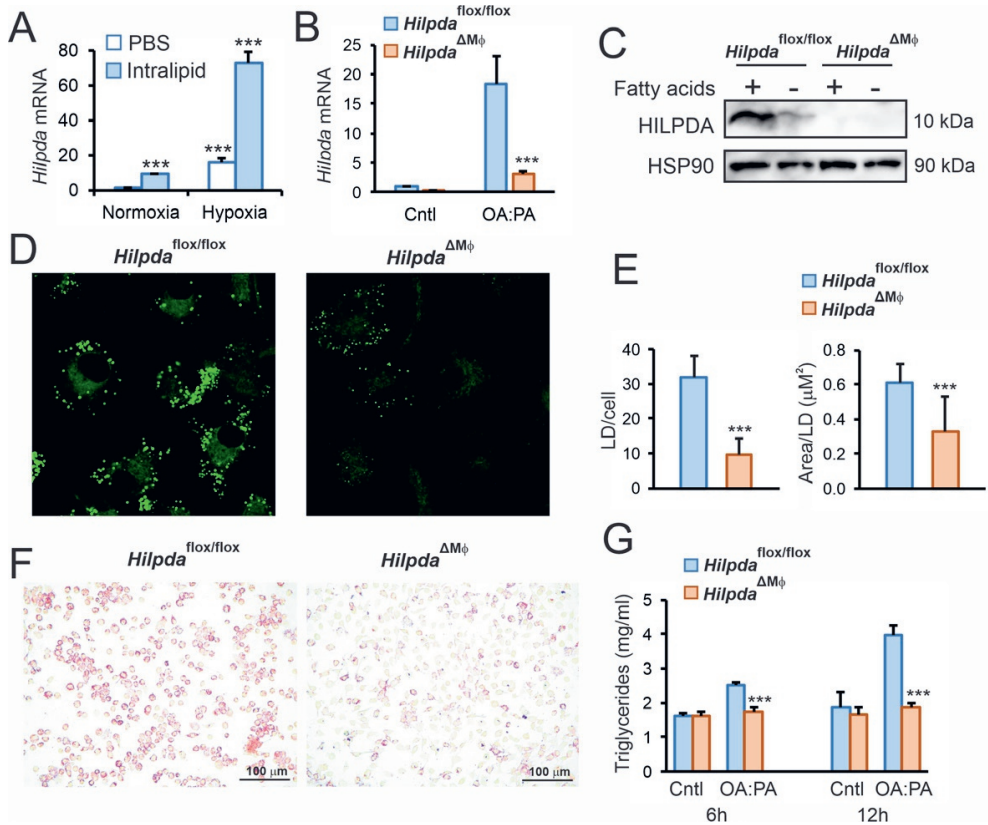


Figure 2. Myeloid-specific HILPDA deficiency impairs lipid droplet formation.

(A) *Hilpda* mRNA expression in C57Bl/6 BMDMs exposed to 1 mM of intralipid or PBS, combined with normoxia or chemical hypoxia induced by 100 μM of 2,2'-bipyridyl for 6 h. (B and C) Gene expression of *Hilpda* (B) and protein levels (C) of HILPDA in *Hilpda*^{flox/flox} and *Hilpda*^{ΔMφ} BMDMs lipid loaded with 400 μM of oleate and 200 μM of palmitate (OA:PA, Fatty acids) or BSA (Cntl) for 12 h (n = 3). HSP90 was used as loading control. (D-F) BODIPY (D and E) and oil Red O (F) staining in *Hilpda*^{flox/flox} and *Hilpda*^{ΔMφ} BMDMs lipid loaded with oleate:palmitate or BSA (Cntl) for 24 h. Data are shown from or are representative of at least three independent experiments. (G) Triglyceride measurement in BMDMs from *Hilpda*^{flox/flox} and *Hilpda*^{ΔMφ} lipid loaded with oleate:palmitate or BSA (Cntl) for 6 or 12 h. See also **Figure S1**. Bar graphs are presented as mean ± SD. Statistical testing was performed by Student's t-test or by two-way ANOVA followed by Bonferroni's post hoc multiple comparisons test. The effect of treatment was significant in (B) and (G). **p* < 0.05, ****p* ≤ 0.001. LD, lipid droplet; OA:PA, oleate:palmitate.

the lipid droplets were significantly lower in *Hilpda*^{ΔMφ} than in *Hilpda*^{flox/flox} macrophages (**Figure 2E**). This reduction of lipid droplets was confirmed by Oil Red O staining (**Figure 2F**). In addition, triglyceride levels were markedly decreased in fatty-acid-loaded *Hilpda*^{ΔMφ} compared to *Hilpda*^{flox/flox} macrophages (**Figure 2G**, **Figure S1**). Together, these data show that HILPDA deficiency in macrophages leads to a pronounced decrease in lipid storage.

HILPDA does not regulate fatty acid uptake or triglyceride synthesis

We next explored potential mechanisms underlying the decreased lipid storage in HILPDA-deficient macrophages. To determine whether the reduction in lipid storage in HILPDA-deficient macrophages is due to decreased lipid uptake, we measured fatty acid uptake 6 and 35 min after addition of a mixture of oleate and BODIPY-labeled C12 (BODIPY FL). Confocal microscopy showed no difference in fluorescence intensity between *Hilpda*^{ΔMΦ} and *Hilpda*^{fllox/fllox} macrophages at 6 and 35 min (**Figure 3A**), which was corroborated by quantitative image analysis (**Figure 3B**), indicating that HILPDA deficiency did not influence fatty acid uptake. Expression of the fatty acid transporter *Cd36* was comparable in *Hilpda*^{ΔMΦ} and *Hilpda*^{fllox/fllox} macrophages (**Figure 3C**). In addition, the early induction of gene expression by fatty acids was not different between *Hilpda*^{ΔMΦ} and *Hilpda*^{fllox/fllox} macrophages, regardless of whether the fatty acids were provided as free fatty acids (**Figure 3D**), or intralipid (**Figure S2**), clearly indicating that HILPDA does not regulate fatty acid uptake. Accordingly, we hypothesized that HILPDA may have two—not necessarily mutually exclusive—functions: (1) activator of fatty acid esterification, and/or (2) inhibitor of triglyceride lipolysis. If HILPDA acts by activating fatty acid esterification in macrophages, suggested before by Maier et al. [14], it would be expected that HILPDA deficiency would lead to accumulation of intermediates in the triglyceride synthesis pathway. To explore that possibility, we performed shotgun lipidomics on *Hilpda*^{ΔMΦ} and *Hilpda*^{fllox/fllox} BMDMs loaded with oleate:palmitate for 24 h. Partial least squares discriminant analysis clearly separated the two genotypes (**Figure 3E**), indicating that the lipidomics profiles of *Hilpda*^{ΔMΦ} and *Hilpda*^{fllox/fllox} macrophages are very distinct. Volcano plot analysis indicated that, although a number of lipids were increased in *Hilpda*^{ΔMΦ} macrophages, most lipids were reduced (**Figure 3F**). Indeed, levels of phosphatidic acids, diacylglycerols, and triglycerides were significantly decreased in *Hilpda*^{ΔMΦ} versus *Hilpda*^{fllox/fllox} macrophages (**Figure 3G**) as were cholesteryl-esters, whereas lysophosphatidic acids were hardly detectable. The decrease in triglycerides and diacylglycerols was accounted for by the major subspecies within each lipid class (**Figure 3H**). These data suggest that HILPDA probably does not regulate the fatty acid esterification pathway in macrophages.

HILPDA regulates lipid droplet mobilization through ATGL inhibition

To further investigate the molecular basis for the decreased lipid storage in HILPDA-deficient macrophages, we determined the trafficking of lipids after loading with a mixture of oleate and BODIPY FL for either 5 or 24 h. Strikingly, after lipid loading *Hilpda*^{fllox/fllox} macrophages for 5 h, the BODIPY FL had largely accumulated in lipid droplets,

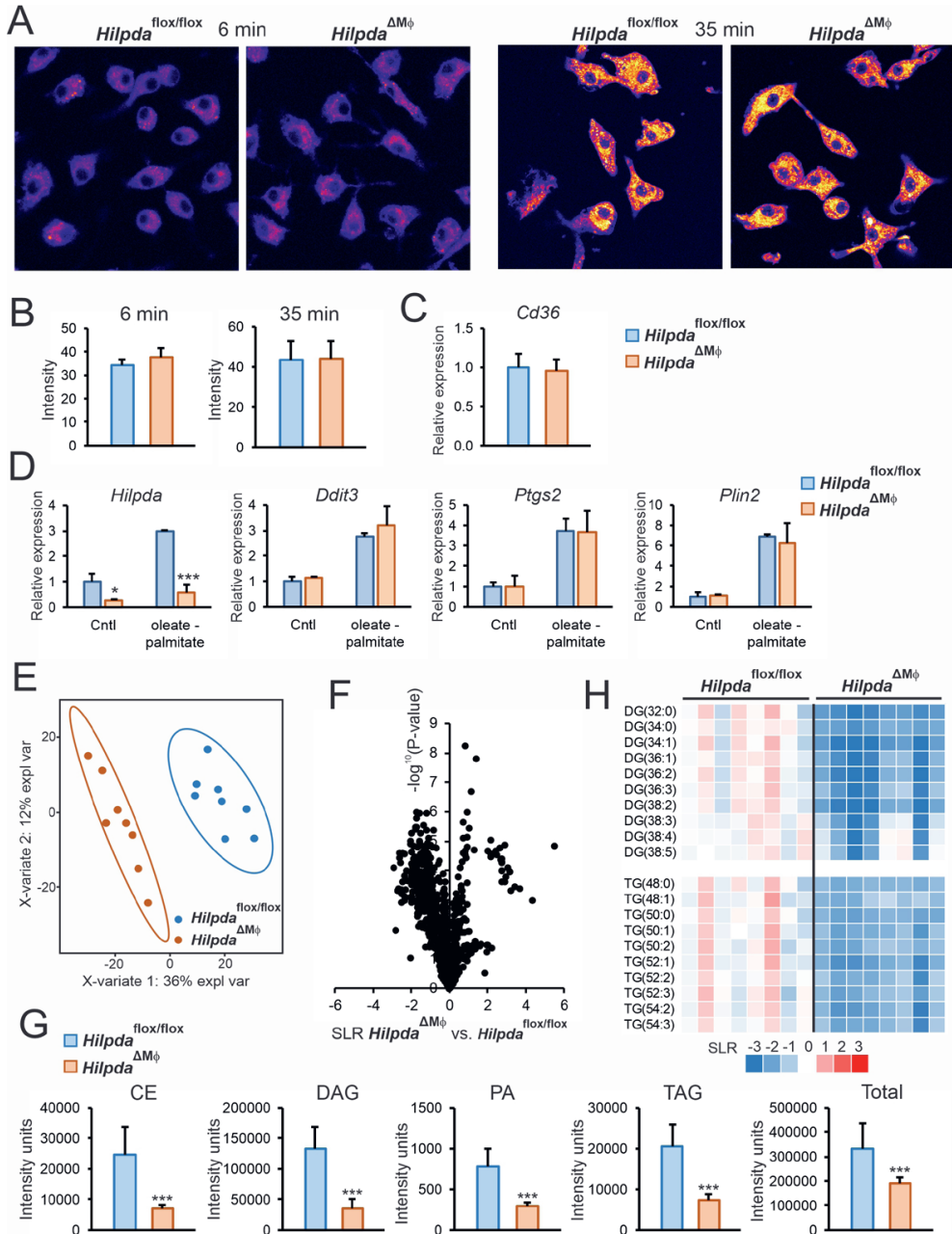


Figure 3. HILPDA does not regulate fatty acid uptake or triglyceride synthesis.

(A) Confocal microscopy of *Hilpda*^{flox/flox} and *Hilpda*^{ΔMφ} BMDMs incubated with BODIPY FL for 6 or 35 min. (B) Fluorescence quantification reflecting fatty acid uptake. (C) *Cd36* mRNA in *Hilpda*^{flox/flox} and *Hilpda*^{ΔMφ} BMDMs. (D) Gene expression of *Hilpda*, *Ddit3*, *Ptgs2* and *Plin2* in BMDMs from *Hilpda*^{flox/flox} and *Hilpda*^{ΔMφ} lipid loaded with oleate:palmitate or BSA (Cntl) for 6 h, (n = 3). See also **Figure S2**. Partial least-square discriminant analysis (E);

volcano plot analysis (**F**); differences in abundance of cholesteryl esters (CE), diacylglycerol (DAG), phosphatidic acid (PA), triacylglycerol (TAG) and total lipid species (**G**); and heatmap of most abundant DAG and TAG species (**H**) based on shotgun lipidomics on *Hilpda*^{fl^{ox}/fl^{ox}} and *Hilpda*^{ΔMΦ} BMDMs loaded with oleate:palmitate for 24 h. Bar graphs are presented as mean ± SD. Statistical testing was performed by Student's t-test or by two-way ANOVA followed by Bonferroni's post hoc multiple comparisons test. The effect of treatment was significant in **C**. **p* < 0.05, ****p* ≤ 0.001. SLR, signal log ratio.

whereas in *Hilpda*^{ΔMΦ} macrophages, the BODIPY FL was mainly distributed throughout the ER and showed only minor presence in lipid droplet-like structures (**Figure 4A**). After lipid loading for 24 h, the size and number of lipid droplets had further increased in *Hilpda*^{fl^{ox}/fl^{ox}} macrophages, whereas in *Hilpda*^{ΔMΦ} macrophages, the lipid-droplet-like structures that had initially formed at 5 h were no longer visible (**Figure 4A**). These data indicate that *Hilpda*^{ΔMΦ} BMDMs, although able to take up similar amounts of fatty acids as *Hilpda*^{fl^{ox}/fl^{ox}} BMDMs, are unable to retain them in lipid droplets.

Using various biochemical and cellular assays, we and others previously found that HILPDA is able to inhibit ATGL, the rate-limiting enzyme for lipolysis [15,16]. However, it is unclear whether HILPDA is a physiological regulator of ATGL in macrophages. To investigate if the decrease in lipid droplet and triglyceride accumulation in *Hilpda*^{ΔMΦ} macrophages is due to enhanced ATGL-mediated lipolysis, we loaded *Hilpda*^{ΔMΦ} and *Hilpda*^{fl^{ox}/fl^{ox}} BMDMs with oleate:palmitate in the presence of Atglistatin, a small-molecule inhibitor of ATGL [19]. Strikingly, inhibiting ATGL markedly increased lipid droplets in *Hilpda*^{ΔMΦ} BMDMs (**Figure 4B**), almost completely rescuing the *Hilpda*^{ΔMΦ} phenotype. Quantitative analysis showed that the lipid droplet surface area was not significantly affected by Atglistatin in *Hilpda*^{fl^{ox}/fl^{ox}} BMDMs and markedly increased by Atglistatin in *Hilpda*^{ΔMΦ} BMDMs (**Figure S3A**). Similarly, the defective retention of BODIPY FL in lipid droplets in *Hilpda*^{ΔMΦ} macrophages was almost completely abolished by Atglistatin (**Figure 4C**, **Figure S3B**). These studies indicate that the decrease in lipid droplet and triglyceride accumulation in *Hilpda*^{ΔMΦ} macrophages is caused by accelerated lipid droplet breakdown via enhanced ATGL-mediated lipolysis. Our data thus suggest that HILPDA functions as a potent endogenous inhibitor of ATGL in macrophages.

To determine whether HILPDA may influence the abundance of ATGL and other lipid droplet-associated proteins in macrophages, we performed Western blot on *Hilpda*^{ΔMΦ} and *Hilpda*^{fl^{ox}/fl^{ox}} BMDMs loaded with oleate:palmitate for 24 h. As expected, lipid loading increased HILPDA levels, as well as PLIN3 levels (**Figure 4D**). Remarkably, ATGL levels were markedly higher in *Hilpda*^{ΔMΦ} than *Hilpda*^{fl^{ox}/fl^{ox}} BMDMs, suggesting that HILPDA not only inhibits ATGL but also decreases ATGL protein levels. G0S2 protein levels, despite being difficult to detect, were also higher in *Hilpda*^{ΔMΦ} than *Hilpda*^{fl^{ox}/fl^{ox}} BMDMs.

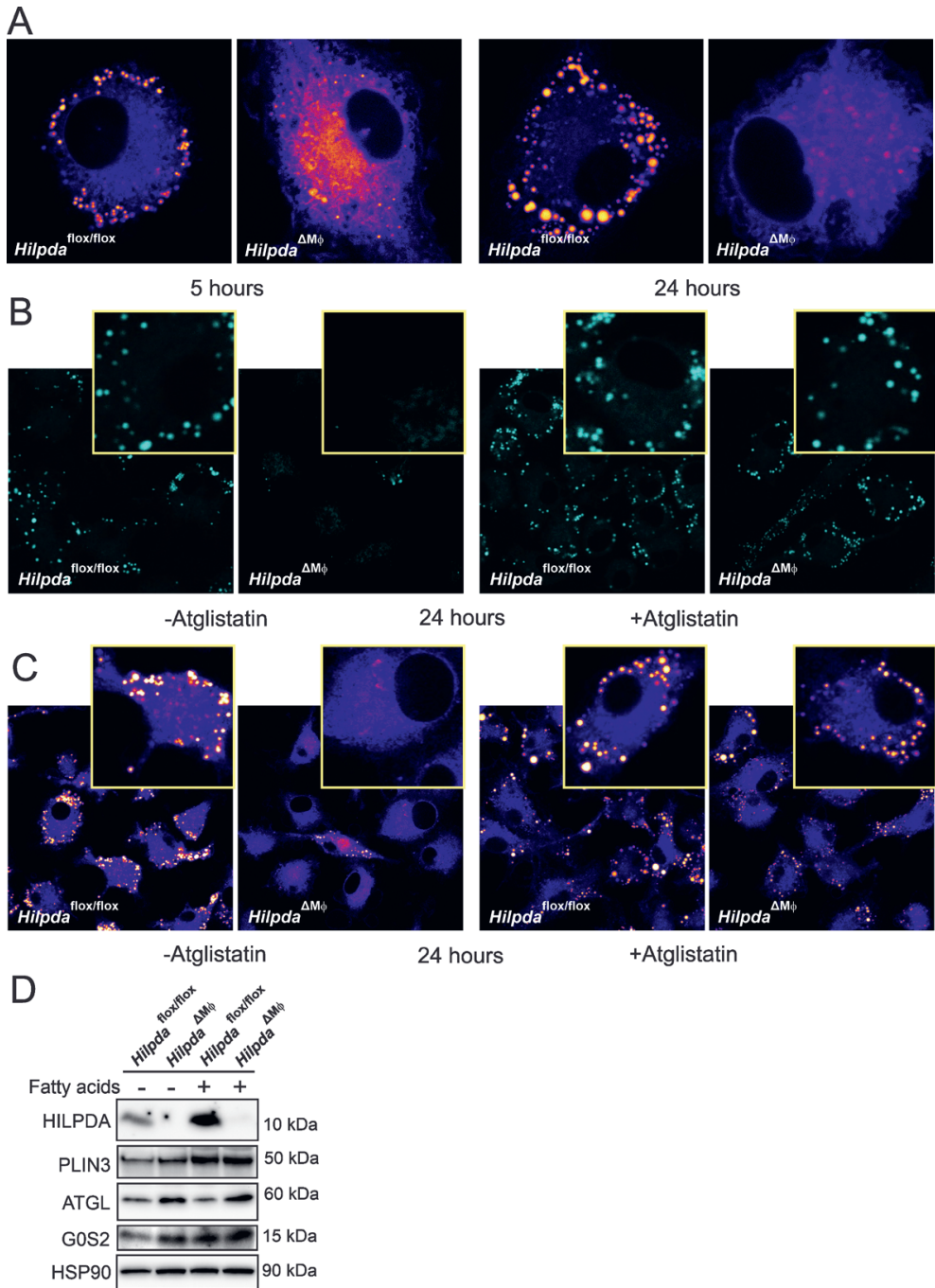


Figure 4. HILPDA regulates lipid droplet mobilization through ATGL inhibition.

(A) Fatty acid trafficking in *Hilpda*^{flox/flox} and *Hilpda*^{ΔMΦ} BMDMs lipid-loaded with oleate and BODIPY FL for 5 or 24 h. (B) BODIPY staining in *Hilpda*^{flox/flox} and *Hilpda*^{ΔMΦ} BMDMs lipid-loaded with oleate:palmitate for 24 h.

and treated with 20 μ M of Atglistatin or vehicle. **(C)** Fatty acid trafficking in *Hilpda*^{flox/flox} and *Hilpda* ^{Δ M Φ} BMDMs lipid-loaded with oleate and BODIPY FL for 24 h and treated with 20 μ M of Atglistatin or vehicle. **(D)** Protein expression of selected lipid droplet-associated proteins in *Hilpda*^{flox/flox} and *Hilpda* ^{Δ M Φ} BMDMs lipid-loaded with oleate:palmitate or BSA for 12 h. HSP90 was used as loading control. See also **Figure S3**. LD, lipid droplet.

HILPDA deficiency promotes respiration

If lipolysis is enhanced, the free fatty acid levels in the cell may rise, thereby stimulating fatty-acid-dependent gene regulation. Consistent with this notion, the expression of fatty-acid-inducible *Gdf15*, *Cpt1a* and *Il7r* was significantly higher in lipid-loaded *Hilpda* ^{Δ M Φ} than in *Hilpda*^{flox/flox} BMDMs (**Figure 5A**). To analyze that further, we performed transcriptomics on *Hilpda* ^{Δ M Φ} and *Hilpda*^{flox/flox} BMDMs loaded with oleate:palmitate for 24 h and co-analyzed the data together with a transcriptomics dataset of Robblee et al. [20] on wild-type BMDMs loaded with stearate for 20 h, as well as with the transcriptomics dataset of adipose tissue macrophages from obese and lean mice. In line with enhanced fatty-acid-dependent gene regulation in *Hilpda*-deficient macrophages, genes that were highly upregulated after stearate in wild-type BMDMs, such as *Gdf15*, *Il7r* and *Ddit3*, were also higher in fatty-acid-loaded *Hilpda* ^{Δ M Φ} than *Hilpda*^{flox/flox} BMDMs (**Figure 5B**). In addition, pro-inflammatory genes, such as *Ccl2* and *Il1b*, were downregulated by stearate in wild-type BMDMs and were also lower in fatty-acid-loaded *Hilpda* ^{Δ M Φ} compared to *Hilpda*^{flox/flox} BMDMs. Interestingly, genes induced by obesity in adipose tissue macrophages, such as *Lpl*, *Lipa*, and *Itgax*, were only weakly regulated by stearate and by HILPDA deficiency, suggesting distinct regulatory mechanisms (**Figure 5B**).

Of the 6,600 genes that passed the expression threshold, only 49 were induced more than 2-fold in fatty-acid-loaded *Hilpda* ^{Δ M Φ} compared with *Hilpda*^{flox/flox} BMDMs. The limited effect of impaired triglyceride retention in *Hilpda* ^{Δ M Φ} BMDMs suggests that the excess fatty acids may be disposed of, for instance by enhanced oxidation. To explore that option, cellular respiration was determined in fatty acid-loaded *Hilpda* ^{Δ M Φ} and *Hilpda*^{flox/flox} BMDMs. As a marker for oxidative phosphorylation, oxygen consumption of fatty acid-loaded *Hilpda* ^{Δ M Φ} and *Hilpda*^{flox/flox} BMDMs was measured by extracellular flux analysis during a mitochondrial stress test (**Figure 5C**). After 6 h of oleate:palmitate loading, basal and maximal respiration were slightly lower in *Hilpda* ^{Δ M Φ} than *Hilpda*^{flox/flox} BMDMs (**Figure 5D**). Remarkably, however, after 24 h of fatty acid loading, basal and maximal respiration were significantly higher in *Hilpda* ^{Δ M Φ} compared to *Hilpda*^{flox/flox} BMDMs (**Figure 5D**), indicating an increased maximal oxidative capacity. These data suggest that the enhanced lipolysis in *Hilpda* ^{Δ M Φ} BMDMs is accompanied by increased fatty acid oxidation through oxidative phosphorylation.

Next, we tested whether HILPDA might influence lipid droplet accumulation in macrophages in adipose tissue. To mimic the adipose environment *in vitro*, BMDMs were treated with conditioned medium of adipose tissue explants. Adipose-conditioned medium markedly increased *Hilpda* expression, along with that of several other lipid-sensitive genes, such as *Plin2*, *Cd36*, and *Angptl4* (Figure 5E). Consistent with our previous studies with fatty-acid-loaded macrophages, *Hilpda*^{ΔMΦ} BMDMs incubated with adipose-conditioned medium showed substantially reduced BODIPY staining compared with *Hilpda*^{flox/flox} BMDMs (Figure 5F). These data suggest that HILPDA may also influence lipid droplet accumulation in macrophages in adipose tissue.

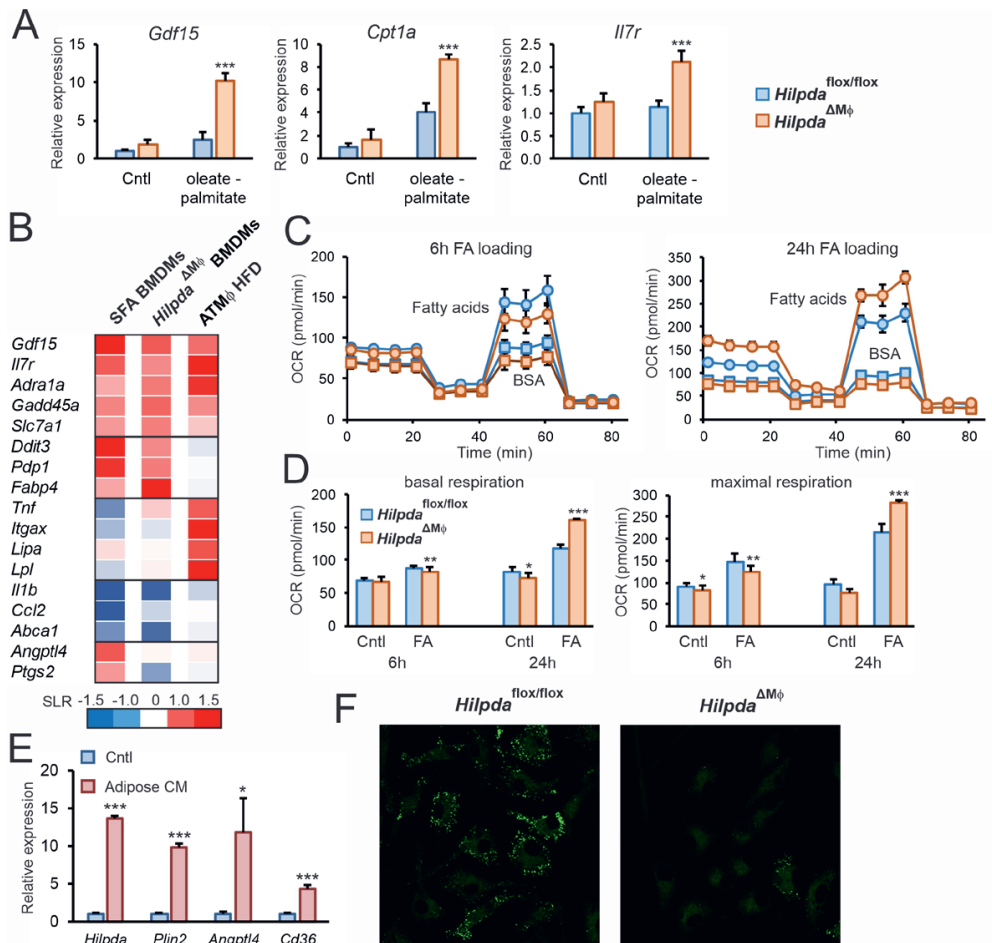


Figure 5. Loss of ATGL inhibition by HILPDA deficiency does not affect lipid-induced inflammation but increases oxidative respiration.

(A) Gene expression of *Gdf15*, *Cpt1a*, *Il7r* and *Fabp4* in *Hilpda*^{flox/flox} and *Hilpda*^{ΔMΦ} BMDMs lipid-loaded with oleate:palmitate or BSA (Cntl) for 12 h (n = 3). (B) Microarray-based gene expression of relevant genes in

wild-type (WT) C57Bl/6 mouse BMDMs loaded with stearate (250 μ M) for 20 h, *Hilpda* ^{Δ M Φ} BMDMs loaded with oleate:palmitate for 24 h and adipose tissue macrophages isolated from mice fed a HFD versus a LFD. (C and D) Oxygen consumption rate of *Hilpda*^{fl Δ /fl Δ} and *Hilpda* ^{Δ M Φ} lipid-loaded with oleate:palmitate or BSA (ctrl) for 6 or 24 h (C) and corresponding basal and maximal respiration levels (D). Data are representative of three independent experiments. (E and F) Gene expression levels of *Hilpda*, *Plin2*, *Angptl4* and *Cd36* in C57Bl/6 mouse BMDMs loaded with adipose-conditioned medium (CM) or Ctrl for 6 h (E) and BODIPY staining after loading with CM for 24 h (F) (n = 3). Bar graphs are presented as mean \pm SD. Statistical testing was performed by Student's t-test or by two-way ANOVA followed by Bonferroni's post hoc multiple comparisons test. The effect of treatment was significant in (A) and (D). * p < 0.05, ** p \leq 0.01, *** p \leq 0.001. FA, fatty acid loading with oleate:palmitate; SLR, signal log ratio.

Myeloid-specific deficiency of HILPDA decreases lipid droplets in adipose tissue macrophages (ATMs) without altering adipose tissue inflammation

To enable studying the effect on HILPDA deficiency in macrophages *in vivo*, we used *Hilpda* ^{Δ M Φ} mice and their *Hilpda*^{fl Δ /fl Δ} littermates. As expected, myeloid-specific inactivation of *Hilpda* significantly decreased *Hilpda* expression in the stromal vascular fraction of adipose tissue but not in the adipocyte fraction (Figure 6A). To test the functional consequences of macrophage HILPDA deficiency in the context of obesity-induced adipose tissue inflammation and foam cell formation, *Hilpda* ^{Δ M Φ} mice and their *Hilpda*^{fl Δ /fl Δ} littermates were rendered obese and insulin resistant by high-fat feeding for 20 weeks, using a low-fat diet as control. Bodyweight gain (Figure 6B), feed intake (Figure 6C), and liver and adipose tissue weights (Figure 6D) were not different between *Hilpda* ^{Δ M Φ} and *Hilpda*^{fl Δ /fl Δ} littermates. Consistent with the data shown in Figure 1C, high-fat feeding increased *Hilpda* mRNA in adipose tissue. Interestingly, the relative increase in *Hilpda* mRNA was considerably lower in *Hilpda* ^{Δ M Φ} than it was in *Hilpda*^{fl Δ /fl Δ} adipose tissue (Figure 6E), suggesting that the increase in *Hilpda* expression by high-fat feeding is mainly driven by its expression in macrophages. Immunoblot for HILPDA confirmed that notion by showing markedly reduced HILPDA protein levels in *Hilpda* ^{Δ M Φ} versus *Hilpda*^{fl Δ /fl Δ} adipose tissue (Figure 6F).

Based on the studies in BMDMs, we hypothesized that lipid accumulation would be reduced in adipose tissue macrophages from *Hilpda* ^{Δ M Φ} mice compared with *Hilpda*^{fl Δ /fl Δ} mice. Indeed, oil Red O staining showed significantly lower lipid droplet content in adipose tissue macrophages isolated from high-fat diet (HFD)-fed *Hilpda* ^{Δ M Φ} mice compared with HFD-fed *Hilpda*^{fl Δ /fl Δ} mice (Figure 7A, B). Interestingly, however, the decrease in lipid droplets was not associated with any change in the secretion of the classical inflammatory cytokines interleukin-6 (IL-6) and tumor necrosis factor alpha (TNF- α) (Figure 7C). These data indicate that HILPDA deficiency reduces lipid accumulation in adipose tissue macrophages but does not have any effect on their *ex vivo* inflammatory properties.

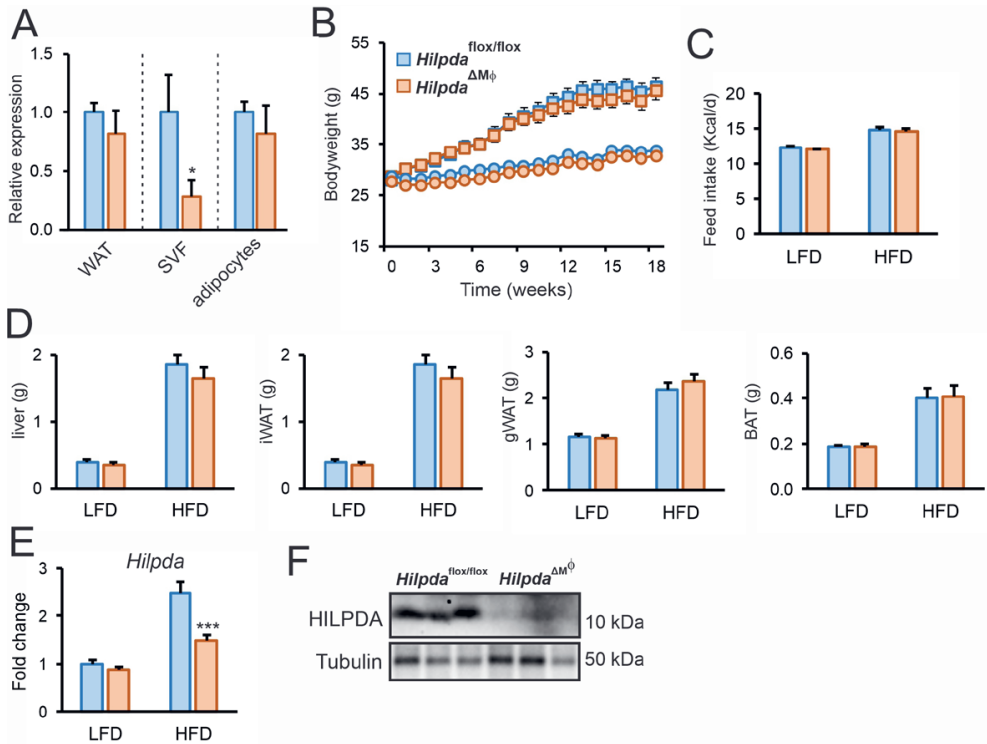


Figure 6. *Hilpda* deficiency in myeloid cells results in a decrease in HILPDA in gonadal white adipose tissue (gWAT) after high-fat feeding, without influencing body and organ weight.

(A) Relative gene expression of *Hilpda* in whole gWAT, stromal vascular fraction, and adipocyte fraction of *Hilpda*^{flx/flx} and *Hilpda*^{ΔMΦ} (n = 3-7). (B-F) Body weight (B), feed intake (C) and weight of liver, inguinal white adipose tissue (iWAT), gWAT and BAT (D) in *Hilpda*^{flx/flx} and *Hilpda*^{ΔMΦ} mice fed a LFD or HFD for 20 weeks. *Hilpda* gene expression in gWAT (E) and HILPDA protein expression in gWAT (F). Bar graphs are presented as mean ± SEM, (n = 10-12 mice per group). Statistical testing was performed by Student's t-test or by two-way ANOVA followed by Bonferroni's post hoc multiple comparisons test. The effect of diet was significant in (C), (D) and (E). *p < 0.05, ***p ≤ 0.001. BAT, brown adipose tissue; gWAT, gonadal adipose tissue; iWAT, inguinal adipose tissue; SVF, stromal vascular fraction.

To investigate the potential effect of macrophage HILPDA on adipose tissue inflammation *in vivo*, we performed flow cytometry analysis of the stromal vascular fraction isolated from the adipose tissue of the various groups of mice. The results showed an increased percentage of populations of CD45+, CD11b+CD206+, and CD11b+CD11c+ cells by high-fat feeding, but no clear differences in the percentages of those populations between *Hilpda*^{ΔMΦ} and *Hilpda*^{flx/flx} mice (Figure 7D). To further examine the influence of macrophage HILPDA deficiency on inflammation in adipose tissue, we determined the expression of selected genes. Interestingly, mRNA levels of both inflammatory macrophage marker *Itgax* (CD11c) and general macrophage marker *Cd68* were significantly lower in

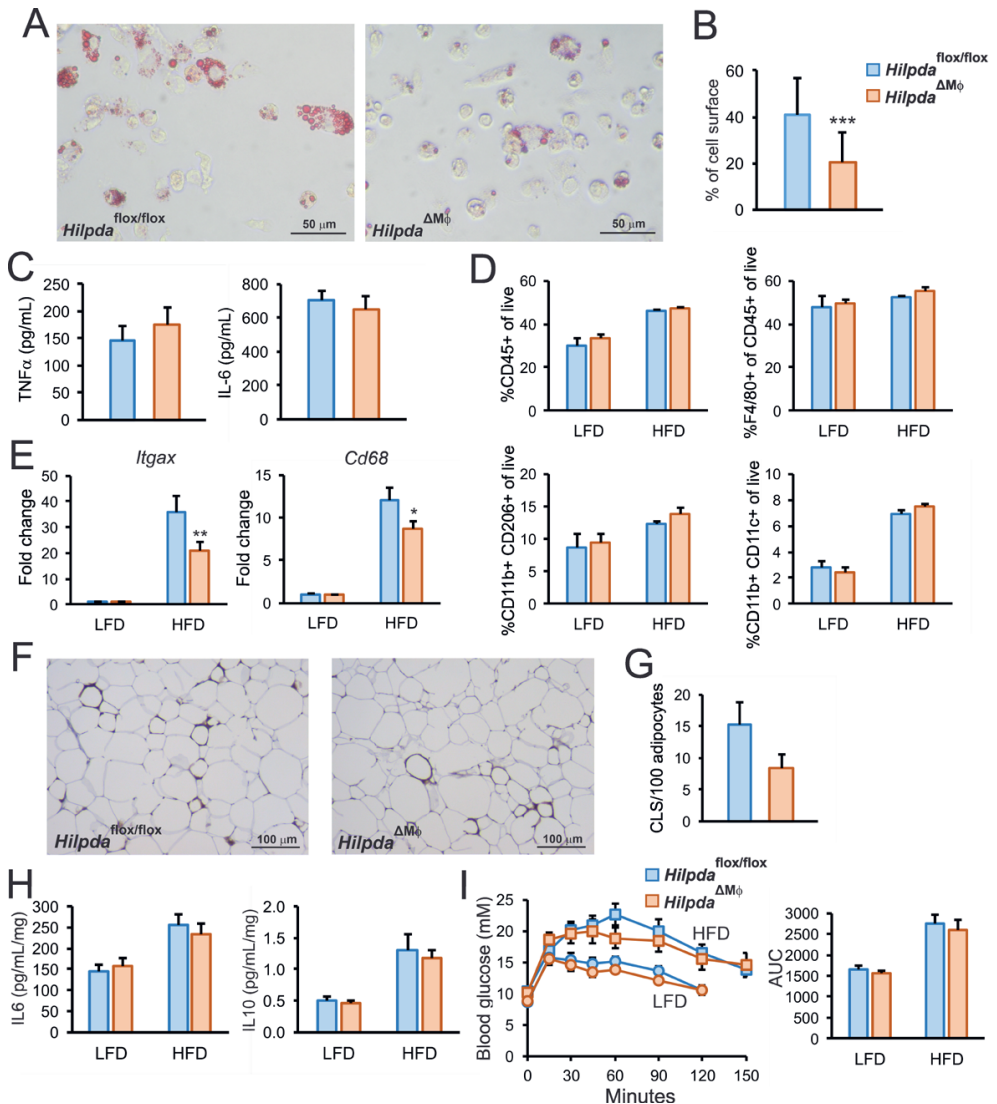


Figure 7. Myeloid-specific deficiency of *Hilpda* decreases lipid droplets in ATMs without altering adipose tissue inflammation or glucose tolerance.

(A) Oil red O staining of adipose tissue macrophages isolated from *Hilpda*^{flox/flox} and *Hilpda*^{ΔMφ} mice fed a HFD for 20 weeks. (B) Quantification of oil red O staining. Data are mean ± SD. (C) Corrected TNF-α and IL-6 secretion of adipose tissue macrophages from *Hilpda*^{flox/flox} and *Hilpda*^{ΔMφ} mice fed a HFD for 20 weeks (n = 10-12 per group, pooled per 3-4). (D) Flow-cytometry-based percentages of CD45+, CD45+F4/80+, CD11b+CD206+ and CD11b+CD11c+ populations in the SVF of gWAT from *Hilpda*^{flox/flox} and *Hilpda*^{ΔMφ} mice (n = 10-12, pooled per 3-4). (E) Gene expression of *Itgax*, *Adgre1*, *Cd68*, *Ccl2*, *Il10*, *Il1ra*, see also Figure S4. (F-H) Density of CLSs in gWAT coupes stained for F4/80 from *Hilpda*^{flox/flox} (F) and *Hilpda*^{ΔMφ} (G) mice (only for HFD) and secretion of IL-6 and IL-10 (H) in gWAT explants (n = 10-12 per group). (I) Glucose tolerance test after 18 weeks of LFD or HFD feeding; see also Figure S5. Bar graphs are presented as mean ± SEM (n = 10-12 mice per group). Statistical testing was

performed by Student's t-test or by two-way ANOVA followed by Bonferroni's post hoc multiple comparisons test. The effect of diet was significant in (D), (E), (H) and the AUCs of (I). * $p < 0.05$, ** $p \leq 0.01$, *** $p \leq 0.001$. AUC, Area under the curve; CLS: crown-like structure; SVF, stromal vascular fraction.

adipose tissue of *Hilpda*^{ΔMΦ} mice versus *Hilpda*^{fllox/fllox} mice fed a HFD (**Figure 7E**), whereas the general macrophage marker *Adgre1* (F4/80) showed a trend toward a decreased expression (**Figure S4**). Despite being induced by high-fat feeding, adipose expression of other pro- or anti-inflammatory genes, such as *Gdf15*, *Il10*, *Arg1*, *Ccl2*, and *Il1ra*, was not significantly different between *Hilpda*^{ΔMΦ} and *Hilpda*^{fllox/fllox} mice (**Figure S4**). Expression of *Adipoq* and *Leptin* also was not different between *Hilpda*^{ΔMΦ} and *Hilpda*^{fllox/fllox} mice (**Figure S4**).

To further investigate the inflammatory status of adipose tissue, the density of crown-like structures was determined in adipose tissue of *Hilpda*^{ΔMΦ} and *Hilpda*^{fllox/fllox} mice fed a HFD. A trend toward lower density was found in the *Hilpda*^{ΔMΦ} mice (**Figure 7F**), which, however, did not reach statistical significance (**Figure 7G**). Additionally, we measured the *ex vivo* release of cytokines from adipose tissue explants. Although high-fat feeding stimulated the release of IL-10 and IL-6, no significant difference in IL-10 and IL-6 release was observed between adipose tissue explants from *Hilpda*^{ΔMΦ} and *Hilpda*^{fllox/fllox} mice (**Figure 7H**).

Finally, to determine whether macrophage HILPDA deficiency has any influence on obesity-induced metabolic derailments, we measured plasma metabolic parameters and assessed glucose tolerance in *Hilpda*^{ΔMΦ} and *Hilpda*^{fllox/fllox} mice fed the low- and high-fat diets. High-fat feeding significantly increased plasma levels of cholesterol, triglycerides, glucose, non-esterified fatty acids, leptin, and insulin (**Figure S5**). However, no difference in these parameters were observed between *Hilpda*^{ΔMΦ} and *Hilpda*^{fllox/fllox} mice, either on a low- or high-fat diet (**Figure S5**). Similarly, although high-fat feeding caused a marked decrease in glucose tolerance, no differences were observed between *Hilpda*^{ΔMΦ} and *Hilpda*^{fllox/fllox} mice (**Figure 7I**).

Collectively, our data indicate that myeloid-specific HILPDA deficiency reduces lipid droplet accumulation in adipose tissue macrophages but does not influence the inflammatory status of adipose tissue and does not have any effect on obesity-induced metabolic complications.

Discussion

Here we show that HILPDA deficiency in macrophages disrupts stable lipid droplet formation after lipid loading. The reduction in lipid droplets is caused by impaired retention of lipids because of elevated ATGL-mediated lipolysis, which, in turn, is associated with increased oxidative metabolism (**Figure S6**). Overall, our data demonstrate that HILPDA is an endogenous and physiological inhibitor of ATGL in macrophages. Strikingly, despite reducing lipid storage in adipose tissue macrophages, HILPDA deficiency in macrophages does not alter the inflammatory status of adipose tissue in diet-induced obesity, arguing against the notion that lipid droplet accumulation in adipose tissue macrophages promotes adipose tissue inflammation and associated metabolic complications, such as insulin resistance.

During obesity, macrophages infiltrate the adipose tissue and take up adipocyte-released lipids. The resulting lipid-laden macrophages are found in crown-like structures in murine and human obesity [7,8,21]. These macrophages form a distinct subpopulation with a characteristic activation that is likely triggered by the adipocyte-released lipids [22–24]. Because lipid droplet formation often serves as a cytoprotective mechanism to prevent lipotoxicity by lipid intermediates or free fatty acids [25], it could be hypothesized that the enhanced lipid droplet breakdown in HILPDA-deficient macrophages may result in elevated inflammation. However, HILPDA deficiency not only reduced intracellular triglyceride levels but also the levels of potentially lipotoxic intermediates, such as diacylglycerols, likely via enhanced fatty acid oxidation, which may be predicted to lead to reduced inflammation [26]. Intriguingly, however, no clear effect of HILPDA deficiency was observed on cytokine release by adipose tissue macrophages, on the percentage of different macrophage populations in adipose tissue, on inflammatory gene expression in adipose tissue, and on cytokine release by adipose tissue explants. In addition, genes typically elevated in adipose tissue macrophages of obese mice, such as *Lipa*, *Lpl*, and *Itgax*, were not induced by fatty acid loading or altered by HILPDA deficiency. The data argue against the notion that excessive lipid droplet accumulation in adipose tissue macrophages is the major driver of adipose tissue inflammation and of the composition of macrophage populations in obese adipose tissue. Rather, the unique profile of adipose tissue macrophages may be determined by other factors active in the obese adipose tissue environment, the identity of which requires further study.

As indicated above, HILPDA-deficient macrophages exhibited a marked decrease in intracellular levels of all the major lipid species, including triglycerides, diacylglycerols, phosphatidic acids, and cholesteryl-esters, likely due to enhanced fatty acid oxidation.

Previously, a strong link was made between ATGL activity and fatty acid oxidation in liver and heart. It was found that ATGL-mediated lipolysis activates a transcriptional network involving PGC-1 α /PPAR- α that controls fatty acid oxidation and mitochondrial biogenesis [27–30]. Accordingly, it is likely that the loss of ATGL inhibition is directly responsible for the enhanced oxidative capacity, reducing the total intracellular lipid levels. In general, increased lipolysis and increased oxidative respiration are two traits essential for macrophage polarization toward alternative, M2-like phenotypes, which may be protective in the context of adipose tissue inflammation [31–33]. In our experiments, increased oxidative respiration seemed a mere consequence following overactive ATGL-mediated lipolysis and did not contribute to any anti-inflammatory effects. Although increased oxidation of fatty acids is often proposed as an alternative cytoprotective pathway in lipid-laden macrophages, the interplay between fatty acid oxidation, concomitant reactive oxygen species (ROS) formation, and ER stress complicates this mechanism [26].

Apart from fatty acid oxidation, ATGL has also been linked to the autophagic degradation of lipid droplets, termed lipophagy [34]. It was suggested that ATGL acts as a signaling node to promote lipophagy, which then controls bulk lipid droplet breakdown. Whether HILPDA, via ATGL, connects to lipophagy requires further study.

In contrast to the cytoprotective effect of normal lipid droplet formation, the adverse effects of excessive triglyceride storage becomes apparent in ATGL^{-/-} macrophages, underlining the importance of functional ATGL in macrophages [35–38]. Indeed, the elevated triglyceride accumulation in ATGL^{-/-} macrophages is accompanied by mitochondrial dysfunction and apoptosis, ER stress, reduced macrophage migration, and decreased phagocytosis ability [35–38], suggesting that proper macrophage function is dependent on the liberation of free fatty acids from intracellular triglyceride stores. The ATGL-mediated release of fatty acids is also necessary for the production of lipid mediators, at least in neutrophils [39]. Similar to ATGL^{-/-} macrophages, macrophages deficient in the ATGL activator CGI-58 (also known as ABHD5) also have elevated lipid storage and decreased phagocytic capacity but show no signs of mitochondrial apoptosis and ER stress, suggesting that triglyceride accumulation per se does not drive mitochondrial dysfunction [40]. Our data show that HILPDA deficiency, despite leading to markedly reduced lipid storage, raises markers of ER stress, suggesting that triglyceride storage protects against lipid-induced ER stress. Presumably, the mechanism leading to ER stress is different in HILPDA-deficient macrophages as compared with ATGL/CGI-58-deficient macrophages.

HILPDA was initially identified in a screen for hypoxia-inducible genes in human cervical cancer cells and was later found to be associated with lipid droplets [10,17]. We identified

Hilpda as a novel PPAR- α target gene in liver [9]. In addition, *Hilpda* is well expressed in adipocytes [11,13]. Several studies have shown that overexpression of *Hilpda* increases intracellular lipid storage in cells [9–11]. In the present study, *Hilpda* emerged from a screen for genes elevated by obesity in adipose tissue macrophages and upregulated in macrophages by fatty acids. Induction of HILPDA by fatty acids and subsequent inhibition of triglyceride hydrolysis is likely part of a lipid-buffering effort of the cell to effectively store excess energy and neutralize the potentially reactive free fatty acids (**Figure S6**).

The observation that the decrease in lipid storage in HILPDA-deficient macrophages can be almost completely abolished by inhibition of ATGL indicates that HILPDA is an endogenous inhibitor of ATGL in macrophages, which is in line with previous data showing direct inhibition of ATGL by HILPDA [15,16]. Intriguingly, HILPDA reduced ATGL protein levels in BMDMs, which supports our previous finding that HILPDA reduces ATGL protein levels in 3T3-L1 adipocytes [11]. It can be hypothesized that binding of HILPDA to ATGL might destabilize it, leading to enhanced ATGL degradation. This option should be investigated in future experiments. Of note, our observation that forced upregulation of HILPDA levels in macrophages does not noticeably increase lipid droplet accumulation suggests that inhibition of ATGL is nearly maxed out in lipid-loaded macrophages.

The inhibition of ATGL by HILPDA is analogous to the inhibition by G0/G1 switch gene 2 (G0S2), with which HILPDA shares extensive sequence homology [15,16,41]. However, the inhibitory potency of HILPDA was low compared to G0S2, which raised questions on the physiological relevance of HILPDA as ATGL inhibitor. Our studies demonstrate that HILPDA is a potent endogenous inhibitor of ATGL-mediated lipolysis in macrophages. A number of questions emerge from this work. First, why does HILPDA, despite allegedly being a much weaker ATGL inhibitor than G0S2, have such a marked influence on lipid storage in macrophages? We hypothesize that HILPDA may require an interaction with an auxiliary factor for full activity. Further research is necessary to identify the mechanism for the differential potency of HILPDA in cell-free systems compared to live cells. Second, what is the reason for having two related ATGL inhibitors? Although our preliminary data suggest that in BMDMs, HILPDA is much more abundant than G0S2; it seems that in certain cells, such as cultured hepatocytes, HILPDA and G0S2 co-exist. Inasmuch as HILPDA and G0S2 are induced by different stimuli, they may be active under different circumstances. So far, there is no evidence for any functional dependency between the two proteins. Further research is necessary to better characterize the relationship and relative roles of these two homologous proteins in different cell types.

In conclusion, our data demonstrate that HILPDA is a lipid-inducible physiological inhibitor

of ATGL-mediated lipolysis in macrophages. In obese mice, HILPDA uncouples lipid droplet accumulation in adipose tissue macrophages from inflammation and metabolic dysregulation. Overall, our data question the importance of lipid storage in adipose tissue macrophages in obesity-induced inflammation and metabolic dysregulation.

Acknowledgements

We would like to thank Shohreh Keshtkar, Karin Mudde, Jenny Jansen, Anneke Hijmans, Tessa de Bie, and Jacqueline Ratter for their technical assistance. This work was financed by grants from the Netherlands Organisation of Scientific Research (2014/12393/ALW), the Dutch Diabetes Foundation (2015.82.1824), and the Netherlands Heart Foundation (ENERGISE grant CVON2014-02).

Author contributions

X.v.D., M.d.I.R., A.G., F.M., W.D., J.B. R.St. and S.K. conceived and planned the research and experiments. X.v.D. carried out the *Hilpda*^{ΔM⁰} mouse studies. X.v.D., M.d.I.R., A.G., F.M. and W.D. carried out the experiments and analyzed the data. M.v.W. carried out the lipidomics analysis. R.Si. and J.B. contributed to the interpretation of the results. X.v.D. carried out the statistical analyses. X.v.D., R.St. and S.K. wrote the manuscript. All authors provided critical feedback and helped to shape the research, analysis and manuscript.

Declaration of interests

The authors declare no competing interests.

STAR METHODS

LEAD CONTACT AND MATERIALS AVAILABILITY

Further information and requests for resources should be directed to and will be fulfilled by the Lead Contact, Sander Kersten (sander.kersten@wur.nl). This study did not generate new unique reagents.

EXPERIMENTAL MODEL AND SUBJECT DETAILS

Animal studies

Studies were performed using purebred wildtype C57BL/6 mice, *Hilpda*^{ΔM^Φ} mice and their *Hilpda*^{flox/flox} littermates. *Hilpda*^{flox/flox} were acquired (Jackson Laboratories, Bar Harbor, ME; *Hilpda*^{tm1.1Nat/J}, JAX: #017360, RRID: MGI:5285399) and backcrossed onto a C57BL/6 background in our facility for at least 5 generations. *LysM-Cre* transgenic mice (B6.129P2-Lyz2tm1^(cre)/J, JAX:#004781, RRID: IMSR_JAX:004781) were acquired from Jackson laboratories. Prior to arrival at Jackson laboratories, the *LysM-Cre* transgenic mice have been backcrossed onto a C57BL/6 background for at least six generations. In our facility, the *Hilpda*^{flox/flox} were crossed with *LysM-Cre* transgenic mice to generate mice with a mature myeloid cell-specific Cre-mediated deletion of *Hilpda* on a C57BL/6 background. The identity of the C57BL/6 background strain was not confirmed by sequencing. Mice were individually housed under normal light-dark cycles in temperature- and humidity-controlled specific pathogen-free conditions. Mice had *ad libitum* access to food and water. The experimenter was blinded to group assignments during all analyses. For *in vivo* studies, male mice were used with an age of 9-12 weeks. For the isolation of primary cell cultures, both male and female mice were used with an age of 8-12 weeks. All animal experiments were approved by the local animal welfare committee of Wageningen University (AVD104002015236, 2016.W-0093.001).

Cell lines and primary cultures

RAW264.7 macrophage cells (Cat#91062702; RRID: CVCL_0493, Sigma-Aldrich, Darmstadt, Germany) and bone-marrow derived macrophages were cultured in Dulbecco's modified Eagle's medium (DMEM, Corning, NY, USA), supplemented with 1% penicillin/streptomycin (P/S, Corning). Adipose tissue macrophages and peritoneal macrophages were cultured in Roswell Park Memorial Institute (RPMI)-1630 medium (Lonza, Basel, Zwitserland) supplemented with 10% FCS and 1% P/S. All cells were kept in incubators at 37°C/5% CO₂. Primary cell cultures were isolated from male and female wildtype C57BL/6, *Hilpda*^{ΔM^Φ} and *Hilpda*^{flox/flox} mice aged 8-12 weeks. RAW264.7 macrophages were purchased as authenticated cell line from Sigma-Aldrich.

METHOD DETAILS

Mouse studies

Per genotype, 12 male *Hilpda*^{ΔM^Φ} mice aged 9-12 weeks or their male *Hilpda*^{flox/flox} littermates were randomly allocated using an online randomisation tool to either a standardized high-fat diet or a low-fat diet (formula D12451 and formula D12450H respectively, Research Diets, New Brunswick, USA; γ -irradiated with 10-20 kGy) for 20 weeks. Body weight and feed intake were assessed weekly. At the end of the study, mice were anaesthetised with isoflurane and blood was collected via orbital puncture in tubes containing EDTA (Sarstedt, Nümbrecht, Germany). Subsequently, mice were immediately euthanized by cervical dislocation, after which tissues were excised, weighed and frozen in liquid nitrogen or prepared for histology. Frozen samples were stored at -80°C.

Intraperitoneal glucose tolerance test

In the HFD-LFD study, an intraperitoneal glucose tolerance test was performed after 18 weeks. Mice were fasted for 5 hours and blood was collected via tail bleeding at 0, 15, 30, 45, 60, 90 and 120 minutes after i.p. injection of 1g/kg bodyweight glucose (Baxter, Deerfield, IL, USA). Blood glucose was measured with a GLUCOFIX Tech glucometer and glucose sensor test strips (GLUCOFIX Tech, Menarini Diagnostics, Valkenswaard, The Netherlands). A time point of 150 minutes after injection of glucose was added for the high-fat diet fed groups.

Plasma measurements

Blood collected in EDTA tubes was spun down for 15 minutes at 5000 RPM at 4°C. Plasma was aliquoted and stored at -80°C until measurement of cholesterol (Liquicolor, Human GmbH, Wiesbaden, Germany), triglycerides (Liquicolor), glucose (Liquicolor), NEFAs (NEFA-HR set R1, R2 and standard, WAKO Diagnostics, Instruchemie, Delfzijl, The Netherlands), adiponectin (ELISA duoset kit, R&D Systems, Bio-technie, MN, USA), leptin (ELISA duoset kit, R&D Systems) and insulin (ultra-sensitive mouse insulin ELISA kit, Crystal Chem Inc., IL, USA) following manufacturer's instructions.

gWAT explants and adipose macrophage isolation

For SVF, adipocytes and adipose tissue macrophages isolation, gonadal adipose tissue (gWAT) was collected and kept in with DMEM supplemented with 1% P/S and 1% FFA-free Bovine Serum Albumin (BSA fraction V, Roche via Merck, Darmstadt, Germany) on ice. gWAT explants were taken into culture for 24h in DMEM, supplemented with 10% fetal calf serum (FCS, BioWest, Nuaille, France) and 1% P/S. Supernatant was stored for ELISA measurements or as conditioned medium. For high-fat diet groups, the stromal

vascular fractions were isolated by digesting gWAT for 45 minutes in Roswell Park Memorial Institute (RPMI)-1630 medium (Lonza, Basel, Zwitserland) supplemented with 10% FCS, 1% P/S, 0.5% FFA-free BSA, 1M CaCl₂, 1M HEPES and 0.15% collagenase (from *Clostridium histolyticum*, Sigma-Aldrich, Cat#C6885; CAS: 9001-12-1). Per three mice of the same group, gWAT was pooled after digestion, filtered through a 100µm cell strainer and centrifuged at 200g for 10 min. Floating mature adipocytes were removed and stored separately and stromal vascular pellet was resuspended in erythrocyte lysis buffer and subsequently washed twice in phosphate buffered saline (PBS, Corning) supplemented with 0.5% FFA-free BSA and 2mM EDTA. Resulting stromal vascular fractions were used to isolate ATMs using mouse anti-F4/80-FITC antibodies (Cat#130-117-509; RRID: AB_2727970, Miltenyi Biotec, Bergisch Gladbach, Germany), anti-FITC MicroBeads (Cat#130-048-701; RRID: AB_244371, Miltenyi Biotec) and MS columns (Miltenyi Biotec) on an OctoMACS™ Cell Separator system (Miltenyi Biotec). ATMs were cultured for 24h in RPMI-1630 supplemented with 10% FCS and 1% P/S. ATMs were either cultured for 2h after which cells were washed with PBS, fixed in 3.7% paraformaldehyde and stained with Oil red O following standard protocols, or were cultured for 24h to obtain supernatants.

Flow cytometry of SVF

Before isolation of ATMs, SVF pools were resuspended in PBS containing 0.5% BSA and 2mM EDTA and 500 000 cells were sampled and stained with antibodies against CD45-ECD (Cat#A07784, Beckman Coulter, Brea, CA, USA), F4/80-FITC (Cat#123107; RRID: AB_893500), CD206-APC (Cat#141707; RRID: AB_10896057), CD11c-PE-Cy7 (Cat#117317; RRID: AB_493569) and CD11b-PE (Cat#101207; RRID: AB_312790, Biolegend, San Diego, CA, USA). Samples were measured on a flow cytometer (FC500, Beckman Coulter) and results were analyzed using Kaluza analysis software 2.1 (RRID: SCR_016182, Beckman Coulter).

Histological studies

Samples of gWAT for histological analysis were fixed in 3.7% paraformaldehyde immediately upon collection, embedded in paraffin, sectioned and stained with hematoxylin eosin according to standard protocols. After preincubation with 20% normal goat serum, paraffin-embedded sections were incubated at 4°C overnight with antibodies for F4/80 (Cat#MCA497G; RRID: AB_872005, Bio-Rad Laboratories, Hercules, CA, USA), HILPDA (sc-137518 HIG2 Antibody (C-14); RRID: AB_2011522, Santa-Cruz Biotechnology, Dallas, TX, USA Biotechnology) or CD68 (Cat#MCA1957; RRID: AB_322219, AbD Serotec, Bio-Rad Laboratories) dissolved in PBS supplemented with 1% BSA (Merck). Anti-rat or anti-rabbit IgG conjugated to HRP (Cell Signaling Technology, Danvers, MA, USA) were used as

secondary antibody. Negative controls were prepared without using primary antibody.

Peritoneal macrophages and BMDMs

To harvest peritoneal macrophages, 8-12 week old WT C57Bl/6 mice were injected intraperitoneally with 1mL 4% thioglycolic acid. Three days post-injection, mice were anesthetised with isoflurane and euthanized by CO₂. Peritoneal cells were harvested by washing the peritoneal cavity with ice-cold RPMI-1630 supplemented with 10% heat-inactivated FCS (BioWest) and 1% P/S. Cells were plated after lysis of erythrocytes and non-adherent cells were washed away three hours post plating. To isolate BMDMs, 8-12 week old *Hilpda*^{ΔMΦ} mice and their *Hilpda*^{fl^{ox}/fl^{ox}} littermates were euthanized by cervical dislocation. Both femurs and hind legs were isolated at the hip joint, keeping femur and tibia intact. Bone marrow was extracted from the femur and tibia and differentiated in DMEM, supplemented with 10% FCS, 1% P/S and 15% L929-conditioned medium. After seven days of differentiation, BMDMs were scraped and plated as appropriate.

Cell culture experiments

RAW 264.7 macrophage cells (Cat#91062702; RRID: CVCL_0493, Sigma-Aldrich) were cultured in DMEM supplemented with 10% FCS and 1% P/S. Overexpression of *Hilpda* was achieved by transfection with an adenoviral construct containing either *Hilpda* (Ad-m-2310016C08RIK, ADV-250639, Vector Biolabs, Malvern, USA) or *Gfp* (Ad-GFP, Cat#1060, Vector Biolabs, Malvern, USA) in a dose of 500 MOI for 48 hours. Palmitate (Cat#P0500; CAS: 57-10-3, Sigma-Aldrich) and oleate (Cat#O1008; CAS: 112-80-1, Sigma-Aldrich) were solubilized using EtOH and KOH and conjugated to FFA-free BSA in sterile water (Versol, Aguetant, Lyon, France) at 37°C for 30 min. Palmitate was used in concentrations of 200, 250 or 500μM. Oleate was used in a concentration of 250μM or 400μM together with 20 μM BODIPY-FL C12 (Cat#D3822, ThermoFisher Scientific, MA, USA) for fatty acid trafficking experiments. A mixture of oleate and palmitate (oleate:palmitate) was made in a ratio of 1:2 and used in a final concentration of 600 μM. Intralipid (Fresenius Kabi AB, Uppsala, Sweden) was used in a concentration of 1 or 2mM. The addition of 100μM iron chelator 2,2'-bipyridyl (Cat#D216305; CAS: 366-18-7, Sigma-Aldrich) was used to chemically mimic hypoxia. Atglistatin (Cat#SML1075, Sigma-Aldrich) was used in a concentration of 20μM in 100% DMSO and cells were pre-treated for 2 hours before fatty acid loading. 24 hour treatments containing Atglistatin were refreshed every 12 hours. All cells were washed with PBS (Corning) after treatment. BMDMs were stained with Oil Red O following standard procedures.

Confocal Imaging

To visualise fatty acid uptake, accumulation and trafficking, BMDMs were plated on 8-well μ glass bottom slides (Ibidi, Martinsried, Germany). Confocal imaging was performed on a Leica confocal TCS SP8 X system equipped with a 63 \times 1.20 NA water-immersion objective lens. Images were acquired using 1,024 \times 1,024 pixels with pinhole set at 1 Airy Unit (AU). Excitation of the fluorescent probes used in this study was performed using white light laser (WLL, 50% laser output) selecting the 488 nm laser line. Fluorescence emission was detected using internal Hybrid (HyD) detector selecting a spectral window from either 520 - 580 nm (fatty acid uptake) or from 510 - 565 nm (fatty acid trafficking).

Fatty acid uptake was measured on paraformaldehyde fixed cells after 35 minutes incubation with the QBT™ Fatty acid uptake assay kit (Cat#R6132, Molecular Devices, California, USA) according to manufacturer's instructions. Image analysis was performed with Fiji (<https://fiji.sc/>) [42,43]. Pixels were selected for analysis using Otsu threshold, mean intensity was quantified. The WLL laser line (488 nm) was set at a laser power of 0.2%. The pinhole was adjusted at 5.7 AU for fluorescence intensity measurements, whereas confocal imaging was done with a pinhole of 1 AU.

Fatty acid trafficking was assessed after lipid loading for 5h and 24h with 400 μ M oleate and 20 μ M BODIPY® FL C12, treated either with vehicle or Atglistatin. The WLL laser line (488 nm) was set at a laser power of 1.6% for 5 h incubated cells and 0.3% for 24 h incubated cells. Cells were washed with PBS, fixed for 15 min with 3.7% formaldehyde and mounted with Vectashield-H (Vector Laboratories, Peterborough, UK). Fire LUT was applied using Fiji.

To assess fatty acid accumulation, BMDMs treated with oleate:palmitate were washed with PBS and fixed for 15 minutes with 3.7% paraformaldehyde. Fixed cells were stained with 2 μ g/mL BODIPY® 493/503 (Thermo Fisher Scientific) and mounted with Vectashield-H (Vector Laboratories). Images were processed and analyzed with Fiji. Briefly, images were converted to binary, watershed and LD size and number was measured with particle analysis set 0.07 μ m²-infinity.

Extracellular flux assay

Extracellular flux of lipid-loaded BMDMs was measured using the Agilent Seahorse XF96 Analyzer (Agilent Technologies, Santa Clara, CA, USA). Cells were seeded in a density of 200 000 cells per well in XF-96 plates (Agilent Technologies), treated appropriately and kept in a 37°C/5% CO₂ incubator. An hour before the measurement, cells were washed and cultured in Seahorse XF base medium (Agilent Technologies) without sodium bicarbonate, supplemented with 25mM glucose and 2mM L-glutamine for one hour at 37°C in a non-

CO₂ incubator. For the mitochondrial stress test, the following compounds were added during four injections: oligomycin (1.5 μM), FCCP (1.5 μM), pyruvate (1 mM), antimycin A (2.5 μM) and rotenone (1.25 μM). The oxygen consumption rate (OCR) was automatically measured by the sensor cartridge at baseline and following injections. Calculations were made using the Seahorse XF-96 software Wave Desktop 2.6 (RRID: SCR_014526, Agilent Technologies).

Real-time PCR

For cells, total RNA was isolated using TRIzol[®] Reagent (Invitrogen, ThermoFisher Scientific). For tissues, total RNA was isolated using the RNeasy Micro Kit (Qiagen, Venlo, The Netherlands). cDNA was synthesized from 500 ng RNA using the iScript cDNA kit (Bio-Rad Laboratories, Hercules, CA, USA) according to manufacturer's instructions. Real time polymerase chain reaction (RT-PCR) was performed with the CFX96 or CFX384 Touch[™] Real-Time detection system (Bio-Rad Laboratories), using a SensiMix[™] (BioLine, London, UK) protocol for SYBR green reactions. Mouse *36b4* expression was used for normalization.

Immunoblotting

Cell or tissue protein lysates were separated by electrophoresis on pre-cast 4-15% polyacrylamide gels and transferred onto nitrocellulose membranes using a Trans-Blot[®] Semi-Dry transfer cell (all purchased from Bio-Rad Laboratories), blocked in non-fat milk and incubated overnight at 4°C with primary antibody for HILPDA (Cat#sc-137518; RRID: AB_2011522, Santa Cruz Biotechnology), ATGL (Cat#sc-365278, RRID: AB_10859044, Santa Cruz Biotechnology), PLIN3 (Cat#10694-1-AP, RRID: AB_2297252, Proteintech), G0S2 (Cat#sc-518067, Santa Cruz Biotechnology), ACTIN (Cat#5057; RRID: AB_10694076, Cell Signaling Technology), TUBULIN (Cat#2146; RRID: AB_2210545, Cell Signaling Technology) or HSP90 (Cat#48745; RRID: AB_2121214, Cell Signaling Technology). Membranes were incubated with secondary antibody (Anti-rabbit IgG, HRP-linked Antibody, 7074, Cell Signaling Technology) and developed using Clarity ECL substrate (Bio-Rad Laboratories). Images were captured with the ChemiDoc MP system (Bio-Rad Laboratories).

Enzyme-linked immunosorbent assay (ELISA)

DuoSet sandwich ELISA kits for TNFα, IL-10 and IL-6 (Cat#DY410/Cat#DY417/Cat#DY406, R&D systems) were used to measure cytokine concentrations in cell or explant supernatant according to manufacturer's instructions. Data was normalized for the amount of adipose tissue macrophages by determining the concentration of DNA per well (Quant-iT dsDNA Assay Kit high sensitivity, Thermo Fisher Scientific) and normalized for gWAT explants to the weight per explant.

Lipidomics

Lipidomics analysis was performed as described [44]. The HPLC system consisted of an Ultimate 3000 binary HPLC pump, a vacuum degasser, a column temperature controller, and an auto sampler (Thermo Fisher Scientific). The column temperature was maintained at 25°C. The lipid extract was injected onto a "normal phase column" LiChrospher 2x250-mm silica-60 column, 5 µm particle diameter (Merck) and a "reverse phase column" Acquity UPLC HSS T3, 1.8 µm particle diameter (Waters, Milford, MA, USA). A Q Exactive Plus Orbitrap (Thermo Fisher Scientific) mass spectrometer was used in the negative and positive electrospray ionization mode. Nitrogen was used as the nebulizing gas. The spray voltage used was 2500 V, and the capillary temperature was 256°C. S-lens RF level: 50, auxiliary gas: 11, auxiliary temperature 300°C, sheath gas: 48, sweep cone gas: 2. In both the negative and positive ionization mode, mass spectra of the lipid species were obtained by continuous scanning from m/z 150 to m/z 2000 with a resolution of 280,000 full width at half maximum (FWHM). Data was analyzed and visualised using R programming language (CRAN, RRID: SCR_003005, <https://www.r-project.org>).

Microarray analyses

Microarray analysis was performed on a several experiments: 1) Peritoneal macrophages treated with various fatty acids (500 µM) for 6 hours. 2) Peritoneal macrophages treated with intralipid (2mM) for 6 hours. 3) BMDM samples from *Hilpda*^{ΔMΦ} mice and *Hilpda*^{fllox/fllox} mice lipid loaded with oleate:palmitate (600µM) for 12 and 24 hours. RNA was isolated as described above and purified with the RNeasy Micro kit from Qiagen. Integrity of the RNA was verified with RNA 6000 Nano chips using an Agilent 2100 bioanalyzer (Agilent Technologies). Purified RNA (100 ng per sample) was labeled with the Whole-Transcript Sense Target Assay kit (Affymetrix, Santa Clara, CA, USA; P/N 900652) and hybridized to an Affymetrix Mouse Gene 1.0 arrays or 2.1 ST array plate (Affymetrix). Hybridization, washing, and scanning were carried out on an Affymetrix GeneTitan platform according to the manufacturer's instructions.

Visualisation

The 3D scatterplot of signal log ratio's (**Figure 1A**) was created using R programming language (<https://www.r-project.org>) and the R package "plot3D". Heat-maps for the lipidomics were created using the package "gplots" and. The graphical abstract was created with BioRender.

QUANTIFICATION AND STATISTICAL ANALYSIS

Power calculation

From earlier studies it is known that fasting glucose values of mice fed a high-fat diet differs on average 3 mM (+ 8 mM – 11mM) compared to mice fed a low-fat diet. Differences in responses lead to a standard deviation around 2mM or higher. For the power calculation, we used a one-way ANOVA with a significance level of 0.05 and a power of 90%, leading to an estimation of around $n = 11$ mice needed per group. To allow compensation for unforeseen circumstances or potential loss of mice during the study, $n = 12$ mice were included per group.

Statistical analysis

Normalization of the arrays was performed with the Robust Multi-array Average method [45,46]. Probe sets were redefined according to Dai et al. [47] based on annotations provided by the Entrez Gene database. Data for the 3D scatterplot of signal log ratio's (**Figure 1A**) was created using R programming language (<https://www.r-project.org>). Partial least squares regression analysis for the lipidomics data was performed using the R package "mixOMICS".

Details on statistical analyses are given in figure legends. In experiments where animals were included, n represents the number of animals used. For cell experiments, n represents the number of replications performed. Data are represented as means \pm SD or SEM as indicated. Assumptions for statistical methods were tested and statistical analyses were carried out using an unpaired Student's t test or two-way ANOVA followed by Bonferroni's post hoc multiple comparisons test, if genotype and diet or genotype and treatment both were found significant (GraphPad Software, San Diego, CA, USA). A value of $p < 0.05$ was considered statistically significant.

DATA AND CODE AVAILABILITY

A publicly available dataset (GSE77104) was downloaded from Gene Expression Omnibus and further processed as described above to obtain individual gene expression data [20]. The microarray analysis of the adipose tissue macrophages (GSE84000) and peritoneal macrophages treated with intralipid (GSE136240) are already described elsewhere [3,48]. The microarray datasets generated during this study have been submitted to the Gene Expression Omnibus (GSE142296).

Key resources table

REAGENT or RESOURCE	SOURCE	IDENTIFIER
Antibodies		
CD45-ECD anti-mouse	Beckman Coulter	Cat#A07784
F4/80-FITC anti-mouse	BioLegend	Cat#123107; RRID: AB_893500
CD206-APC anti-mouse	BioLegend	Cat#141707; RRID: AB_10896057
CD11c-PE-Cy7 anti-mouse	BioLegend	Cat#117317; RRID: AB_493569
CD11b-PE anti-mouse	BioLegend	Cat#101207; RRID: AB_312790
F4/80 anti-mouse	Bio-Rad	Cat#MCA497G; RRID: AB_872005
CD68 anti-mouse	AbD Serotec, Bio-Rad	Cat#MCA1957; RRID: AB_322219
HILPDA (HIG2, C-14) anti-mouse	Santa Cruz, Biotechnology	Cat#sc-137518; RRID: AB_2011522
ATGL	Santa Cruz Biotechnology	Cat#sc-365278, RRID:AB_10859044
PLIN3 (TIP47, M6PRBP1)	Proteintech	Cat#10694-1-AP, RRID:AB_2297252
GOS2	Santa Cruz Biotechnology	Cat#sc-518067
ACTIN	Cell Signaling	Cat#5057; RRID: AB_10694076
TUBULIN	Cell Signaling	Cat#2146; RRID: AB_2210545
HSP90	Cell Signaling	Cat#4874S; RRID: AB_2121214
F4/80-FITC anti-mouse for MACS	Miltenyi Biotec	Cat#130-117-509; RRID: AB_2727970
Anti-FITC microbeads	Miltenyi Biotec	Cat#130-048-701; RRID: AB_244371
Bacterial and Virus Strains		
Ad-m-2310016C08RIK (<i>AV-Hilpda</i>)	Vector Biolabs	Cat#ADV-250639
Ad-GFP	Vector Biolabs	Cat#1060
Chemicals, Peptides, and Recombinant Proteins		
Atglistatin	Sigma-Aldrich	Cat#SML1075
BODIPY [®] 493-503	ThermoFisher Scientific	Cat#D3922; CAS: 121207-31-6
BODIPY-FL [®] C12	ThermoFisher Scientific	Cat#D3822
2,2'-bipyridyl	Sigma-Aldrich	Cat#D216305; CAS: 366-18-7
Critical Commercial Assays		
GeneChip Whole-Transcript Sense Target Assay kit	Affymetrix	P/N 900652
QBT Fatty Acid Uptake Assay Kit	Molecular Devices	Cat#R6132
IL6 DuoSet Sandwich ELISA	R&D Systems	Cat#DY406
TNF α DuoSet Sandwich ELISA	R&D Systems	Cat#DY410

IL10 DuoSet Sandwich ELISA	R&D Systems	Cat#DY417
Deposited Data		
Microarray dataset peritoneal macrophages treated with fatty acids	This paper	GSE142296
Microarray dataset: peritoneal macrophages treated with intralipid	Oteng et al., 2019	GSE136240
Microarray dataset: Hilpda ^{AMΦ} and Hilpda ^{flox/flox} BMDMs treated with oleate:palmitate	This paper	GSE142296
Microarray dataset: WT BMDMs treated fatty acids or LPS	Robblee et al., 2016	GSE77104
Microarray dataset: adipose tissue macrophages	Boutens et al., 2016	GSE84000
Experimental Models: Cell Lines		
RAW264.7 authenticated murine macrophage cell line	Sigma-Aldrich	Cat#91062702; RRID: CVCL_0493
Experimental Models: Organisms/Strains		
Mouse: Hilpda ^{tm1.1Nat/J}	Jackson Laboratories	JAX: 017360; RRID: MGI:5285399
Mouse: B6.129P2-Lyz2 ^{tm1(cre)lfo/J}	Jackson Laboratories	JAX: 004781; RRID: IMSR_JAX:004781
Oligonucleotides		
Primers for RT-PCR, see table S1	This paper	N/A
Software and Algorithms		
Fiji	Schindelin et al., 2012, Rueden et al., 2017	https://fiji.sc/
Kaluza	Beckman Coulter	RRID: SCR_016182
Seahorse XF-96 Wave	Agilent Technologies	RRID: SCR_014526
CRAN for R programming language	http://cran.r-project.org/	CRAN, RRID: SCR_003005
Other		
Palmitic acid	Sigma-Aldrich	Cat#P0500; CAS: 57-10-3
Oleic acid	Sigma-Aldrich	Cat#O1008; CAS: 112-80-1
Intralipid	Baxter	Cat#0338-0519-58
Collagenase from <i>Clostridium histolyticum</i>	Sigma-Aldrich	Cat#C6885; CAS: 9001-12-1
Standardized rodent high-fat diet	Research Diets	Cat#D12451
Standardized rodent low-fat diet	Research Diets	Cat#D12450H

References

1. Gregor MF, Hotamisligil GS. Inflammatory Mechanisms in Obesity. *Annual Review of Immunology*. 2011; 29(1): 415–45.
2. Hotamisligil GS. Inflammation, metaflammation and immunometabolic disorders. *Nature*. 2017; 542(7640): 177–85.
3. Boutens L, Stienstra R. Adipose tissue macrophages: going off track during obesity. *Diabetologia*. 2016; 59(5): 879–94.
4. Cinti S, Mitchell G, Barbatelli G, Murano I, Ceresi E, Faloia E, et al. Adipocyte death defines macrophage localization and function in adipose tissue of obese mice and humans. *Journal of Lipid Research*. 2005; 46(11): 2347–55.
5. Lumeng CN, Bodzin JL, Saltiel AR. Obesity induces a phenotypic switch in adipose tissue macrophage polarization. *Journal of Clinical Investigation*. 2007; 117(1): 175–84.
6. Xu X, Grijalva A, Skowronski A, van Eijk M, Serlie MJ, Ferrante AW. Obesity Activates a Program of Lysosomal-Dependent Lipid Metabolism in Adipose Tissue Macrophages Independently of Classic Activation. *Cell Metabolism*. 2013; 18(6): 816–30.
7. Shapiro H, Pecht T, Shaco-Levy R, Harman-Boehm I, Kirshtein B, Kuperman Y, et al. Adipose Tissue Foam Cells Are Present in Human Obesity. *The Journal of Clinical Endocrinology & Metabolism*. 2013; 98(3): 1173–81.
8. Lumeng CN, DelProposto JB, Westcott DJ, Saltiel AR. Phenotypic Switching of Adipose Tissue Macrophages With Obesity Is Generated by Spatiotemporal Differences in Macrophage Subtypes. *Diabetes*. 2008; 57(12): 3239–46.
9. Mattijssen F, Georgiadi A, Andasarie T, Szalowska E, Zota A, Krones-Herzig A, et al. Hypoxia-inducible Lipid Droplet-associated (HILPDA) Is a Novel Peroxisome Proliferator-activated Receptor (PPAR) Target Involved in Hepatic Triglyceride Secretion. *Journal of Biological Chemistry*. 2014; 289(28): 19279–93.
10. Gimm T, Wiese M, Teschemacher B, Deggerich A, Schödel J, Knaup KX, et al. Hypoxia-inducible protein 2 is a novel lipid droplet protein and a specific target gene of hypoxia-inducible factor-1. *The FASEB Journal*. 2010; 24(11): 4443–58.
11. Dijk W, Mattijssen F, de la Rosa Rodriguez M, Loza Valdes A, Loft A, Mandrup S, et al. Hypoxia-Inducible Lipid Droplet-Associated Is Not a Direct Physiological Regulator of Lipolysis in Adipose Tissue. *Endocrinology*. 2017; 158(5): 1231–51.
12. DiStefano MT, Danai L V., Roth Flach RJ, Chawla A, Pedersen DJ, Guilherme A, et al. The Lipid Droplet Protein Hypoxia-inducible Gene 2 Promotes Hepatic Triglyceride Deposition by Inhibiting Lipolysis. *Journal of Biological Chemistry*. 2015; 290(24): 15175–84.
13. DiStefano MT, Roth Flach RJ, Senol-Cosar O, Danai L V., Virbasius J V., Nicoloso SM, et al. Adipocyte-specific Hypoxia-inducible gene 2 promotes fat deposition and diet-induced insulin resistance. *Molecular Metabolism*. 2016; 5(12): 1149–61.
14. Maier A, Wu H, Cordasic N, Oefner P, Diel B, Thiele C, et al. Hypoxia-inducible protein 2 Hlg2/Hilpda mediates neutral lipid accumulation in macrophages and contributes to atherosclerosis in apolipoprotein E-deficient mice. *The FASEB Journal*. 2017; : 4971–84.
15. Zhang X, Saarinen AM, Hitosugi T, Wang Z, Wang L, Ho TH, et al. Inhibition of Intracellular Lipolysis Promotes Cancer Cell Adaptation to Hypoxia. *eLife*. 2017; 6: e31132.
16. Padmanabha Das KM, Wechselberger L, Liziczai M, De la Rosa Rodriguez M, Grabner GF, Heier C, et al. Hypoxia-inducible lipid droplet-associated protein inhibits adipose triglyceride lipase.

- Journal of lipid research. 2018; 59(3): 531–41.
17. Denko N, Schindler C, Koong A, Laderoute K, Green C, Giaccia A. Epigenetic regulation of gene expression in cervical cancer cells by the tumor microenvironment. *Clinical cancer research : an official journal of the American Association for Cancer Research*. 2000; 6(2): 480–7.
 18. Rausch ME, Weisberg S, Vardhana P, Tortoriello D V. Obesity in C57BL/6J mice is characterized by adipose tissue hypoxia and cytotoxic T-cell infiltration. *International Journal of Obesity*. 2008; 32(3): 451–63.
 19. Mayer N, Schweiger M, Romauch M, Grabner GF, Eichmann TO, Fuchs E, et al. Development of small-molecule inhibitors targeting adipose triglyceride lipase. *Nature Chemical Biology*. 2013; 9(12): 785–7.
 20. Robblee MM, Kim CC, Abate JP, Valdearcos M, Sandlund KLM, Shenoy MK, et al. Saturated Fatty Acids Engage an IRE1 α -Dependent Pathway to Activate the NLRP3 Inflammasome in Myeloid Cells. *Cell Reports*. 2016; 14(11): 2611–23.
 21. Prieur X, Mok CYL, Velagapudi VR, Núñez V, Fuentes L, Montaner D, et al. Differential Lipid Partitioning Between Adipocytes and Tissue Macrophages Modulates Macrophage Lipotoxicity and M2/M1 Polarization in Obese Mice. *Diabetes*. 2011; 60(3): 797–809.
 22. Kratz M, Coats BR, Hisert KB, Hagman D, Mutskov V, Peris E, et al. Metabolic Dysfunction Drives a Mechanistically Distinct Proinflammatory Phenotype in Adipose Tissue Macrophages. *Cell Metabolism*. 2014; 20(4): 614–25.
 23. Coats BR, Schoenfelt KQ, Barbosa-Lorenzi VC, Peris E, Cui C, Hoffman A, et al. Metabolically Activated Adipose Tissue Macrophages Perform Detrimental and Beneficial Functions during Diet-Induced Obesity. *Cell Reports*. 2017; 20(13): 3149–61.
 24. Hill DA, Lim H-W, Kim YH, Ho WY, Foong YH, Nelson VL, et al. Distinct macrophage populations direct inflammatory versus physiological changes in adipose tissue. *Proceedings of the National Academy of Sciences of the United States of America*. 2018; 115(22): E5096–105.
 25. Saraswathi V, Hasty AH. Inhibition of Long-Chain Acyl Coenzyme A Synthetases During Fatty Acid Loading Induces Lipotoxicity in Macrophages. *Arteriosclerosis, Thrombosis, and Vascular Biology*. 2009; 29(11): 1937–43.
 26. Namgaladze D, Brüne B. Macrophage fatty acid oxidation and its roles in macrophage polarization and fatty acid-induced inflammation. *Biochimica et Biophysica Acta (BBA) - Molecular and Cell Biology of Lipids*. 2016; 1861(11): 1796–807.
 27. Reid BN, Ables GP, Otlivanchik OA, Schoiswohl G, Zechner R, Blaner WS, et al. Hepatic Overexpression of Hormone-sensitive Lipase and Adipose Triglyceride Lipase Promotes Fatty Acid Oxidation, Stimulates Direct Release of Free Fatty Acids, and Ameliorates Steatosis. *Journal of Biological Chemistry*. 2008; 283(19): 13087–99.
 28. Sapiro JM, Mashek MT, Greenberg AS, Mashek DG. Hepatic triacylglycerol hydrolysis regulates peroxisome proliferator-activated receptor α activity. *Journal of Lipid Research*. 2009; 50(8): 1621–9.
 29. Ong KT, Mashek MT, Bu SY, Greenberg AS, Mashek DG. Adipose triglyceride lipase is a major hepatic lipase that regulates triacylglycerol turnover and fatty acid signaling and partitioning. *Hepatology*. 2011; 53(1): 116–26.
 30. Haemmerle G, Moustafa T, Woelkart G, Büttner S, Schmidt A, van de Weijer T, et al. ATGL-mediated fat catabolism regulates cardiac mitochondrial function via PPAR- α and PGC-1. *Nature Medicine*. 2011; 17(9): 1076–85.
 31. Huang SC-C, Everts B, Ivanova Y, O'Sullivan D, Nascimento M, Smith AM, et al. Cell-intrinsic lysosomal lipolysis is essential for alternative activation of macrophages. *Nature immunology*.

- 2014; 15(9): 846–55.
32. Van den Bossche J, Baardman J, Otto NA, van der Velden S, Neele AE, van den Berg SM, et al. Mitochondrial Dysfunction Prevents Repolarization of Inflammatory Macrophages. *Cell Reports*. 2016; 17(3): 684–96.
 33. Jung S-B, Choi MJ, Ryu D, Yi H-S, Lee SE, Chang JY, et al. Reduced oxidative capacity in macrophages results in systemic insulin resistance. *Nature Communications*. 2018; 9(1): 1551.
 34. Sathyanarayan A, Mashek MT, Mashek DG. ATGL Promotes Autophagy/Lipophagy via SIRT1 to Control Hepatic Lipid Droplet Catabolism. *Cell Reports*. 2017; 19(1): 1–9.
 35. Chandak PG, Radović B, Aflaki E, Kolb D, Buchebner M, Fröhlich E, et al. Efficient Phagocytosis Requires Triacylglycerol Hydrolysis by Adipose Triglyceride Lipase. *Journal of Biological Chemistry*. 2010; 285(26): 20192–201.
 36. Aflaki E, Radović B, Chandak PG, Kolb D, Eisenberg T, Ring J, et al. Triacylglycerol Accumulation Activates the Mitochondrial Apoptosis Pathway in Macrophages. *Journal of Biological Chemistry*. 2011; 286(9): 7418–28.
 37. Aflaki E, Balenga NAB, Luschnig-Schratl P, Wolinski H, Povoden S, Chandak PG, et al. Impaired Rho GTPase activation abrogates cell polarization and migration in macrophages with defective lipolysis. *Cellular and Molecular Life Sciences*. 2011; 68(23): 3933–47.
 38. Aflaki E, Doddapattar P, Radović B, Povoden S, Kolb D, Vujić N, et al. C16 ceramide is crucial for triacylglycerol-induced apoptosis in macrophages. *Cell death & disease*. 2012; 3(3): e280.
 39. Schlager S, Goeritzer M, Jandl K, Frei R, Vujic N, Kolb D, et al. Adipose triglyceride lipase acts on neutrophil lipid droplets to regulate substrate availability for lipid mediator synthesis. *Journal of Leukocyte Biology*. 2015; 98(5): 837–50.
 40. Goeritzer M, Schlager S, Radovic B, Madreiter CT, Rainer S, Thomas G, et al. Deletion of CGI-58 or adipose triglyceride lipase differently affects macrophage function and atherosclerosis. *Journal of lipid research*. 2014; 55(12): 2562–75.
 41. Yang X, Lu X, Lombès M, Rha GB, Chi Y-I, Guerin TM, et al. The G0/G1 Switch Gene 2 Regulates Adipose Lipolysis through Association with Adipose Triglyceride Lipase. *Cell Metabolism*. 2010; 11(3): 194–205.
 42. Rueden CT, Schindelin J, Hiner MC, DeZonia BE, Walter AE, Arena ET, et al. ImageJ2: ImageJ for the next generation of scientific image data. *BMC Bioinformatics*. 2017; 18(1): 529.
 43. Schindelin J, Arganda-Carreras I, Frise E, Kaynig V, Longair M, Pietzsch T, et al. Fiji: An open-source platform for biological-image analysis. *Nature Methods*. 2012; 9(7): 676–82.
 44. Herzog K, Pras-Raves ML, Vervaart MAT, Luyf ACM, van Kampen AHC, Wanders RJA, et al. Lipidomic analysis of fibroblasts from Zellweger spectrum disorder patients identifies disease-specific phospholipid ratios. *Journal of lipid research*. 2016; 57(8): 1447–54.
 45. Bolstad BM, Irizarry RA, Astrand M, Speed TP. A comparison of normalization methods for high density oligonucleotide array data based on variance and bias. *Bioinformatics (Oxford, England)*. 2003; 19(2): 185–93.
 46. Irizarry RA, Bolstad BM, Collin F, Cope LM, Hobbs B, Speed TP. Summaries of Affymetrix GeneChip probe level data. *Nucleic acids research*. 2003; 31(4): e15.
 47. Dai M, Wang P, Boyd AD, Kostov G, Athey B, Jones EG, et al. Evolving gene/transcript definitions significantly alter the interpretation of GeneChip data. *Nucleic Acids Research*. 2005; 33(20): e175.
 48. Oteng A-B, Ruppert PMM, Boutens L, Dijk W, van Dierendonck XAMH, Olivecrona G, et al. Characterization of ANGPTL4 function in macrophages and adipocytes using Angptl4-knockout and Angptl4-hypomorphic mice. *Journal of lipid research*. 2019; 60(10): 1741–54.

Supplemental material

Primer name	Forward	Reverse
<i>mHilpda</i>	TCGTGCAGGATCTAGCAGCAG	GCCCAGCACATAGAGGTTCA
<i>mAdgre1</i>	CTTTGGCTATGGGCTTCCAGTC G	CAAGGAGGACAGAGTTTATCGTG
<i>mCcl2</i>	CCAATGAGTAGGCTGGAGA	TCTGGACCCATTCTTCTTG
<i>mCd68</i>	CCAATCAGGGTGAAGAAA	CTCGGGCTCTGATGTAGGTC
<i>mltgax</i>	CTGGATAGCCTTTCTTCTGCTG	GCACACTGTGTCGAACTCA
<i>mLep</i>	AGAAGATCCCAGGGAGGAAA T	GATGAGGGTTTTGGTGTCA
<i>mCd36</i>	TCCAGCCAATGCCTTTGC	TGGAGATTACTTTTCAGTGCAGAA
<i>mDdit3</i>	TATCTCATCCCAGGAAACG	GGGCACTGACCACTCTGTTT
<i>mPtgs2</i>	TGAGCAACTATTCCAACCAGC	GCACGTAGTCTTCGATCACTATC
<i>mPlin2</i>	CTTGTGTCTCCGCTTATGTC	GCAGAGGTCACGGTCTTCAC
<i>mGdf15</i>	GAAGTGCCTTACGGGTAG	CTGCACAGTCTCCAGGTGA
<i>mCpt1a</i>	CTCAGTGGAGCGACTCTTCA G	GCCTCTGTGGTACACGACAA
<i>ml17r</i>	GCGGACGATCACTCTTCTG A	GCCCCACATATTTGAAATTCCA
<i>mAngptl4</i>	GTTTGCAGACTCAGCTCAAGG	CCAAGAGGTCTATCTGGCTCTG

Table S1, related to STAR methods. Primers used for qPCR.

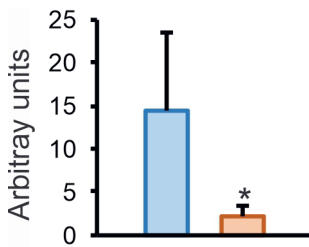


Figure S1, related to Figure 2G.

(A) Quantification of triglycerides on Thin Layer Chromatography plates in *Hilpda*^{flox/flox} and *Hilpda*^{ΔMΦ} BMDMs lipid loaded with oleate:palmitate for 24 h. (B) BODIPY staining in *Hilpda*^{flox/flox} and *Hilpda*^{ΔMΦ} BMDMs treated with palmitate for 6 or 24 h. Bar graphs are presented as mean ± SD. **p* < 0.05.

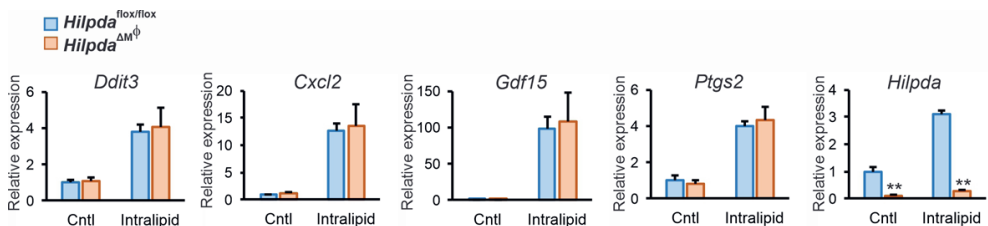


Figure S2, related to Figure 3D.

Gene expression of *Ddit3*, *Cxcl2*, *Gdf15*, *Ptgs2* and *Hilpda* in *Hilpda*^{flox/flox} and *Hilpda*^{ΔMΦ} BMDMs treated with 1 mM of intralipid or PBS control (Cntl) for 6 h. Bar graphs are presented as mean ± SD. The effect of treatment was significant. ***p* ≤ 0.01. Cntl: Control.

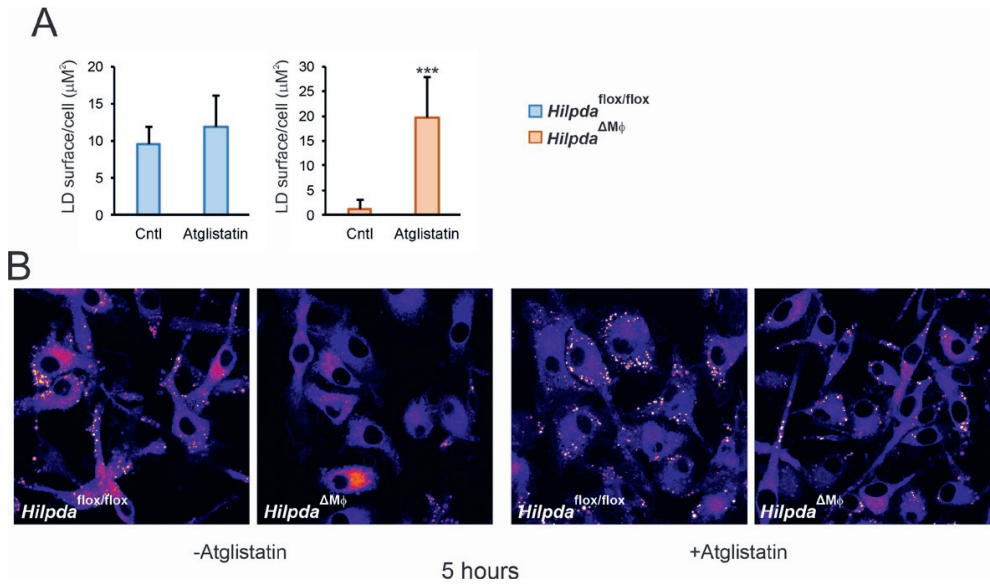


Figure S3, related to Figure 4.

(A) Quantification of the amount of lipid droplet surface area per cell in *Hilpda*^{flox/flox} and *Hilpda*^{ΔMφ} BMDMs lipid loaded with oleate:palmitate for 24 h and treated with 20 μM of atglistatin or vehicle (DMSO). (B) BODIPY FL trafficking and incorporation in lipid droplets in *Hilpda*^{flox/flox} and *Hilpda*^{ΔMφ} BMDMs lipid loaded with 400 μM of oleate and 20 μM of BODIPY FL, treated with 20 μM of atglistatin or vehicle (DMSO) for 5 h. Bar graphs are presented as mean \pm SD. *** $p < 0.001$ LD: lipid droplet, Cntl: Control.

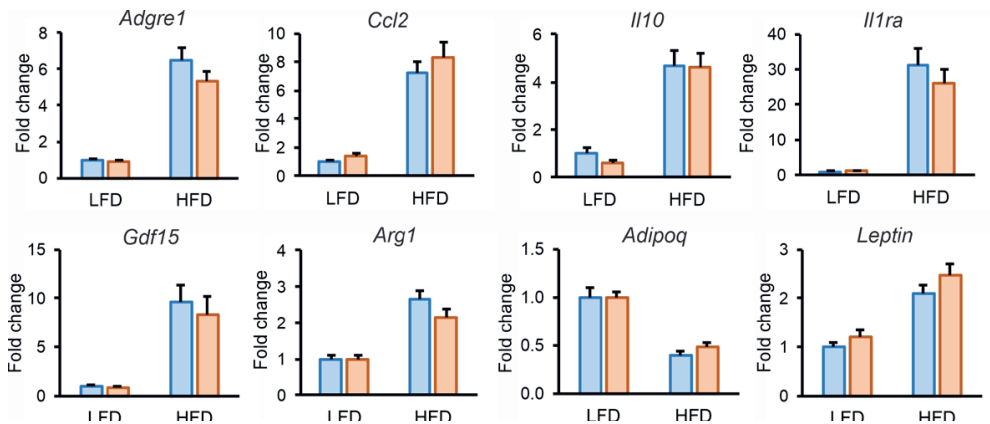


Figure S4, related to Figure 7E.

Gene expression of *Adgre1*, *Ccl2*, *Il10*, *Il1ra*, *Gdf15*, *Arg1*, *Adipoq* and *Leptin* in gWAT of *Hilpda*^{flox/flox} and *Hilpda*^{ΔMφ} mice fed a LFD or HFD for 20 weeks. Gene expression levels in gWAT from *Hilpda*^{flox/flox} fed a LFD diet are set to one. Bar graphs are presented as mean \pm SEM. The effect of diet was significant. LFD: low-fat diet, HFD: high-fat diet.

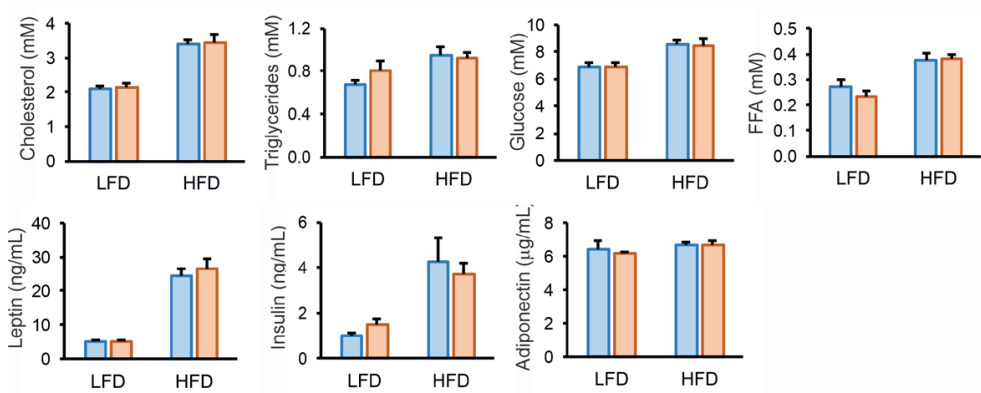


Figure S5, related to Figure 71.

Plasma levels of cholesterol, triglycerides, glucose, free-fatty acids, leptin, insulin and adiponectin in *Hilpda^{flox/flox}* and *Hilpda^{ΔMΔ}* mice fed a LFD or HFD for 20 weeks. Bar graphs are presented as mean ± SEM, (n = 10 – 12 mice per group). Statistical testing was performed by two-way ANOVA followed by Bonferroni's post hoc multiple comparisons test. The effect of diet was significant in cholesterol, triglycerides, glucose, FFA, leptin and insulin. LFD: low-fat diet, HFD: high-fat diet.

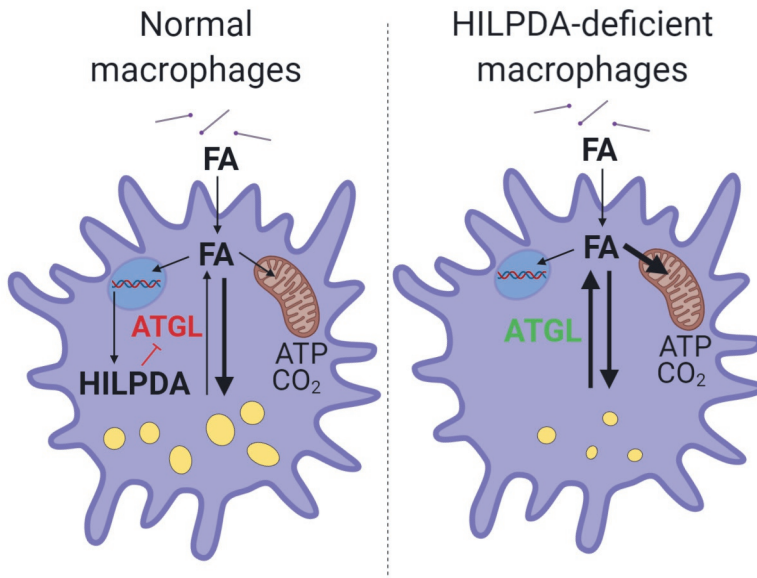


Figure S6.

Effect of HILPDA deficiency on lipid metabolism in BMDMs. In normal BMDMs, HILPDA is produced in response to lipid load, resulting in enhanced lipid storage via inhibition of ATGL-mediated lipolysis. HILPDA deficiency in BMDMs relieves inhibition of adipose tissue lipolysis, leading to enhanced degradation of lipid droplets and promoting oxidation of fatty acids in mitochondria.



Triglyceride breakdown from lipid droplets regulates the inflammatory response in macrophages

Xanthe A.M.H. van Dierendonck^{1,2}, Frank Vrieling¹, Lisa Smeehuijzen¹, Joline P. Boogaard¹, Cresci-Anne Croes¹, Lieve Temmerman³, Suzan Wetzels³, Erik Biessen^{3,4}, Sander Kersten¹, Rinke Stienstra^{1,2}

¹Nutrition, Metabolism and Genomics Group, Division of Human Nutrition and Health, Wageningen University, Wageningen, the Netherlands

²Department of Internal Medicine, Radboud University Medical Center, Nijmegen, the Netherlands

³Department of Pathology, Cardiovascular Research Institute Maastricht (CARIM), University of Maastricht, Maastricht, The Netherlands

⁴Institute for Molecular Cardiology, Klinikum RWTH Aachen, Aachen, Germany

Manuscript in preparation

Abstract

In response to inflammatory activation by pathogens, macrophages accumulate triglycerides in intracellular lipid droplets. The mechanisms underlying triglyceride accumulation and its exact role in the inflammatory response are not yet fully understood. Here, we aim to further elucidate the mechanism and function of triglyceride accumulation in the inflammatory response of activated macrophages by modulating the interaction between hypoxia-inducible lipid droplet associated (HILPDA) and the intracellular lipase adipose triglyceride lipase (ATGL). LPS-mediated inflammatory activation markedly induced upregulation of HILPDA, and downregulation of ATGL protein levels in macrophages, leading to triglyceride accumulation. Deletion of HILPDA abolished the regulation of ATGL, leading to overactive ATGL-mediated lipolysis of triglycerides and decreased lipid droplet accumulation. The myeloid-specific deletion of HILPDA and the subsequent induction of triglyceride breakdown led to an increased pro-inflammatory signature in macrophages after *ex vivo* and *in vitro* activation, characterized by increased production of PGE2 and IL-6. Overall, we find that regulation of ATGL-mediated lipolysis by HILPDA directs the inflammatory response in macrophages, regulating the production of PGE2 and IL-6.

Introduction

Lipid droplets (LDs) are ubiquitous organelles that serve as intracellular energy stores by compartmentalizing lipids, mainly in the form of triglycerides (TGs). While LDs were originally identified in adipocytes, their presence has been confirmed in the majority of mammalian cells. The outside of LDs is covered by numerous LD-related proteins, many of which are involved in the regulation of the storage and release of lipids [1]. Besides mediating energy storage, LDs are increasingly recognized to be directly or indirectly involved in the regulation of other cellular processes, ranging from the storage of hydrophobic vitamins and signalling precursors to the management of endoplasmic reticulum and oxidative stress and the production of inflammatory mediators [2,3].

Macrophages are innate immune cells that play distinct roles in tissue homeostasis and form the frontline in host defence against pathogens. Inflammatory activation of macrophages consistently induces the accumulation of TGs [4,5]. In particular, various pathogen-associated molecular patterns (PAMPs), including LPS, are able to induce specific reprogramming of lipid metabolism in macrophages leading to increased lipid storage [5]. However, rather than being an unintentional consequence of lipid metabolic reprogramming, there is growing evidence that LDs are actively involved in the inflammatory response of macrophages [5]. Studies suggest that besides being hijacked by infectious pathogens as a source of energy [6,7], LDs may also serve as a sink for proteins involved in antimicrobial defence mechanisms [8]. Currently, how PAMPs promote the accumulation of TGs in LDs of macrophages is unclear.

Adipose triglyceride lipase (ATGL) is a lipid-droplet associated protein that is present in numerous cell types, which catalyzes the first step in the hydrolytic cleavage of intracellular TGs, generating non-esterified fatty acids [9–11]. Intriguingly, in macrophages, ATGL is not only responsible for the degradation of stored TGs but also appears to be involved in the immune response. Indeed, deficiency of ATGL in lipid-laden macrophages was shown to attenuate the release of the proinflammatory cytokine IL-6, simultaneously increasing the release of anti-inflammatory IL-10 [12]. In addition, deficiency of ATGL was found to promote macrophage apoptosis [13]. Although these studies have pointed to a role for intracellular lipolysis in the functional properties of macrophages, the precise role of TG accumulation and lipolysis in the immune function of macrophages remains undefined.

HILPDA (hypoxia-inducible lipid droplet-associated) is a small LD-associated protein [14] that was found to promote lipid storage in several cell types, including macrophages [15,16]. Previously, we and others showed that HILPDA functions as a direct physiological inhibitor of ATGL in macrophages [16,17]. Consistent with the role of HILPDA as an inhibitor

of ATGL, HILPDA deficiency was accompanied by a marked reduction in lipid storage in fatty acid-treated macrophages [16]. Whether HILPDA plays a role in the stimulation of TG storage by PAMPs is unknown. In principle, modification of ATGL-mediated lipolysis by HILPDA could be leveraged to further elucidate the role of TG accumulation in the inflammatory response of macrophages. Accordingly, here we set out to investigate the mechanism by which LPS enhances LD formation in macrophages, as well as investigate the role of TG accumulation in the inflammatory response of LPS-treated macrophages, using HILPDA-deficient macrophages as a model. By modulating HILPDA and ATGL, we find that tight regulation of lipolysis directs the pro-inflammatory response of macrophages, involving the production of PGE2 and pro-inflammatory IL-6.

Results

TLR stimulation leads to lipid droplet accumulation through inhibition of ATGL by HILPDA

In order to investigate how LPS promotes lipid accumulation in macrophages, we first verified the stimulatory effect of LPS and various other TLR ligands on TG accumulation in bone marrow-derived macrophages (BMDM), including Pam3Cysk (P3C; TLR-2), lipopolysaccharide (LPS; TLR-4), flagellin (TLR-5), polyinosinic-polycytidylic acid (Poly:IC; TLR-3) and opsonized zymosan (TLR-2) (**Figure 1A**). All TLR ligands increased TG accumulation in BMDMs, with LPS showing the largest effect (**Figure 1B**). To gain insight into the mechanism underlying the increased TG storage upon LPS treatment, BMDMs were treated with the metabolic modulators C75, an inhibitor of fatty acid synthase (FASN) [18], and atglistatin, an inhibitor of ATGL [19]. Whereas inhibition of fatty acid synthesis by C75 decreased LD accumulation, inhibition of ATGL by atglistatin markedly increased accumulation of LDs in LPS-treated BMDMs (**Figure 1C and D**). Although *de novo* synthesis of fatty acids thus appears to be partly responsible for the increased accumulation of lipids, decreased lipolysis by ATGL inhibition likely also plays a role in LPS-induced LD accumulation. Previously, we showed that besides serving as a direct substrate for TG synthesis, fatty acids promote LD accumulation in BMDMs by raising protein levels of the endogenous ATGL inhibitor HILPDA. To investigate if HILPDA may play a role in LPS-induced LD accumulation, we first studied the effect of different TLR ligands on HILPDA levels. Interestingly, various TLR ligands, especially LPS, markedly induced *Hilpda* mRNA levels (**Figure 1E**). Concurrent with the increase in *Hilpda* mRNA, 24 h treatment with LPS dramatically increased HILPDA protein levels (**Figure 1F**), simultaneously reducing ATGL protein levels, hinting at a potential role of HILPDA and ATGL in the augmentation of lipid storage after LPS treatment (**Figure 1F**).

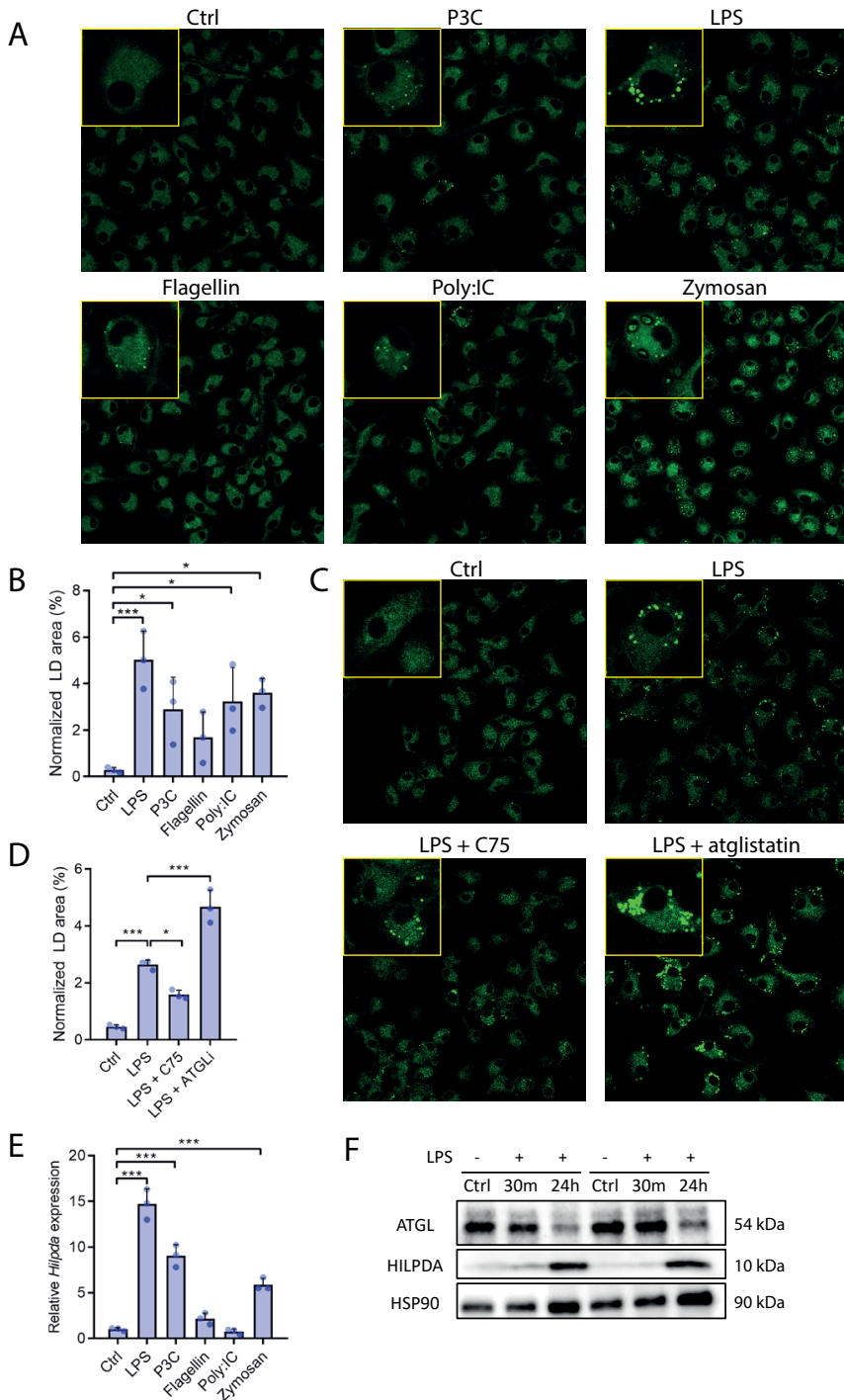


Figure 1. TLR stimulation leads to lipid droplet accumulation through HILPDA and ATGL.

(A and B) BODIPY staining and LD quantification in wild-type BMDMs treated with vehicle (Ctrl), P3C, LPS, flagellin, poly:IC or opsonized zymosan for 24 h. (C and D) BODIPY staining in wild-type BMDMs treated with vehicle (Ctrl), LPS, LPS and C75 or LPS and atglistatin (ATGLi). (E) Gene expression levels of *Hilpda* in wild-type BMDMs treated with vehicle (Ctrl, LPS, P3C, flagellin, poly:IC or opsonized zymosan for 24 h. (F) Protein expression levels of ATGL and HILPDA in wild-type BMDMs treated with vehicle (Ctrl) or LPS for 30 min or 24 h. HSP90 was used as the loading control. Bar graphs are represented as mean \pm SD. LD: lipid droplet; Ctrl: control; P3C: Pam3CysK4; LPS: lipopolysaccharide; poly:IC: polyinosinic:polycytidylic acid; ATGLi: atglistatin. * $p < 0.05$, ** $p < 0.01$, *** $p < 0.001$

To verify this notion, we used a murine myeloid-specific knockout model for HILPDA [16]. BMDMs derived from myeloid-specific HILPDA-deficient mice (*Hilpda* ^{Δ LysM}) expressed little to no HILPDA protein after LPS stimulation, whereas BMDMs derived from their floxed littermates (*Hilpda*^{fl/fl}) showed substantial upregulation of HILPDA protein in response to LPS (**Figure 2A**). Consistent with an important role of HILPDA in LPS-induced TG accumulation, the LD area was significantly lower in LPS-treated *Hilpda* ^{Δ LysM} macrophages compared with *Hilpda*^{fl/fl} macrophages (**Figure 2B and C**), whereas no differences in LD area were observed under control conditions (**Supplemental Figure 1**). The difference in TG accumulation between LPS-treated *Hilpda* ^{Δ LysM} and *Hilpda*^{fl/fl} macrophages was almost completely abolished by atglistatin, indicating that the reduced TG accumulation in LPS-treated *Hilpda* ^{Δ LysM} macrophages is mostly due to enhanced ATGL activity (**Figure 2B and C**). To further investigate the connection between HILPDA and ATGL, we determined ATGL protein levels. In *Hilpda*^{fl/fl} BMDMs, ATGL protein tended to be downregulated already after 30 min of LPS stimulation, with an even stronger downregulation after 24 h, again showing an inverse pattern compared with HILPDA protein (**Figure 2A**). Strikingly, ATGL protein levels were much higher in *Hilpda* ^{Δ LysM} compared with *Hilpda*^{fl/fl} BMDMs, which was most evident after 24 h LPS treatment (**Figure 2A**). These data indicate that the induction of HILPDA mediates the decrease in ATGL protein levels upon LPS treatment.

Subsequently, we tried to clarify the mechanism by which HILPDA decreases ATGL protein expression. HILPDA deficiency in BMDMs did not influence ATGL (*Pnpla2*) mRNA levels (**Figure 2D**). Accordingly, we hypothesized that HILPDA might promote ATGL protein degradation. To verify this hypothesis, we treated *Hilpda* ^{Δ LysM} and *Hilpda*^{fl/fl} macrophages with specific lysosomal protease (e64d and leupeptin) or ubiquitin-proteasome (MG132) inhibitors. Treatment with e64d or leupeptin did not influence ATGL protein levels, suggesting that ATGL is not degraded via the lysosomes (**Figure 2E and F**). In contrast, treatment of *Hilpda*^{fl/fl} macrophages with MG132 markedly induced ATGL protein levels, suggesting that ATGL is degraded via the ubiquitin-proteasome pathway (**Figure 2G**). Consistent with a stimulatory effect of HILPDA on proteasomal degradation of ATGL, MG132 failed to increase ATGL protein levels in *Hilpda* ^{Δ LysM} macrophages (**Figure 2G**). Differences in ATGL protein levels between *Hilpda* ^{Δ LysM} and *Hilpda*^{fl/fl} macrophages were

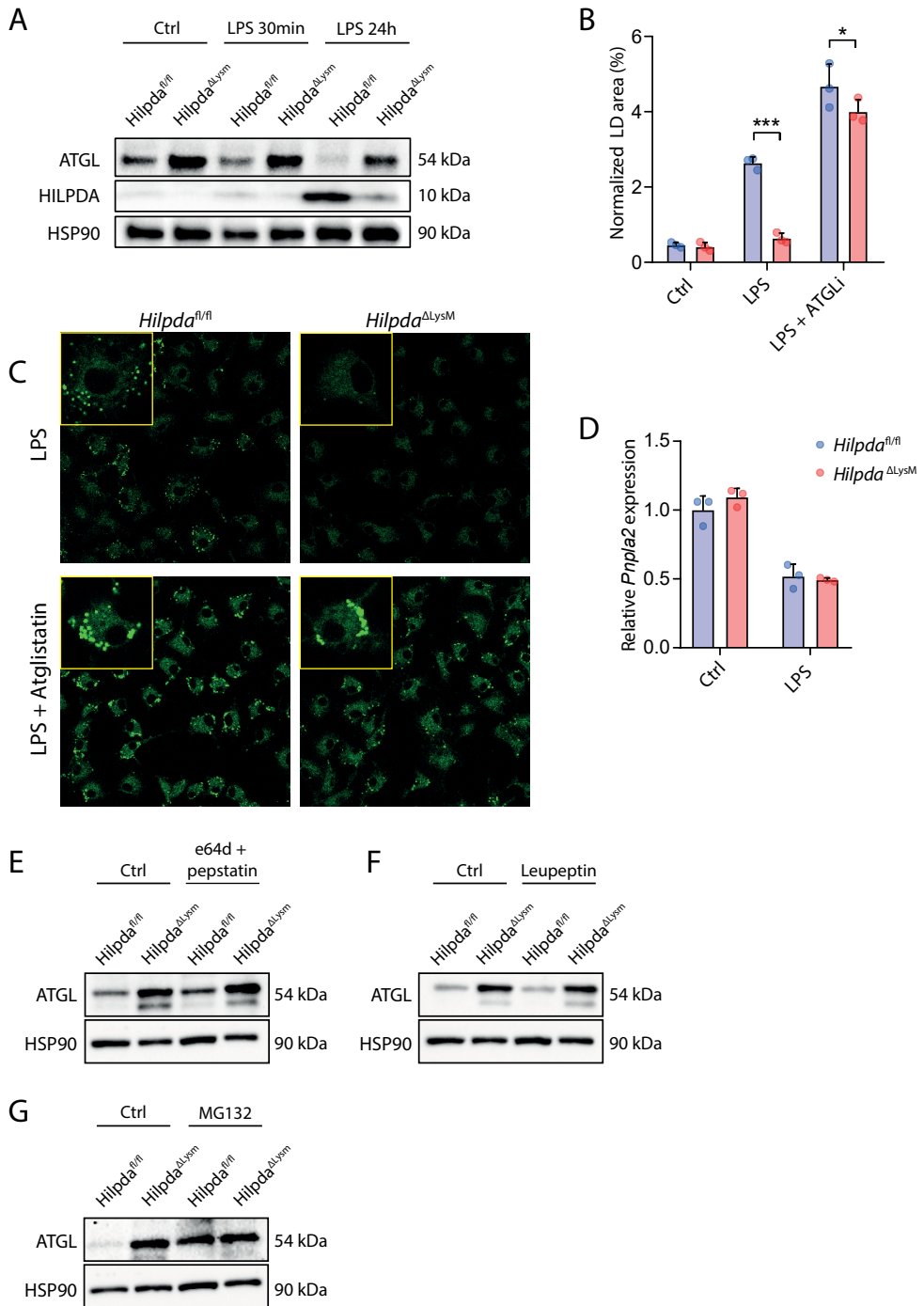


Figure 2. LPS promotes TG accumulation in macrophages by inducing HILPDA, which inhibits TG lipolysis by stimulating proteasomal degradation of ATGL.

(A) Protein expression levels of ATGL and HILPDA in *Hilpda*^{ΔLysM} and *Hilpda*^{fl/fl} BMDMs treated with vehicle (Ctrl) or LPS for 30 min or 24 h. HSP90 was used as loading control. (B and C) BODIPY staining and LD quantification of *Hilpda*^{ΔLysM} and *Hilpda*^{fl/fl} BMDMs treated with LPS or LPS and atglistatin for 24 h. (D) Gene expression levels of *Pnpla2* (ATGL) in *Hilpda*^{ΔLysM} and *Hilpda*^{fl/fl} BMDMs treated with vehicle (Ctrl) or LPS for 24 h. Protein expression of ATGL in *Hilpda*^{ΔLysM} and *Hilpda*^{fl/fl} BMDMs treated with vehicle (Ctrl) or e64d and pepstatin (E), vehicle (Ctrl) or Leupeptin (F) and vehicle (Ctrl) or MG132 (G). HSP90 was used as loading control. Bar graphs are represented as mean ± SD. LD: lipid droplet; Ctrl: control; LPS: lipopolysaccharide; ATGLi: atglistatin. * $p < 0.05$, *** $p < 0.001$

completely abolished after MG132 treatment, suggesting that the repressive effect of HILPDA on ATGL protein levels is entirely mediated by enhanced proteasomal degradation of ATGL. Overall, these data suggest that LPS promotes TG accumulation in macrophages by inducing HILPDA, which in turn decreases ATGL protein levels and consequent TG lipolysis by stimulating proteasomal degradation of ATGL.

HILPDA deficiency in myeloid cells facilitates the inflammatory phenotype *in vivo*

Based on the findings presented above, myeloid-specific HILPDA-deficient mice provide an excellent model to examine the impact of modulating macrophage TG accumulation on LPS-induced whole-body inflammation. To pursue this question, classical inflammation was induced by intraperitoneal injection of LPS in *Hilpda*^{ΔLysM} and *Hilpda*^{fl/fl} mice for 2, 4, 8 or 24 h. Similar to the observation in BMDMs, LPS stimulated *Hilpda* expression in splenic *Hilpda*^{fl/fl} macrophages, with a maximal effect observed after 4 h (**Figure 3A**). Although LPS also upregulated *Hilpda* mRNA in splenic *Hilpda*^{ΔLysM} macrophages, *Hilpda* expression levels were much lower compared with *Hilpda*^{fl/fl} macrophages (**Figure 3A**). To study the effect of macrophage-specific HILPDA deficiency on plasma inflammatory markers, plasma collected at different time points of LPS-induced inflammation was subjected to proteomic profiling, allowing for the semi-quantification of a protein biomarker panel consisting of 92 biomarkers (Olink®). Both principal component analyses (PCA) and partial least squares discriminant analyses (PLS-DA) clearly separated the different time points (**Supplemental Figure 2A and B**). In addition, at each time point, clear separation by genotype could be observed by PLS-DA (**Figure 3B and Supplemental Figure 2C**). Relative differences in the biomarkers between *Hilpda*^{ΔLysM} and *Hilpda*^{fl/fl} mice were mapped in volcano plots. Protein biomarkers were given further consideration if they met the very lenient statistical threshold of uncorrected p -value < 0.05 . For both the control groups and the 4 h time point groups, the number of indicated proteins was 2 or none (**Supplemental Figure 2D**). However, for the 2 h, 8 h and 24 h time points, a higher number of proteins met the significance threshold (**Figure 3C**). Interestingly, proteins such as TNF and IL-6 were higher in the *Hilpda*^{ΔLysM} mice than their *Hilpda*^{fl/fl} littermates at several time points, hinting at a potentially higher degree of inflammation in the *Hilpda*^{ΔLysM} mice.

immune cell populations in the circulation by flow cytometry. Although the relative abundance of the measured immune cell populations in the circulation clearly changed over time upon LPS-induced inflammation, no differences were found between the two genotypes in populations of B cells, T cells, neutrophils, eosinophils and three subsets of monocytes (CD11b+Ly6G-Ly6C-, CD11b+Ly6G-Ly6C+ and CD11b+Ly6G-CCR2+) (**Figure 4C**). Additionally, no differences were found in the relative abundance of T-cell subsets (**Supplemental Figure 3**).

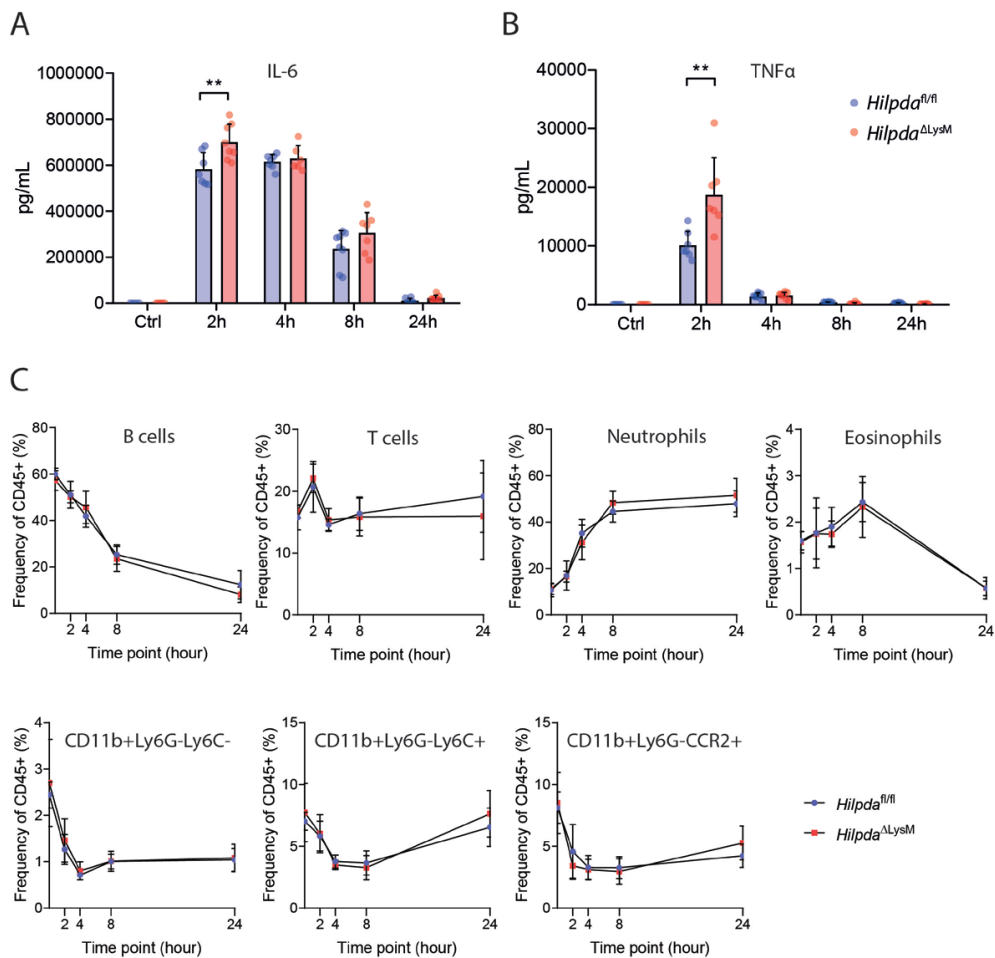


Figure 4. Myeloid deletion of HILPDA affects inflammatory parameters without altering relative immune cell populations *in vivo*.

(**A** and **B**) Plasma concentration of IL-6 and TNFα in *Hilpda^{ΔLysM}* and *Hilpda^{fl/fl}* mice 2, 4, 8 or 24 h after intraperitoneal injection of LPS or 24 h after intraperitoneal injection of saline (Ctrl). (**C**) Relative circulating immune cell populations in *Hilpda^{ΔLysM}* and *Hilpda^{fl/fl}* mice 2, 4, 8 or 24 h after intraperitoneal injection of LPS or 24 h after intraperitoneal injection of saline (baseline). Bar graphs are represented as mean ± SD. Ctrl: control. ***p*<0.01

HILPDA-deficient macrophages show an increased pro-inflammatory phenotype *ex vivo*

Next, we asked whether modulation of lipid storage by HILPDA could influence the secretion of inflammatory mediators in peritoneal macrophages. To that end, peritoneal macrophages were isolated from *Hilpda*^{ΔLysM} and *Hilpda*^{fl/fl} mice at different time points after LPS injection, and the release of several inflammatory mediators was measured. In agreement with the data in BMDMs, LPS caused a clear induction in lipid storage in the *Hilpda*^{fl/fl} macrophages but not in *Hilpda*^{ΔLysM} macrophages, becoming most evident 8 to 24 h after LPS injection (**Figure 5A and B**). Since we observed increased pro-inflammatory markers *in vivo*, we set out to investigate the pro-inflammatory phenotype of the peritoneal macrophages by measuring cytokine release (**Figure 5C**). Interestingly, 4 and 8 h after LPS injection, IL-6 release was significantly higher in *Hilpda*^{ΔLysM} compared with *Hilpda*^{fl/fl} macrophages, suggesting an increased inflammatory phenotype in peritoneal macrophages (**Figure 5C**). By contrast, 4 h after LPS injection, the release of TNFα was significantly lower in *Hilpda*^{ΔLysM} compared with *Hilpda*^{fl/fl} macrophages (**Figure 5C**).

IL-10 release showed a trend toward a reduction in *Hilpda*^{ΔLysM} compared with *Hilpda*^{fl/fl} macrophages for most time points, which reached significance 24 h after LPS injection (**Figure 5C**). No significant differences were observed for IL-1RA (**Figure 5C**). Since a decreased presence of LDs was found in the *Hilpda*^{ΔLysM} compared with *Hilpda*^{fl/fl} macrophages over time (**Figure 5A**), we wondered whether this could impact the release of lipid-derived inflammatory mediators. Indeed, 8 h after LPS injections, the release of prostaglandin-E2 (PGE2) by peritoneal macrophages was significantly higher in *Hilpda*^{ΔLysM} macrophages than in *Hilpda*^{fl/fl} macrophages (**Figure 5D**), potentially indicating an increased direction of lipids from LDs toward the production of prostaglandins.

HILPDA deficiency does not affect key macrophage effector functions

After observing clear differences in the inflammatory activation between *Hilpda*^{fl/fl} and *Hilpda*^{ΔLysM} macrophages, we wondered whether similar differences could be observed in effector functions that are associated with inflammation. Interestingly, previous research highlighted the importance of TG hydrolysis by ATGL for phagocytosis [20] and linked ATGL deficiency to increased apoptosis in macrophages [13]. Since HILPDA-deficient macrophages consistently show increased ATGL protein expression levels, we set out to study whether apoptosis may be downregulated and whether efferocytosis and phagocytosis may be amplified in *Hilpda*^{ΔLysM} and *Hilpda*^{fl/fl} macrophages. For the study of these three characteristics, we used a high-content analysis (HCA) approach based on live-cell fluorescent labelling assays, assessed using an automated confocal image

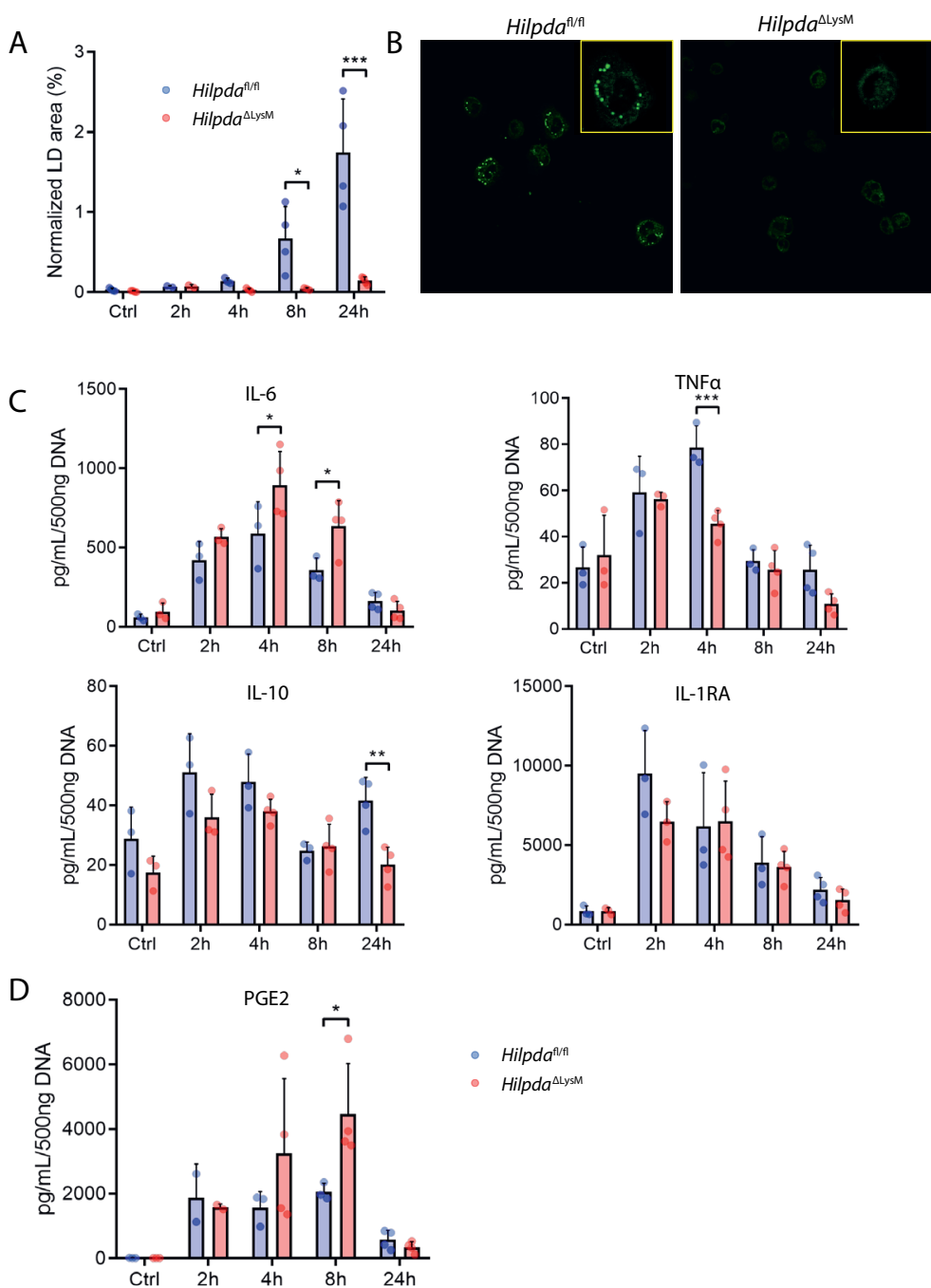


Figure 5. HILPDA-deficient macrophages show an increased pro-inflammatory phenotype after *in vivo* LPS treatment.

(A and B) BODIPY staining and LD quantification in peritoneal macrophages isolated from *Hilpda^{ΔLysM}* and *Hilpda^{fl/fl}*

^{fl} mice 2, 4, 8 or 24 h after intraperitoneal injection of LPS or 24 h after intraperitoneal injection of saline (Ctrl). (C) Concentrations of IL-6, TNF α , IL-10 and IL-1RA or (D) PGE2 in *ex vivo* supernatant from peritoneal macrophages isolated from *Hilpda* ^{Δ LysM} and *Hilpda*^{fl/fl} mice 2, 4, 8 or 24 h after intraperitoneal injection of LPS or 24 h after intraperitoneal injection of saline (Ctrl). Bar graphs are represented as mean \pm SD. LD: lipid droplet; Ctrl: control. * p <0.05, *** p <0.001

reader and single-cell based image analysis. To measure relative levels of apoptosis, BMDMs were stained with Annexin-V. Both the percentage of positive cells and the mean fluorescent intensity were similar in *Hilpda* ^{Δ LysM} and *Hilpda*^{fl/fl} macrophages, indicating that apoptosis is not affected by HILPDA deficiency (**Figure 6A and B**). To assess efferocytosis, *Hilpda* ^{Δ LysM} or *Hilpda*^{fl/fl} BMDMs were co-cultured with apoptotic Jurkat E6.1 cells. Both the percentage of cells positive for the efferocytosis as the mean count of ingested Jurkat cells per macrophage did not differ between *Hilpda* ^{Δ LysM} and *Hilpda*^{fl/fl} BMDMs (**Figure 6C and D**). Lastly, to assess phagocytosis, BMDMs were co-incubated with fluorescently labelled Zymosan bioparticles. No differences in the percentage of positive cells or mean fluorescent intensity were found between *Hilpda* ^{Δ LysM} and *Hilpda*^{fl/fl} macrophages (**Figure 6E and F**). Taken together, our data suggest that deletion of HILPDA does not affect apoptosis in *Hilpda* ^{Δ LysM} versus *Hilpda*^{fl/fl} macrophages, nor does it increase the capacity for efferocytosis or phagocytosis. Since recent research has highlighted the important role of LDs in the bacterial killing capacity of macrophages [8], we investigated whether the decreased retention of LDs after LPS treatment in *Hilpda* ^{Δ LysM} macrophages could impact their killing capacity. The microbial killing of *E. coli* was consistent at control or atglitastatin-treated *Hilpda* ^{Δ LysM} and *Hilpda*^{fl/fl} macrophages, and treatment with LPS did not lead to significant differences in remaining *E. coli* load after 4 or 24 h of LPS treatment (**Figure 6G**).

Increased production of PGE2 in HILPDA-deficient macrophages drives increased production of IL-6

Next, we further investigated the mechanism underlying the effect of HILPDA deficiency on PGE2 and IL-6 production using BMDMs. Confirming the results obtained in peritoneal macrophages, IL-6 production was significantly higher in *Hilpda* ^{Δ LysM} compared with *Hilpda*^{fl/fl} macrophages after 8 and 24 h of LPS treatment. Subsequently, we determined whether the observed differences in PGE2 and IL-6 might have been due to differential activation of transcriptional factors controlling the inflammatory response. However, phosphorylation of cJUN, STAT3 and NF κ B was not significantly different between *Hilpda* ^{Δ LysM} and *Hilpda*^{fl/fl} macrophages (**Supplemental Figure 4A-C**), indicating that the acute regulation of inflammatory pathways is intact. Alternatively, since we previously showed that lipid loading leads to increased oxidation of excess fatty acids in *Hilpda* ^{Δ LysM} compared with *Hilpda*^{fl/fl} macrophages [16], we determined whether the oxidation of fatty acids or other metabolic parameters were differently regulated in *Hilpda* ^{Δ LysM} macrophages.

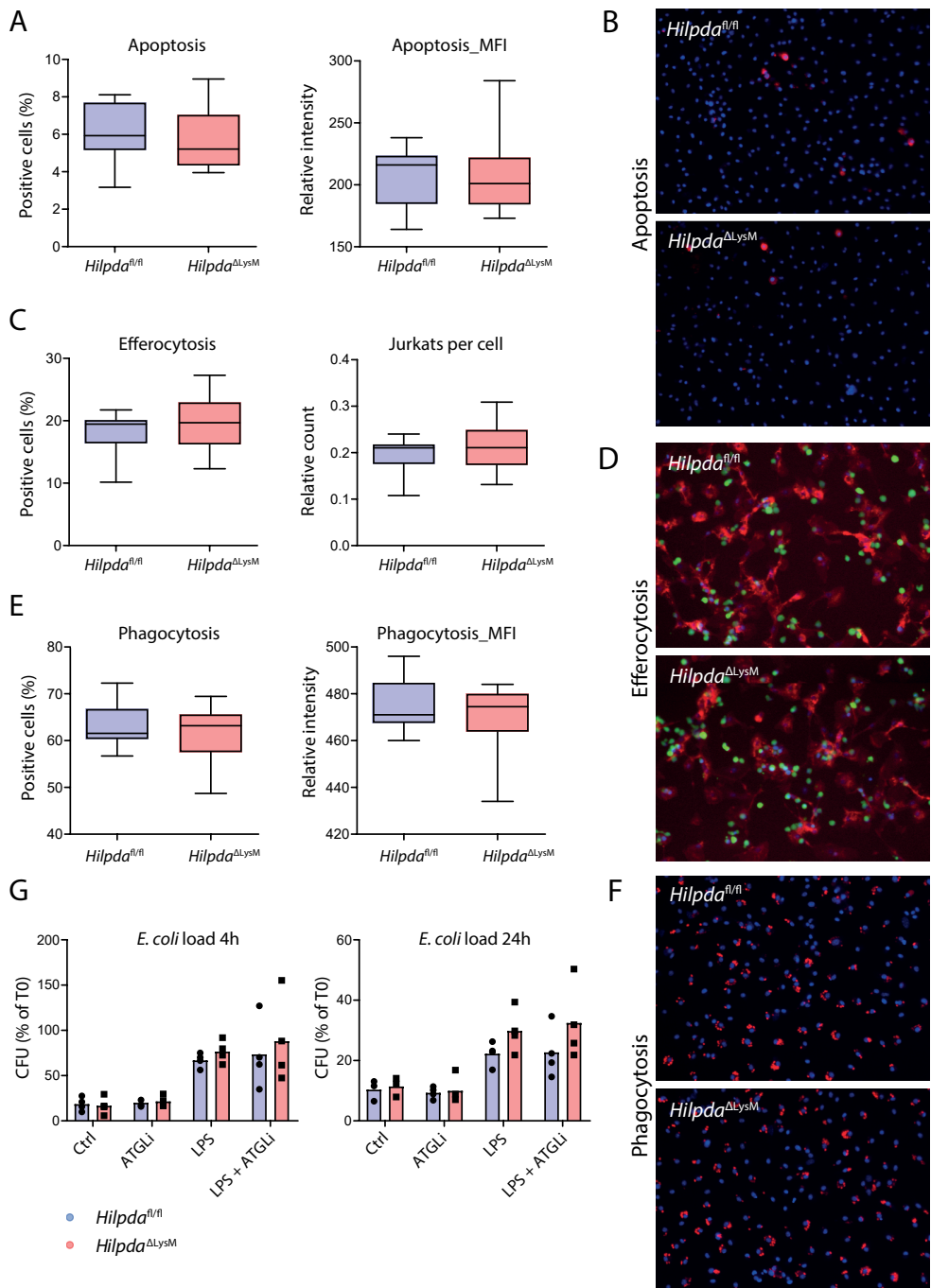


Figure 6. HILPDA deficiency does not affect key macrophage effector functions.

(A and B) Percentage of positive cells and mean fluorescence intensity following Annexin-V and Hoechst staining in *Hilpda^{ΔLysM}* and *Hilpda^{fl/fl}* BMDMs after treatment with LPS for 24 h. (C and D) Percentage of positive cells and

amount of ingested Jurkat cells (green) following efferocytosis assay and subsequent staining in *Hilpda*^{ΔLysM} and *Hilpda*^{fl/fl} BMDMs (actin in red, nuclei in blue) after treatment with LPS for 24 h. **(E and F)** Percentage of positive cells and mean fluorescence intensity after phagocytosis assay and subsequent staining in *Hilpda*^{ΔLysM} and *Hilpda*^{fl/fl} BMDMs (beads in red, nuclei in blue) after treatment with LPS for 24 h. **(G)** Relative *E. coli* load after 4 or 24 h of bacterial killing in *Hilpda*^{ΔLysM} and *Hilpda*^{fl/fl} BMDMs after treatment with LPS for 24 h. MFI: mean fluorescence intensity; CFU: colony-forming units.

Comparing oxygen consumption rate (OCR) before and after addition of etomoxir, an inhibitor of fatty acid oxidation (FAO), did not reveal consistent and significant differences in FAO in LPS-treated BMDMs (24 h) between the two genotypes (**Supplemental Figure 5A**). Additionally, no differences were observed in the extracellular acidification rate (ECAR) after 24 h of LPS treatment, suggesting the absence of long-term differences in glycolytic rate (**Supplemental Figure 5B**). These results suggest that deletion of HILPDA does not affect metabolism in macrophages.

We subsequently hypothesized that the observed increase in PGE2 in *Hilpda*^{ΔLysM} macrophages could be driven by an increased conversion of excess fatty acids into lipid-related inflammatory mediators, which in turn may drive the increase in IL-6 release [21]. To examine this hypothesis, we first measured whether the increased production of IL-6 and PGE2 in *Hilpda*^{ΔLysM} macrophages could be confirmed *in vitro*. Indeed, after 8 and 24 h of LPS treatment, the production of both IL-6 and PGE2 was significantly higher in *Hilpda*^{ΔLysM} than *Hilpda*^{fl/fl} macrophages (**Figure 7A and B**). Next, we measured the release of PGE2 in BMDMs from *Hilpda*^{ΔLysM} and *Hilpda*^{fl/fl} mice treated with LPS and vehicle or LPS and atglistatin for 24 h. Although the production of PGE2 was found to be consistently higher in BMDMs from *Hilpda*^{ΔLysM} versus *Hilpda*^{fl/fl} mice, the production of PGE2 in both genotypes was markedly and similarly inhibited by the addition of atglistatin (**Figure 7C**), validating the importance of lipolysis by ATGL for the endogenous production of PGE2. Subsequently, we tested whether the increased levels of PGE2 could drive the observed increase in IL-6 production. The addition of exogenous PGE2 to BMDMs from *Hilpda*^{ΔLysM} and *Hilpda*^{fl/fl} mice treated with LPS significantly increased the production of IL-6 in both genotypes after 4, 8 and 24 h (**Figure 7D**). Inhibiting cyclooxygenase (COX)1 and COX2, the alleged drivers of PGE2 synthesis, by a general COX1/2 inhibitor (indomethacin) or a specific COX2 inhibitor (NS-398), drastically decreased the production of PGE2 in both genotypes after 8 or 24 h of LPS stimulation (**Supplemental Figure 5C**). Accordingly, these inhibitors also significantly decreased the production of IL-6 in macrophages from both genotypes, abolishing the difference between *Hilpda*^{ΔLysM} and *Hilpda*^{fl/fl} macrophages (**Figure 7E**) and verifying the association between increased PGE2 production and subsequent IL-6 production in *Hilpda*^{ΔLysM} macrophages.

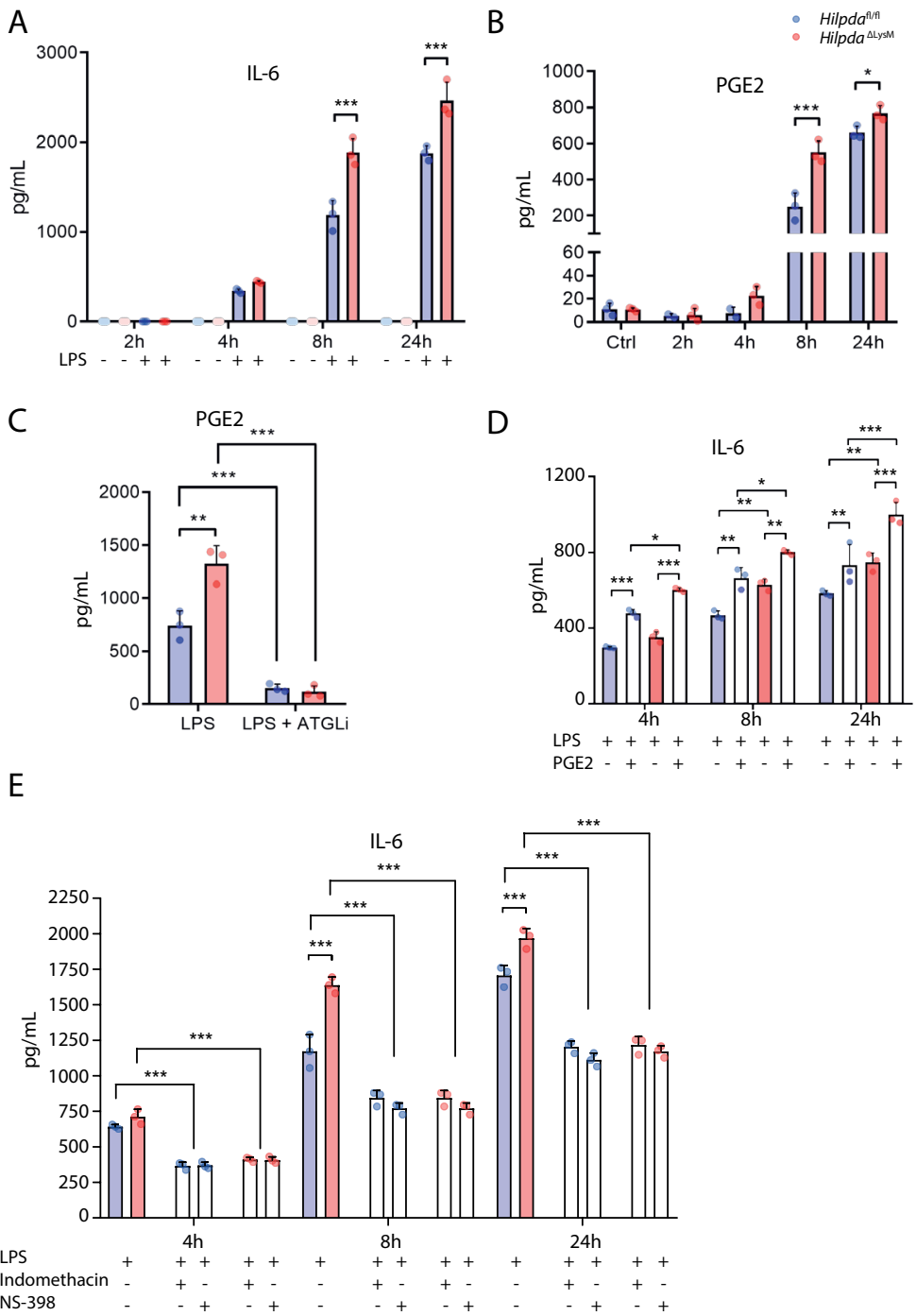


Figure 7. Increased production of PGE2 in HILPDA-deficient macrophages drives increased production of IL-6.

(A) Concentration of IL-6 or (B) PGE2 from *Hilpda*^{ΔLysM} and *Hilpda*^{fl/fl} BMDMs after treatment with vehicle (Ctrl) or LPS for 2, 4, 8 or 24 h. (C) Concentration of PGE2 from *Hilpda*^{ΔLysM} and *Hilpda*^{fl/fl} BMDMs after treatment with LPS or LPS and atglistatin for 24 h. (D) Concentration of IL-6 from *Hilpda*^{ΔLysM} and *Hilpda*^{fl/fl} BMDMs after treatment with LPS and/or PGE2 for 4, 8 or 24 h. (E) Concentration of IL-6 from *Hilpda*^{ΔLysM} and *Hilpda*^{fl/fl} BMDMs after treatment with LPS and indomethacin or NS-398 for 4, 8 or 24 h. Bar graphs are represented as mean ± SD. LPS: lipopolysaccharide; PGE2: prostaglandin-E2; ATGLi: atglistatin. * $p < 0.05$, ** $p < 0.01$, *** $p < 0.001$

Discussion

In the current study, we investigated the mechanism underlying the LPS-induced accumulation of TG in macrophages, and the role of TG accumulation in LPS-induced inflammation. Our data demonstrate that LPS promotes TG accumulation in macrophages by inducing HILPDA, which, in turn, lowers ATGL protein levels by enhancing the proteasomal degradation of ATGL. The decrease in TGs in HILPDA-deficient myeloid cells is associated with a heightened inflammatory response, both *in vivo* and *ex vivo*, and with elevated production of PGE₂. Our data suggest that the tight regulation of lipid efflux from LDs by ATGL is important for the regulation of the inflammatory response by directing the production of PGE₂, which in turn modulates the release of IL-6.

Although a decrease in ATGL-mediated lipolysis evidently plays an important part in stimulating the accumulation of TGs in LDs during inflammation, this phenomenon is likely the result of an interplay between several variables. As observed, the expression of HILPDA increases during inflammation, decreasing ATGL protein levels and thereby limiting the breakdown of TGs from LDs. At the same time, oxidation of fatty acids is often limited in inflammatory macrophages [22,23]. Additionally, the synthesis or uptake of fatty acids [4] and subsequent synthesis of TGs [24] are also significantly enhanced after inflammatory activation. Together, these processes likely lead to the physical accumulation of LDs in macrophages. However, deletion of HILPDA prevents the inducing effects of LPS on TG accumulation in LDs, underlining the importance of ATGL inhibition in this process.

Lack of visible LDs in our HILPDA-deficient macrophages is distinct from the lack of LDs that results from the inhibition of TG synthesis, as seen by Castoldi and colleagues [24]. In their DGAT1-deficient macrophages, the inhibition of TG synthesis caused a lack of lipid storage in LDs. Consequently, a decreased amount of precursors for the production of prostaglandins were available, leading to an attenuated inflammatory response in macrophages [24]. In our study, deletion of HILPDA in myeloid cells led to increased ATGL-mediated lipolysis and thus likely increased the availability of fatty acids as precursors for inflammatory mediators. Accordingly, we observed an increased inflammatory phenotype, exemplified by consistently increased production of IL-6, likely effectuated by increased levels of PGE₂. Hence, our data confirm the importance of the availability of TG pools in the inflammatory process in macrophages. Moreover, the results of this study pinpoint ATGL-mediated lipolysis as an important factor in the inflammatory process by tightly controlling the flow of lipids from LDs toward the synthesis of inflammatory mediators, thereby precisely determining the magnitude of the inflammatory response.

In both neutrophils and mast cells lacking ATGL, decreased release of inflammatory lipid

mediators can be seen [25,26]. These results are in accordance with our results using the ATGL inhibitor atglistatin, which directly inverted the increased levels of PGE2 in *Hilpda*^{ΔLysM} macrophages. Eicosanoids, including PGE2, are signalling lipids synthesized from arachidonic acid by highly organized cyclooxygenase enzymes that can be directly recruited to LD membranes. Although not only directed by, synthesis of eicosanoids during LPS-induced inflammation is heavily dependent on the liberation of esterified arachidonic acid from intracellular phospholipid or neutral lipid pools [27]. Whereas specific hydrolysis of membrane glycerophospholipids or neutral lipids by phospholipase A2 enzymes was conventionally regarded as the main source of fatty acids for eicosanoid production [28,29], the current study builds upon the increasing evidence that ATGL also controls the release of fatty acid precursors from LDs for the production of eicosanoids in immune cells [25,26].

It has been established that prostaglandins, including PGE2, can directly regulate the inflammatory response by influencing the release of cytokines. The regulation of different cytokines by PGE2 is complex and determined by separate molecular mechanisms [30,31]. Whether PGE2 exerts pro- or anti-inflammatory effects is likely also dependent on the timing of experiments and the use of different *in vitro* or *in vivo* systems. Endogenous production of PGE2 in macrophages has led to inhibition of TNF α release, but also the induction of either transcription or release of IL-10, IL-1 β and IL-6 [21,30–33]. Especially the direct role between PGE2 and IL-6 is often highlighted to be specific [21] and formed the basis of the observed phenotypes within the current study.

The fact that careful regulation of ATGL is crucial for an adequate immune response in macrophages, besides providing fatty acid precursors for inflammatory mediators, becomes further apparent in studies using ATGL^{-/-} macrophages. In macrophages lacking ATGL, TGs can be seen to accumulate, leading to mitochondrial dysfunction, defects in macrophage polarization, ER stress, decreased ability to migrate and decreased ability to use phagocytosis, accompanied by increased induction of mitochondrial apoptosis [12,13,20]. A decreased activation of ATGL in macrophages, for instance by deleting its coactivator CGI-58, also diminishes phagocytosis, although this phenotype is not accompanied by mitochondrial dysfunction [34]. Intriguingly, in our results, which in many ways show to be the exact opposite of the processes found in macrophages with decreased ATGL activity, no proof of increased phagocytosis or efferocytosis ability was perceived. Thus, whereas active ATGL was identified as a crucial factor to enable phagocytosis, further increase of ATGL expression clearly does not increase the phagocytic ability of macrophages.

To enable precise control of ATGL in macrophages, ATGL expression is regulated by several inhibitors, including HILPDA. It is shown that HILPDA is inducible by lipid influx [16] and, as observed in this study, inflammatory activation by LPS. Previous studies have also shown that HILPDA inhibits ATGL via direct physical interaction [16,17]. Here we show that HILPDA promotes the proteasomal degradation of ATGL in BMDMs, explaining the direct effects of HILPDA on LD homeostasis in macrophages [15,16]. The exact mechanism whereby HILPDA enhances ATGL degradation is unclear. It can be hypothesized that by binding to ATGL, HILPDA may cause a conformational change in ATGL, leading to the recruitment of a particular ubiquitin ligase. Further studies are necessary to carefully dissect the underlying mechanism.

In conclusion, our study demonstrates that HILPDA is directly involved in regulating the breakdown of ATGL during inflammatory activation in macrophages, thereby controlling ATGL-mediated lipolysis and mediating the increase of TG accumulation upon LPS treatment. Furthermore, we establish an important role for ATGL-mediated lipolysis in the production of PGE2 and subsequent modulation of IL-6 release.

Acknowledgements

We kindly thank Merel Defour, Benthe van der Lugt, Julia van Heck, Jenny Janssen, Anneke Hijmans, Gregorio Fazzi and Ricky Siebeler for their practical assistance. We are indebted to dr. Christina Warnecke for providing us with the HILPDA antibody. This work was financed by grants from the Netherlands Organisation of Scientific Research (2014/12393/ALW), the Dutch Diabetes Foundation (2015.82.1824), and the Netherlands Heart Foundation (ENERGISE grant CVON2014-02).

Methods

Animal Studies

All animal experiments were approved by the animal welfare committee of Wageningen University (2016.W-0093.015). *Hilpda*^{ΔLysM} and *Hilpda*^{fl/fl} mice were bred as described before [16]. Mice had unlimited access to food (standard chow) and water and were housed under normal light-dark cycles in humidity- and temperature-controlled specific pathogen-free conditions. Both male and female mice were used for the isolation of primary cell cultures. For the *in vivo* study, male *Hilpda*^{ΔLysM} and *Hilpda*^{fl/fl} mice, aged 9 – 12 weeks, were housed with two or three littermates per cage and randomly allocated to the different time points. Mice were weighed prior to injection to calculate specific concentrations of LPS. At each time point, 8 mice per genotype received an intraperitoneal injection of lipopolysaccharide (from *E. coli* O55:B5, Cat#L6529, Sigma-Aldrich, MO, USA) in a concentration of 2 mg/kg body weight in an end volume of 200 μL sterile saline solution. Control groups were injected with 200 μL sterile saline solution. After indicated time points, mice were anaesthetized with isoflurane and blood was collected via orbital puncture in EDTA containing tubes (Sarstedt, Nümbrecht, Germany). After blood collection, mice were immediately euthanized by cervical dislocation. Subsequently, peritoneal macrophages and tissues were harvested.

Flow Cytometry

Before collection of blood plasma, 25 uL blood was aliquoted from each sample and stained with antibodies against CD45-Alexa700 (Cat#103127), CD11b-FITC (Cat#101205), F4/80-PE (Cat#123109), Ly6C-Brilliant Violet 421™ (Cat#128031), CCR2-PE/Cy7 (Cat#150611), CD3-APC (Cat#100235), CD4-PerCP/Cy5.5 (Cat#100539), CD8-Brilliant Violet 785™ (Cat#100749), CD19-PE/Dazzle™ 594 (Cat#115553), Ly6G-APC/Fire™ 750 (Cat#127651) (all purchased from BioLegend, San Diego, CA, USA). Red blood cells were lysed with RBC lysis buffer (Cat#00-4333-57, eBioscience, ThermoFisher Scientific), and samples were measured on the CytoFLEX flow cytometry system (Beckman Coulter, Brea, CA, USA). Results were analyzed using CytExpert acquisition and analysis software, version 2.4 (Beckman Coulter) and FlowJo™ analysis software (BD BioSciences San Jose, CA, USA).

Plasma Measurements

EDTA tubes containing blood samples were centrifuged for 15 min at 5000 RPM at 4°C. Plasma was aliquoted and stored at –80°C until further measurements. The V-PLEX Mouse Cytokine 19-Plex Kit (Cat# K15255D-1, Meso Scale Diagnostics, MD, USA) and MESO QuickPlex SQ 120 (Meso Scale Diagnostics) were used to determine the concentrations of

IL27p28/IL30, IP-10, MCP-1, MIP-1 α , MIP-2, IFN γ , IL-10, IL-1 β , IL-6 and TNF α in the plasma. A high-multiplex biomarker panel (Olink[®] Target Mouse Exploratory) was used to explore 92 biomarkers in the mouse plasma using the proprietary Proximity Extension Assay technology (Olink Proteomics, Uppsala, Sweden).

Primary Cell Isolation

Peritoneal macrophages were harvested by flushing the peritoneal cavity with ice-cold PBS. The macrophage fractions were pooled per two mice from the same group, and purified by magnetic selection using anti-F4/80-FITC antibody (Cat#130-117-509; RRID: AB_2727970, Miltenyi Biotec, Bergisch Gladbach, Germany), anti-FITC MicroBeads (Cat#130-048-701; RRID: AB_244371, Miltenyi Biotec) and MS columns (Miltenyi Biotec) on the OctoMACS Cell Separator system (Miltenyi Biotec). Peritoneal macrophages were plated in 96-well plates for collection of supernatant or in 8-well glass-bottom μ -slides (Ibidi, Martinsried, Germany) for confocal imaging, and cultured in Roswell Park Memorial Institute (RPMI)-1630 medium (Lonza, Basel, Zwitterland) supplemented with 10% fetal calf serum (FCS, BioWest, Nuaille, France) and 1% penicillin/streptomycin (P/S, Corning) at 37°C and 5% CO₂ for 24 h. The supernatant was collected and stored at -80°C, 96-well plates were stored at -20°C. Macrophages in glass-bottom slides were fixed immediately in 3.7% paraformaldehyde, washed with PBS and stored at 4°C before staining.

After euthanizing the mice, spleens were immediately stored on ice in RPMI-1630 supplemented with 10% FCS and 1% P/S. Spleens were strained through 100 μ m cell strainers, and red blood cells were lysed with RBC lysis buffer (eBioscience, ThermoScientific). Splenic macrophages were isolated by magnetic selection using anti-F4/80-FITC antibody (Cat#130-117-509; RRID: AB_2727970, Miltenyi Biotec), anti-FITC MicroBeads (Cat#130-048-701; RRID: AB_244371) and MS columns (Miltenyi Biotec) with the OctoMACS Cell Separator system (Miltenyi Biotec). Splenic macrophages were centrifuged, and cell pellets were directly dissolved in TRIzol[®] Reagent (Invitrogen, ThermoFisher Scientific) and stored at -80°C.

For the isolation of BMDMs for *in vitro* experiments, 8-12 week old *Hilpda*^{ALysM} and *Hilpda*^{fl/fl} mice were euthanized by cervical dislocation and femurs and hind legs were isolated at the hip joint. Bone marrow was flushed from both femur and tibia and differentiated in Dulbecco's modified Eagle's medium (DMEM, Corning, NY, USA), supplemented with 10% FCS, 1% P/S and 15% L929-conditioned medium. After differentiation for seven days, cells were scraped and plated as appropriate.

In vitro Experiments

BMDMs were treated with LPS from *E. coli* (O55:B5, Cat#L6529, Sigma-Aldrich) and flagellin from *S. typhimurium* (Sigma-Aldrich) in the concentration of 100 ng/mL, Pam3CysK4 (Cat#L2000, EMC Microcollections, Tübingen, Germany) in the concentration of 5 µg/mL, Poly:IC (Sigma-Aldrich) in the concentration of 20 µg/mL and Zymosan from *S. cerevisiae* (Sigma-Aldrich) in the concentration of 100 µg/mL. Zymosan was opsonized to increase uptake by phagocytosis and sonicated just before use. Timing of treatments are indicated in the figure legends. Atglistatin (Cat#SML1075, Sigma-Aldrich) was used in a concentration of 20 µM, and cells were pre-treated for 1 h before further treatment. C75 (Cat#C5490, Sigma-Aldrich) was used in a concentration of 5 µg/mL, and cells were pre-treated for 1 h before further treatment. Indomethacin (Cat#I7378, Sigma-Aldrich) was used in a concentration of 10 µM and NS-398 (Cat#N194, Sigma-Aldrich) was used in a concentration of 1 µM, cells were pre-treated for 1 h before further treatment. PGE2 (Cat#2296, Tocris, Bio-Techne, UK) was added in a concentration of 0.1 µM 1 h after treatment with LPS.

Confocal Imaging

The visualization of lipid droplet accumulation was studied by plating BMDMs on 8- or 18-well glass-bottom µ-slides (Cat#80807 and 81817 Ibidi, Martinsried, Germany) coated with collagen type I (Cat#50201, Ibidi, Martinsried, Germany). After treatment, cells were washed with PBS and fixed with 3.7% paraformaldehyde. Next, cells were stained with 2µg/mL BODIPY® 493/503 (Cat#D3922, Invitrogen, ThermoFisher Scientific) and ActinRed™555 (Cat#R37112 ThermoFisher Scientific) and mounted with Vectashield antifade mounting medium (Cat#H-1000-10, Vector Laboratories, Peterborough, UK). Imaging was performed on the Leica Confocal TCS SP8 X system (Leica Microsystems, Wetzlar, Germany) using the 63 x 1.20 NA water-immersion objective lens. The pinhole was set to 1 Airy Unit (AU), and fluorescent probes were excited using the white light laser (WLL, 50% laser output) with laser power set to 1.5%. Fluorescent emission was detected using internal Hybrid (HyD) detectors. Images were processed and analyzed for lipid droplets with Cell Profiler Software [35].

Immunoblotting

After treatment, cells were lysed in RIPA lysis buffer (Cat#89900, ThermoFisher Scientific) supplemented with phosphatase and protease inhibitors. Pre-cast 4%-15% polyacrylamide gels were used to separate protein lysates and proteins were transferred onto nitrocellulose membranes using the Trans-Blot® Turbo™ Semi-Dry transfer cell with Trans-Blot® Turbo™ PVDF Transfer Packs (all purchased from Bio-Rad Laboratories). After blocking in non-fat

milk, membranes were incubated overnight at 4°C with primary antibody for HILPDA (a kind gift of dr. Christina Warnecke), ATGL (Cat#2138S, Cell Signaling Technology, MA, USA), Phospho-NF-κB p65 (Ser536, Cat#3033T, Cell Signaling Technology), Phospho-STAT3 (Tyr705, Cat#9145T, Cell Signaling Technology), Phospho-c-JUN (Ser63, Cat#9261S, Cell Signaling Technology), ACTIN (Cat#5057; RRID: AB_10694076, Cell Signaling Technology) or HSP90 (Cat#4874S; RRID: AB_2121214, Cell Signaling Technology). Membranes were subsequently incubated with secondary antibody (Anti-rabbit IgG, HRP-linked Antibody, 7074, Cell Signaling Technology) for 1 h at 4°C. Membranes were developed using Clarity ECL substrate (Bio-Rad Laboratories) and images were acquired with the ChemiDoc MP system (Bio-Rad Laboratories).

Enzyme-Linked Immunosorbent Assay (ELISA)

IL-6, TNFα, IL-10 and IL-1RA concentrations were measured in cell supernatants with the DuoSet sandwich ELISA kits (Cat#DY406/Cat#DY410/Cat#DY417/Cat#DY490, R&D systems, Bio-Techne) according to manufacturer's instructions. PGE2 was measured with the PGE2 monoclonal ELISA kit (Cat#514010, Cayman Chemicals, MI, USA). Normalization for peritoneal macrophages was performed by determining the DNA concentration per well (Quant-iT dsDNA Assay Kit high sensitivity, Cat#Q33120, ThermoFisher Scientific).

Functional Assays

Before measuring apoptosis, efferocytosis and phagocytosis, all BMDMs were treated with LPS (100 ng/mL) for 24 h to induce lipid droplet accumulation. Apoptosis was measured in BMDMs from *Hilpda*^{ΔLysM} and *Hilpda*^{fl/fl} mice by incubating with 2.5 ng/μL FITC-conjugated Annexin-V-FP488 (kindly provided by prof. Reutelingsperger [35]) for 15 minutes in annexin binding buffer, adding 300 nM Staurosporine (from *Streptomyces* sp., Cat#S4400, Sigma-Aldrich) to positive control wells to induce phagocytosis. Staining was quenched with 200 mM potassium iodide (KI). Efferocytosis was measured by staining Jurkat E6.1 cells (Cat#88042803, Sigma-Aldrich) with calcein (AM, Cat#C1430, Invitrogen, ThermoFisher Scientific) and rendering them apoptotic by treatment with staurosporine (from *Streptomyces* sp., Cat#S4400, Sigma-Aldrich) in a concentration of 5 μM for 1 h. Jurkats were co-incubated for 1.5 h with BMDMs from *Hilpda*^{ΔLysM} and *Hilpda*^{fl/fl} mice (approximately 3 Jurkat cells per BMDM). Not-internalized Jurkats were detached and BMDMs were stained with antibodies against CD11b-Alexa Fluor 647 (Cat#101218, BioLegend). Phagocytosis was assessed by incubating cells with pHrodo™ Red Zymosan Bioparticles™ (Cat#P35364, Life Technologies, ThermoFisher Scientific) for 1 h, while Cytochalasin D (Cat#C2618, Sigma-Aldrich) was added to negative control wells to inhibit phagocytosis. For all assays, nuclei of BMDMs were stained with Hoechst 33342

(Cat#B2261, Sigma-Aldrich). All the above described functional assays were processed on the BD Pathway 855 High Content Analyzer (BD Biosciences, NJ, USA) using the 10-fold objective, making 9 images per well (3x3). Data was analyzed with AttoVision™ software (BD Biosciences), FACSDiva™ software (BD Biosciences) and Cell Profiler Software [36]. Shortly, background signals were subtracted, Flat Field correction was performed, cells were segmented on each image based on the nuclei and intensity of the stainings were recorded. Data were subsequently analyzed in FACSDiva software, calculated the mean fluorescence intensity and percentage of positive cells. For the efferocytosis assay, Cell Profiler Software was used to calculate the average number of internalized Jurkats per BMDM.

Bacterial killing assay

E. coli were grown to an O.D. of 1 at 600 nm and diluted toward 1×10^5 colony-forming units (CFU) per mL. BMDMs from *Hilpda*^{ΔLysM} and *Hilpda*^{fl/fl} mice were seeded in a density of 50 000 cells per well in 96-well plates and treated overnight with atglistatin, LPS or LPS + atglistatin for 24 h. BMDMs were co-incubated with *E. coli* (total MOI 100) for 30 min and subsequently washed with 200 µg/mL gentamycin. Cells were lysed directly after 30 min (t = 0), or after 4 (t = 4) or 24 h (t = 24) of incubation at 37°C and 10% CO₂. BMDMs were lysed and bacteria were plated in serial dilutions on LB-agar plates overnight at 30°C, after which the colony-forming units were counted.

Extracellular Flux Assay

To estimate metabolic fluxes, the extracellular flux of *Hilpda*^{ΔLysM} and *Hilpda*^{fl/fl} BMDMs was measured after 24 h treatment with LPS (100ng/mL) using the Agilent Seahorse XF96 Analyzer (Agilent Technologies, Santa Clara, CA, USA). BMDMs were seeded in 100 000 cells per well in XF-96 plates (Agilent Technologies) and cultured at 37°C/5% CO₂. Before measuring extracellular flux, BMDMs were washed and cultured in Seahorse XF base medium (Agilent Technologies) without sodium bicarbonate, supplemented with 2 mM L-glutamine for the glycolytic stress test, or with 2 mM L-glutamine and 25 mM glucose for the measurement of oxidative phosphorylation. Cells were kept for 1 h at 37°C in a non-CO₂ incubator. For the glycolytic stress test, the following compounds were added during three injections: glucose (25 mM), oligomycin (1.5 µM), and 2-DG (50 mM) and the extracellular acidification rate (ECAR) was automatically measured by the sensor cartridge at baseline and following injections. For the measurement of the OXPHOS and fatty acid oxidation, etomoxir (50 µM) was injected and the oxygen consumption rate (OCR) measured by the sensor cartridge at baseline and following the injection. Calculations were made using the Seahorse XF-96 software Wave Desktop 2.6 (RRID: SCR_014526, Agilent Technologies).

Quantitative PCR

Total RNA was isolated from treated cells with TRIzol® Reagent (Invitrogen, ThermoFisher Scientific), and from isolated spleen macrophages using the RNeasy Micro Kit (QIAGEN, Venlo, the Netherlands). cDNA was synthesized from 500ng RNA with the iScript cDNA kit (Bio-Rad Laboratories, Hercules, CA, USA) according to manufacturer's instructions. The CFX384 Touch Real-Time detection system (Bio-Rad Laboratories) was used to assess amplification of *Pnpla2* templates (ATGL, forward primer CAACGCCACTCACATCTACGG; reverse primer GGACACCTCAATAATGTTGGCAC) or *Hilpda* templates (forward primer TCGTGCAGGATCTAGCAGCAG; reverse primer GCCCAGCACATAGAGGTTCA) with the SensiMix kit for SYBR green reactions (Cat#QT650-05, BioLine, London, UK). Mouse *36b4* expression was used to normalize the quantification (forward primer ATGGGTACAAGCGCGTCCTG; reverse primer GCCTTGACCTTTTCAGTAAG).

Power Calculation Animal Study

From a pilot study, we concluded that macrophages from *Hilpda*^{ΔLysM} mice after stimulation with LPS showed a 1.4-fold upregulation in the mRNA expression of *Il6*, compared with *Hilpda*^{n/n} mice. Standard deviations between several experiments were tested between 0.1 – 0.2. The group size was estimated with a power calculation assuming use of a one-way ANOVA with a significance level of 0.05 and a power of 80%, including at least ten pairwise comparisons between groups, leading to an estimation of around $n = 7$ mice needed per group. To allow compensation for unforeseen circumstances and account for potential loss of mice during the study, we included 8 mice per genotype, per group.

Statistical Analysis

Analyses and visualization for the Olink data were performed with the R programming language (CRAN, RRID: SCR_003005, <https://www.r-project.org>) using the R packages “ggbiplot” (PCA) “mixOmics” (PLS-DA) and “ggplot2” (volcano plots). Details on statistical analyses can be found in figure legends. The number n represents either the number of animals used or in case of *in vitro* data the number of replications performed. Data are represented as means \pm SD or as indicated. Statistical analyses were performed using the unpaired Student's t-test, Mann-Whitney U test or two-way ANOVA followed by either Bonferroni's or Sidak's post hoc multiple comparisons test, if both genotype and treatment were found significant. A value of $p < 0.05$ was considered statistically significant. All data were visualized and analyzed using Prism version 5.0 or 8.0 (GraphPad Software, La Jolla, California, USA) or R Studio (PBC, Boston, MA <http://www.rstudio.com/>).

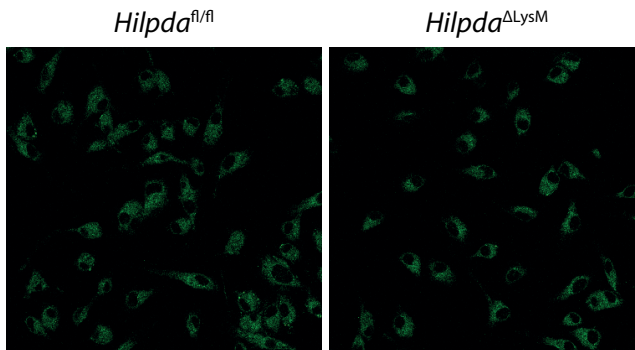
References

1. Gross DA, Silver DL. Cytosolic lipid droplets: From mechanisms of fat storage to disease. *Critical Reviews in Biochemistry and Molecular Biology*. 2014; 49(4): 304–26.
2. den Brok MH, Raaijmakers TK, Collado-Camps E, Adema GJ. Lipid Droplets as Immune Modulators in Myeloid Cells. *Trends in Immunology*. 2018; 39(5): 380–92.
3. Welte MA, Gould AP. Lipid droplet functions beyond energy storage. *Biochimica et Biophysica Acta - Molecular and Cell Biology of Lipids*. 2017; 1862(10): 1260–72.
4. Feingold KR, Shigenaga JK, Kazemi MR, McDonald CM, Patzek SM, Cross AS, et al. Mechanisms of triglyceride accumulation in activated macrophages. *Journal of Leukocyte Biology*. 2012; 92(4): 829–39.
5. Hsieh WY, Zhou QD, York AG, Williams KJ, Scumpia PO, Kronenberger EB, et al. Toll-Like Receptors Induce Signal-Specific Reprogramming of the Macrophage Lipidome. *Cell Metabolism*. 2020; 32(1): 128-143.e5.
6. Peán CB, Schiebler M, Tan SWS, Sharrock JA, Kierdorf K, Brown KP, et al. Regulation of phagocyte triglyceride by a STAT-ATG2 pathway controls mycobacterial infection. *Nature Communications*. 2017; 8, 14642.
7. Cocchiari JL, Kumar Y, Fischer ER, Hackstadt T, Valdivia RH. Cytoplasmic lipid droplets are translocated into the lumen of the Chlamydia trachomatis parasitophorous vacuole. *Proceedings of the National Academy of Sciences of the United States of America*. 2008; 105(27): 9379–84.
8. Bosch M, Sánchez-Álvarez M, Fajardo A, Kapetanovic R, Steiner B, Dutra F, et al. Mammalian lipid droplets are innate immune hubs integrating cell metabolism and host defense. *Science*. 2020; 370(6514):eaay8085.
9. Zimmermann R, Strauss JG, Haemmerle G, Schoiswohl G, Birner-Gruenberger R, Riederer M, et al. Fat mobilization in adipose tissue is promoted by adipose triglyceride lipase. *Science*. 2004; 306(5700): 1383–6.
10. Villena JA, Roy S, Sarkadi-Nagy E, Kim KH, Hei SS. Desnutrin, an adipocyte gene encoding a novel patatin domain-containing protein, is induced by fasting and glucocorticoids: Ectopic expression of desnutrin increases triglyceride hydrolysis. *Journal of Biological Chemistry*. 2004; 279(45): 47066–75.
11. Jenkins CM, Mancuso DJ, Yan W, Sims HF, Gibson B, Gross RW. Identification, cloning, expression, and purification of three novel human calcium-independent phospholipase A2 family members possessing triacylglycerol lipase and acylglycerol transacylase activities. *Journal of Biological Chemistry*. 2004; 279(47): 48968–75.
12. Aflaki E, Balenga NAB, Luschnig-Schratl P, Wolinski H, Povoden S, Chandak PG, et al. Impaired Rho GTPase activation abrogates cell polarization and migration in macrophages with defective lipolysis. *Cellular and Molecular Life Sciences*. 2011; 68(23): 3933–47.
13. Aflaki E, Radović B, Chandak PG, Kolb D, Eisenberg T, Ring J, et al. Triacylglycerol Accumulation Activates the Mitochondrial Apoptosis Pathway in Macrophages. *Journal of Biological Chemistry*. 2011; 286(9): 7418–28.
14. Mattijssen F, Georgiadi A, Andasarie T, Szalowska E, Zota A, Kronenberger A, et al. Hypoxia-inducible Lipid Droplet-associated (HILPDA) Is a Novel Peroxisome Proliferator-activated Receptor (PPAR) Target Involved in Hepatic Triglyceride Secretion. *Journal of Biological Chemistry*. 2014; 289(28): 19279–93.

15. Maier A, Wu H, Cordasic N, Oefner P, Dietel B, Thiele C, et al. Hypoxia-inducible protein 2 Hig2/Hilpda mediates neutral lipid accumulation in macrophages and contributes to atherosclerosis in apolipoprotein E-deficient mice. *The FASEB Journal*. 2017; : 4971–84.
16. van Dierendonck XAMH, de la Rosa Rodriguez MA, Georgiadi A, Mattijssen F, Dijk W, van Weeghel M, et al. HILPDA Uncouples Lipid Droplet Accumulation in Adipose Tissue Macrophages from Inflammation and Metabolic Dysregulation. *Cell Reports*. 2020; 30(6):1811-1822.
17. Padmanabha Das KM, Wechselberger L, Liziczai M, De la Rosa Rodriguez M, Grabner GF, Heier C, et al. Hypoxia-inducible lipid droplet-associated protein inhibits adipose triglyceride lipase. *Journal of lipid research*. 2018; 59(3): 531–41.
18. Kuhajda FP, Pizer ES, Nong Li J, Mani NS, Frehywot GL, Townsend CA. Synthesis and antitumor activity of an inhibitor of fatty acid synthase. *Proceedings of the National Academy of Sciences*. 2000; 97(7): 3450–4.
19. Mayer N, Schweiger M, Romauch M, Grabner GF, Eichmann TO, Fuchs E, et al. Development of small-molecule inhibitors targeting adipose triglyceride lipase. *Nature Chemical Biology*. 2013; 9(12): 785–7.
20. Chandak PG, Radović B, Aflaki E, Kolb D, Buchebner M, Fröhlich E, et al. Efficient Phagocytosis Requires Triacylglycerol Hydrolysis by Adipose Triglyceride Lipase. *Journal of Biological Chemistry*. 2010; 285(26): 20192–201.
21. Williams JA, Shacter E. Regulation of macrophage cytokine production by prostaglandin E₂. Distinct roles of cyclooxygenase-1 and -2. *Journal of Biological Chemistry*. 1997; 272(41): 25693–9.
22. Vats D, Mukundan L, Odegaard JI, Zhang L, Smith KL, Morel CR, et al. Oxidative metabolism and PGC-1 β attenuate macrophage-mediated inflammation. *Cell Metabolism*. 2006; 4(1): 13–24.
23. Rodríguez-Prados J-C, Través PG, Cuenca J, Rico D, Aragonés J, Martín-Sanz P, et al. Substrate Fate in Activated Macrophages: A Comparison between Innate, Classic, and Alternative Activation. *The Journal of Immunology*. 2010; 185(1): 605–14.
24. Castoldi A, Monteiro LB, van Teijlingen Bakker N, Sanin DE, Rana N, Corrado M, et al. Triacylglycerol synthesis enhances macrophage inflammatory function. *Nature Communications*. 2020; 11(1):4107.
25. Schlager S, Goeritzer M, Jandl K, Frei R, Vujic N, Kolb D, et al. Adipose triglyceride lipase acts on neutrophil lipid droplets to regulate substrate availability for lipid mediator synthesis. *Journal of Leukocyte Biology*. 2015; 98(5): 837–50.
26. Dichlberger A, Schlager S, Maaninka K, Schneider WJ, Kovanen PT. Adipose triglyceride lipase regulates eicosanoid production in activated human mast cells. *Journal of Lipid Research*. 2014; 55(12): 2471–8.
27. Pacheco P, Bozza FA, Gomes RN, Bozza M, Weller PF, Castro-Faria-Neto HC, et al. Lipopolysaccharide-Induced Leukocyte Lipid Body Formation In Vivo: Innate Immunity Elicited Intracellular Loci Involved in Eicosanoid Metabolism. *The Journal of Immunology*. 2002; 169(11): 6498–506.
28. Leslie CC. Cytosolic phospholipase A2: Physiological function and role in disease. *Journal of Lipid Research*. 2015; 56(8): 1386–402.
29. Jarc E, Petan T. A twist of FATE: Lipid droplets and inflammatory lipid mediators. *Biochimie*. 2020; 169: 69–87.
30. Williams JA, Pontzer CH, Shacter E. Regulation of macrophage interleukin-6 (IL-6) and IL-10 expression by prostaglandin E₂: The role of p38 mitogen-activated protein kinase. *Journal of Interferon and Cytokine Research*. 2000; 20(3): 291–8.

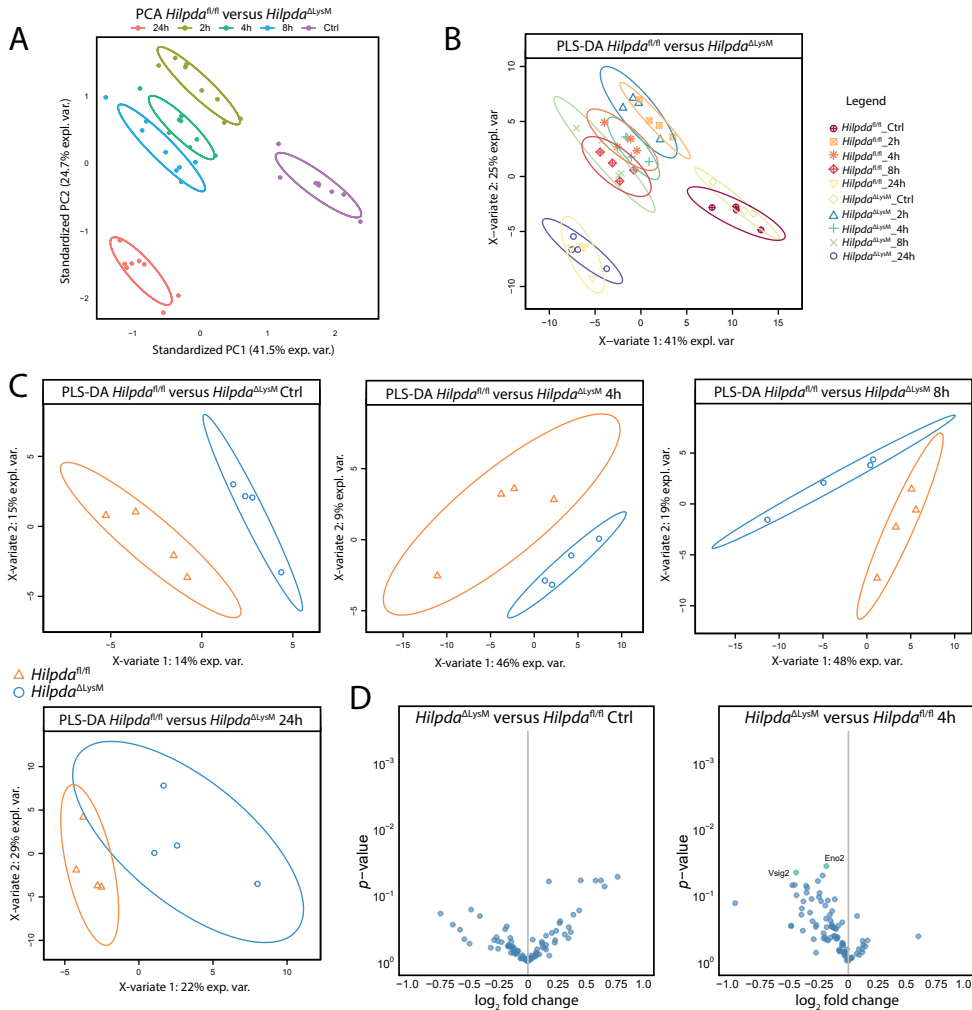
31. MacKenzie KF, Clark K, Naqvi S, McGuire VA, Nöehren G, Kristariyanto Y, et al. PGE2 Induces Macrophage IL-10 Production and a Regulatory-like Phenotype via a Protein Kinase A–SIK–CRTC3 Pathway. *The Journal of Immunology*. 2013; 190(2): 565–77.
32. Hinson RM, Williams JA, Shacter E. Elevated interleukin 6 is induced by prostaglandin E2 in a murine model of inflammation: Possible role of cyclooxygenase-2. *Proceedings of the National Academy of Sciences of the United States of America*. 1996; 93(10): 4885–90.
33. Kim SH, Serezani CH, Okunishi K, Zaslona Z, Aronoff DM, Peters-Golden M. Distinct protein kinase A anchoring proteins direct prostaglandin E 2 modulation of toll-like receptor signaling in alveolar macrophages. *Journal of Biological Chemistry*. 2011; 286(11): 8875–83.
34. Goeritzer M, Schlager S, Radovic B, Madreiter CT, Rainer S, Thomas G, et al. Deletion of CGI-58 or adipose triglyceride lipase differently affects macrophage function and atherosclerosis. *Journal of lipid research*. 2014; 55(12): 2562–75.
35. van Genderen H, Kenis H, Lux P, Ungeth L, Maassen C, Deckers N, et al. In vitro measurement of cell death with the annexin A5 affinity assay. *Nature Protocols*. 2006; 1, 363–367.
36. Carpenter AE, Jones TR, Lamprecht MR, Clarke C, Kang IH, Friman O, et al. CellProfiler: Image analysis software for identifying and quantifying cell phenotypes. *Genome Biology*. 2006; 7(10):R100.

Supplemental material



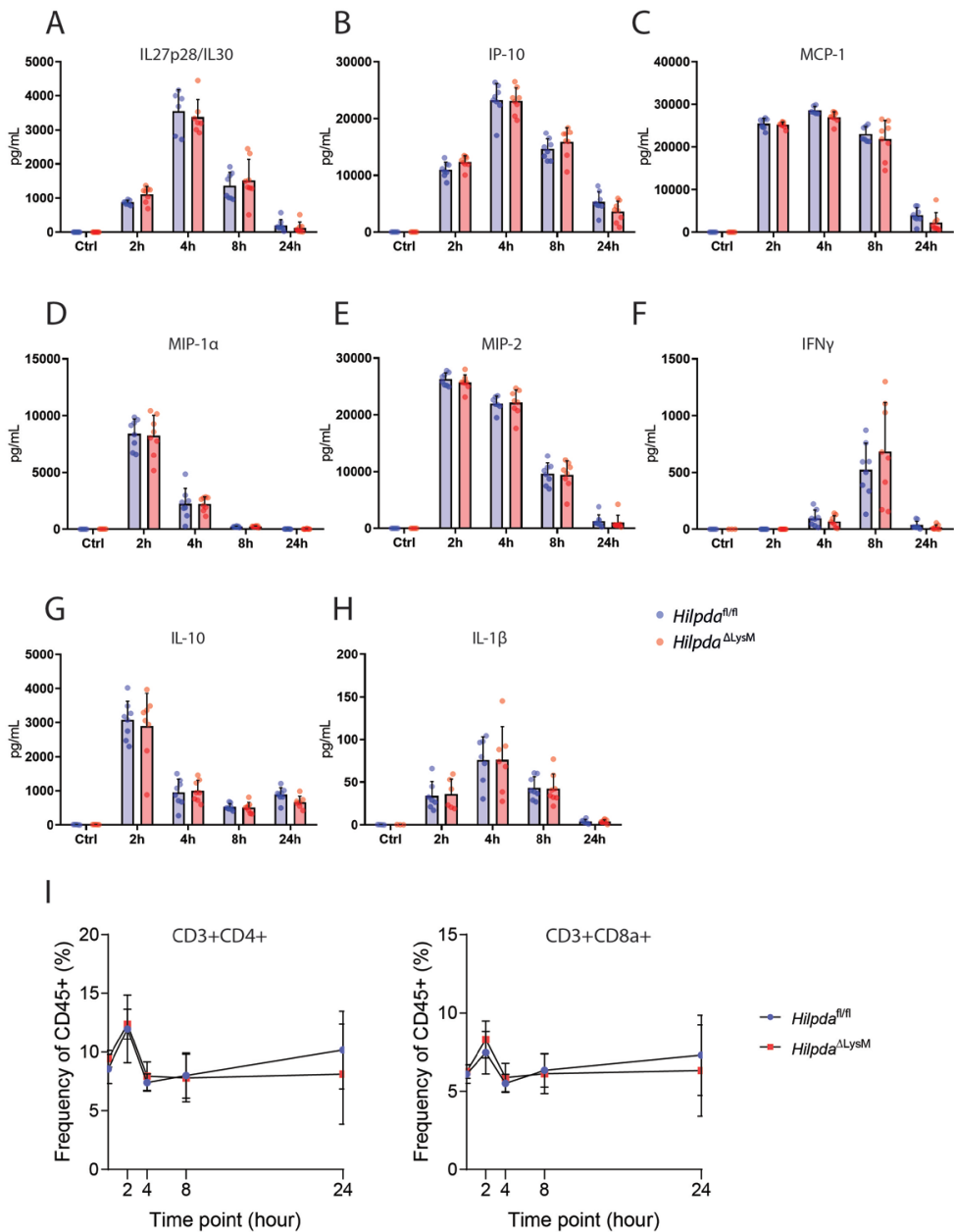
Supplemental Figure 1, corresponds to Figure 2.

BODIPY staining of *Hilpda*^{fl/fl} (A) and *Hilpda*^{ΔLysM} (B) BMDMs treated with vehicle for 24 h.



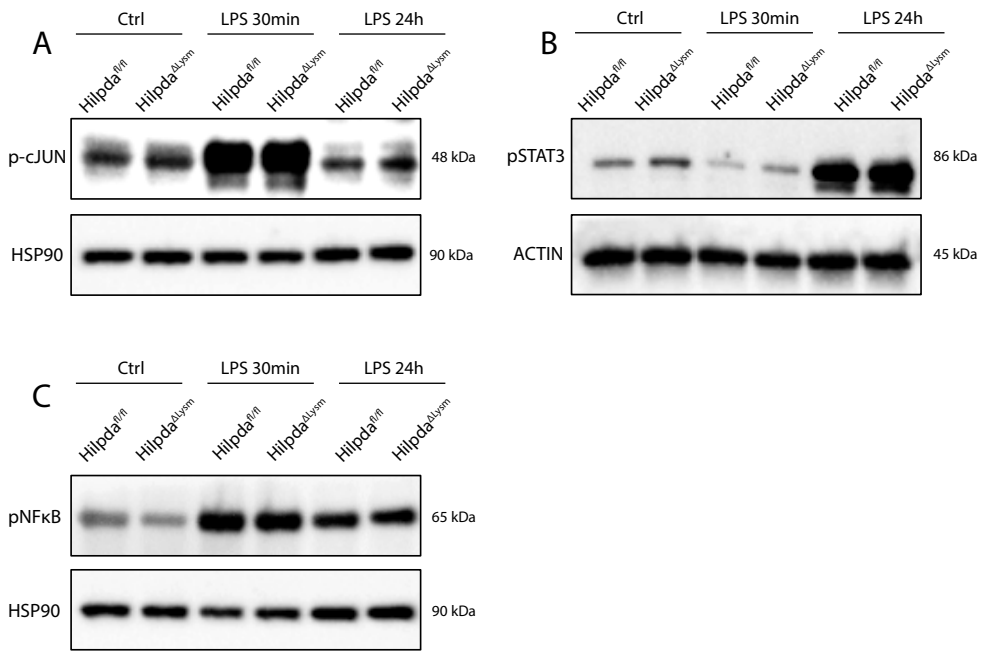
Supplemental Figure 2, corresponds to Figure 3.

(A) PCA of targeted plasma proteomic profiles (Olink) in *Hilpda*^{ΔLysM} and *Hilpda*^{fl/fl} mice (grouped per time point) 2, 4, 8 or 24 h after intraperitoneal injection of LPS or 24 h after intraperitoneal injection of saline (Ctrl). (B) PLS-DA of targeted plasma proteomic profiles in *Hilpda*^{ΔLysM} and *Hilpda*^{fl/fl} mice 2, 4, 8 or 24 h after intraperitoneal injection of LPS or 24 h after intraperitoneal injection of saline (Ctrl). (C) PLS-DA of targeted plasma proteomic profiles in *Hilpda*^{ΔLysM} and *Hilpda*^{fl/fl} mice 4, 8 or 24 h after intraperitoneal injection of LPS or 24 h after intraperitoneal injection of saline (Ctrl), separated for time point. (D) Relative fold change and uncorrected *p*-values in plasma proteomic profiles in *Hilpda*^{ΔLysM} and *Hilpda*^{fl/fl} mice 4 h after intraperitoneal injection of LPS, or 24 h after intraperitoneal injection of saline (Ctrl). Ctrl: control; PCA: principal component analysis; PLS-DA: partial least-squares discriminant analysis.



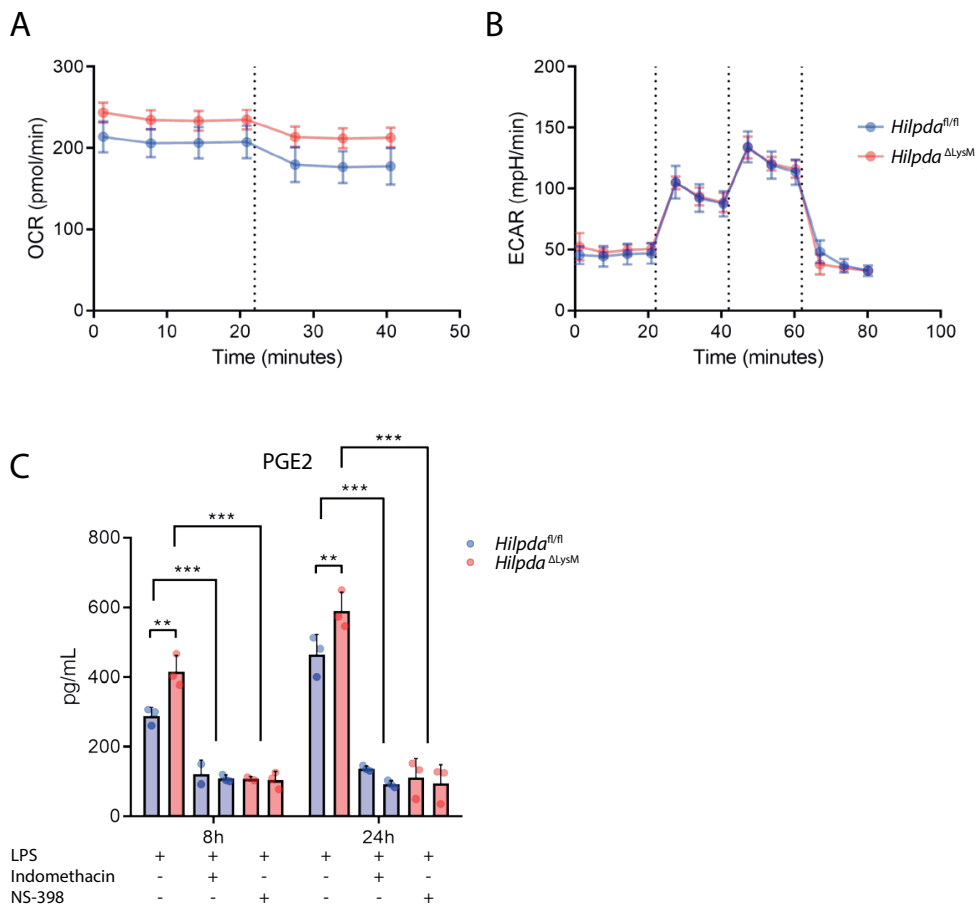
Supplemental Figure 3, corresponds to Figure 4.

(A - H) Plasma concentration of IL27p28/IL30, IP-10, MCP-1, MIP-1 α , MIP-2, IFN γ , IL-10 and IL-1 β in *Hilpda*^{ALysM} and *Hilpda*^{fl/fl} mice 2, 4, 8 or 24 h after intraperitoneal injection of LPS or 24 h after intraperitoneal injection of saline (Ctrl). (I) Relative circulating T cell subpopulations in *Hilpda*^{ALysM} and *Hilpda*^{fl/fl} mice 2, 4, 8 or 24 h after intraperitoneal injection of LPS or 24 h after intraperitoneal injection of saline (baseline). Bar graphs are represented as mean \pm SD. Ctrl: control.



Supplemental Figure 4.

Protein expression of (A) p-cJUN, (B) p-STAT3 and (C) p-NFκB in *Hilpda^{ΔLysM}* and *Hilpda^{fl/fl}* BMDMs after treatment with vehicle (Ctrl) or LPS for 30 min or 24 h. HSP90 and ACTIN are used as loading controls. Ctrl: control; LPS: lipopolysaccharide.



Supplemental Figure 5.

(A) Oxygen consumption rate of *Hilpda*^{ΔLysM} and *Hilpda*^{fl/fl} BMDMs after treatment with LPS for 24 h, measured by extracellular flux analysis. Injection of etomoxir is indicated with dotted line. (B) Extracellular acidification rate of *Hilpda*^{ΔLysM} and *Hilpda*^{fl/fl} BMDMs after treatment with LPS for 24 h, measured by extracellular flux analysis. Injection of glucose, oligomycin and 2-deoxyglucose are indicated with dotted lines. (C) Concentration of PGE2 derived from *Hilpda*^{ΔLysM} and *Hilpda*^{fl/fl} BMDMs after treatment with LPS and indomethacin or NS-398 for 8 or 24 h. Bar graphs are represented as mean ± SD. OCR: oxygen consumption rate; ECAR: extracellular acidification rate; LPS: lipopolysaccharide; PGE2: prostaglandin-E2. ** $p < 0.01$, *** $p < 0.001$



General summary

Xanthe A.M.H. van Dierendonck

The prevalence of obesity has tripled since 1975 and is projected to exponentially increase in the coming years. In 2016, already 39% of adults worldwide were overweight, with 13% of them being obese. Obesity increases the risk of diabetes mellitus and various other complications, which may be partly driven by aberrations in innate immune cell functioning. Intracellular metabolism can be an important driver of functional properties in innate immune cells. By driving immune cell dysfunction, it may also contribute to disease progression during obesity and diabetes mellitus. For the development of diabetes mellitus and the progression of its long-term complications, dysfunctional innate immune cells form a common denominator. In this thesis, we aimed to explore the role of immunometabolism in monocytes and macrophages in the development of diabetes mellitus and associated complications. Furthermore, we investigated whether immunometabolism could be targeted in these cells to avert disease development or progression.

Increased aerobic glycolysis is a metabolic hallmark of immune cell activation. To understand the close interplay between glycolytic metabolism and functional output in humans, we define the contribution of aerobic glycolysis to the production of cytokines in **chapter 2**. Our results demonstrate that although different PAMPs lead to robust upregulation of cytokine and lactate production, the strength of the association between these two parameters can differ. Additionally, the production of specific cytokines is differentially associated with the upregulation of aerobic glycolysis, with stronger associations for IL-10 and IL-1RA. Inter-individual variations in lactate production revealed groups with different glycolytic flexibility, linked to the magnitude of cytokine responses. In patients with T1DM, associations between lactate and cytokine production were generally similar, although slightly attenuated, compared with healthy subjects. Overall, intra-individual differences in immune cell responses could be driven by differences in aerobic glycolysis, although specific TLRs and cytokines differentially rely on the use of aerobic glycolysis.

Many diabetes-related complications, including increased susceptibility to infections and increased cardiovascular risk, suggest an inadequate functioning of innate immune cells. Several studies have indeed demonstrated innate immune dysfunction in diabetes mellitus. However, a link to metabolic rewiring of immune cells in the diabetic microenvironment driving these functional alterations was lacking. In **chapter 3**, we examined diabetes-dependent alterations in monocyte function and metabolism. We revealed that a high glycemic burden, reflected by high HbA_{1c} levels, was coupled to reduced cytokine secretion in stimulated monocytes from patients with T1DM. Interestingly, decreased cytokine secretion was associated with increased relative glycolytic rates. High HbA_{1c} levels

were subsequently linked to a pro-inflammatory transcriptional signature in circulating monocytes. This observation suggests the existence of immune tolerance in monocytes from patients with a high glycemic burden, where chronic inflammatory activation of circulating monocytes may lead to immune dysfunction upon acute activation. Together, these findings could partly explain the increased risk of infections and cardiovascular disease in patients with diabetes mellitus.

Besides driving diabetes-related complications, aberrations in innate immune responses can also contribute to the development of diabetes mellitus itself. Obesity-driven inflammation of adipose tissue can promote peripheral and systemic resistance to insulin, advancing the development of T2DM. In **chapter 4**, we set out to elucidate the role of UCP2 in adipose tissue macrophages in the context of adipose tissue inflammation. We confirmed the importance of UCP2 in regulating both the inflammatory response and metabolism in LPS-activated macrophages. Deletion of UCP2 resulted in a generally attenuated pro-inflammatory response to LPS, whereas glycolytic and oxidative metabolism were upregulated. However, the metabolic differences were normalized in a lipid-rich environment, potentially representative for the adipose tissue. These findings suggest that UCP2 is not a crucial component in controlling macrophage metabolism in a lipid-rich environment. Hence, in the context of obesity, deletion of UCP2 did not affect the development of adipose tissue inflammation or insulin resistance.

Metabolic activation of ATMs in obese adipose tissue leads to a unique rewiring of lipid metabolism, allowing macrophages to cope with a lipid-enriched environment. Eventually, macrophages residing in obese adipose tissue develop into foam cells characterized by excessive lipid droplet formation. To determine whether lipid accumulation itself contributes to ATM dysfunction and the development of adipose tissue inflammation or insulin resistance, we studied the function of lipid droplet-related protein HILPDA in macrophages in **chapter 5**. We found HILPDA expression to be strongly upregulated in obese adipose tissue, where it colocalized with crown-like structures. Fatty acids and triglycerides induced HILPDA expression, and specific myeloid deletion of HILPDA led to the abolishment of lipid droplet accumulation in macrophages after lipid loading. From a mechanistic perspective, our data revealed that HILPDA is a direct inhibitor of ATGL, and lack of lipid accumulation after HILPDA deletion was caused by enhanced ATGL-mediated lipolysis. The decreased accumulation of lipid droplets after HILPDA deletion was confirmed in adipose tissue macrophages isolated from obese adipose tissue. However, decreased lipid droplet accumulation did not lead to altered secretion of cytokines from ATMs, nor did it affect the development of adipose tissue inflammation and insulin resistance. Based on these data, we show that excessive lipid droplet accumulation in ATMs is not the sole

driver of adipose tissue inflammation.

Besides the lipid-rich environment of the obese adipose tissue, the accumulation of triglycerides in lipid droplets also characterizes the metabolic response of macrophages toward classical inflammatory stimuli. In **chapter 6**, we studied triglyceride accumulation in pro-inflammatory macrophages and the involvement of HILPDA and ATGL in this process. The expression of HILPDA in response to inflammatory TLR ligands corresponded with the visual accumulation of lipid droplets, especially after treatment with LPS. Decreased expression of ATGL was found to be an important contributor to lipid droplet accumulation after the inflammatory activation of macrophages. Our data revealed that HILPDA is directly involved in enhancing the proteasomal degradation of ATGL. Specific deletion of HILPDA in macrophages emphasized their inflammatory phenotype in response to LPS, characterized by increased production of PGE₂ and IL-6 both *ex vivo* and *in vitro*. Together, our findings suggest that ATGL-mediated lipolysis is partly responsible for the production of PGE₂, which can, in turn, enhance the production of IL-6 and regulate the inflammatory response in macrophages.



General discussion

Xanthe A.M.H. van Dierendonck

Innate immune cells play important roles in supporting whole-body (systemic) metabolism and healthy tissue homeostasis. However, in the context of obesity and diabetes mellitus, innate immune cell dysfunction may contribute to a state of chronic inflammation. In this thesis, we have focused on intracellular metabolism as a potential key determinant of the innate immune response. We studied the role of metabolic changes in monocytes and macrophages and their contribution to the aggravation of obesity and diabetes mellitus (**Figure 1**), focusing on two aspects: the development of diabetes and the progression of diabetes-related complications.

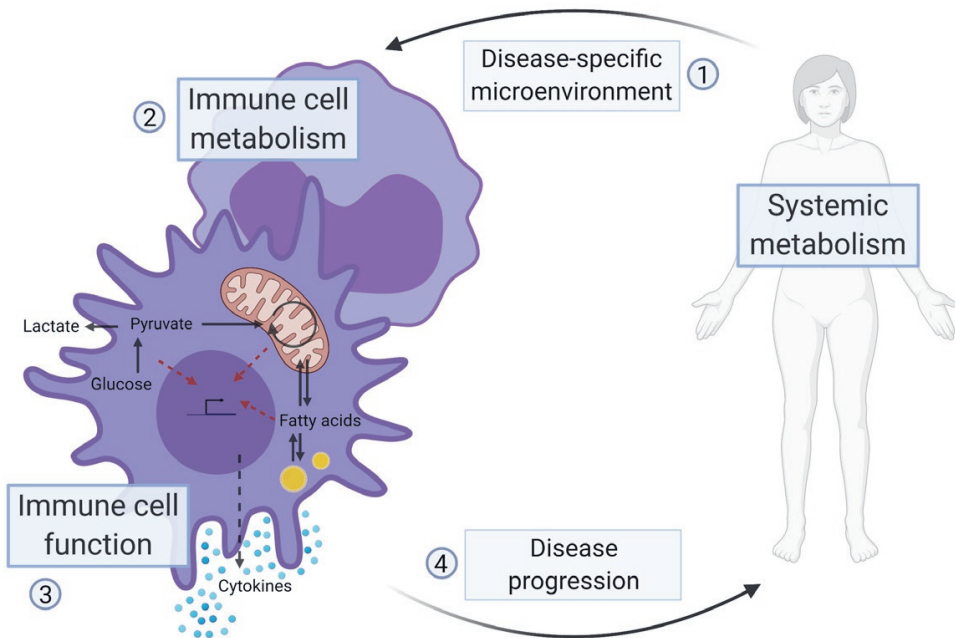


Figure 1. The vicious cycle between systemic metabolism, immune cell metabolism and immune cell functioning.

During obesity or diabetes mellitus, loss of equilibrium in systemic metabolic processes leads to changes in signals and cues in the disease-specific microenvironment (1). These cues may induce disease-specific rewiring of immune cell metabolism (2), possibly contributing to immune dysfunction (3), which can subsequently advance the development of diabetes mellitus or promote the progression of diabetes-related complications (4).

Regarding the first aspect, we focused on the role of innate immune cell metabolism in obesity-driven diabetes development. Specific cues in the obese adipose tissue microenvironment (**Figure 1**, part 1) promote unique metabolic rewiring of adipose tissue macrophages (**Figure 1**, part 2), affecting their function (**Figure 1**, part 3). Subsequent dysfunction may contribute to derailment of the inflammatory response in obese adipose tissue and further advancement of insulin resistance (**Figure 1**, part 4). In this

context, we determined that metabolic regulators such as UCP2 and HILPDA play a role in linking macrophage metabolism to the inflammatory response (**chapter 4, 5 and 6**) and investigated whether targeting these regulators affects the development of obesity-induced adipose tissue inflammation and insulin resistance (**chapter 4 and 5**).

In the second aspect, we explored the role of innate immune cell metabolism and dysfunctional immune responses in driving diabetes-associated complications. Diabetes mellitus is characterized by hyperglycemia, which shapes the disease-specific microenvironment for circulating monocytes (**Figure 1**, part 1). The hyperglycemic microenvironment could affect their metabolism (**Figure 1**, part 2) and may modify their function (**Figure 1**, part 3). Eventually, the altered function of monocytes could contribute to the progression of diabetes-associated complications (**Figure 1**, part 4). Our results support the strong association between aerobic glycolysis and cytokine production in human immune cells (**chapter 2**). However, in patients with diabetes mellitus, a high glycemic burden leads to increased aerobic glycolysis and a basal inflammatory profile in monocytes, coupled to a decreased secretion of cytokines after acute stimulation. These alterations potentially contribute to the development of complications such as increased cardiovascular risk and increased susceptibility to infections (**chapter 3**).

In this chapter, we will discuss and integrate our findings involving monocyte and macrophage immunometabolism in the context of diabetes development and the progression of diabetes-related complications. Although multiple metabolic pathways play a role in both aspects, we will primarily focus on the role of lipid and glucose metabolism in monocytes and macrophages, as these are two important pathways expected to contribute to immune dysfunction during obesity and diabetes mellitus. We will end by highlighting future perspectives and considerations to investigate disease-specific immunometabolic targets that may ultimately be used in therapeutic strategies.

The role of immune cell metabolism in driving immune cell function during health and obesity-induced development of diabetes mellitus

In monocytes and macrophages, different functional phenotypes are associated with the activation of specific metabolic pathways [1,2]. The metabolism of lipid and glucose are two important pathways involved in functional reprogramming of immune cells in the context of obesity and diabetes [3]. Here, we will specifically highlight the role of lipid metabolism. First, we will focus on fatty acid (FA) and triglyceride (TG) synthesis and accumulation in the context of classical inflammation. Subsequently, we will discuss lipid metabolism and accumulation in the context of obesity-driven development of insulin resistance and diabetes mellitus.

Fatty acid synthesis in inflammatory immune cell phenotypes

Both the oxidation and the synthesis of fatty acids are of importance for the adequate functioning of innate immune cells. The oxidation of fatty acids, primarily important for the generation of ATP, is a characteristic that is often associated with anti-inflammatory activation of immune cells [4]. However, whether it is an indispensable trait for the polarization of anti-inflammatory macrophages is under discussion [5,6]. In contrast, the synthesis of fatty acids is thought to be indispensable for pro-inflammatory activation of macrophages. Fatty acid synthase (FAS) is a lipogenic enzyme that can play a crucial role in activating the NLRP3 inflammasome [7] and may support the conduction of signals through TLRs and MYD88. FAS is thought to be involved in regulating inflammation directly through the synthesis of FAs, which is likely essential to support palmitoylation of inflammatory regulators [8], or independent of full FA synthesis through the action of its intermediates [9]. UCP2 was found to be a crucial regulator of FAS-dependent activation of the NLRP3 inflammasome [7], which may explain the attenuated inflammatory phenotype of UCP2-deficient macrophages after stimulation with LPS (**chapter 4**). Although the involvement of FAS in the inflammatory response seems firmly established, the carbon source for de novo lipogenesis is still under debate, as direct incorporation of glucose-derived carbons into fatty acid synthesis is questioned, at least after treatment with IFN γ [10].

Triglyceride synthesis and accumulation in inflammatory phenotypes

In addition to increased synthesis of FAs, decreased FA oxidation and decreased ATGL-mediated lipolysis also contribute to the synthesis and accumulation of TGs in pro-inflammatory macrophages (**chapter 6**) [11–13]. Independent of FA synthesis, the synthesis of TGs was also found to be important for pro-inflammatory signalling in macrophages [14]. Furthermore, changes in the intracellular composition of lipids can modulate immune responses in innate immune cells, for example by affecting membrane composition [15]. The lipidome of immune cells can be altered through specific activation by different pathogen-associated molecular patterns (PAMPs) [16,17]. Additionally, the regulation of TG accumulation in lipid droplets (LDs) can determine the magnitude of the inflammatory response in macrophages (chapter 6). The importance of TG accumulation in inflammatory signalling seems substantially contingent on providing intracellular lipid pools that deliver precursors for inflammatory mediators, such as prostaglandins and leukotrienes. This theory would explain why the inhibition of TG synthesis [14] or ATGL-mediated lipolysis (**chapter 6**) [18,19] attenuates the pro-inflammatory response in activated immune cells. Accordingly, overactivation of ATGL increases the liberation of fatty acids that could serve as precursors, apparently leading to an increased release of

inflammatory intermediates and cytokines after activation (**chapter 6**).

Whereas accumulation of TGs in LDs seems to regulate the inflammatory response in macrophages, the overall role of LDs in the inflammatory response appears to be much more than being an intracellular energy storage or providing a pool of precursors for inflammatory mediators. Next to LD-related proteins that are indirectly involved in immune regulation, including ATGL and HILPDA, the LD monolayer may also accumulate proteins directly involved in the immune response, such as anti-microbial peptides [20]. Since it is unknown whether this recruitment is intact when LDs are not visible replete with TGs due to increased TG breakdown (**chapter 6**), it would be interesting to investigate whether these pathways are functional when TG accumulation in LDs is prevented, for instance by deletion of DGAT1. Furthermore, similar to the direct regulatory roles described to TCA-cycle intermediates, lipid intermediates that are synthesized within the synthesis pathways of FAs, cholesterol, and TGs may reveal interesting regulatory roles in inflammatory activation, as has already been suggested for acetoacetyl-CoA [9] and mevalonate [21]. Altogether, these findings demonstrate that LDs are important in the regulation of the inflammatory response and could provide interesting therapeutic immunometabolic targets to modulate inflammatory responses.

Lipid metabolism as driver of macrophage dysfunction

In healthy adipose tissue, macrophages generally show anti-inflammatory phenotypes and play a role in supporting cell turnover and tissue homeostasis [22,23]. In obese adipose tissue, adipose tissue macrophages (ATMs) start to accumulate around dead adipocytes and undergo metabolic activation, resulting in a unique inflammatory phenotype [24–26]. Metabolic activation is characterized by increased lipid metabolism and lysosomal biogenesis [27,28], but ATMs also display excess accumulation of lipids [29,30]. In healthy adipose tissue, ATMs may start to buffer lipids in situations where adipocyte lipolysis is upregulated, thereby supporting a gradual release of lipids into the circulation [31,32]. In these situations, including weight loss or fasting, lipid accumulation in ATMs is not coupled to the development of a pro-inflammatory phenotype [31,33,34]. However, in the obese adipose tissue microenvironment, excessive buffering of lipids by ATMs and subsequent development into foam cells has been suggested to overwhelm ATM metabolism [35]. Hence, although lipid accumulation does not lead to macrophage dysfunction by definition, excessive lipid accumulation in ATMs in the obese microenvironment could precede dysfunction. The disproportionate influx of lipids may lead to an exorbitant skewing of ATM metabolism toward lipid processing. Due to the close association of metabolism and function, this type of enforced metabolic skewing could contribute to macrophage dysfunction and may eventually drive adipose tissue inflammation [30,36,37].

Lipid uptake and accumulation in macrophages in the development of adipose tissue inflammation

Following the theory of metabolic skewing by lipid accumulation in ATMs, it could be hypothesized that prevention of excess lipid accumulation could improve ATM functioning. In turn, improvement of ATM functioning would eventually result in the attenuation of adipose tissue inflammation and insulin resistance. However, preventing lipid uptake in ATMs during obesity did not seem to attenuate adipose tissue inflammation and insulin resistance, but even exacerbated glucose intolerance in obese mice [38]. This finding underlines the importance of lipid buffering by ATMs in obese adipose tissue, similar to situations of increased lipolysis or lipid spillover in healthy adipose tissue [31,32]. We have shown that physical accumulation of lipids was not the sole driver of ATM dysfunction, since increased ATGL-mediated breakdown of accumulated lipids did not improve ATM phenotype or attenuate adipose tissue inflammation (**chapter 5**). On the contrary, increasing the storage of TGs in ATMs, for instance through enhancement of DGAT1 expression, was even suggested to slightly improve insulin sensitivity in obese mice [39]. Additionally, *Pten*^{Δmyel} ATM subsets that were generally characterized by increased lipid uptake and catabolism, generated through sustaining the macrophage-intrinsic PI3K signalling pathway, were found to promote metabolic health in obese mice [40]. Together, these findings suggest that neither lipid uptake nor lipid accumulation per se seems to lie at the basis of ATM dysfunction, adipose tissue inflammation or insulin resistance in obese adipose tissue. Moreover, enhancing both lipid uptake and increasing lipid catabolism may provide a strategy to reinforce ATM functioning and thereby support metabolic health in the adipose tissue [40].

In classical inflammation, intracellular storage of TGs was found to be important for regulating the release of lipid-related inflammatory mediators [14], including prostaglandins, which can be enhanced by increased lipolysis (**chapter 6**). Following these results, it could be hypothesized that inducing lipolysis in lipid-laden ATMs would lead to enhanced inflammatory signalling by increasing the release of inflammatory mediators. In practice, this process may prove to be less straightforward compared with classical inflammation. This may also be due to the dual nature of prostaglandins, which can exert either pro- or anti-inflammatory signalling depending on the context. On the one hand, PGE2 has been suggested to promote anti-inflammatory phenotypes in ATMs [41], whereas on the other hand, inhibition of PGE2 production by adipocytes was found to potentially be protective against macrophage-mediated adipose tissue inflammation during obesity [42]. Therefore, it could be interesting to investigate whether activation of ATGL would lead to increased formation of inflammatory lipid mediators, including PGE2,

in metabolically activated ATMs and their role in driving adipose tissue inflammation.

Lipid-related signalling in adipose tissue inflammation

Although physical lipid accumulation in ATMs may not be the major cause for adipose tissue inflammation, the excessive flux of lipids from the obese microenvironment and the inability of ATMs to cope with it likely still contributes to ATM dysfunction [40]. The release of FAs or lipid-filled exosomes by adipocytes exponentially increases in obese adipose tissue, and these may promote the development of insulin resistance through the induction of ATM accumulation and activation [31,43,44]. Even when internalization is left out of the equation, the increased presence of saturated FAs in obese adipose tissue still provokes inflammatory signalling in ATMs and may contribute to insulin resistance [45,46]. This process could be partly mediated through TLR-4 [47,48], although saturated FAs likely do not directly bind to TLR-4 [49]. Through TLR-4 signalling, saturated FAs may activate the NLRP3 inflammasome, NFκB or JNK signalling pathways, which contribute to the induction of insulin resistance [45,50–53]. Interestingly, macrophage-specific deletion of TLR-4 was observed to increase circulating inflammatory markers after high-fat diet feeding in mice and thereby did not alleviate the development of insulin resistance [54], suggesting that these inflammatory processes are not solely driven through TLR-4 signalling. Thus, affecting downstream inflammatory signalling cues mediated by external lipid influx may be a better approach, for instance by preventing the conversion of saturated FAs into phosphatidylcholine [50,52]. Thereby, fatty acid-induced activation of the NLRP3, NFκB or JNK-mediated pathways could be specifically targeted to attenuate obesity-induced insulin resistance and diabetes development [45,51,53].

The NLRP3 inflammasome seems to be a notorious and central player in adipose tissue inflammation in the context of diabetes mellitus [55]. Monocyte-derived macrophages from patients with type-2 diabetes mellitus (T2DM) show an upregulated activation of the NLRP3 inflammasome [56]. In turn, the increased inflammasome activation may directly interfere with insulin signalling [53]. UCP2 was suggested to be involved in activating the NLRP3 inflammasome through its ability to regulate FAS [7]. Moreover, FAS-mediated production of endogenous lipids is likely crucial for maintaining the plasma membrane, and myeloid deletion of FAS led to improved diet-induced glucose intolerance and insulin resistance [57]. Based on these findings, it could be expected that deletion of UCP2 would decrease adipose tissue inflammation, which was not observed (**chapter 4**). Possibly, the induction of NLRP3 by saturated FAs during obesity overrides its association with FAS-related signalling, decreasing the effect of myeloid UCP2 deletion in the obese adipose tissue microenvironment. Confirming this hypothesis, lipid loading indeed abolished the observed metabolic differences in macrophages with *Ucp2*-deletion (**chapter 4**).

Additionally, the improvement of glucose tolerance by myeloid deletion of FAS was mainly mediated by reducing ATM recruitment toward the obese adipose tissue [57], which likely cannot be modelled by deletion of UCP2. Therefore, despite the effect of UCP2 in the context of classical inflammation, it does not appear to be an effective target to improve macrophage functioning in the context of adipose tissue inflammation.

Concluding remarks

During metabolic activation of ATMs in obese adipose tissue, excessive lipid flux may not just induce subtle metabolic adjustments, but even drive extensive skewing of metabolism, contributing to ATM dysfunction. Targeting the influx or accumulation of lipids does not solve this metabolic inflexibility and is thus insufficient to attenuate adipose tissue inflammation. In combination with the heterogeneous macrophage phenotypes that can be found in the obese microenvironment [22], it could be difficult to find a single metabolic target that can be used to regulate inflammation in ATMs, to eventually decrease adipose tissue inflammation and slow down the development of insulin resistance. Instead, recent approaches focused on promoting lipid uptake and catabolism in ATMs, thereby supporting metabolic flexibility, might provide more successful strategies [40]. Furthermore, an important role could be reserved for using high-resolution methods, including single-cell techniques, to find approaches specific for distinct ATM subsets [58].

The role of immune cell metabolism in driving immune cell function during health and diabetes-related complications

Aerobic glycolysis as an inducer of inflammatory phenotypes

In innate immune cells, the upregulation of glucose metabolism in the form of aerobic glycolysis is seen as a robust hallmark of metabolic rewiring following TLR-mediated activation [59,60]. Limitation of the glycolytic pathway leads to suppression of the inflammatory response, including a dampening of the production of inflammatory cytokines [61–67]. Alterations in this metabolic route thereby robustly affect the effectiveness of innate immune cells to orchestrate an appropriate inflammatory response. Here, the focus will first be on the association between glycolysis and the immune response in the context of classical inflammation. Subsequently, glycolytic changes in monocytes in the diabetic microenvironment will be discussed in the context of diabetes-related complications.

Glycolysis and cytokine production in classical inflammation

The investigation of immune responses in response to different TLR agonists reveals large inter-individual variations in cytokine production [68–71]. Similarly, the upregulation of

glycolytic metabolism may be subject to inter-individual variations, reflecting a healthy range of glycolytic flexibility in immune cells (**chapter 2**). Underlining the strong link between glycolytic metabolism and the cytokine response, the release of cytokines can effectively be inhibited by limiting glycolysis, for instance by using the glycolytic inhibitor 2-deoxyglucose (2-DG) [72]. Interestingly, some cytokines, including TNF α , seem to be less affected by the inhibition of glycolysis. In contrast, other cytokines, such as IL-1 β , play key roles in the interplay between glycolytic metabolism and inflammatory activation [72–74]. Next to the production of IL-1 β , glycolysis also seems to be crucial for the regulation of IL-10. However, whereas IL-1 β could further increase glycolysis after inflammatory activation [75], IL-10 was observed to inhibit glycolysis [59,76]. Our work in **chapter 2** has confirmed this apparent cytokine-related specificity, where we observed specificity in the strength of the association between cytokine and lactate production. Differences in the direct interaction of glycolysis-associated transcription factors with the production of cytokines [73] or positive feedback mechanisms between cytokines and aerobic glycolysis [75] could partly drive this specificity. Additionally, the findings in **chapter 2** suggest that certain TLR-signalling pathways are more dependent on aerobic glycolysis than others, leading to different patterns in cytokine production. Differences in the kinetics and timing of cytokines could also play an important part in their associations with aerobic glycolysis. For instance, IL-1 β is often produced in low concentrations, which nevertheless conduct large effects. In contrast, IL-1RA, which has antagonistic properties to IL-1 signalling, is produced in much higher concentrations, as a high molar ratio is needed to inhibit IL-1 bioactivity [77]. Therefore, although IL-1RA itself does not convey pro-inflammatory signalling, it may serve as a more accessible surrogate marker for the biological effect of IL-1 β .

Metabolic flexibility and the inflammatory response

Whereas inhibition of aerobic glycolysis in the context of inflammatory activation consistently seems to be associated with an attenuated inflammatory phenotype [60–66], less evidence exists for the opposite process. In that case, an increase in aerobic glycolysis would directly lead to elevated inflammatory activation. The induction of glucose metabolism by overexpression of glucose transporter-1 (GLUT-1), the main glucose transporter in myeloid cells, increased pro-inflammatory signalling in murine macrophages *in vitro* [62]. However, this association does not always seem to be evident, as these results were not replicable *in vivo* [78]. This association is also lacking in UCP2-deficient macrophages, where a clear induction of glycolysis can be observed after inflammatory activation [79,80], which is coupled to decreased production of TNF α and IL-6 and increased production of IL-10 (**chapter 4**). Based on these observations, deletion

of UCP2 may lead to enforced restriction of metabolic flexibility in macrophages, which could lead to a disconnection between glycolytic metabolism and the inflammatory response.

Glycolytic skewing as driver of monocyte dysfunction in diabetes

The apparent possibility to uncouple glycolytic metabolism from the inflammatory response during enforced metabolic inflexibility is an interesting phenomenon that could provide new insights in the context of diabetes mellitus. Chronic hyperglycemia is an important characteristic of diabetes mellitus [81] and results in the exposure of circulating immune cells to increased concentrations of glucose. Increased glucose availability in the context of diabetes mellitus consistently associates with an inflammatory activation of monocytes [56,82–86]. Whether this is directly connected to glucose metabolism in monocytes is unclear, although monocytes from patients with type 1 diabetes mellitus (T1DM) with high HbA_{1c} levels did display higher baseline and maximal glycolytic capacity than patients with T1DM that had lower HbA_{1c} levels (**chapter 3**). Whereas monocytes from patients with T1DM displayed increased basal expression of pro-inflammatory genes, acute stimulation with P3C actually resulted in significantly lower production of TNF α , IL-1 β and IL-1RA compared with healthy controls (**chapter 3**). These findings resemble the development of immune tolerance, where chronic activation of monocytes in patients with a high glycemic burden contributes to attenuation of acute inflammatory responses. A higher glycemic burden may impose excessive metabolic skewing towards a continuous induction of glycolysis in these monocytes. The resulting metabolic inflexibility may drive uncoupling of the inflammatory response from the regulation of glycolysis upon inflammatory activation. Consequentially, glycolysis is increased, whereas the secretion of cytokines is decreased, despite the enhanced pro-inflammatory gene signature of unstimulated monocytes.

Aerobic glycolysis as driver of diabetes-related complications

Hyperglycemia increases the risk of developing cardiovascular diseases in patients with diabetes mellitus, particularly via chronic inflammatory activation of immune cells [87–89]. This chronic inflammatory state may have been reflected in the basal inflammatory transcriptional signature observed in monocytes from patients with T1DM in **chapter 3**. Aberrations in the glycolytic metabolism of monocytes that are induced by a high glycemic burden may still underlie the observed basal inflammatory signature. In this case, glycolytic metabolism and the inflammatory response are only uncoupled in response to an additional stressor, for instance P3C. Thereby, a high glycemic burden could partly contribute to cardiovascular risk by driving metabolic inflexibility in monocytes. However,

it is more likely that the major link between monocyte function and cardiovascular risk lies in the increased monocytosis that is frequently associated with hyperglycemia, promoting atherosclerosis progression [87,88]. Besides cardiovascular complications, increased susceptibility to infections is another consistent complication linked to glycemic burden and immune cell dysfunction in patients with diabetes mellitus [90–93]. During the possible development of immune tolerance by a high glycemic burden, continuous chronic inflammatory activation of monocytes may impede acute inflammatory responses. This hypothesis is endorsed by the immune tolerance observed in monocytes following *ex vivo* activation with P3C (**chapter 3**). If these findings are predictive for the inadequate acute immune response *in vivo*, immune tolerance in monocytes may partly explain the increased occurrence and severity of infections in patients with a high glycemic burden. Therefore, the excessive skewing towards glycolysis and the uncoupling of glycolytic metabolism and the inflammatory response may partly contribute to an increased susceptibility to infections (**chapter 3**).

Concluding remarks

The upregulation of aerobic glycolysis is consistently associated with a pro-inflammatory phenotype in monocytes and macrophages. In healthy subjects, determining aerobic glycolysis in the form of lactate production can therefore be an additional measurement of immune cell activation. Additionally, inter-individual differences in glycolytic upregulation may underlie differential immune responses. In patients with diabetes mellitus, the link between aerobic glycolysis and the inflammatory response may become uncoupled during a high glycemic burden combined with an inflammatory stressor. Possibly, the hyperglycemic microenvironment could be responsible for metabolic inflexibility in monocytes. Thereby, it may promote a state of chronic inflammation and immune dysregulation, which could eventually contribute to the development of diabetes-related complications. The selective uncoupling of glycolytic metabolism and inflammatory function that might occur in patients with high glycemic burden could undermine the suitability of targeting glycolysis as an anti-inflammatory strategy to combat chronic inflammation. Rather, future research should focus on identifying the molecular mechanisms underlying this uncoupling, its link to hyperglycemia and whether the observed alterations are reversible by providing better glycemic control.

Metabolic inflexibility in innate immune cells in the context of obesity and diabetes

Metabolic flexibility is the ability to efficiently adjust intracellular metabolism [94]. It is an important trait in immune cells to enable their functional adaptation to specific microenvironments. Evidently, diabetes-associated microenvironments can lead to the development of metabolic inflexibility in innate immune cells. In macrophages in the

obese adipose tissue, the inability to cope with an excessive influx of lipids is associated with an ineffective skewing of metabolism toward lipid processing [27,28]. Similarly, monocytes in the hyperglycemic microenvironment of patients with a high glycemic burden may be driven toward increased glycolytic metabolism (**chapter 3**). Both types of metabolic rewiring may initially reflect a protective response. However, passing a certain threshold, functional metabolic rewiring could shift toward metabolic inflexibility, contributing to immune dysfunction (**Figure 2**). In monocytes and macrophages, this metabolic inflexibility could potentially promote chronic inflammation in the context of diabetes mellitus. Although functional metabolic rewiring could, in theory, be reversed by targeting single genes or proteins, the induction of metabolic inflexibility by diabetes-related microenvironments could be difficult to modulate with a single metabolic target (**chapter 4 and 5**). Similarly, the uncoupling between glycolytic metabolism and inflammatory regulation observed in monocytes from patients with T1DM (**chapter 3**) could undermine the suitability of targeting glycolysis as a strategy to combat chronic inflammation. Potentially, metabolic flexibility could be partly restored by decreasing stressors in the diabetic microenvironment, for instance by improving glycemic control or decreasing the presence of FAs. Next to that, the focus could primarily be on preventing immune dysfunction by finding ways to increase metabolic flexibility in innate immune cells, thereby increasing immune cell fitness and raising the threshold leading to immune cell dysfunction.

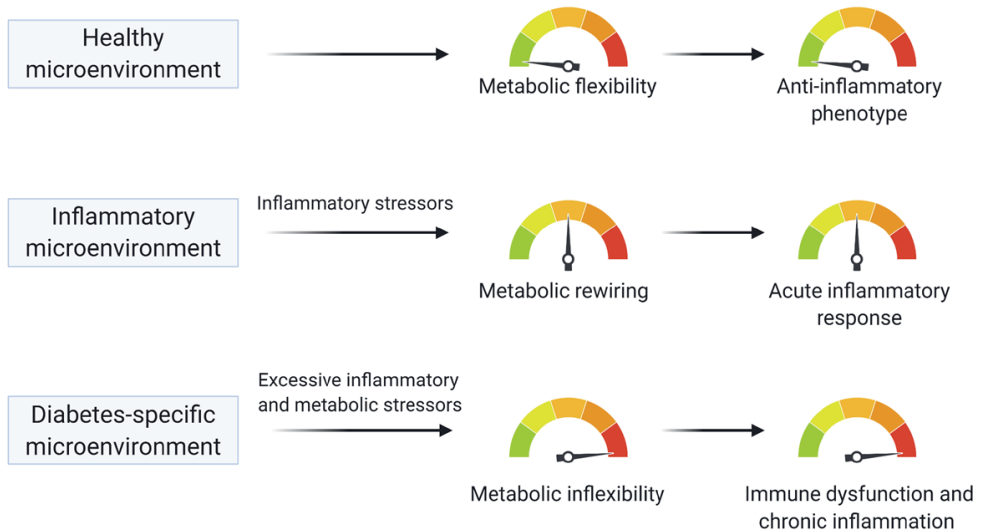


Figure 2. Metabolic inflexibility as driver of macrophage and monocyte dysfunction in diabetes-specific microenvironments.

Monocytes and macrophages are cells with high metabolic plasticity, enabling them to rapidly adapt to changes

in their microenvironment. Inflammatory stressors in inflammatory microenvironments induce extensive metabolic rewiring, facilitating adequate functional adjustments. In diabetes-specific microenvironments, the combination of inflammatory and metabolic stressors, including an excessive influx of lipids or a hyperglycemic milieu, induces not just metabolic rewiring, but enforces metabolic inflexibility. Whereas full metabolic flexibility and a healthy range of metabolic rewiring supports the initiating and resolving of acute inflammation, enforced metabolic inflexibility may underlie innate immune cell dysfunction and chronic inflammation.

Investigating immune cell metabolism to improve immune cell function during obesity and diabetes: challenges and perspectives

Monocytes and macrophages are greatly affected by microenvironmental changes that emanate from a disbalance in systemic metabolic processes. The cues and stressors originating from these microenvironments can modulate their metabolism and cause functional modifications. These modifications may eventually result in the derailment of inflammatory responses and a vicious cycle in disease progression [95], effectively fuelling the inflammatory ‘fire’. However, with their capacity for metabolic and functional plasticity, innate immune cells may also emerge as part of the solution. If it proves to be possible to improve monocyte or macrophage functioning by specifically increasing metabolic flexibility, this may contribute to the prevention of chronic inflammation and insulin resistance. In exploring this possibility, understanding the complex aspects of immunometabolism in the context of disease-specific microenvironments is crucial. Here, we will discuss the challenges and perspectives in studying immunometabolism, including techniques to extensively characterize metabolism, the importance of disease-specific models and the potential for therapeutic applications in the context of obesity and diabetes.

A combination of many different measurements is needed to comprehensibly measure changes occurring within the complex network of intracellular metabolic pathways. Although techniques to measure metabolism in immune cells have rapidly evolved over the past years, there often seems to be a trade-off between detail, dynamics and high-throughput measurements. Detailed information is essential for understanding the intricate shifts in metabolism and elucidating the underlying mechanisms that link them to changing phenotypes in immune cells. Taking dynamics and timing into account also proves to be crucial, as the inclusion of several time points already exposes distinct phases in metabolic rewiring [96] (**chapter 4, 5 and 6**). Lastly, high-throughput methods are of utmost importance, especially in translating murine data to large human populations.

Techniques to measure metabolism

Measuring a single metabolite can already provide substantial general information about the metabolic activity of immune cells in large cohorts (**chapter 2**). This information

increases exponentially when measuring large arrays of metabolites. Moreover, large arrays of metabolomic or lipidomic intermediates can be measured in a high-throughput manner. A disadvantage of these techniques is that they may not allow the elucidation of complex time-related dynamics of metabolic pathways. Furthermore, interpretation of these data could be complex, since the accumulation of specific intermediates could either indicate increased flux, decreased flux, or even a break in the corresponding pathway. Many of these complications could be overcome by using tracer-containing nutrients, such as D-glucose-¹³C, and repeating the measurement at multiple time points. In the concept of these “fluxomics” strategies, incorporation of the tracer into metabolites will indicate how the energetic flux shifts between the chosen time points [97]. However, the need for repeated experiments decreases the feasibility of using these techniques in high-throughput studies and measuring large cohorts. The same applies to the measurement of extracellular acidification or oxygen consumption through metabolic flux assays. This technique measures extracellular flux in live cells, thereby decreasing the importance of estimating appropriate time points. However, in contrast to metabolomics analyses, this method uses surrogate markers that are limited to glycolytic flux and mitochondrial respiration. Additionally, the measurement of immunometabolism in large cohorts in a high-throughput manner is challenging, and live cells can only be followed acutely over a limited amount of time.

The techniques mentioned above primarily offer the characterization of metabolites or energetic fluxes in groups of cells. To draw conclusions based on single cell types, the contribution of different cell populations should be estimated (**chapter 2**), or specific cell populations should be isolated from their *in vivo* environment and studied separately. The latter involves omitting important cell-cell interactions (**chapter 3, 4, 5 and 6**) and may potentially influence their metabolic state [98]. Recent advances in single-cell technologies show that these techniques are able to overcome this limitation and often lend themselves to measure a broad array of metabolic pathways in a high-throughput manner [99]. These techniques enable single-cell metabolic profiling through single-cell transcriptomics [100], proteomics [101], mass spectrometry [102], (spectral) flow cytometry [103,104], mass cytometry [105] or multiplex imaging techniques [106]. These techniques and their corresponding computational frameworks allow for the simultaneous characterization of multiple cell populations, or even the target tissue as a whole [107,108], without isolating subpopulations. Thereby, they can bring momentum to the identification of specific immunometabolic shifts in the context of diabetes mellitus in the future [58].

Modifying metabolism to determine immunometabolic rewiring

Besides determining a detailed metabolic characterization, restricting or modifying metabolic pathways can provide additional insight into the interplay between metabolic rewiring of immune cells and subsequent functional effects (**chapter 4** and **5**). These modifications include compounds that can activate or inhibit metabolic pathways, but also gene knockout models. Although both types of modifications can give crucial insights into the importance of specific metabolic pathways in driving immune cell phenotypes, the complexity and interdependency of the network of metabolic pathways often make it challenging to draw strong conclusions. Additionally, several metabolic compounds, including 2-DG or etomoxir, may lead to broad off-target effects or affect immune cell function separate from metabolic modulation [109–112].

Gene deletion

The deletion of key metabolic enzymes can reveal the importance of distinct metabolic pathways for disease-specific activation of immune cells. As an example, glycolysis has been seen to strongly associate with inflammatory signalling (**chapter 2**) [59,60]. Therefore, silencing key players in the glycolytic pathway, including *Glut1*, *Hk1*, or *Pkm2*, logically interferes with inflammatory signalling [66,74,113,114]. Likewise, the importance of triglyceride accumulation in the regulation of inflammation is emphasized by the effects of deletion of *Dgat1* and *Atgl* [14,115,116].

As cells with high metabolic plasticity, monocytes and macrophages can compensate for these inhibitions by shifting energetics to other metabolic pathways, which may facilitate phenotypic changes. Consequentially, in some cases, it can be complicated to discern whether resulting phenotypic adjustments depend on the decreased flux through the inhibited pathway or the increased flux through the compensatory pathway. It could thus be argued that deleting metabolic genes that are not indispensable, such as inhibitors or activators of rate-limiting enzymes, would lead to a more focused activation or inhibition of the selected metabolic pathway. Deletion of these genes may decrease the chance of general immune cell dysfunction, thereby enabling a more explicit interpretation of the involvement of the selected metabolic pathway in disease-specific metabolic rewiring. For instance, targeting ATGL in macrophages leads to lipid accumulation, which results in increased ER stress, mitochondrial dysfunction and apoptosis [116,117]. Interestingly, macrophages deficient in the ATGL activator CGI-58 display a similar increase in lipid storage, without the induction of ER stress or apoptosis [118]. The obvious downside to exploring immunometabolism based on the deletion of these types of genes or proteins is that the effect of their deletion may be too subtle to lead to effective phenotypic changes.

For instance, deletion of either *Hilpda* or *Ucp2* showed that both targets could influence macrophage metabolism without being indispensable, rate-limiting regulators of general metabolic pathways. These findings suggested that both HILPDA and UCP2 might have been useful targets to modulate macrophage metabolism and inflammatory phenotype. However, their deletion in macrophages did not seem to exert sufficient influence to affect adipose tissue inflammation (**chapter 4, 5 and 6**).

In the context of adipose tissue inflammation, proof for positive effects on disease outcome following metabolic gene deletions in myeloid cells is generally scarce. Even the targeted myeloid deletion of HIF-1 α , a key transcriptional regulator of hypoxia, glycolysis and the inflammatory response, was seen to have mixed success in affecting the development of adipose tissue inflammation and insulin resistance [119,120]. An exception can be made for targeting FAS or HMG-CoA reductase (HMGCR), the rate-limiting enzyme of the mevalonate pathway. Deletion of *Fasn* or *Hmgcr* reduced ATM infiltration by decreasing chemotaxis or recruitment, thereby improving glucose tolerance and insulin sensitivity [57,121]. Interestingly, both deletions prevented excessive accumulation of macrophages instead of resolving individual macrophage dysfunction by targeting their metabolism. As such, the effect of these deletions is somewhat reminiscent of more general measures that prevent macrophage accumulation in the obese adipose tissue, including the use of clodronate liposomes or targeted removal of CD11c-positive cells. After all, effectively ablating all (inflammatory) macrophages through these measures also improves insulin sensitivity in obese adipose tissue [122,123]. Potentially, targeting metabolism to prevent macrophage accumulation in obese adipose tissue, rather than focus on correcting macrophage dysfunction, may also prove to be a successful strategy to decrease inflammation and insulin resistance.

In vivo versus in vitro disease models

The complexity of disease-specific environments is important to keep in mind when translating *in vitro* findings to *in vivo* phenotypes [124]. Measuring immune cell metabolism in humans *ex vivo* enables a direct look at how diseases can direct specific metabolic and functional rewiring, although assessment of the underlying molecular mechanisms remains complicated (**chapter 2 and 3**). In contrast, a simplified *in vitro* model provides a convenient way to investigate disease-specific metabolic rewiring in great detail and could resemble the *in vivo* microenvironment sufficiently to lead to similar phenotypes [28]. However, oversimplification may lead to inaccurate assumptions, especially in the context of heterogeneous metabolic diseases, including obesity and diabetes mellitus. In **chapter 4** and **chapter 6**, both HILPDA and UCP2 were seen to affect inflammation in the

context of classical inflammation *in vitro* (**chapter 4** and **6**) [7], although these findings did not translate to similar effects in the context of adipose tissue inflammation *in vivo* (**chapter 4** and **5**). However, the regulatory effect of HILPDA in the context of classical inflammation *in vitro* was reflected *in vivo* (**chapter 6**). This observation emphasizes that, besides finding the right translation of disease models from *in vitro* to *in vivo*, also disease-specific changes *in vivo* are crucial in determining the effect of immunometabolic rewiring on the inflammatory response.

Disease-specific phenotypes need disease-specific immunometabolic therapies

The complex composition of cues and stressors in different disease-specific microenvironments can induce unique metabolic and functional rewiring in innate immune cells, of which metabolic activation of ATMs in the obese microenvironment is an excellent example [27,35]. Logically, the metabolic and functional rewiring underlying this unique signature is very distinct from monocyte or macrophage activation in the context of atherosclerosis [125,126] or the tumour microenvironment [127,128]. Therefore, in order to apply metabolic rewiring to modulate immune phenotypes, the specificity of disease-related microenvironments and their potential differential effects on immune cells should be taken into account.

An interesting example underlining the importance of disease-specific differences can be found in comparing the development of atherosclerosis and adipose tissue inflammation. The pathophysiology of both diseases includes the encounter between macrophages and an excess flux of lipids, leading to foam cell formation and promotion of unresolved inflammation [30,125]. However, notable differences come to light in comparing the effects on the outcome of both disease models following deletion of immunometabolic genes in macrophages. For instance, in the context of atherosclerosis, *Hilpda* deletion in macrophages was seen to have a beneficial effect through decreasing aortic plaque area [129], whereas no protective effects of its deletion were observed in adipose tissue macrophages in the obesity-induced development of adipose tissue inflammation and insulin resistance (**chapter 5**). Furthermore, leukocyte-specific deletion of *Ucp2* was seen to increase atherosclerotic lesion size, suggesting a protective effect role for UCP2 during atherosclerosis development [130]. In contrast, no effects were observed in the context of obese adipose tissue inflammation following myeloid-specific *Ucp2* deletion (**chapter 4**). Similarly, targeting the key glycolytic regulator HIF-1 α in myeloid cells has successfully attenuated atherosclerosis [131,132], whereas mixed results were found in the context of adipose tissue macrophages [119,120]. Although differences in experimental setup should be considered, single metabolic gene myeloid knockout models seem more likely

to affect atherosclerosis progression than adipose tissue inflammation development. Thus, whereas the formation of foam cell-like macrophages characterizes the disease aetiology of both, the different microenvironmental cues, potentially including the interplay with other (immune) cell populations, likely lead to distinct activation of innate immune cells. Thereby, both microenvironments give rise to distinct macrophage subsets with unique metabolic rewiring [58,133,134]. These examples emphasize the fact that there is no single blueprint for monocyte or macrophage activation. Therefore, extensive disease-specific knowledge of metabolic rewiring or inflexibility is needed as the first essential step to combat immune dysregulation through immunometabolism in different diseases. In the context of metabolic diseases, the solution may be to identify ways to increase metabolic flexibility [40], which could be modulated in specific immune cell subpopulations.

Targeting identified metabolic pathways

After identifying promising and disease-specific targets that have the potential to increase metabolic flexibility and improve disease outcome, the final hurdle to take is determining how these can be used for therapeutic strategies. The key aspects to consider for immunometabolic strategies are temporality and specificity. Temporality could be achieved by developing small-molecule inhibitors or activators or identifying specific immunometabolites that can affect metabolic pathways acutely. The concept of targeting activated immune cells already provides a certain specificity, as activated regulatory immune cells often have high metabolic requirements and are thereby more effectively targeted by metabolic strategies [135]. Additionally, specific delivery methods toward monocytes or macrophages could be explored using micro- or nano-particles, liposomes, or oligopeptide complexes [136]. Particles or liposomes can be conjugated to antibodies or nanobodies that specifically target monocyte or macrophage subsets to ensure specificity, preventing off-target effects toward regulatory immune cells in other tissues besides the target tissue. This approach has already proven to be successful, for instance in the specific delivery of rapamycin, an inhibitor of the mTOR pathway, to reprogram metabolism and polarization of tumour-associated macrophages in a murine model of colon cancer [137], and may offer potential for specifically targeting immunometabolism in monocytes and macrophages in other disease models.

Concluding remarks and future perspectives

The studies in this thesis emphasize the intricate functional and metabolic rewiring that disease-specific microenvironments can induce. In the context of obesity- and diabetes-specific microenvironments, our observations are confirmative of a restriction in metabolic flexibility in monocytes and macrophages. This metabolic inflexibility may

induce aberrations in inflammatory responses, thereby contributing to the development and progression of diabetes and diabetes-related complications. To successfully target immunometabolism to improve disease progression in general, identifying disease-specific inhibitors or activators of rate-limiting enzymes could be a fitting approach. However, in the context of obesity and diabetes, metabolic inflexibility and the complex heterogeneity of monocyte and macrophage microenvironments may undermine the suitability of using single metabolic targets as an effective strategy to combat disease progression. Instead, the focus should be on preventing innate immune dysfunction by finding methods to increase or restore metabolic flexibility in innate immune cells, thereby raising the threshold leading to immune cell dysfunction and preventing disease progression.

References

Figures are created with BioRender.com

1. Stienstra R, Netea-Maier RT, Riksen NP, Joosten LAB, Netea MG. Specific and Complex Reprogramming of Cellular Metabolism in Myeloid Cells during Innate Immune Responses. *Cell Metabolism*. 2017; 26(1): 142–56.
2. O'Neill LAJ, Kishton RJ, Rathmell J. A guide to immunometabolism for immunologists. *Nature Reviews Immunology*. 2016; 16(9): 553–65.
3. Biswas SK, Mantovani A. Orchestration of metabolism by macrophages. *Cell metabolism*. 2012; 15(4): 432–7.
4. Namgaladze D, Brüne B. Macrophage fatty acid oxidation and its roles in macrophage polarization and fatty acid-induced inflammation. *Biochimica et Biophysica Acta (BBA) - Molecular and Cell Biology of Lipids*. 2016; 1861(11): 1796–807.
5. Namgaladze D, Brüne B. Fatty acid oxidation is dispensable for human macrophage IL-4-induced polarization. *Biochimica et Biophysica Acta - Molecular and Cell Biology of Lipids*. 2014; 1841(9): 1329–35.
6. Nomura M, Liu J, Rovira II, Gonzalez-Hurtado E, Lee J, Wolfgang MJ, et al. Fatty acid oxidation in macrophage polarization. *Nature Immunology*. 2016; 17(3): 216–7.
7. Moon J-S, Lee S, Park M-A, Siempos II, Haslip M, Lee PJ, et al. UCP2-induced fatty acid synthase promotes NLRP3 inflammasome activation during sepsis. *The Journal of Clinical Investigation*. 2015; 125(2): 665–80.
8. Kim YC, Lee SE, Kim SK, Jang HD, Hwang I, Jin S, et al. Toll-like receptor mediated inflammation requires FASN-dependent MYD88 palmitoylation. *Nature Chemical Biology*. 2019; 15(9): 907–16.
9. Carroll RG, Zastona Z, Galván-Peña S, Koppe EL, Sévin DC, Angiari S, et al. An unexpected link between fatty acid synthase and cholesterol synthesis in proinflammatory macrophage activation. *Journal of Biological Chemistry*. 2018; 293(15): 5509–21.
10. Rosas-Ballina M, Guan XL, Schmidt A, Bumann D. Classical Activation of Macrophages Leads to Lipid Droplet Formation Without de novo Fatty Acid Synthesis. *Frontiers in Immunology*. 2020; 11: 131.
11. Feingold KR, Shigenaga JK, Kazemi MR, McDonald CM, Patzek SM, Cross AS, et al. Mechanisms of triglyceride accumulation in activated macrophages. *Journal of Leukocyte Biology*. 2012; 92(4): 829–39.
12. Im SS, Yousef L, Blaschitz C, Liu JZ, Edwards RA, Young SG, et al. Linking lipid metabolism to the innate immune response in macrophages through sterol regulatory element binding protein-1a. *Cell Metabolism*. 2011; 13(5): 540–9.
13. Infantino V, Iacobazzi V, Palmieri F, Menga A. ATP-citrate lyase is essential for macrophage inflammatory response. *Biochemical and Biophysical Research Communications*. 2013; 440(1): 105–11.
14. Castoldi A, Monteiro LB, van Teijlingen Bakker N, Sanin DE, Rana N, Corrado M, et al. Triacylglycerol synthesis enhances macrophage inflammatory function. *Nature Communications*. 2020; 11(1).
15. Köberlin MS, Snijder B, Heinz LX, Baumann CL, Fauster A, Vladimer GI, et al. A Conserved Circular Network of Coregulated Lipids Modulates Innate Immune Responses. *Cell*. 2015; 162(1): 170–83.
16. Dennis EA, Deems RA, Harkewicz R, Quehenberger O, Brown HA, Milne SB, et al. A mouse

- macrophage lipidome. *Journal of Biological Chemistry*. 2010; 285(51): 39976–85.
17. Hsieh WY, Zhou QD, York AG, Williams KJ, Scumpia PO, Kronenberger EB, et al. Toll-Like Receptors Induce Signal-Specific Reprogramming of the Macrophage Lipidome. *Cell Metabolism*. 2020; 32(1): 128-143.e5.
 18. Schlager S, Goeritzer M, Jandl K, Frei R, Vujic N, Kolb D, et al. Adipose triglyceride lipase acts on neutrophil lipid droplets to regulate substrate availability for lipid mediator synthesis. *Journal of Leukocyte Biology*. 2015; 98(5): 837–50.
 19. Dichlberger A, Schlager S, Maaninka K, Schneider WJ, Kovanen PT. Adipose triglyceride lipase regulates eicosanoid production in activated human mast cells. *Journal of Lipid Research*. 2014; 55(12): 2471–8.
 20. Bosch M, Sánchez-Álvarez M, Fajardo A, Kapetanovic R, Steiner B, Dutra F, et al. Mammalian lipid droplets are innate immune hubs integrating cell metabolism and host defense. *Science*. 2020; 370(6514).
 21. Bekkering S, Arts RJW, Novakovic B, Kourtzelis I, van der Heijden CDCC, Li Y, et al. Metabolic Induction of Trained Immunity through the Mevalonate Pathway. *Cell*. 2018; 172(1–2): 135-146.e9.
 22. Lumeng CN, DelProposto JB, Westcott DJ, Saltiel AR. Phenotypic Switching of Adipose Tissue Macrophages With Obesity Is Generated by Spatiotemporal Differences in Macrophage Subtypes. *Diabetes*. 2008; 57(12): 3239–46.
 23. Lumeng CN, Bodzin JL, Saltiel AR. Obesity induces a phenotypic switch in adipose tissue macrophage polarization. *Journal of Clinical Investigation*. 2007; 117(1): 175–84.
 24. Weisberg SP, McCann D, Desai M, Rosenbaum M, Leibel RL, Ferrante AW. Obesity is associated with macrophage accumulation in adipose tissue. *Journal of Clinical Investigation*. 2003; 112(12): 1796–808.
 25. Cinti S, Mitchell G, Barbatelli G, Murano I, Ceresi E, Faloia E, et al. Adipocyte death defines macrophage localization and function in adipose tissue of obese mice and humans. *Journal of Lipid Research*. 2005; 46(11): 2347–55.
 26. Strissel KJ, Stancheva Z, Miyoshi H, Perfield JW, DeFuria J, Jick Z, et al. Adipocyte death, adipose tissue remodeling, and obesity complications. *Diabetes*. 2007; 56(12): 2910–8.
 27. Xu X, Grijalva A, Skowronski A, van Eijk M, Serlie MJ, Ferrante AW. Obesity Activates a Program of Lysosomal-Dependent Lipid Metabolism in Adipose Tissue Macrophages Independently of Classic Activation. *Cell Metabolism*. 2013; 18(6): 816–30.
 28. Kratz M, Coats BR, Hisert KB, Hagman D, Mutskov V, Peris E, et al. Metabolic Dysfunction Drives a Mechanistically Distinct Proinflammatory Phenotype in Adipose Tissue Macrophages. *Cell Metabolism*. 2014; 20(4): 614–25.
 29. Muir LA, Kiridena S, Griffin C, DelProposto JB, Geletka L, Martinez-Santibañez G, et al. Frontline Science: Rapid adipose tissue expansion triggers unique proliferation and lipid accumulation profiles in adipose tissue macrophages. *Journal of Leukocyte Biology*. 2018; 103(4): 615–28.
 30. Shapiro H, Pecht T, Shaco-Levy R, Harman-Boehm I, Kirshtein B, Kuperman Y, et al. Adipose Tissue Foam Cells Are Present in Human Obesity. *The Journal of Clinical Endocrinology & Metabolism*. 2013; 98(3): 1173–81.
 31. Kosteli A, Sogut E, Haemmerle G, Martin JF, Lei J, Zechner R, et al. Weight loss and lipolysis promote a dynamic immune response in murine adipose tissue. *The Journal of Clinical Investigation*. 2010; 120(10): 3466–79.
 32. Rao RR, Long JZ, White JP, Svensson KJ, Lou J, Lokurkar I, et al. Meteorin-like is a hormone that regulates immune-adipose interactions to increase beige fat thermogenesis. *Cell*. 2014; 157(6):

- 1279–91.
33. Asterholm IW, McDonald J, Blanchard PG, Sinha M, Xiao Q, Mistry J, et al. Lack of “immunological fitness” during fasting in metabolically challenged animals. *Journal of Lipid Research*. 2012; 53(7): 1254–67.
 34. Lee YH, Petkova AP, Granneman JG. Identification of an adipogenic niche for adipose tissue remodeling and restoration. *Cell Metabolism*. 2013; 18(3): 355–67.
 35. Boutens L, Stienstra R. Adipose tissue macrophages: going off track during obesity. *Diabetologia*. 2016; 59(5): 879–94.
 36. Prieur X, Mok CYL, Velagapudi VR, Núñez V, Fuentes L, Montaner D, et al. Differential Lipid Partitioning Between Adipocytes and Tissue Macrophages Modulates Macrophage Lipotoxicity and M2/M1 Polarization in Obese Mice. *Diabetes*. 2011; 60(3): 797–809.
 37. Hill DA, Lim HW, Kim YH, Ho WY, Foong YH, Nelson VL, et al. Distinct macrophage populations direct inflammatory versus physiological changes in adipose tissue. *Proceedings of the National Academy of Sciences of the United States of America*. 2018; 115(22): E5096–105.
 38. Aouadi M, Vangala P, Yawe JC, Tencerova M, Nicoloso SM, Cohen JL, et al. Lipid storage by adipose tissue macrophages regulates systemic glucose tolerance. *American Journal of Physiology-Endocrinology and Metabolism*. 2014; 307(4): E374–83.
 39. Koliwad SK, Streeper RS, Monetti M, Cornelissen I, Chan L, Terayama K, et al. DGAT1-dependent triacylglycerol storage by macrophages protects mice from diet-induced insulin resistance and inflammation. *Journal of Clinical Investigation*. 2010; 120(3): 756–67.
 40. Brunner JS, Vogel A, Lercher A, Caldera M, Korosec A, Pühringer M, et al. The PI3K pathway preserves metabolic health through MARCO-dependent lipid uptake by adipose tissue macrophages. *Nature Metabolism*. 2020; 2(12): 1427–42.
 41. Luan B, Yoon YS, Lay J Le, Kaestner KH, Hedrick S, Montminy M. CREB pathway links PGE2 signaling with macrophage polarization. *Proceedings of the National Academy of Sciences of the United States of America*. 2015; 112(51): 15642–7.
 42. Chan P-C, Hsiao F-C, Chang H-M, Wabitsch M, Hsieh PS. Importance of adipocyte cyclooxygenase-2 and prostaglandin E2-prostaglandin E receptor 3 signaling in the development of obesity-induced adipose tissue inflammation and insulin resistance. *FASEB journal*. 2016; 30(6): 2282–97.
 43. Flaherty SE, Grijalva A, Xu X, Ables E, Nomani A, Ferrante AW. A lipase-independent pathway of lipid release and immune modulation by adipocytes. *Science*. 2019; 363(6430): 989–93.
 44. Deng Z Bin, Poliakov A, Hardy RW, Clements R, Liu C, Liu Y, et al. Adipose tissue exosome-like vesicles mediate activation of macrophage-induced insulin resistance. *Diabetes*. 2009; 58(11): 2498–505.
 45. Shi H, Kokoeva M V., Inouye K, Tzameli I, Yin H, Flier JS. TLR4 links innate immunity and fatty acid-induced insulin resistance. *Journal of Clinical Investigation*. 2006; 116(11): 3015–25.
 46. Huang S, Rutkowsky JM, Snodgrass RG, Ono-Moore KD, Schneider DA, Newman JW, et al. Saturated fatty acids activate TLR-mediated proinflammatory signaling pathways. *Journal of Lipid Research*. 2012; 53(9): 2002–13.
 47. Wong SW, Kwon M-J, Choi AMK, Kim H-P, Nakahira K, Hwang DH. Fatty acids modulate Toll-like receptor 4 activation through regulation of receptor dimerization and recruitment into lipid rafts in a reactive oxygen species-dependent manner. *The Journal of biological chemistry*. 2009; 284(40): 27384–92.
 48. Lee JY, Sohn KH, Rhee SH, Hwang D. Saturated fatty acids, but not unsaturated fatty acids, induce the expression of cyclooxygenase-2 mediated through Toll-like receptor 4. *The Journal*

- of biological chemistry. 2001; 276(20): 16683–9.
49. Lancaster GI, Langley KG, Berglund NA, Kammoun HL, Reibe S, Estevez E, et al. Evidence that TLR4 Is Not a Receptor for Saturated Fatty Acids but Mediates Lipid-Induced Inflammation by Reprogramming Macrophage Metabolism. *Cell Metabolism*. 2018; 27(5): 1096-1110.e5.
 50. Robblee MM, Kim CC, Abate JP, Valdearcos M, Sandlund KLM, Shenoy MK, et al. Saturated Fatty Acids Engage an IRE1 α -Dependent Pathway to Activate the NLRP3 Inflammasome in Myeloid Cells. *Cell Reports*. 2016; 14(11): 2611–23.
 51. Han MS, Jung DY, Morel C, Lakhani SA, Kim JK, Flavell RA, et al. JNK expression by macrophages promotes obesity-induced insulin resistance and inflammation. *Science*. 2013; 339(6116): 218–22.
 52. Gianfrancesco MA, Dehairs J, L'homme L, Herinckx G, Esser N, Jansen O, et al. Saturated fatty acids induce NLRP3 activation in human macrophages through K⁺ efflux resulting from phospholipid saturation and Na, K-ATPase disruption. *Biochimica Et Biophysica Acta (BBA)-Molecular and Cell Biology of Lipids*. 2019; 1864(7): 1017–30.
 53. Wen H, Gris D, Lei Y, Jha S, Zhang L, Huang MTH, et al. Fatty acid-induced NLRP3-ASC inflammasome activation interferes with insulin signaling. *Nature Immunology*. 2011; 12(5): 408–15.
 54. Jia L, Vianna CR, Fukuda M, Berglund ED, Liu C, Tao C, et al. Hepatocyte toll-like receptor 4 regulates obesity-induced inflammation and insulin resistance. *Nature Communications*. 2014; 5.
 55. Barra NG, Henriksbo BD, Anhe FF, Schertzer JD. The NLRP3 inflammasome regulates adipose tissue metabolism. *Biochemical Journal*. 2020; 477(6): 1089–107.
 56. Lee HM, Kim JJ, Kim HJ, Shong M, Ku BJ, Jo EK. Upregulated NLRP3 inflammasome activation in patients with type 2 diabetes. *Diabetes*. 2013; 62(1): 194–204.
 57. Wei X, Song H, Yin L, Rizzo MG, Sidhu R, Covey DF, et al. Fatty acid synthesis configures the plasma membrane for inflammation in diabetes. *Nature*. 2016; 539(7628): 294–8.
 58. Jaitin DA, Adlung L, Thaïss CA, Weiner A, Li B, Descamps H, et al. Lipid-Associated Macrophages Control Metabolic Homeostasis in a Trem2-Dependent Manner. *Cell*. 2019; 178(3).
 59. Krawczyk CM, Holowka T, Sun J, Blagih J, Amiel E, DeBerardinis RJ, et al. Toll-like receptor-induced changes in glycolytic metabolism regulate dendritic cell activation. *Blood*. 2010; 115(23): 4742–9.
 60. Rodríguez-Prados J-C, Través PG, Cuenca J, Rico D, Aragonés J, Martín-Sanz P, et al. Substrate Fate in Activated Macrophages: A Comparison between Innate, Classic, and Alternative Activation. *The Journal of Immunology*. 2010; 185(1): 605–14.
 61. Michl J, Ohlbaum DJ, Silverstein SC. 2-Deoxyglucose selectively inhibits fc and complement receptor-mediated phagocytosis in mouse peritoneal macrophages. *Journal of Experimental Medicine*. 1976; 144(6): 1484–93.
 62. Freerman AJ, Johnson AR, Sacks GN, Milner JJ, Kirk EL, Troester MA, et al. Metabolic reprogramming of macrophages: Glucose transporter 1 (GLUT1)-mediated glucose metabolism drives a proinflammatory phenotype. *Journal of Biological Chemistry*. 2014; 289(11): 7884–96.
 63. Pålsson-Mcdermott EM, Curtis AM, Goel G, Lauterbach MAR, Sheedy FJ, Gleeson LE, et al. Pyruvate kinase M2 regulates hif-1 α activity and il-1 β induction and is a critical determinant of the warburg effect in LPS-activated macrophages. *Cell Metabolism*. 2015; 21(1).
 64. Tan Z, Xie N, Cui H, Moellering DR, Abraham E, Thannickal VJ, et al. Pyruvate Dehydrogenase Kinase 1 Participates in Macrophage Polarization via Regulating Glucose Metabolism. *The Journal of Immunology*. 2015; 194(12): 6082–9.

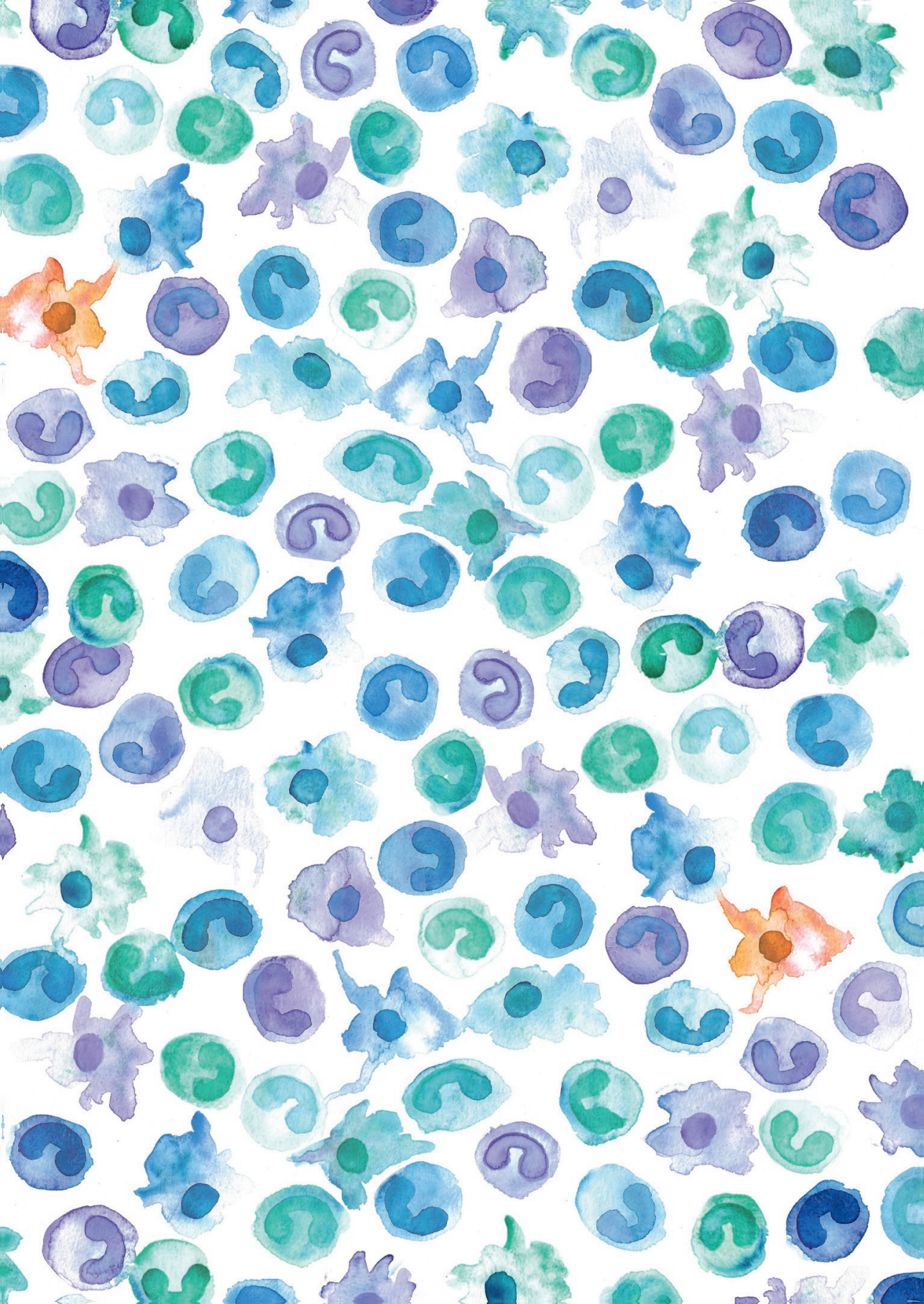
65. Galván-Peña S, Carroll RG, Newman C, Hinchey EC, Palsson-McDermott E, Robinson EK, et al. Malonylation of GAPDH is an inflammatory signal in macrophages. *Nature Communications*. 2019; 10(1).
66. Xie M, Yu Y, Kang R, Zhu S, Yang L, Zeng L, et al. PKM2-Dependent glycolysis promotes NLRP3 and AIM2 inflammasome activation. *Nature Communications*. 2016; 7.
67. Cheng SC, Quintin J, Cramer RA, Shepardson KM, Saeed S, Kumar V, et al. MTOR- and HIF-1 α -mediated aerobic glycolysis as metabolic basis for trained immunity. *Science*. 2014; 345(6204).
68. Li Y, Oosting M, Deelen P, Ricaño-Ponce I, Smeekens S, Jaeger M, et al. Inter-individual variability and genetic influences on cytokine responses to bacteria and fungi. *Nature Medicine*. 2016; 22(8): 952–60.
69. Li Y, Oosting M, Smeekens SP, Jaeger M, Aguirre-Gamboa R, Le KTT, et al. A Functional Genomics Approach to Understand Variation in Cytokine Production in Humans. *Cell*. 2016; 167(4): 1099-1110.e14.
70. ter Horst R, Jaeger M, Smeekens SP, Oosting M, Swertz MA, Li Y, et al. Host and Environmental Factors Influencing Individual Human Cytokine Responses. *Cell*. 2016; 167(4): 1111-1124.e13.
71. Bakker OB, Aguirre-Gamboa R, Sanna S, Oosting M, Smeekens SP, Jaeger M, et al. Integration of multi-omics data and deep phenotyping enables prediction of cytokine responses. *Nature Immunology*. 2018; 19(7): 776–86.
72. Izquierdo E, Cuevas VD, Fernández-Arroyo S, Riera-Borrull M, Orta-Zavalza E, Joven J, et al. Reshaping of Human Macrophage Polarization through Modulation of Glucose Catabolic Pathways. *The Journal of Immunology*. 2015; 195(5): 2442–51.
73. Tannahill G, Curtis A, Adamik J, Palsson-McDermott E, McGettrick A, Goel G, et al. Succinate is a danger signal that induces IL-1 β via HIF-1 α . *Nature*. 2013; 496(7444): 238–42.
74. Moon JS, Hisata S, Park MA, DeNicola GM, Ryter SW, Nakahira K, et al. MTORC1-Induced HK1-Dependent Glycolysis Regulates NLRP3 Inflammasome Activation. *Cell Reports*. 2015; 12(1): 102–15.
75. Finucane OM, Sugrue J, Rubio-Araiz A, Guillot-Sestier MV, Lynch MA. The NLRP3 inflammasome modulates glycolysis by increasing PFKFB3 in an IL-1 β -dependent manner in macrophages. *Scientific Reports*. 2019; 9(1).
76. Ip WKE, Hoshi N, Shouval DS, Snapper S, Medzhitov R. Anti-inflammatory effect of IL-10 mediated by metabolic reprogramming of macrophages. *Science*. 2017; 356(6337): 513–9.
77. Dinarello CA. Biologic basis for interleukin-1 in disease. *Blood*. 1996; 87(6): 2095–147.
78. Nishizawa T, Kanter JE, Kramer F, Barnhart S, Shen X, Vivekanandan-Giri A, et al. Testing the Role of Myeloid Cell Glucose Flux in Inflammation and Atherosclerosis. *Cell Reports*. 2014; 7(2): 356–65.
79. Vozza A, Parisi G, De Leonardis F, Lasorsa FM, Castegna A, Amorese D, et al. UCP2 transports C4 metabolites out of mitochondria, regulating glucose and glutamine oxidation. *Proceedings of the National Academy of Sciences*. 2014; 111(3): 960–5.
80. Pecqueur C, Alves-Guerra C, Ricquier D, Bouillaud F. UCP2, a metabolic sensor coupling glucose oxidation to mitochondrial metabolism? *IUBMB Life*. 2009; 61(7): 762–7.
81. Brownlee M. The pathobiology of diabetic complications: A unifying mechanism. In: *Diabetes*. Diabetes; 2005. p. 1615–25.
82. Shanmugam N, Reddy MA, Guha M, Natarajan R. High glucose-induced expression of proinflammatory cytokine and chemokine genes in monocytic cells. *Diabetes*. 2003; 52(5): 1256–64.
83. Dasu MR, Devaraj S, Jialal I. High glucose induces IL-1 β expression in human monocytes:

- Mechanistic insights. *American Journal of Physiology - Endocrinology and Metabolism*. 2007; 293(1): 337–46.
84. Devaraj S, Glaser N, Griffen S, Wang-Polagruto J, Miguelino E, Jialal I. Increased monocytic activity and biomarkers of inflammation in patients with type 1 diabetes. *Diabetes*. 2006; 55(3): 774–9.
 85. Devaraj S, Dasu MR, Rockwood J, Winter W, Griffen SC, Jialal I. Increased toll-like receptor (TLR) 2 and TLR4 expression in monocytes from patients with type 1 diabetes: Further evidence of a proinflammatory state. *Journal of Clinical Endocrinology and Metabolism*. 2008; 93(2): 578–83.
 86. van Diepen JA, Thiem K, Stienstra R, Riksen NP, Tack CJ, Netea MG. Diabetes propels the risk for cardiovascular disease: sweet monocytes becoming aggressive? *Cellular and Molecular Life Sciences*. 2016; 73(24): 4675–84.
 87. Nagareddy PR, Murphy AJ, Stirzaker RA, Hu Y, Yu S, Miller RG, et al. Hyperglycemia promotes myelopoiesis and impairs the resolution of atherosclerosis. *Cell Metabolism*. 2013; 17(5): 695–708.
 88. Flynn MC, Kraakman MJ, Tikellis C, Lee MKS, Hanssen NMJ, Kammoun HL, et al. Transient Intermittent Hyperglycemia Accelerates Atherosclerosis by Promoting Myelopoiesis. *Circulation Research*. 2020; 127(7): 877–92.
 89. Basu S, Larsson A, Vessby J, Vessby B, Berne C. Type 1 Diabetes Is Associated With Increased Cyclooxygenase- and Cytokine-Mediated Inflammation. *Diabetes Care*. 2005; 28(6): 1371 LP – 1375.
 90. Carey IM, Critchley JA, Dewilde S, Harris T, Hosking FJ, Cook DG. Risk of infection in type 1 and type 2 diabetes compared with the general population: A matched cohort study. *Diabetes Care*. 2018; 41(3): 513–21.
 91. Critchley JA, Carey IM, Harris T, DeWilde S, Hosking FJ, Cook DG. Glycemic control and risk of infections among people with type 1 or type 2 diabetes in a large primary care cohort study. *Diabetes Care*. 2018; 41(10): 2127–35.
 92. McGovern AP, Hine J, de Lusignan S. Infection risk in elderly people with reduced glycaemic control. *The Lancet Diabetes and Endocrinology*. 2016; 4(4): 303–4.
 93. Dooley KE, Chaisson RE. Tuberculosis and diabetes mellitus: convergence of two epidemics. *The Lancet Infectious Diseases*. 2009; 9(12): 737–46.
 94. Smith RL, Soeters MR, Wüst RCI, Houtkooper RH. Metabolic flexibility as an adaptation to energy resources and requirements in health and disease. *Endocrine Reviews*. 2018; 39(4): 489–517.
 95. Donath MY, Shoelson SE. Type 2 diabetes as an inflammatory disease. *Nature reviews Immunology*. 2011; 11(2): 98–107.
 96. Seim GL, Britt EC, John S V., Yeo FJ, Johnson AR, Eisenstein RS, et al. Two-stage metabolic remodelling in macrophages in response to lipopolysaccharide and interferon- γ stimulation. *Nature Metabolism*. 2019; 1(7): 731–42.
 97. Alves TC, Pongratz RL, Zhao X, Yarborough O, Sereda S, Shirihai O, et al. Integrated, Step-Wise, Mass-Isotopomeric Flux Analysis of the TCA Cycle. *Cell Metabolism*. 2015; 22(5): 936–47.
 98. Llufrío EM, Wang L, Naser FJ, Patti GJ. Sorting cells alters their redox state and cellular metabolome. *Redox Biology*. 2018; 16: 381–7.
 99. Artyomov MN, Van den Bossche J. Immunometabolism in the Single-Cell Era. *Cell Metabolism*. 2020; 32(5): 710–25.
 100. Mereu E, Lafzi A, Moutinho C, Ziegenhain C, McCarthy DJ, Álvarez-Varela A, et al. Benchmarking single-cell RNA-sequencing protocols for cell atlas projects. *Nature Biotechnology*. 2020; 38(6):

- 747–55.
101. Slavov N. Unpicking the proteome in single cells. *Science*. 2020; 367(6477): 512–3.
 102. Pareek V, Tian H, Winograd N, Benkovic SJ. Metabolomics and mass spectrometry imaging reveal channeled de novo purine synthesis in cells. *Science*. 2020; 368(6488): 283–90.
 103. Ferrer-Font L, Pellefigues C, Mayer JU, Small SJ, Jaimes MC, Price KM. Panel Design and Optimization for High-Dimensional Immunophenotyping Assays Using Spectral Flow Cytometry. *Current Protocols in Cytometry*. 2020; 92(1).
 104. Argüello RJ, Combes AJ, Char R, Gigan JP, Baaziz AI, Bousiquot E, et al. SCENITH: A Flow Cytometry-Based Method to Functionally Profile Energy Metabolism with Single-Cell Resolution. *Cell Metabolism*. 2020; 32(6): 1063-1075.e7.
 105. Spitzer MH, Nolan GP. Mass Cytometry: Single Cells, Many Features. *Cell*. 2016; 165(4): 780–91.
 106. Hartmann FJ, Bendall SC. Immune monitoring using mass cytometry and related high-dimensional imaging approaches. *Nature Reviews Rheumatology*. 2020; 16(2): 87–99.
 107. Gerner MY, Kastenmuller W, Ifrim I, Kabat J, Germain RN. Histo-Cytometry: A Method for Highly Multiplex Quantitative Tissue Imaging Analysis Applied to Dendritic Cell Subset Microanatomy in Lymph Nodes. *Immunity*. 2012; 37(2): 364–76.
 108. Miller A, Nagy C, Knapp B, Laengle J, Ponweiser E, Groeger M, et al. Exploring Metabolic Configurations of Single Cells within Complex Tissue Microenvironments. *Cell Metabolism*. 2017; 26(5): 788-800.e6.
 109. Divakaruni AS, Hsieh WY, Minarrieta L, Duong TN, Kim KKO, Desousa BR, et al. Etomoxir Inhibits Macrophage Polarization by Disrupting CoA Homeostasis. *Cell Metabolism*. 2018; 28(3): 490-503.e7.
 110. Raud B, Roy DG, Divakaruni AS, Tarasenko TN, Franke R, Ma EH, et al. Etomoxir Actions on Regulatory and Memory T Cells Are Independent of Cpt1a-Mediated Fatty Acid Oxidation. *Cell Metabolism*. 2018; 28(3): 504-515.e7.
 111. O'Connor RS, Guo L, Ghassemi S, Snyder NW, Worth AJ, Weng L, et al. The CPT1a inhibitor, etomoxir induces severe oxidative stress at commonly used concentrations. *Scientific Reports*. 2018; 8(1): 6289.
 112. Wang F, Zhang S, Vuckovic I, Jeon R, Lerman A, Folmes CD, et al. Glycolytic Stimulation Is Not a Requirement for M2 Macrophage Differentiation. *Cell Metabolism*. 2018; 28(3): 463-475.e4.
 113. Freerman AJ, Zhao L, Pingili AK, Teng B, Cozzo AJ, Fuller AM, et al. Myeloid Slc2a1 -Deficient Murine Model Revealed Macrophage Activation and Metabolic Phenotype Are Fueled by GLUT1. *The Journal of Immunology*. 2019; 202(4): 1265–86.
 114. Yang L, Xie M, Yang M, Yu Y, Zhu S, Hou W, et al. PKM2 regulates the Warburg effect and promotes HMGB1 release in sepsis. *Nature Communications*. 2014; 5: 4436.
 115. Aflaki E, Balenga NAB, Luschnig-Schratl P, Wolinski H, Povoden S, Chandak PG, et al. Impaired Rho GTPase activation abrogates cell polarization and migration in macrophages with defective lipolysis. *Cellular and Molecular Life Sciences*. 2011; 68(23): 3933–47.
 116. Chandak PG, Radović B, Aflaki E, Kolb D, Buchebner M, Fröhlich E, et al. Efficient Phagocytosis Requires Triacylglycerol Hydrolysis by Adipose Triglyceride Lipase. *Journal of Biological Chemistry*. 2010; 285(26): 20192–201.
 117. Aflaki E, Radović B, Chandak PG, Kolb D, Eisenberg T, Ring J, et al. Triacylglycerol Accumulation Activates the Mitochondrial Apoptosis Pathway in Macrophages. *Journal of Biological Chemistry*. 2011; 286(9): 7418–28.
 118. Goeritzer M, Schlager S, Radovic B, Madreiter CT, Rainer S, Thomas G, et al. Deletion of CGI-58 or adipose triglyceride lipase differently affects macrophage function and atherosclerosis.

- Journal of lipid research. 2014; 55(12): 2562–75.
119. Boutens L, Hooiveld GJ, Dhingra S, Cramer RA, Netea MG, Stienstra R. Unique metabolic activation of adipose tissue macrophages in obesity promotes inflammatory responses. *Diabetologia*. 2018; 61(4): 942–53.
 120. Sharma M, Boytard L, Hadi T, Koelwyn G, Simon R, Ouimet M, et al. Enhanced glycolysis and HIF-1 α activation in adipose tissue macrophages sustains local and systemic interleukin-1 β production in obesity. *Scientific Reports*. 2020; 10(1).
 121. Takei A, Nagashima S, Takei S, Yamamuro D, Murakami A, Wakabayashi T, et al. Myeloid HMG-CoA reductase determines adipose tissue inflammation, insulin resistance, and hepatic steatosis in diet-induced obese mice. *Diabetes*. 2020; 69(2): 158–64.
 122. Patsouris D, Li P-P, Thapar D, Chapman J, Olefsky JM, Neels JG. Ablation of CD11c-Positive Cells Normalizes Insulin Sensitivity in Obese Insulin Resistant Animals. *Cell Metabolism*. 2008; 8(4): 301–9.
 123. Feng B, Jiao P, Nie Y, Kim T, Jun D, van Rooijen N, et al. Clodronate liposomes improve metabolic profile and reduce visceral adipose macrophage content in diet-induced obese mice. *PLoS ONE*. 2011; 6(9).
 124. Mazumdar C, Driggers EM, Turka LA. The Untapped Opportunity and Challenge of Immunometabolism: A New Paradigm for Drug Discovery. *Cell Metabolism*. 2020; 31(1): 26–34.
 125. Moore KJ, Tabas I. Macrophages in the pathogenesis of atherosclerosis. *Cell*. 2011; 145(3): 341–55.
 126. Koelwyn GJ, Corr EM, Erbay E, Moore KJ. Regulation of macrophage immunometabolism in atherosclerosis. *Nature Immunology*. 2018; 19(6).
 127. Kaymak I, Williams KS, Cantor JR, Jones RG. Immunometabolic Interplay in the Tumor Microenvironment. *Cancer Cell*. 2021; 39(1): 28–37.
 128. Vitale I, Manic G, Coussens LM, Kroemer G, Galluzzi L. Macrophages and Metabolism in the Tumor Microenvironment. *Cell Metabolism*. 2019; 30(1): 36–50.
 129. Maier A, Wu H, Cordasic N, Oefner P, Dietel B, Thiele C, et al. Hypoxia-inducible protein 2 Hif2/Hilpda mediates neutral lipid accumulation in macrophages and contributes to atherosclerosis in apolipoprotein E-deficient mice. *The FASEB Journal*. 2017; : 4971–84.
 130. Blanc J, Alves-Guerra MC, Esposito B, Rousset S, Gourdy P, Ricquier D, et al. Protective Role of Uncoupling Protein 2 in Atherosclerosis. *Circulation*. 2003; 107(3): 388–90.
 131. Aarup A, Pedersen TX, Junker N, Christoffersen C, Bartels ED, Madsen M, et al. Hypoxia-inducible factor-1 α expression in macrophages promotes development of atherosclerosis. *Arteriosclerosis, Thrombosis, and Vascular Biology*. 2016; 36(9): 1782–90.
 132. Tawakol A, Singh P, Mojena M, Pimentel-Santillana M, Emami H, Macnabb M, et al. HIF-1 α and PFKFB3 mediate a tight relationship between proinflammatory activation and anerobic metabolism in atherosclerotic macrophages. *Arteriosclerosis, Thrombosis, and Vascular Biology*. 2015; 35(6): 1463–71.
 133. Cochain C, Vafadarnejad E, Arampatzi P, Pelisek J, Winkels H, Ley K, et al. Single-cell RNA-seq reveals the transcriptional landscape and heterogeneity of aortic macrophages in murine atherosclerosis. *Circulation research*. 2018; 122(12): 1661–74.
 134. Silva HM, Báfica A, Rodrigues-Luiz GF, Chi J, D'Emery Alves Santos P, Reis BS, et al. Vasculature-associated fat macrophages readily adapt to inflammatory and metabolic challenges. *Journal of Experimental Medicine*. 2019; 216(4).
 135. Pålsson-McDermott EM, O'Neill LAJ. Targeting immunometabolism as an anti-inflammatory strategy. *Cell Research*. 2020; 30(4): 300–14.

136. Peterson KR, Cottam MA, Kennedy AJ, Hasty AH. Macrophage-Targeted Therapeutics for Metabolic Disease. *Trends in Pharmacological Sciences*. 2018; 39(6): 536–46.
137. Chen B, Gao A, Tu B, Wang Y, Yu X, Wang Y, et al. Metabolic modulation via mTOR pathway and anti-angiogenesis remodels tumor microenvironment using PD-L1-targeting codelivery. *Biomaterials*. 2020; 255: 120187.



Dutch summary | Nederlandse samenvatting

Dutch Summary | Nederlandse samenvatting

Introductie

Metabole ziekten, waaronder obesitas en suikerziekte (diabetes mellitus), zijn een wereldwijd probleem. Momenteel kampt meer dan één op de drie volwassenen met overgewicht en er wordt verwacht dat dit aantal de komende jaren zal blijven toenemen. Het ontstaan van metabole ziekten gaat vaak gepaard met complicaties die grote gevolgen hebben voor de gezondheid, bijvoorbeeld een verhoogde vatbaarheid voor infecties en een verhoogd risico op hart- en vaatziekten (cardiovasculaire ziekten). Het afweersysteem (immuunsysteem) kan een belangrijke rol spelen bij het ontstaan van deze complicaties. Obesitas kan bijvoorbeeld leiden tot een disfunctie van verschillende typen immuuncellen. Hierbij is een belangrijke rol weggelegd voor het witte vetweefsel. Bij overgewicht en obesitas leidt een overmatige opslag van vetten in het vetweefsel tot een verslechterde functie van zowel vetcellen (adipocyten) als immuuncellen, waardoor er lokaal een laaggradige ontsteking (inflammatie) kan ontstaan. Wanneer deze laaggradige inflammatie chronisch wordt, kan dit de werking van het hormoon insuline verstoren. Aangezien insuline de controle van glucose in de bloedcirculatie reguleert, kan hierdoor de glucoseregulatie uit balans raken, met als uiteindelijk gevolg het ontstaan van diabetes mellitus.

Diabetes mellitus type 2 (T2DM) is de meest voorkomende vorm van diabetes, en tevens de vorm die kan ontstaan als een gevolg van overgewicht en laaggradige inflammatie. Diabetes mellitus type 1 (T1DM) wordt daarentegen veroorzaakt door een gebrek aan de productie van insuline. T1DM wordt gekarakteriseerd als een auto-immuunziekte, waarbij immuuncellen de insulineproducerende beta-cellen in de alvleesklier aanvallen. Hoewel T1DM en T2DM een andere oorzaak hebben, zijn de gevolgen vergelijkbaar. Bij beide types is het lichaam niet meer goed in staat om voldoende glucose uit de circulatie op te nemen, met een te hoge bloedsuikerspiegel (hyperglycemie) als gevolg. Daarnaast gaan beide types ook vaak gepaard met een algemene disfunctie van immuuncellen, chronische ontstekingen, een verminderde acute immunrespons en een verhoogd risico op hart- en vaatziekten.

Vooraf cellen van het aangeboren immuunsysteem lijken een belangrijke rol te spelen bij de ontwikkeling van aan diabetes gerelateerde complicaties. Het aangeboren immuunsysteem vormt de eerste verdedigingslinie van het lichaam en helpt daarmee bij de bescherming tegen ziekteverwekkers. Twee belangrijke celtypen van het aangeboren immuunsysteem zijn monocyten en macrofagen. Bij het ontstaan van infecties of beschadigingen kunnen monocyten vanuit de bloedsomloop naar weefsels gerekruteerd

worden. Monocyten passen zich vervolgens gemakkelijk aan hun nieuwe omgeving aan door zich om te vormen naar macrofagen met weefsel- en situatie-specifieke functies. Macrofagen spelen vervolgens een belangrijke rol in de initiatie en de resolutie van ontstekingen, en kunnen daarnaast het herstel van weefsels ondersteunen en helpen bij het opruimen van dode cellen. Zowel monocyten als macrofagen zijn zeer plastische cellen die zich snel kunnen aanpassen aan een veranderende omgeving, waarbij ze effectief de benodigde functies kunnen uitoefenen.

De intracellulaire stofwisseling (metabolisme) blijkt bij monocyten en macrofagen van cruciaal belang voor hun functioneren. Dat betekent dat een afwijkend functioneren van deze immuuncellen ook veroorzaakt kan worden door veranderingen in het metabolisme. De interacties tussen het metabolisme en het functioneren van immuuncellen worden vaak beschreven met de algemene term 'immunometabolisme'. Bij monocyten en macrofagen kunnen bepaalde functies of karakteristieken zelfs afhankelijk zijn van specifieke metabole processen. Hieronder vallen processen die met het ontstaan of oplossen van ontstekingen te maken hebben, maar ook met uitvoerende taken zoals het opruimen van dode cellen.

Aangezien monocyten en macrofagen plastische cellen zijn die zich snel kunnen aanpassen aan een nieuwe omgeving, zijn ze zeer sensitief voor (metabole) veranderingen in het lichaam. Veranderingen in de metabole status van het lichaam, bijvoorbeeld door overgewicht of resistentie tegen insuline, kunnen daardoor bijdragen aan het ontstaan of het versterken van een chronische ontstekingsstaat. Veranderingen in het metabolisme van immuuncellen zouden hierbij een belangrijke rol kunnen spelen.

Het doel van dit proefschrift was dan ook om te onderzoeken welke rol de interactie tussen het metabolisme en de functie van monocyten en macrofagen speelt tijdens de ontwikkeling van diabetes en diabetes-gerelateerde complicaties.

Immuuncelmetabolisme en diabetes-gerelateerde complicaties

Een ontstekingsgerichte activering van immuuncellen gaat vaak samen met een verhoogd verbruik van suikers (glucose) als brandstof. Door de directe verbranding van glucose, waarbij melkzuur (lactaat) vrijkomt, kunnen immuuncellen snel energie vrijmaken en daarmee adequaat reageren op een infectie of activatie. Een wissel in het metabolisme van vetten (lipiden) naar het metabolisme van glucose wordt daarom vaak gezien als een kenmerk van ontstekingsgerichte, inflammatoire immuuncellen. In **hoofdstuk 2** hebben we onderzocht welke samenhang er bestaat tussen de uitscheiding van lactaat als marker voor glucosemetabolisme en de uitscheiding van specifieke ontstekingsstoffen (cytokines)

door immuuncellen van gezonde personen en patiënten met T1DM. Het verband tussen de aanwezigheid van lactaat en specifieke cytokines blijkt voor een aantal onderzochte cytokine verschillend te zijn, maar lijkt ook beïnvloed te worden door activering van de immuuncellen met verschillende ziekteverwekkers. We ontdekten dat er grote variaties bestaan in de immuunrespons en het glucosemetabolisme van immuuncellen bij gezonde personen, die wijzen op verschillen in de flexibiliteit van immuuncellen om over te schakelen op het metabolisme van glucose. Bij patiënten met T1DM vonden we grotendeels dezelfde verbanden als bij gezonde personen, met kleine verschillen in de associatie tussen glucosemetabolisme en de immuunrespons.

Veel aan diabetes gerelateerde complicaties, bijvoorbeeld een verhoogde vatbaarheid voor infecties of een verhoogd risico op hart- en vaatziekten, lijken geassocieerd te zijn met een inadequate functie van aangeboren immuuncellen. De rol van het immuuncelmetabolisme in deze associatie was echter nog niet onderzocht. Daarom hebben we diabetes-afhankelijke veranderingen in het functioneren en het metabolisme van monocyten van gezonde personen en patiënten met T1DM in kaart gebracht in **hoofdstuk 3**. Bij monocyten van patiënten met T1DM met een slechte glycemische controle, blijkend uit hoge HbA1c gehalten, vonden we na inflammatoire activatie een verminderde productie van cytokines. Deze reductie in cytokines was echter geassocieerd met een verhoogd glucosemetabolisme en een verhoogd ontstekingsprofiel voorafgaand aan de activatie. Deze observaties wijzen op de aanwezigheid van een bepaalde immuuntolerantie (onderdrukte immuunreacties) bij patiënten met een slechte glycemische controle, waarbij een chronische inflammatoire activatie gepaard gaat met een disfunctionele immuunrespons. Deze bevindingen zouden gedeeltelijk het verhoogde risico op infecties en hart- en vaatziekten bij patiënten met T1DM kunnen verklaren.

Immuuncelmetabolisme en het ontstaan van diabetes

Naast een rol in de ontwikkeling van aan diabetes gerelateerde complicaties, kunnen monocyten en macrofagen ook betrokken zijn bij het ontstaan van diabetes. Aangeboren immuuncellen kunnen in het vetweefsel een ontsteking versterken, die vervolgens resistentie tegen insuline in de hand kan werken. Van de verschillende typen immuuncellen die in het vetweefsel aanwezig zijn, is er bij het ontstaan van overgewicht en obesitas vooral een sterke stijging te zien in het aantal macrofagen. Bij overgewicht groeit het vetweefsel en de omgeving van macrofagen verandert daardoor sterk. Hierdoor raken deze macrofagen op een unieke manier geactiveerd, de zogenoemde 'metabole activatie', die waarschijnlijk bijdraagt aan de progressie van vetweefselontsteking. Bij deze metabole activatie wordt ook vaak een grote verandering in het metabolisme van macrofagen

waargenomen. Aangezien veranderingen in het metabolisme van immuuncellen sterke effecten kunnen hebben op hun functioneren, zou het veranderde metabolisme van vetweefselmacrofagen misschien ook een directe oorzaak kunnen zijn van de verhoogde ontstekingsgraad in het vetweefsel.

Om de onderliggende mechanismen te kunnen doorgronden die immuuncelmetabolisme, vetweefselontsteking en uiteindelijk resistentie tegen insuline met elkaar verbinden, is het belangrijk om zoveel mogelijk betrokken genen en eiwitten te identificeren. In **hoofdstuk 4** onderzochten we daarom de rol van het eiwit uncoupling protein 2 (UCP2) in vetweefselmacrofagen binnen de context van vetweefselontsteking. We bevestigden het belang van UCP2 bij het reguleren van zowel het metabolisme als de inflammatoire functie van macrofagen. Het uitschakelen van de werking van UCP2 (UCP2-deletie) leidde namelijk tot een verlaagde ontstekingsrespons, terwijl deze macrofagen wel een verhoogde glucose- en oxidatief metabolisme lieten zien ten opzichte van normale macrofagen. Deze metabole veranderingen waren echter niet meer waar te nemen in een lipiderijke omgeving. Daarnaast zagen we in een experimenteel model voor dieetgeïnduceerde obesitas bij muizen met of zonder UCP2-deletie geen verschillen in vetweefselontsteking of insulineresistentie. Op basis hiervan concludeerden we dat UCP2 geen cruciale rol speelt in de link tussen vetweefselmacrofagen, vetweefselontsteking en insulineresistentie.

Een belangrijk kenmerk van metabole activatie is een verhoogd metabolisme van lipiden, waardoor vetweefselmacrofagen waarschijnlijk beter kunnen omgaan met de hogere lipidegehalten in groeiend vetweefsel. Doordat macrofagen veel meer lipiden kunnen opnemen dan ze verbruiken, worden vetweefselmacrofagen bij obesitas vaak getypeerd door een excessieve opslag van lipiden in lipidedruppeltjes. Onze hypothese was dat de excessieve toename van lipidedruppeltjes in vetweefselmacrofagen een rol zou spelen in het ontstaan van disfunctionele macrofagen en daardoor ook bij zou kunnen dragen aan vetweefselontsteking. Om dit vast te kunnen stellen, onderzochten we in **hoofdstuk 5** de precieze functie van het eiwit hypoxia-inducible lipid droplet-associated (HILPDA), dat geassocieerd was met de aanwezigheid van lipidedruppeltjes in macrofagen. Uit onze data bleek dat HILPDA sterk gereguleerd was na behandeling van macrofagen met lipiden, maar ook in obees vetweefsel hoog tot uiting kwam. Na een specifieke deletie van HILPDA in macrofagen namen we bijna geen lipidedruppeltjes meer waar in macrofagen die waren behandeld met lipiden. Bij het ontrafelen van het mechanisme bleek dat HILPDA een directe remmer was van het enzym ATGL, dat lipiden kan afbreken. Een gebrek aan HILPDA zorgt dus voor een overactiviteit van ATGL, waardoor lipidedruppeltjes

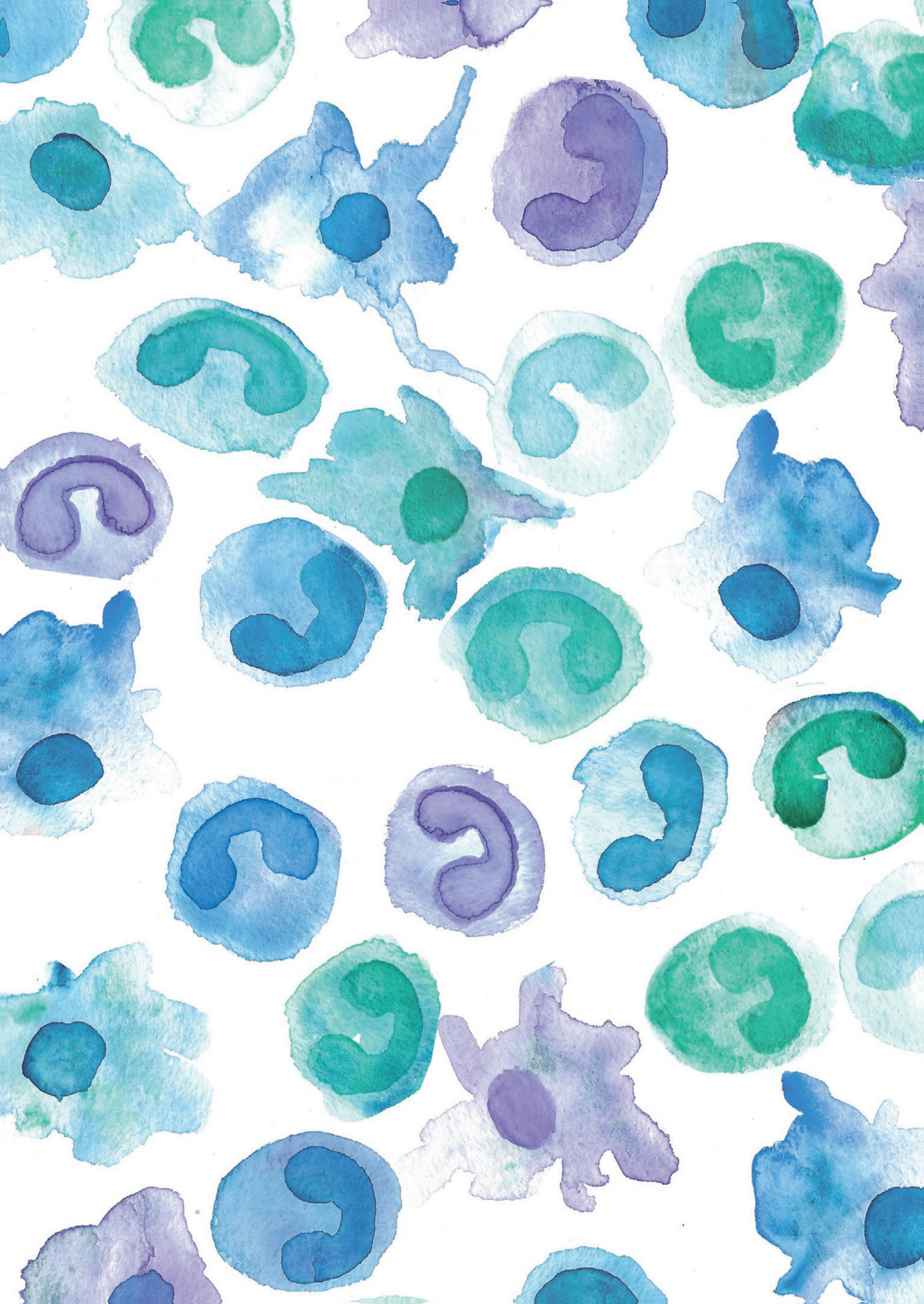
constant worden afgebroken. De verminderde ophoping van lipidedruppeltjes werd ook geobserveerd in HILPDA-deficiënte vetweefselmacrofagen geïsoleerd uit obeerse vetweefsel van muizen. In tegenstelling tot onze verwachtingen zorgde het voorkomen van de ophoping van lipidedruppeltjes echter niet tot een verminderde inflammatoire activatie van vetweefselmacrofagen. Daarnaast waren er in dieet-geïnduceerde obese muizen met een macrofaag-specifieke HILPDA-deletie ook geen verbeteringen te zien in vetweefselontsteking of insulineresistentie. Deze bevindingen tonen aan dat excessieve ophoping van lipidedruppeltjes in vetweefselmacrofagen niet de directe oorzaak is van vetweefselontsteking en insulineresistentie.

Ook buiten een lipide-rijke omgeving kunnen macrofagen lipiden opslaan in lipidedruppeltjes. Een toename van lipidedruppeltjes karakteriseert namelijk ook de metabole respons in reactie op verschillende ziekteverwekkers. In **hoofdstuk 6** bestudeerden we de accumulatie van lipidedruppeltjes na inflammatoire activatie van macrofagen als reactie op blootstelling aan een bacteriële component: LPS. We onderzochten de betrokkenheid van HILPDA en ATGL in dit proces, en vonden dat de remmende werking van HILPDA op ATGL waarschijnlijk te maken heeft met een verhoogde afbraak van het ATGL enzym. Daarnaast stelden we vast dat een afname van ATGL, waarschijnlijk door een verhoogde expressie van HILPDA, een rol speelt bij het ophopen van lipidedruppeltjes na LPS-behandeling in macrofagen. Specifieke deletie van HILPDA zorgde ook in de context van LPS-geïnduceerde inflammatoire activatie voor een gebrek aan lipidedruppeltjes in macrofagen. In deze HILPDA-deficiënte macrofagen vonden we een versterking van de inflammatoire reactie op LPS waarmee we een duidelijke link tussen vetdruppeltjes in macrofagen en de ontstekingsreactie ontdekten. De versterkte inflammatoire reactie van HILPDA-deficiënte macrofagen werd gekarakteriseerd door een verhoogde uitscheiding van ontstekingsstoffen PGE2 en IL-6, waartussen onze data een direct verband suggereerden. Deze bevindingen ondersteunen dat de afbraak van lipiden door ATGL een belangrijke rol speelt bij de regulatie van ontstekingen middels productie van PGE2 en IL-6 in macrofagen.

Conclusie

Bij veranderingen in de metabole status van het lichaam tijdens metabole ziekten zoals obesitas en diabetes, kunnen het metabolisme en de functie van aangeboren immuuncellen, zoals monocytten en macrofagen, beïnvloed worden. De studies in dit proefschrift laten gezamenlijk zien dat veranderingen in het metabolisme van monocytten en macrofagen een belangrijke rol kunnen spelen in de verdere ontwikkeling van diabetes en diabetes-gerelateerde complicaties, waaronder een chronische ontstekingsstaat. Door

deze veranderingen beter in kaart te brengen, kunnen we in de toekomst mogelijk het metabolisme van monocyten en macrofagen beïnvloeden om verdere progressie van metabole ziekten te voorkomen.



Acknowledgements | Dankwoord

Acknowledgements | Dankwoord

Na iets meer dan vier jaar pipetteren, discussiëren, schrijven, experimenteren, onderzoeken en herhalen, ligt hier dan uiteindelijk mijn Ph.D. thesis. Ik kijk met ontzettend veel trots en dankbaarheid terug op deze bijzondere tijd en alles wat ik de afgelopen jaren heb mogen leren en bereiken. Het grootste deel hiervan was echter nooit mogelijk geweest zonder de onmisbare directe of indirecte hulp van collega's, vrienden en familie, die ik in dit dankwoord hier graag persoonlijk voor wil bedanken.

Allereerst natuurlijk Dr Stienstra, beste **Rinke!** Ontzettend bedankt voor alle steun en mooie kansen die je me de afgelopen jaren hebt gegeven. Je gaf me ontzettend veel vrijheid en vertrouwen in mijn onderzoek, maar stond ook altijd klaar met honderden nieuwe ideeën. Jouw deur stond altijd, maar dan ook altijd open: om (niet zo heel) snel resultaten of experimenten te bespreken, even frustraties los te laten, maar ook voor allerhande grapjes en praatjes. "Komt wel goed" en "Er komt vast wat uit" waren zo ongeveer jouw zinspreuken, en je wist al snel dat die woorden vaak precies waren wat ik even moest horen. Je hebt een eeuwig positieve insteek, die je alleen even losliet in één van de vele rants in de auto op weg naar Nijmegen. Ik heb superveel van je geleerd en daar ben ik je heel erg dankbaar voor!

Ook Prof. Dr Kersten, **Sander**, bedankt voor al jouw kritische input, vragen en suggesties. Ik vond het super om met je samen aan het eerste HILPDA project te mogen werken, en heb daar ook enorm veel van geleerd. Niet alleen was het heel leerzaam en fijn om met jou over de inhoud van projecten te kunnen sparren, ook zal ik je wilde verhalen en (slechte) grapjes tijdens ITT/GTT's of secties niet snel vergeten. Dank voor je supervisie de afgelopen jaren!

Prof. Dr Tack, beste **Cees**, dank voor je input de afgelopen jaren. Ik heb bewondering voor de bodemloze putten aan kennis en interesses die je bezit, van de frequentie van achternamen in Nederland tot Duitse spreekwoorden en DJ-software. Alleen al het feit dat je een van de weinige professoren was die tijdens de ADDRDM meetings op de dansvloer te vinden was, dwingt een diep respect af. Dank!

Natuurlijk ook hartelijk dank aan mijn thesis commissie: Prof. Dr **Huub Savelkoul**, Prof. Dr **Esther Lutgens**, Dr **Marianne Boes** en Dr **Kristiaan Wouters**, voor het plaatsnemen in mijn promotiecommissie en het kritisch beoordelen van mijn proefschrift.

I would also like to thank all co-authors and collaborators: **Lieve Temmerman**, **Suzan Wetzels**, **Erik Biessen**, **Niels Riksen**, **Frits Mattijssen**, **Wieneke Dijk**, **Anastasia Georgiadi**, **Michel van Weeghel**, **Rajat Singh**, **Jan Willem Borst**, **Tiphaine Sancerni** and **Marie-Clotilde Alves Guerra** for their indispensable help, and for providing valuable information, experimental input or data. Lieve en Suzan, dank voor het mogelijk maken van de supergave ervaring op het pathologie lab in Maastricht, met jullie openheid en al jullie onmisbare hulp bij de MacroScreen! Tiphaine, thank you so much for being so open to share your expertise on UCP2!

Lisa, **Frank**, mijn macrofaag-vriendjes en fantastische paranimfen, ik ben ontzettend blij dat ik jullie aan mijn zijde heb tijdens mijn verdediging! Jullie laten menig loodje een stuk minder zwaar wegen. Met jullie was er opeens een macrofaag/monocyt-groepje (stienstreet!) en daarmee ruimte om te sparren, maar vooral ook veel (echt veel) koffietjes en borreltjes te drinken en flauwe grapjes te maken. Lisa, stiekem borrelen in Maastricht, samen met Solex in een B&B, elkaar spontaan tegenkomen op een festival (natuurlijk samen met Jelle), en samen feesten wanneer het maar kan.

Ik waardeer je openheid en eerlijkheid, je gekkigheid, je vermogen om te relativeren, maar ook dat je altijd klaar staat om even te kletsen of te sparren (of koffie te drinken bij je favo barista). Je bent supergoed op weg met je PhD, en ik weet zeker dat je het fantastisch gaat doen! En Frank, het voelde net alsof ik jou al jaren kende. Naast een snelle binding over ons SSR verleden, en je bizarre puzzel-oplossende vermogen, was je als DE POSTDOC vanaf moment 1 mijn go-to person om mee te sparren. En, wat doorzag je mij goed (en wij jou, met je volwassen schoenen). Je bent mega zorgzaam, fantastisch in peptalks & opvrolijkmomentjes en ik ben je super dankbaar voor al je hulp in het lab en daarbuiten! Ik wens jou, Maria en Sam alle geluk toe!

Natuurlijk ook alle lof voor **Merel**, zonder jou was er van mij ook zeker weten niks terecht gekomen ;) Bedankt voor de duizenden theetjes, kletsmomentjes en crisisoverleggen. Ik ben echt ontzettend blij dat jij er was en dat ik altijd op je terug mocht vallen. Ik waardeer hoe jij altijd mensen weet te verbinden, met verjaardagen en feesten die niet te overtreffen zijn (natuurlijk ook dankzij topkooktalent & entertainer Ingmar). Heel veel succes met je afronding, ik ben al zo ontzettend trots op je! En natuurlijk wens ik jullie heel veel geluk samen met Tristan.

Dan mijn lieve kantoorgenootjes: kletsen, serieuze dingen bespreken, tranen, boosheid (dinnergame!), en vooral heel veel lachen met elkaar, ik had jullie steun niet kunnen missen. **Charlotte!** Ik vond het heerlijk om samen te dansen als jonkies, en heb zoveel aan jouw steun gehad de laatste jaren. Je bent naast karaoketalent een super sterke vrouw die weet wat ze wil en dat bewonder ik in je. Een ding weet ik ook zeker, als wij samen in een team waren gezet tijdens de dinner game waren we onoverwinnelijk geweest en hadden de andere teams al na een week huilend opgegeven! **Anouk**, ik bewonder je positiviteit en standvastigheid! Als eloquente en belezen Amsterdammer ben je altijd in voor een goede discussie, maar ook de Anouk die bij carnaval naar boven kwam waardeerde ik zeer! **Brecht**, ik vind het super dat ik jou nog in mijn laatste tijd heb mogen meemaken. Je hebt veel zelfreflectie & alle ingrediënten om een fantastische PhD neer te zetten. Succes! En **Judith**, het was super om naast iemand te zitten met wie ik zo open en fijn kon praten. Ik heb veel respect voor hoe jij met je PhD traject omgaat, je doet het echt super! En natuurlijk ook vroeger kantoorgenootje **Nikkie** heel erg bedankt voor je positieve insteek en fijne kletsmomentjes!

Dan zijn er nog veel meer PhD-collega's die de NMG experience zo top hebben gemaakt. **Benthe** (Besse?), van Barcelona tot hier hebben we allebei een enorme weg afgelegd, het was super om dat met jou tegelijk te doen. Ik had onze flauwe grapjes, gekkigheid, biertjes, tv-experience, gesprekken en rants in de celkweek absoluut niet willen missen. En ook **Mara**, ik heb enorme bewondering voor jouw positieve instelling! Ondanks tegenslagen ga jij altijd gewoon door en blijf je altijd lachen (en dat is aanstekelijk!). En natuurlijk was carnaval bij jou absoluut onvergetelijk (gelukkig hebben we de foto's nog..). Jullie zijn allebei super lekker bezig, heel veel succes allebei met de laatste loodjes en ik kan niet wachten om er samen een biertje op te drinken!

Danny, you are such a lovely person with a big heart! You were easy to connect with, bold with your questions and a kind, honest and hardworking colleague. I will miss your jokes in the lab & I'm confident you will do a great job finishing your PhD! **Xiaolin**, I wish I had your sense of fashion. You were a kind colleague, always smiling and happy to help. I enjoyed connecting with you over PGE2 ;) good luck with finishing your PhD! **Rieneke**, jij was een superfijne collega! Ik heb groot respect voor jouw enorme sportiviteit, positiviteit en doorzettingsvermogen. Ik vond het super leuk om af en toe met jou over immuuncellen te praten! **Iris**, ook bij jou stond de deur altijd open, dankjewel daarvoor. Veel succes met je onderzoek! **Montse**, thanks for the collaboration on our HILPDA paper.

It's absolutely incredible how you manage to combine your PhD with being a great mom! **Philip**, we were already in the lab together during our MSc theses. I appreciate your honesty and challenging attitude, but also your jokes (although I'm never sure if you are serious). You are great company for parties, borrels and of course power yoga! **Antwi**, thanks for your help in the lab. You were a super kind and helpful colleague, always quick with a smile, thanks! **Miranda**, ik ga jou zeker nog wel een keer tegenkomen op een festival of op een camping. Jij ook veel succes met het afronden van je PhD! **Ian**, het was tof om jou als mede-Zeeuw de laatste tijd als labbench-buurman te hebben. Succes met je verdediging! **Joline**, jij was een topper om in het lab te hebben! Jij maakte Stienstreet helemaal af, en ik ben super blij dat ik je in Amsterdam nu niet meer hoef te missen ;) **Tessa**, als ergens tomato of potato lees, dan hoor ik dat in jouw stem. Heel veel succes verder met je PhD! Ook veel succes aan **Monique & Mingjuan**. Ook een aantal PhD's van de oude stempel bedankt: **Lily, Aafke, Wieneke, Sophie** en **Inge** voor alle hulp & gezelligheid!

Besides I would like to thank all other colleagues in Wageningen. **Guido**, bedankt voor al je hulp, kletsmomentjes, slechte grapjes en (goedbedoelde) wijze raad. Het beeld van jou in je gouden jas en hoed staat op mijn netvlies gebrand. Daarnaast **Lydia, Wilma, Dieuwertje, Shauna, Mark, Marco, Jocelijn, Klaske, Michiel, Marlies, Pieter, Anna, Suzanne, Paulien** en **Renger**, erg bedankt voor jullie waardevolle input, belangstelling en kritische vragen, maar ook fijne gesprekken bij het koffieapparaat of tijdens de lunch. Daarnaast ook **Adriëne, Riekie, Jasmijn** en **Gea** bedankt voor al jullie ondersteuning!

Also a big thanks to all the technicians, without you the lab would not be ~~the same~~ running at all. Dankjewel labmama **Mieke** voor alle goede zorgen en op zijn tijd een goede dosis liefde, bier&friet en wijze raad. Ik zal nog met smart wachten tot ik aan de slag kan op The Poland lab. **Jenny**, bedankt voor je hulp bij alle microarrays en RNA-gerelateerde dingen, maar ook je zangkunsten als je dacht dat je veilig in het microarray lab zat. **Karin, Nhien** en **Mechteld**, bedankt voor al jullie hulp en fijne gesprekken! **Susanne**, jammer dat ik jou en je science memes niet wat langer kon meemaken! And also a big thanks to **Shohreh**, especially for all the lastminute crisis management and much needed worktime (or long-past-worktime) snacks! Ook een enorme dank aan **Anneke** voor de bergen aan hulp die je me in het AIG lab in Nijmegen gegeven hebt, je stond altijd voor me klaar en was super om je af en toe aan mijn zijde te kunnen hebben! Daarnaast ook **Kiki** bedankt voor de hulp, maar natuurlijk ook de vele uurtjes kletsen!

Also a big thanks to **Wendy, Desiree, Hanne, Daan, Yanlin, Anna** and **Cresci-Anne**, it was an honour to (partly or fully) supervise you during your M.Sc. projects in the lab!

Ook alle medewerkers van het CKP ontzettend bedankt: **René, Wilma, Bert, Marleen, Froukje** en **Noortje**. Zonder jullie was een groot deel van dit onderzoek niet mogelijk geweest. Lieve Wilma en Bert (en later ook Marleen), bedankt voor al jullie goede zorgen, het altijd klaarstaan voor hulp met de muizen (niet alleen overdag maar ook 's avond/'s nachts/in de vroege ochtend/weekenden, niks was jullie te gek), al het lastminute geregeld en de altijd aanwezige vers gezette koffie, geklets en luisterende oren. Ik kon altijd bij jullie terecht en er was altijd wel iets te regelen, en daar ben ik jullie super dankbaar voor!

Anne, wat begon met een wild idee is geëindigd in een prachtig avontuur samen in de bergen in Nepal. Ik bewonder je als een sterk mens en een superfijne vriendin om mee te filosoferen. Onze gesprekken, etentjes, wandelingen, drankjes en mensen-zeggen-dingen-avonden brachten vaak veel in perspectief en hebben me de nodige energie en rust gegeven. Dankjewel daarvoor!

Mariëlle, bedankt voor alle heerlijke etentjes, drankjes, en avondjes uit. Hoe jij en Anne als verrassing opeens op kwamen dagen tijdens een ScienceBattle was zo tof! En alle verjaardagen bij jou waren altijd fantastisch. Ik wens je heel veel succes met het afronden van je PhD!

Also all my colleagues from the AIG lab in Nijmegen, thank you for making me feel welcome on all my Seahorse, monocyte & lactate assay trips to Nijmegen, and of course thank you for the unforgettable great parties conference talks in Cluj, and the great weekend to the Ardennen! Of course a very special thanks to the 'sugar'-girls: **Jacqueline**, thanks for all your help in the lab, the great pasta evenings and our nice week 'off' together in Rotterdam! **Kathrin** (Kat), thanks for the collaboration on the Diabetes paper, your very wise job advice to become the next Antje (I'm still considering), and all your (very special) jokes! **Anouk** en **Lian**, ik zal nooit al onze NEYDM/ADDRM feestjes/avonturen vergeten (al zou ik het willen), en natuurlijk het iets te gezellige beddentekort in de Ardennen. Gelukkig hebben we de foto's (...en filmpjes...) nog! En natuurlijk **Julia**, het Nijmegen-lid van de stienstreet groep, nooit een gebrek aan gezelligheid op het lab met jou. Jouw positiviteit is mega aanstekelijk, zal ik dan ook maar een macrofaag-tattoo nemen? Natuurlijk zijn er meer mensen uit Nijmegen die ik hier wil noemen, bedankt **Steef** voor de gezelligheid, biertjes en fijne gesprekken. **Julia, Siroon, Jorge, Inge, Martin, Laszlo, Leonie, Michelle, Charlotte, Jessica, Katrin, Nico, Jelmer, Intan and all others**, thanks for your helpfulness and the fun days!

Naast al mijn collega's was ik uiteraard ook helemaal nergens geweest zonder al mijn lieve vrienden en familie. Voor jaren hebben jullie te pas en te onpas mijn macrofaag-en-diabetes-verhalen aan moeten horen op borrels, feestjes, en in filmpjes, en hebben velen van jullie zelfs het halve land afgereisd om me er op een random podium nog eens over te horen vertellen. Dank voor jullie geduld, dankzij jullie onvoorwaardelijke steun ben ik gekomen waar ik nu ben!

Dan is daar natuurlijk mijn clubje. De chille weekendjes, dagjes weg, goede gesprekken en harten onder de riem had ik niet kunnen missen. Duizenden blokjes voor jullie. Stoere **Marieke**, niet alleen prijkt jouw fantastische creativiteit op de kaft en in dit boekje, ook ben ik je super dankbaar voor al je steun en vrijwel dagelijkse motivatie-appjes. Ik heb super veel bewondering voor jouw veerkracht! **Helen**, ook jij hebt me er (zeker door de laatste maanden) doorheen gesleept met wandelingen, lieve kaartjes en goede gesprekken. Je bent een superlieve en zorgzame vriendin, en ik bewonder jouw doorzettingsvermogen! **Jildou**, met jouw gelijke doses (vieze?) grappen en hele wijze eloquente raad weet je altijd de kern uit elk gesprek te halen en de juiste vragen te stellen. Dankjewel voor je belangstelling, liefde en openheid! **Marion**, jij wereldvrouw, wat ben ik blij dat je weer even terug in Nederland bent. Je kan zo heerlijk relativiseren en jouw aanwezigheid staat gelijk aan ontspanning en gezelligheid! **Gerben**, bedankt voor de goede gesprekken, gezellige avonden en (soms te felle) discussies ;) En dan natuurlijk ook **Folkert** bedankt voor alle grapjes, Enka-verkoop-trucjes&tips, de liefde van Budde en goede gesprekken. En **Nick**, bedankt voor je oprechte interesse, spontane plant- en natuur-colleges en gezelligheid!

En niet te missen is ook het dansfeestje groepje, het was altijd weer (letterlijk) thuiskomen en opladen met jullie op honderdduizend mooie feestjes, festivals en dagjes weg. **Jeremy & Mariëlle**, mijn eerste jaar was ik vrijwel elke zondagavond bij jullie, en ook in mijn laatste jaren voelde jullie huis als mijn tweede thuis in Wageningen. J, we go way back, dankjewel voor al je rauwe enthousiasme en no-nonsense-gewoon-een-beetje-lekker-doen-inspiratie. M, jij bent echt een rustpunt :) dankjewel voor al je steun & liefde! **Daan & Simoon**, dank voor alle keren dat ik in Nimma op ravilla mocht crashen als ik weer een week vol experimenten had, maar ook voor alle chille avondjes, spontaan langskomen, biertjes, spelletjes en kletspraatjes over het leven. Daan,

dank voor al je steun de afgelopen jaren, etentjes, dansjes, goede gesprekken, ik weet dat je er altijd bent. Simoon, we waren samen richting het einde van onze Ph.D., en daarbij was het superfijn om zo gelijk met jou op te trekken. Ik ben ook zo ontzettend trots op jou! **Frank**: bij twijfel, volg Frank. Op een festival of daarbuiten. Dankjewel voor just being Frank, knuffels, steun, filosofieën en zoveel meer. Dan natuurlijk lieve **Fen**, alle knuffels, gesprekken, dansjes, gekkigheid, peptalks (voor elkaar) en zoektochten naar avonturen zijn me superveel waard. En ook **Lou** natuurlijk, dank voor alle fijne dansjes en gesprekken!

Also thanks to the lovely **Jaap, Pauline, Rob** and **Sun** for being awesome roommates and tolerating me during the last years of my PhD! Especially Sun, thanks for all the beers, coffee, yoga and talks together :) Also to all YOPI-people & **Ynske**, thanks for providing such a great community, you really helped me find my homebase!

Ook lieve mensen van HMD De Zwevelpin, bedankt voor alle laatste jaren aan borrels, feestjes, weekenden, IRs en gekkigheid, maar ook de interesse die velen van jullie toonden in mijn onderzoek. Met jullie is er altijd wel wat te beleven! **Petra**, bedankt voor alle heerlijke wandelingen, gekke verhalen en spontane ideeën en natuurlijk ons grote Noorwegen-avontuur met Buck en de prinsessenknop! **Sas**, ons jaarlijkse uitje is altijd iets om naar uit te kijken. Dank voor je oprechte vragen en onze fijne gesprekken. Gaan we snel weer bij Beers-en-donck onbedekt aan de bar zitten? Ook **Joeri** en **Ellen** bedankt voor alle etentjes en gezelligheid. Ook **Alex, Tessa** en alle anderen nog actieve "oudjes", bedankt! Ook **Jochem** (je haat het vast om in deze alinea erbij te staan), toch bedankt voor alle dagjes zeilen en de gezellige etentjes op Binnenveld, en absoluut niet bedankt voor het zo vaak vragen wanneer ik nou eens ging publiceren ;)

Tania, in mijn hele Wageningen-tijd kende jij me het allerlangst. Ik vind het superfijn dat we in contact zijn gebleven en waardeer jouw steun en vriendschap ontzettend! **Michelle**, jij bent altijd een inspiratie. Blijf lekker je eigen weg volgen! Dan ook de lieve Zeeuwsche dames, vooral **Merel, Charlotte** en **Mignon**, heel erg bedankt voor het brengen van perspectief, de aanmoedigen en onze vriendschap!

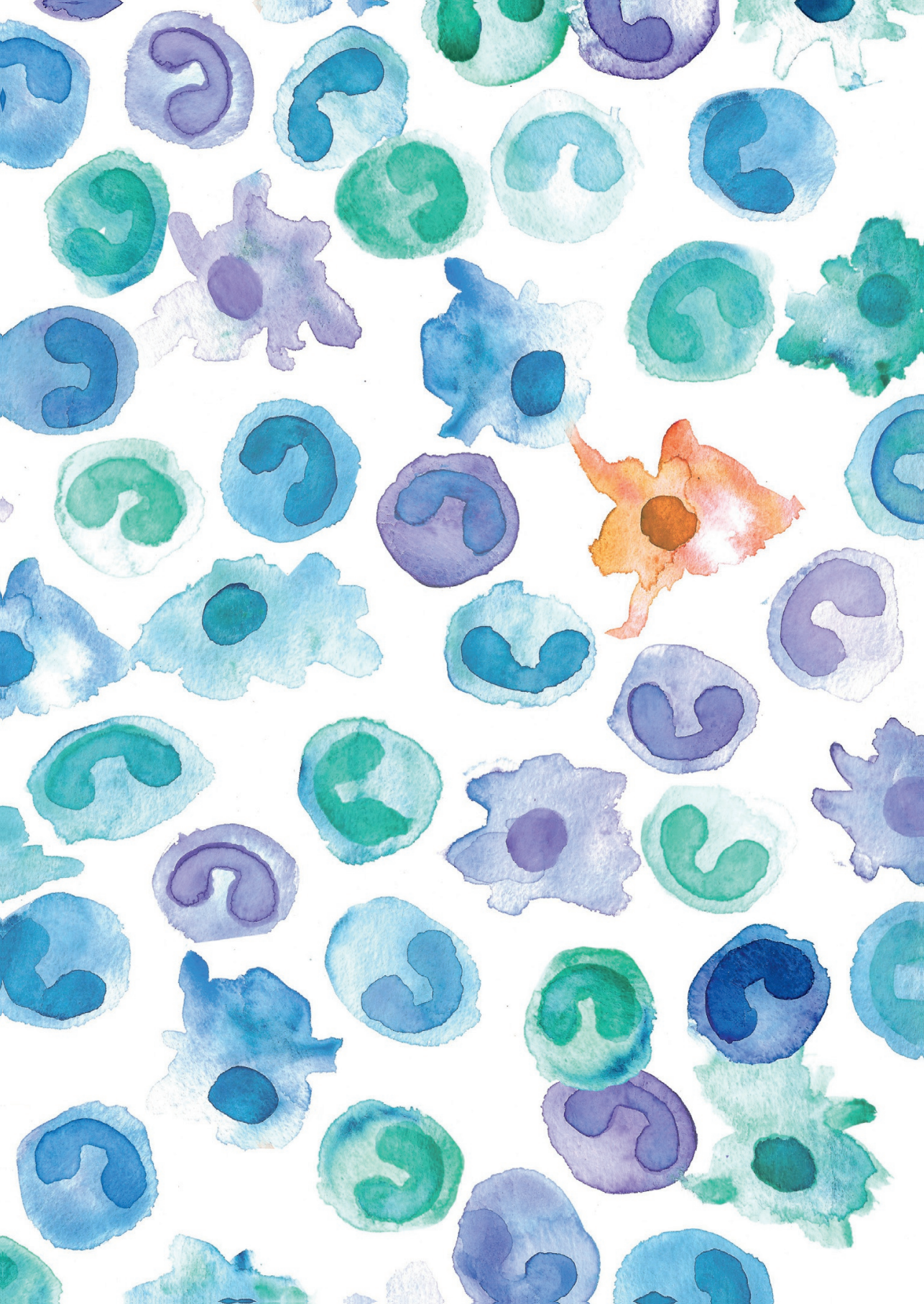
Natuurlijk wil ik ook mijn lieve schoonfamilie bedanken: **Milou, Patrick, Eva, Edwin** en **Jolanda** heel erg bedankt voor jullie steun, jullie interesse in mijn onderzoek en hoe welkom jullie me altijd laten voelen!

En daarnaast wil ik ook mijn eigen familie heel erg bedanken. Natuurlijk mijn lieve broers, die allebei een gouden hart hebben en altijd voor me klaar staan. **Merlijn**, ik heb ontzettend veel respect voor jouw veerkracht en doorzettingsvermogen. Dankjewel voor je steun & vertrouwen, samen met **Sophie** zorgden jullie voor genoeg fijne opvrolijkmomentjes, heerlijke je-kunt-het snacks en natuurlijk het regelmatig uitlenen van Tobi & Mia. **Quirijn**, dankjewel voor het altijd steunen van je kleine zusje, ik ben echt super trots op jou en hoe je de afgelopen jaren gegroeid bent. En natuurlijk ook op **Trang**! Straks twee Dr's in de familie binnen één week! Ik heb veel bewondering voor jouw harde werken, heel veel succes straks!

Allerliefste **pap & mam**, daar sta ik dan. Het was soms een flinke bevalling, maar jullie hebben mij altijd onvoorwaardelijk gesteund en mij nooit laten twijfelen over hoe ongelofelijk trots jullie op me zijn. Ik ben een gelukkig mens dat ik zulke lieve ouders heb, waar ik altijd op terug mag en kan vallen, en dat waardeer ik ontzettend. De basis van mijn nieuwsgierigheid en affiniteit met onderzoek is zonder twijfel door jullie gelegd. Mam, jij hebt me de afgelopen jaren altijd in mezelf laten geloven, ook als ik het soms zelf even niet meer zag. Je goede raad is altijd on point, en het

doet me altijd goed als we weer even een dag samen weg zijn. Pap, dan is daar toch de eerste dr. van Dierendonck.. Bedankt dat je de trots die van je afstraalt nooit, maar dan ook nooit onder stoelen of banken steekt en dat ik altijd bij jou terecht kan voor een goed gesprek!

Lieve **Richard**, de afgelopen jaren heb ik 100% dankzij jou kunnen doorzetten. En nu is het gelukt! Je moedigt me aan om buiten mijn comfortzone te gaan, maar je bent er ook altijd om me weer op te vangen als ik een paar stappen te veel neem. Je maakt me altijd weer aan het lachen. Wat er ook gebeurt, door jouw rust en de vanzelfsprekendheid waarmee je mij vertrouwen geeft, weet je vaak al mijn zorgen te relativeren. Ik kan je niet genoeg bedanken voor de niet aflatende stroom van (eindeloze bergen aan) geduld, support, kampeerweekendjes, knuffels, mountainbike-ritjes, liefde, wandelingen, afleiding, koffie, (on)gezond eten en puppyfilmpjes die de brandstof vormden voor het afronden van deze thesis. Ik ben super mega ongelofelijk blij met jou, op naar een mooie toekomst samen!



About the author

Curriculum vitae

Xanthe A.M.H. van Dierendonck was born in Apeldoorn, The Netherlands, on August 5th 1992. As most children, she showed an interest in food from a very young age. During her childhood, this interest escalated into a strong curiosity towards the effect of nutrition on metabolism and health. After graduating from secondary school in 2010, she therefore started the bachelor program Nutrition and Health at Wageningen University. During her bachelor thesis, she investigated how disruption of circadian day-night rhythms could affect glucose metabolism in the body. Bringing her thesis into practice, she frequently disrupted her own circadian day-night rhythms at her student association S.S.R-W.



In 2013, Xanthe obtained her bachelor's degree, after which she was elected as a full-time member in the Student Council for a board year. With her student party VeSte, she focused on safeguarding financial compensation for active students and monitoring the quality of education. In 2014, she continued her academic career by starting the master program Nutrition and Health, specializing in Molecular Nutrition and Toxicology. Next to that, she was appointed as academic writing tutor at the Wageningen Writing Lab (WWL), where she provided coaching for students who experienced difficulties in academic writing. During her M.Sc. thesis at the Nutrition, Metabolism and Genomics group, which was focused on the interaction between macrophages and adipocytes, she discovered a passion for macrophages that would linger on for years. After successfully finishing her M.Sc. thesis, she moved to Newcastle, United Kingdom for an internship at the Institute for Cell and Molecular Biosciences at Newcastle University. Here, she examined the circadian rhythms of autophagy in muscle tissue. She obtained her M.Sc. degree cum laude in 2016.

After backpacking on the other side of the world, she returned to Wageningen to start as a Ph.D. candidate under supervision of Dr Rinke Stienstra. During her Ph.D. research, she investigated the mechanisms and functional relevance of monocyte and macrophage metabolism in the context of obesity and diabetes, the results of which are described in this thesis. Next to her research, she supervised several M.Sc. students and was a member of the Ph.D. committee of the Division of Human Nutrition and Health.

Besides presenting her findings by oral and poster presentations at national and international conferences such as the Annual Dutch Diabetes Research Meeting, the European Atherosclerosis Society Meeting and the North European Young Diabetologists Meeting, she developed an interest to communicate her scientific results to a broader audience. She started participating in the Dutch theatre show 'ScienceBattle'; was selected for a pitch at the Pioneering Nutrition symposium; and recorded a video lecture for the University of the Netherlands (Universiteit van Nederland), which can be found online. In the last year of her Ph.D. Xanthe was awarded a travel grant from the VVAO, a travel grant for Translational Research from ZonMW, a Keystone Scholarship grant and a grant from Kennisinstituut Suiker & Voeding.

In 2021, Xanthe continued following her interest in all things concerning macrophage metabolism by starting as a postdoctoral researcher in the Van den Bossche lab within the Department of Molecular Cell Biology and Immunology at Amsterdam UMC, location VUmc.

List of publications

This thesis:

van Dierendonck XAMH*, de la Rosa Rodriguez MA*, Georgiadi A, Mattijssen F, Dijk W, van Weeghel M, Singh R, Borst JW, Stienstra R, Kersten S. HILPDA Uncouples Lipid Droplet Accumulation in Adipose Tissue Macrophages from Inflammation and Metabolic Dysregulation. *Cell Reports*. 2020 11;30(6):1811-1822.e6. doi: 10.1016/j.celrep.2020.01.046.

Thiem K*, **van Dierendonck XAMH***, Janssen AWM*, Boogaard JP, Riksen NP, Tack CJ#, Stienstra R#. A High Glycemic Burden Relates to Functional and Metabolic Alterations of Human Monocytes in Patients With Type 1 Diabetes. *Diabetes*. 2020;69(12):2735-2746. doi: 10.2337/db20-0568.

van Dierendonck XAMH, Sancerni T, Alves-Guerra MC, Stienstra R. The role of uncoupling protein 2 in macrophages and its impact on obesity-induced adipose tissue inflammation and insulin resistance. *Journal of Biological Chemistry*. 2020 18;295(51):17535-17548. doi: 10.1074/jbc.RA120.014868.

van Dierendonck XAMH, Vrieling F, Jaeger M, Janssen AWM, Hijmans A, Netea MG, Tack CJ, Stienstra R. Glycolytic activity in human immune cells: focus on inter-individual variation and functional implications during health and diabetes. In preparation.

van Dierendonck XAMH, Vrieling F, Smeehuijzen L, Boogaard JP, Croes C, Temmerman L, Wetzels S, Biessen E, Kersten S, Stienstra R. Triglyceride breakdown from lipid droplets regulates the inflammatory response in macrophages. In preparation.

Others:

Oteng AB*, Ruppert PMM*, Boutens L, Dijk W, **van Dierendonck XAMH**, Olivecrona G, Stienstra R, Kersten S. Characterization of ANGPTL4 function in macrophages and adipocytes using Angptl4-knockout and Angptl4-hypomorphic mice. *Journal of Lipid Research*. 2019 Oct;60(10):1741-1754. doi: 10.1194/jlr.M094128.

Petkevicius K, Bidault G, Virtue S, Jenkins B, **van Dierendonck XAMH**, Dugourd A, Saez-Rodriguez J, Stienstra R, Koulman A, Vidal-Puig A. Norepinephrine promotes triglyceride storage in macrophages via beta2-adrenergic receptor activation. *FASEB Journal*. 2021 Feb;35(2):e21266. doi: 10.1096/fj.202001101R.

Pecht T, **van Dierendonck XAMH**, Braune J, Boutens L, Haim Y, Vatarescu M, Gordon M, Chalifa-Caspi V, Gericke M, Rudich A, Stienstra R. Increased adipose tissue macrophage proliferation and glucose uptake occur early in obesity development, preceding immunophenotypic changes. Submitted.

*#Equal contribution

Overview of completed training activities

Discipline specific activities

Conferences and symposia

- North European Young Diabetologists meeting (NEYD), 2017 (oral)
Warwickshire, United Kingdom
- New Frontiers in Innate Immunity and Inflammation, 2018 (poster)
Radboud Centre for Infectious Diseases, Cluj-Napoca, Romania
- Dutch Diabetes Research Meeting (NVDO), 2017 (oral)
Oosterbeek, The Netherlands
- Dutch Diabetes Research Meeting (NVDO), 2018 (oral)
Oosterbeek, The Netherlands
- North European Young Diabetologists meeting (NEYD), 2019 (oral, first prize)
Copenhagen, Denmark
- Immunology symposium, Nederlandse vereniging voor Immunologie (NVVI) 2019
Lunteren, The Netherlands
- Immunometabolism EAS satellite meeting, 2019 (oral)
Maastricht, The Netherlands
- European Atherosclerosis Society conference (EAS), 2019 (oral/poster)
Maastricht, The Netherlands
- ImmunoMetNet symposium, 2019
Amsterdam, The Netherlands
- Pioneering Nutrition symposium, 2019 (selected pitch)
Wageningen, The Netherlands
- ImmunoMetNet symposium, 2020
Online

General courses and activities

- VLAG PhD week (VLAG) 2017
Baarlo, The Netherlands
- Project and Time Management course (WGS), 2017
Wageningen, The Netherlands
- Competence Assessment course (VLAG), 2018
Wageningen, The Netherlands
- Basic Course on R Software (Erasmus MC), 2018
Rotterdam, The Netherlands
- Teaching and Supervising Thesis Students course (WGS), 2019

Wageningen, The Netherlands

- Big Data analysis in the Life Sciences (VLAG), 2019
Wageningen, The Netherlands
- Last Stretch of the PhD Programme (WGS), 2020
Online

Optional activities

- MSc Course on Laboratory Animal Science (Radboud UMC), 2017
Nijmegen, The Netherlands
- PhD study tour United Kingdom, 2017
- Weekly scientific meetings/journal clubs, 2016 - 2021
Wageningen
- Weekly scientific meeting NMG/NB, 2016 - 2021
Wageningen
- Preparation of research proposal, 2016

Colophon

The research described in this thesis was financially supported by grants from the Netherlands Organisation of Scientific Research (2014/12393/ALW), the Dutch Diabetes Foundation (2015.82.1824), and the Netherlands Heart Foundation (ENERGISE grant CVON2014-02).

Financial support from Wageningen University and the Netherlands Association for the Study of Obesity (NASO) for printing this thesis is greatly acknowledged.

Cover design Marieke Oostveen

Layout Xanthe van Dierendonck

Printed by DigiForce | ProefschriftMaken.nl

©Xanthe van Dierendonck, 2021

